THE IMPACT OF INFLAMMATION ON PREGNANCY OUTCOMES

Laura Gillian Howe

00659359

A thesis submitted in fulfillment of the requirements for the degree of Doctor of Philosophy at Imperial College London, 2015

Institute of Reproductive and Developmental Biology
Department of Surgery and Cancer
Faculty of Medicine
Imperial College London
Hammersmith Hospital Campus
London
W12 0NN

i. Declaration of Originality

I confirm that all of the work included in this thesis is my own. Where data have been obtained by others, this is clearly stated in the text.



Laura Howe
September 2015

ii. Copyright Declaration

The copyright of this thesis rests with the author and is made available under a Creative Commons Attribution Non-Commercial No Derivatives licence. Researchers are free to copy, distribute or transmit the thesis on the condition that they attribute it, that they do not use it for commercial purposes and that they do not alter, transform or build upon it. For any reuse or redistribution, researchers must make clear to others the licence terms of this work.

iii. Acknowledgements

I would like to take this opportunity to extend my sincere gratitude to the people who have made this PhD possible. I would also like the reader to bear with me as I have a tendency to be effusively sentimental.

First and foremost, I would like to thank my supervisors, Prof Mark Johnson and Dr James Leiper. Mark it has been an absolute privilege to work with you. Your overflowing ideas and enthusiasm for the field have been truly inspirational. Thank you so much for your supervision and guidance throughout. I feel very lucky to have had James as my second supervisor; I am indebted for your time, input and insightful feedback as well as those off-topic discussions about politics and life and its meaning.

I am truly beholden to Dr Julia Zöllner: my work wife and my partner in crime. I have so many things to thank you for both in the context of science and friendship (far more than I could possibly discuss here). Thank you for your huge contribution to this project, from valuable discussions on the complexities of the immune system ('a modulated immunologic condition') and immeasurably appreciated comments on my chapter drafts, to sharing mouse mating duties and organising our calendars. On more than one occasion you made my 'happy Monday' in the form of biscuits and starburst and surprised me with flowers. Every time I go past the Le Creuset shop now I cannot but think of you. In this last year I feel extremely fortunate to have worked with you so closely and I hope you feel it's been an asset to you as well. I wish I could take you with me!

I would also like to say a huge thank you the rest of my IRDB family, who have had to put up with me hanging around the office since doing my masters degree and never leaving. Firstly to the MJ group and Dev, whose pastoral care has been invaluable. Thanks for doing all the ordering (even from the other side of the world on occasion), doing the chasing up every time my multiplex plate didn't arrive on time and working out the courier system to send the probes back for exchange. It has been my pleasure to sit next to Dr Kaiyu Lei for the past three years. I hope that I haven't had too much of a bad influence on your English and that my daily idioms helped. I know that I am now aware of many 'cultural differences' I did not realise existed previously. A tip for the future: in England you shouldn't tell a girl she needs more exercise (even if it is true), or try to sell her for an iPhone. I have very much enjoyed sitting behind Hector who I am sure will one day come into the office smiling. Thanks for sharing your food and moaning about life with me. Maybe we should both take a leaf out of Ana's book and try and remain more positive. Thank you Ana for being such an asset to the office – and thanks also to your grandma who unwittingly fed us all. It also goes without saying that I did not truly understand what a work ethic was until I met Angela. Credit goes to anyone who can pull off 20 gels in a day and 30 PCRs in a week.

Secondly to the PB group and to Kim, who has been there for me from the beginning. You are truly the lab pantomath, but if it all goes wrong you should call me and we'll start that coffee shop! Thanks also for introducing me to the culinary delights of Korea and sharing all the baked goods (I'm still not over how good that birthday cake was). Thanks also to Roberta, the cool one (for being the only one to ever turn up to my house parties), we'll go climbing again soon -promise! In all seriousness I would also like to thank Dr David MacIntyre for his insight into this work, constructive comments and

statistical advice (I would say this advice was average but that would be pretty mean). Also, many thanks go to Dr Yooni Lee for all of her helpful comments and advice throughout this PhD. I am also grateful to Jo for allowing me to distract her on many occasions for a quick chat; I'm sorry for further disrupting your concentration with baffling mouse talk.

I am also hugely appreciative of the work done towards this thesis by Steph. It was a pleasure to supervise you. Thank you to all the other masters students over the years and to Richard and Lindsay and all other 3rd floor IRDB-ers.

Also I would like to extend my appreciation to those members of the MJ lab who are based elsewhere either at Chelsea and Westminster Hospital or University College London. A big thank you to Dr Bronwen Herbert for originally agreeing to take me on as a fresh-faced and enthusiastic MRes student! Your expert guidance through the magical world of mice gave me the confidence and know-how to make myself a satellite set-up at Hammersmith. Many thanks also to Lydia without whom my nights collecting samples in BSU would be even more sleepless/awful. You have been a true asset to have around when I needed to moan to someone who knew. Thanks also for contributing your FACS data. Thanks also to Pei, Sophia, Nish, Raj, Natasha, Juliet and all MJ group members past and present. It has been a pleasure to work as part of such a talented and dedicated team, especially when that team went to exciting places for conferences. It took a lot of effort to convince my friends at home I was actually working (the pictures of us at Disneyworld didn't really help matters)!

I would like to also say thank you to all members of the Leiper (NOS signalling) group. Whenever I turned up in the lab/office it was generally because I wanted something, so thank you all for not running and hiding! Laura, thank you for guiding me step by step through the NO Analyser, to this day I have no idea how my VCl_3 managed to be green, navy, brown and almost every colour it shouldn't be. I could not have navigated through all that trouble-shooting without you. Sophie, I will miss our monthly gossip cocktail sessions and general chats about life. Thanks also to Matt for looking after my mice for me when I was constantly quarantined and unable to go into H2; also sorry for all the pestering when I needed another cohort! I also owe many thanks to Zhen for being extra patient whilst trying to teach me the telemetry surgery and how to use the DSI software. Thanks to Konstantinos for his charming, if not slightly sexist banter, and also to Simon, James T, Ben, Eliza and Harpreet for being so welcoming and inclusive.

Originally members of the Leiper group, now the highly talented MRC Whole Animal Physiology group, I am extremely grateful for the help of Anna and Olga. I owe special thanks to Anna for running the wire myography experiments for me. I am sorry for making you come in early so I didn't have to stay too late- whose idea was 12 hour time points?! And to Olga for helping me out with the surgery when the bookings didn't quite work out, for running the CLAMS room with an iron fist, and for stepping in and checking my mice when I couldn't be there.

Further to this, I have to express my appreciation to two people who have made my life much easier in a place that at times felt like my home-from-home. Maeve your willingness to help, patience and diligence has been invaluable; and Reece, well I just counted and over the past 2 years I have sent you 141 emails, which has got to be a bit annoying. Thank you for sending me cute YouTube clips to cheer me up and I will take my stamp-authorised 'good job *smiley face*' post-it note with me to my new desk.

I am extremely fortunate to have started out at Imperial as part of a close-knit group of masters students. Els, Adam, Katie, Kat, Erica, and Claire (honorary CIMPP) thank you for organising my social life for at least the first year I was in London. We started this endeavour together and I wish you all every success in the future.

I would also like to thank all of my friends outside of the academic bubble; for the seemingly never-ending moaning, for not attending social events because there was a mouse in labour, and for your ear at the end of the phone. In particular I would like to say a huge thank you to Vickie and Mizz for their continuous faith in me. Vickie has, in fact, been telling everyone I am a doctor for years, so it's nice to finally be almost there! An even bigger thank you goes out to those people who had to live with me over the course of this PhD: Kate, Becky and Lauz. Thank you for providing tea, biscuits, the odd meal and light relief in the form of Sunday excursions and snuggling up under copious blankets watching the adonis that is Jessie on our living room sofa/bed.

Huge thanks go out to my extremely supportive family, without whom this PhD would never have begun. To my brother Jake I would like to thank for his occasional statistical advice, general cynical remarks and overall sibling love. Thank you to my Mum, who I can always rely on for a chat - whether that's for advice, to complain, or for just a good gossip. Without your eternal support and generosity there is not a chance I would be where I am today. To my Dad, my WordFeud nemesis, your enthusiasm for understanding what I spend my days doing has been ridiculously appreciated. A special thank you for using your ethics committee experience to proof read parts of this thesis; hopefully it wasn't too painful. I hope I have, and continue to make you all proud.

Lastly, I would like to thank my wonderful fiancé Ian. You knew best what to say/do when things got particularly challenging to keep me on track and motivated; be it those expert words of encouragement, an expertly cooked dinner (I will take the blame for all the puddings), or endless cups of tea. I guess this stemmed from the experience of having been there and done that, but I am profoundly appreciative of that understanding and insider knowledge. You have guided me through several crises of confidence (read: tears and tantrums) and I am in no doubt that without your unending support and patience this thesis would not have been completed. You have been and continue to be a genuine inspiration. And also, a treat.

iv. Table of Contents

I. DECLARATION OF ORIGINALITY **2**
II. COPYRIGHT DECLARATION **2**
III. ACKNOWLEDGEMENTS **3**
IV. TABLE OF CONTENTS **6**
V. LIST OF FIGURES **10**
VI. LIST OF TABLES **14**
VII. ABBREVIATIONS **15**
VIII. PUBLICATIONS AND PRESENTATIONS **18**
IX. ABSTRACT **19**

CHAPTER 1: GENERAL INTRODUCTION **20**

1.1 PHYSIOLOGICAL ADAPTATIONS IN HEALTHY PREGNANCY **21**
1.1.1 CARDIOVASCULAR ADAPTATIONS IN PREGNANCY 21
1.1.2 HORMONAL ADAPTATIONS IN PREGNANCY 23
1.1.3 HORMONAL REGULATION OF CARDIOVASCULAR ADAPTATION IN PREGNANCY 24
1.1.4 IMMUNOLOGICAL ADAPTATIONS IN PREGNANCY 26
1.1.4.1. Innate Immune System Adaptations 29
1.1.4.2 Adaptive Immune System Adaptations 30
1.1.4.3 Adaptations in Cytokine Production 31
1.1.5 THE ROLE OF THE NITRIC OXIDE SIGNALLING PATHWAY IN PREGNANCY 33
1.1.5.1 The DDAH/ADMA/NO Pathway 33
1.1.5.2 DDAH Isoforms 34
1.1.5.3 Role of Nitric Oxide in Pregnancy 34
1.2 MATERNAL INFECTION AND INFLAMMATION **36**
1.2.1 MATERNAL SUSCEPTIBILITY TO INFECTION 36
1.2.1.1 Influenza 36
1.2.1.2. Malaria 38
1.2.1.3 Acute Pyelonephritis 39
1.2.2. THE EFFECTS OF MATERNAL INFECTION AND INFLAMMATION 40
1.2.2.1 Maternal Sepsis 40
1.2.2.2 Role of Chemokines in Sepsis 43
1.2.2.2a CCL2 44
1.2.2.3 Role of Nitric Oxide in Sepsis 45
1.2.2.4 Preterm Labour 46
1.2.2.5 Neonatal Sepsis 47
1.3 ANIMAL MODELS **48**
1.3.1 THE ENDOTOXAEMIC MODEL 48
1.3.2 BACTERIAL INOCULATION MODELS 50
1.3.3 MODELS OF POLYMICROBIAL SEPSIS 51
1.4 CLINICAL RELEVANCE AND JUSTIFICATION OF STUDY **53**
1.4.1 SEPSIS IN PREGNANCY 53
1.4.2 MATERNAL INFECTION AND PRETERM LABOUR 54
1.5 NOVEL HYPOTHESES **55**
1.5.1 AIMS AND OBJECTIVES 55

2. MATERIALS AND METHODS **56**

2.1 MATERIALS **57**
2.1.1 REAGENTS AND BUFFERS 57
2.1.1.1 Chemicals and Solvents 57
2.1.1.2 Buffers 57

2.1.1.3 PCR Reagents and Buffers 58
2.1.1.4 Protein Extraction and Western Blotting Reagents 59
2.1.1.5 FACS Equipment and Reagents 59
2.1.1.6 Kits 60
2.1.2 MICE, SURGICAL CONSUMABLES AND DRUGS 60
2.1.3 EQUIPMENT 61
2.1.4 PRIMER SEQUENCES 62
2.1.5 ANTIBODIES 63
2.2 *IN VIVO* METHODS 64
2.2.1 ANIMALS 64
2.2.2 GENOTYPING 65
2.2.2.1 $CCR2^{-/-}$ Colony 65
2.2.2.2 $DDAH1^{-/-}$ Colony 66
2.2.3 TELEMETRY 67
2.2.3.1 Telemetry Device Implantation 67
2.2.3.2 Telemetry Recording, Acquisition and Analysis 69
2.2.4 PTL MODEL (SYSTEMIC ENDOTOXAEMIA) AND PHARMACOLOGICAL INTERVENTION 70
2.2.4.1 PTL Model (Systemic Endotoxaemia) 70
2.2.4.2 Progesterone Treatment 71
2.2.4.3 CCR2 Antagonism 71
2.2.5 TISSUE COLLECTION 71
2.2.6 WIRE MYOGRAPHY 72
2.2.6.1 Preparation of Vessels 72
2.2.6.2 Normalisation and Viability of Tissues 73
2.2.6.3 Concentration Response Curves 73
2.2.7 PLASMA VOLUME DETERMINATION 74
2.2.8 FLOW CYTOMETRY 75
2.3 *IN VITRO* METHODS 77
2.3.1 REVERSE TRANSCRIPTASE POLYMERASE CHAIN REACTION (RT-PCR) 77
2.3.1.1 mRNA Extraction 77
2.3.1.2 cDNA Synthesis 77
2.3.1.3 Primer design and Production of Standards 77
2.3.1.4 RT-PCR 78
2.3.2 PROTEIN EXPRESSION ANALYSIS 79
2.3.2.1 Protein extraction 79
2.3.2.2 Protein Assay 79
2.3.2.3 SDS-PAGE and Western Blot 80
2.3.2.4 Multiplex Assay 80
2.3.2.5 Placental Growth Factor (PLGF2) Enzyme-linked Immunosorbent Assay (ELISA) 81
2.3.2.6 Cyclic Guanosine Monophosphate (cGMP) ELISA 81
2.3.2.7 Soluble Fms-like Tyrosine Kinase-1 (sFlt-1) ELISA 82
2.3.3 NITRIC OXIDE ANALYSIS 82
2.3.4 METHYLARGININE MEASUREMENT 83
2.3.5 DATA HANDLING AND STATISTICAL ANALYSIS 84

CHAPTER 3: LONGITUDINAL TELEMETRIC RECORDING OF HAEMODYNAMIC PARAMETERS AND ACTIVITY IN MURINE PREGNANCY 86

3.1 INTRODUCTION 87
3.1.1 AIMS AND OBJECTIVES 88
3.2 RESULTS 89
3.2.1 THE HAEMODYNAMIC PROFILE OF PREGNANCY IN CD1 MICE 89
3.2.2 ACTIVITY DURING PREGNANCY IN CD1 MICE 94
3.3. SUMMARY AND DISCUSSION 98

CHAPTER 4: THE RESPONSE TO LIPOPOLYSACCHARIDE-INDUCED INFLAMMATION IN NON-PREGNANT AND PREGNANT MICE 101

4.1 INTRODUCTION 102
4.1.1 AIMS AND OBJECTIVES 103
4.2 RESULTS 104
4.2.1 MATERNAL SYSTEMIC LPS ADMINISTRATION 104
4.2.2 THE HAEMODYNAMIC RESPONSE TO LPS-INDUCED INFLAMMATION IN NON-PREGNANT AND PREGNANT MICE 106
4.2.2.1 The Effect of LPS-induced Inflammation on Labour Time and Pup Survival 106
4.2.2.2 The Effect of LPS-induced Inflammation on Maternal Haemodynamics 107
4.2.2.3 The Effect of LPS-induced Inflammation on Maternal Activity 111
4.2.3 LPS-INDUCED CYTOKINE AND CHEMOKINE PRODUCTION IN NON-PREGNANT AND PREGNANT MICE 114
4.2.4 CIRCULATING AND CARDIAC EXPRESSION OF VASOACTIVE FACTORS IN RESPONSE TO LPS IN NON-PREGNANT AND PREGNANT MICE 118
4.2.5 LPS-INDUCED CHANGES IN VASCULAR FUNCTION IN NON-PREGNANT AND PREGNANT MICE 126
4.2.5.1 Aorta 126
4.2.5.1 Uterine Artery 129
4.2.6 EXPRESSION OF MARKERS OF INFLAMMATION, CARDIAC DYSFUNCTION AND APOPTOSIS IN NON-PREGNANT AND PREGNANT MICE 131
4.2.7 LPS-INDUCED MONOCYTE AND NEUTROPHIL INFILTRATION IN NON-PREGNANT AND PREGNANT MICE 140
4.3. SUMMARY AND DISCUSSION 142

CHAPTER 5: THE EFFECT OF PROGESTERONE SUPPLEMENTATION ON MATERNAL HAEMODYNAMICS 149

5.1 INTRODUCTION 150
5.1.1 AIMS AND OBJECTIVES 151
5.2 RESULTS 152
5.2.1 THE EFFECT OF PROGESTERONE SUPPLEMENTATION ON LABOUR TIME AND PUP SURVIVAL .. 152
5.2.2 THE HAEMODYNAMIC RESPONSE TO LPS-INDUCED INFLAMMATION IN MOUSE PREGNANCIES SUPPLEMENTED WITH PROGESTERONE 154
5.2.3 THE EFFECT OF PROGESTERONE SUPPLEMENTATION ON LPS-INDUCED CYTOKINE, CHEMOKINE, NITRIC OXIDE AND ASYMMETRIC DIMETHYLARGININE PRODUCTION IN PREGNANT MICE 160
5.2.4 THE EFFECT OF PROGESTERONE SUPPLEMENTATION ON THE PRODUCTION OF INFLAMMATORY MARKERS, MARKERS OF CARDIAC DYSFUNCTION AND APOPTOTIC MARKERS IN LEFT VENTRICULAR TISSUE 164
5.3 SUMMARY AND DISCUSSION 167

CHAPTER 6: THE EFFECT OF C-C CHEMOKINE RECEPTOR TYPE 2 DEFICIENCY ON LPS-INDUCED HYPOTENSION IN PREGNANCY 171

6.1 INTRODUCTION 172
6.1.1 AIMS AND OBJECTIVES 174
6.2 RESULTS 175
6.2.2 THE HAEMODYNAMIC PROFILE OF NON-PREGNANT CCR2 KNOCKOUT MICE 175
6.2.2 LATENCY TO LABOUR AND PUP SURVIVAL OUTCOMES AFTER LPS ADMINISTRATION IN CCR2 KNOCKOUT MICE 175
6.2.3 THE HAEMODYNAMIC RESPONSE TO LPS-INDUCED INFLAMMATION IN PREGNANT CCR2 KNOCKOUT MICE 178

6.2.4 The LPS-induced Inflammatory Response in Pregnant CCR2 Knockout Mice 184
6.2.5 Circulating Expression of Vasoactive Factors in Response to LPS in Pregnant CCR2 Knockout Mice 189
6.2.7 The Haemodynamic Response to LPS-induced Inflammation after Pharmacological CCR2 Inhibition in Pregnant Mice 192
6.3 Summary and Discussion 199

CHAPTER 7: THE EFFECT OF DIMETHYLARGININE DIMETHYLAMINOHYDROLASE-1 DEFICIENCY IN PREGNANCY 203

7.1 Introduction 204
7.1.1 Aims and Objectives 206
7.2 Results 207
7.2.1 The Haemodynamic Profile of Non-Pregnant DDAH1 Knockout Mice 207
7.2.2 The Haemodynamic Profile of Pregnancy in DDAH1 Knockout Mice 207
7.2.3 Activity during Pregnancy in CD1 Mice 214
7.2.5 Circulating Expression of Vasoactive Factors in Response to LPS in Pregnant DDAH1 Knockout Mice 221
7.2.6 The Production of Inflammatory Markers, Markers of Cardiac Dysfunction and Apoptotic Markers in Left Ventricular Tissue in Response to LPS in Pregnant DDAH1 Knockout Mice 224
7.2.7 The Production of Vasoactive Factors in DDAH1 Knockout Mouse Placenta 229
7.3 Summary and Discussion 233

CHAPTER 8: GENERAL DISCUSSION 239

8.1 Summary of Main Findings 240
8.2 Limitations of Study 245
8.2.1 Experimental Limitations 245
8.2.2 Technical Limitations 246
8.3 Further Research 251
8.3.1 Future Directions 253
8.4 Conclusions 255

9. REFERENCES 256

10. APPENDIX 1: SUPPLEMENTARY DATA 279

v. List of Figures

Chapter 1

Figure 1.1: Changes in the principal hormone levels and corresponding immune system characteristics during pregnancy
Figure 1.2: 'Signal 1' and 'signal 2' in an immune response to infection and how this is altered in pregnancy
Figure 1.3: Cytokine alterations during pregnancy
Figure 1.4: An overview of the LPS signalling pathway

Chapter 2

Figure 2.1: Genotyping gels of CCR2 expression
Figure 2.2: Genotyping gels of DDAH1 floxed alleles and cre expression
Figure 2.3: Telemetry transmitter placement
Figure 2.4: Calculation of plasma volume using Evan's Blue dilution method

Chapter 3

Figure 3.1: Continuous measurement of mean arterial pressure (MAP) throughout pregnancy
Figure 3.2: Continuous measurement of systolic arterial pressure (SAP) throughout pregnancy
Figure 3.3: Continuous measurement of diastolic arterial pressure (DAP) throughout pregnancy
Figure 3.4: Continuous measurement of heart rate (HR) throughout pregnancy
Figure 3.5: Continuous measurement of the percentage of time spent inactive (%TSI) throughout pregnancy
Figure 3.6: Continuous measurement of activity throughout pregnancy
Figure 3.7: Continuous measurement of activity >0 throughout pregnancy

Chapter 4

Figure 4.1: Dose response to intraperitoneal administration of LPS in CD1 mice
Figure 4.2: Latency to labour and pup survival in CD1 mice administered 10μg LPS or vehicle
Figure 4.3: The haemodynamic response to LPS-induced inflammation in pregnant CD1 mice
Figure 4.4: The haemodynamic response to LPS-induced inflammation in pregnant CD1 mice as assessed by maximum decrease and maximum increase
Figure 4.5: Activity in pregnant and non-pregnant CD1 mice after LPS administration
Figure 4.6: Circulating concentrations of pro-inflammatory cytokines in serum of non-pregnant and pregnant mice treated with LPS or vehicle
Figure 4.7: Circulating concentrations of anti-inflammatory cytokines in serum of non-pregnant and pregnant mice treated with LPS or vehicle
Figure 4.8: Circulating concentrations of chemokines in serum of non-pregnant and pregnant mice treated with LPS or vehicle
Figure 4.9: Nitric oxide, cGMP and ADMA measurements in serum of non-pregnant and pregnant mice treated with LPS or vehicle
Figure 4.10: Circulating concentrations of vasoactive factors in serum of non-pregnant and pregnant mice treated with LPS or vehicle
Figure 4.11: Concentrations of circulating PLGF2 measured at gestational time points in CD1 mice

Figure 4.12: Local concentrations of vasoactive factors in hearts taken from non-pregnant and pregnant mice treated with LPS or vehicle
Figure 4.13: Circulating and localised concentrations of VEGF isoforms in serum and hearts taken from non-pregnant and pregnant mice treated with LPS or vehicle
Figure 4.14: Ex –vivo measurement of aortic endothelial responses in non-pregnant and pregnant mice treated with LPS or vehicle
Figure 4.15: Ex –vivo measurement of uterine artery endothelial responses in non-pregnant and pregnant mice treated with LPS or vehicle
Figure 4.16: mRNA expression of pro- and anti-inflammatory cytokines and inflammatory regulators in heart tissue taken from non-pregnant or pregnant mice treated with LPS or vehicle
Figure 4.17: mRNA expression of markers of cardiac dysfunction in heart tissue taken from non-pregnant or pregnant mice treated with LPS or vehicle
Figure 4.18: mRNA expression of pro- and anti-apoptotic markers in heart tissue taken from non-pregnant or pregnant mice treated with LPS or vehicle
Figure 4.19: Expression of caspase-3 in heart tissue taken from non-pregnant or pregnant mice treated with LPS or vehicle
Figure 4.20: mRNA expression of pro- and anti-inflammatory cytokines and inflammatory regulators in the left ventricle of non-pregnant or pregnant mice treated with LPS or vehicle
Figure 4.21: mRNA expression of markers of cardiac dysfunction in the left ventricle of non-pregnant or pregnant mice treated with LPS or vehicle
Figure 4.22: mRNA expression of pro- and anti-apoptotic markers in the left ventricle of non-pregnant or pregnant mice treated with LPS or vehicle
Figure 4.23: Changes in infiltrating leukocytes in response to LPS in non-pregnant and pregnant mice

Chapter 5

Figure 5.1: Dose response to subcutaneous supplementation of progesterone in LPS-treated pregnant CD1 mice
Figure 5.2: The haemodynamic response to LPS-induced inflammation after progesterone supplementation
Figure 5.3: The heart rate response to LPS-induced inflammation after progesterone supplementation
Figure 5.4: The haemodynamic response to LPS-induced inflammation after progesterone supplementation as assessed by AUC, maximum decrease and maximum increase
Figure 5.5: Activity in pregnant CD1 mice treated with LPS after supplementation with progesterone or vehicle
Figure 5.6: Circulating concentrations of pro- and anti-inflammatory cytokines in the serum of pregnant mice treated with LPS after supplementation with progesterone or vehicle
Figure 5.7: Circulating concentrations of chemokines in the serum of pregnant mice treated with LPS after supplementation with progesterone or vehicle
Figure 5.8: Circulating concentrations of nitric oxide and asymmetric dimethylarginine in the serum of pregnant mice treated with LPS after supplementation with progesterone or vehicle
Figure 5.9: mRNA expression of pro- and anti-inflammatory cytokines and inflammatory regulators in left ventricular tissue taken from pregnant mice treated with LPS after supplementation with progesterone or vehicle
Figure 5.10: mRNA expression of markers of cardiac dysfunction in left ventricular tissue taken from pregnant mice treated with LPS after supplementation with progesterone or vehicle

Figure 5.11: mRNA expression of markers of apoptosis in left ventricular tissue taken from pregnant mice treated with LPS after supplementation with progesterone or vehicle

Chapter 6

Figure 6.1: Latency to labour and pup survival outcomes after LPS administration in CCR2 knockout mice
Figure 6.2: The haemodynamic and activity profile of non-pregnant CCR2$^{-/-}$ mice
Figure 6.3: The haemodynamic response to LPS-induced inflammation in CCR2$^{-/-}$ mice
Figure 6.4: The heart rate response to LPS-induced inflammation in CCR2$^{-/-}$ mice
Figure 6.5: The haemodynamic response to LPS-induced inflammation in CCR2$^{-/-}$ mice compared to CD1s as assessed by AUC, maximum decrease and maximum increase
Figure 6.6: Activity in pregnant CCR2$^{-/-}$ and CD1 mice after LPS administration
Figure 6.7: Circulating concentrations of pro- and anti-inflammatory cytokines in the serum of pregnant CD1 and CCR2$^{-/-}$ mice treated with LPS or vehicle
Figure 6.8: Circulating concentrations of chemokines in the serum of pregnant CD1 and CCR2$^{-/-}$ mice treated with LPS or vehicle
Figure 6.9: mRNA expression of pro-inflammatory cytokines in left ventricular tissue taken from pregnant CCR2$^{-/-}$ and CD1 mice treated with LPS or vehicle
Figure 6.10: Circulating concentrations of nitric oxide and asymmetric dimethylarginine in the serum of pregnant CD1 and CCR2$^{-/-}$ mice treated with LPS or vehicle
Figure 6.11: Circulating concentrations of vasoactive factors in serum of pregnant CD1 and CCR2$^{-/-}$ mice treated with LPS or vehicle
Figure 6.12: The haemodynamic response to LPS-induced inflammation in mice pre-treated with CCR2 inhibitor
Figure 6.13: The heart rate response to LPS-induced inflammation in mice pre-treated with CCR2 inhibitor
Figure 6.14: The haemodynamic response to LPS-induced inflammation in in mice pre-treated with CCR2 inhibitor or vehicle control as assessed by AUC, maximum decrease and maximum increase
Figure 6.15: Activity in pregnant mice pre-treated with CCR2 inhibitor after LPS administration

Chapter 7

Figure 7.1: The haemodynamic and activity profile of non-pregnant female DDAH1 WT and DDAH1$^{-/-}$ mice
Figure 7.2: Continuous measurement of mean arterial pressure (MAP) throughout pregnancy in DDAH1 WT and DDAH1$^{-/-}$ mice
Figure 7.3: Continuous measurement of systolic arterial pressure (SAP) throughout pregnancy in DDAH1 WT and DDAH1$^{-/-}$ mice
Figure 7.4: Continuous measurement of diastolic arterial pressure (DAP) throughout pregnancy in DDAH1 WT and DDAH$^{-/-}$ mice
Figure 7.5: Continuous measurement of heart rate (HR) throughout pregnancy in DDAH1 WT and DDAH1$^{-/-}$ mice
Figure 7.6: Continuous measurement of the percentage of time spent inactive (%TSI) throughout pregnancy in DDAH1 WT and DDAH1$^{-/-}$ mice
Figure 7.7: Continuous measurement of activity throughout pregnancy in DDAH1 WT and DDAH1$^{-/-}$ mice

Figure 7.8: Continuous measurement of activity >0 throughout pregnancy in DDAH1 WT and DDAH1$^{-/-}$ mice
Figure 7.9: Latency to labour and pup survival outcomes after LPS administration in DDAH1 WT and DDAH1$^{-/-}$ mice
Figure 7.10: The extent of failed pregnancies and average litter sizes in DDAH1 WT and DDAH1$^{-/-}$ mice
Figure 7.11: Circulating concentrations of nitric oxide and asymmetric dimethylarginine in the serum of pregnant DDAH1 WT and DDAH1$^{-/-}$ mice treated with LPS or vehicle
Figure 7.12: Circulating concentrations of vasoactive factors in serum of pregnant DDAH1 WT and DDAH1$^{-/-}$ mice treated with LPS or vehicle
Figure 7.13: mRNA expression of pro- and anti-inflammatory cytokines, inflammatory regulators and chemokines in left ventricular tissue taken from DDAH1 WT and DDAH1$^{-/-}$ mice treated with LPS or vehicle
Figure 7.14: mRNA expression of markers of cardiac dysfunction in left ventricular tissue taken from DDAH1 WT or DDAH1$^{-/-}$ mice treated with LPS or vehicle
Figure 7.15: mRNA expression of markers of apoptosis in left ventricular tissue taken from DDAH1 WT or DDAH1$^{-/-}$ mice treated with LPS or vehicle
Figure 7.16: Placental concentrations of vasoactive factors in DDAH1 WT and DDAH1$^{-/-}$ mice
Figure 7.17: Expression of DDAH1 and DDAH2 in placental tissue taken from DDAH1 WT and DDAH1$^{-/-}$ mice

vi. List of Tables

Chapter 1

Table 1.1: Organisms associated with maternal sepsis

Chapter 2

Table 2.1: Mouse primer sequences for use in PCR/ RT-PCR
Table 2.2: Antibodies used for FACS
Table 2.3: Antibodies for use in Western Blotting

Chapter 4

Table 4.1: Summary of LPS dose response outcomes
Table 4.2: Treatment group comparisons between pregnant and non-pregnant haemodynamic responses to LPS
Table 4.3: Treatment group comparisons between pregnant and non-pregnant activity in response to LPS
Table 4.4: Summary of changes in vascular function and sensitivity to vasoactive substances

vii. Abbreviations

α-MHC	Alpha Myosin Heavy Chain
a.u.	Arbitrary Units
AAMs	Alternatively Activated Macrophages
ACh	Acetylcholine
ADMA	Asymmetric Dimethylarginine
AF	Amniotic Fluid
ALI	Acute Lung Injury
ANOVA	Analysis of Variance
ANP	Atrial Natriuretic Peptide
AP	Acute Pyelonephritis
APC	Antigen Presenting Cell
ARDS	Acute Respiratory Distress Syndrome
AUC	Area Under the Curve
AWERB	Animal Welfare and Ethical Review Board
β-MHC	Beta Myosin Heavy Chain
Bad	Bcl-2 Associated Death Promoter
BAL	Bronchoalveolar Lavage
Bax	Bcl-2 Associated X Protein
Bcl-2	B-cell Lymphoma-2
BNF	Brain Natriuretic Factor
BNP	Brain Natriuretic Peptide
BSA	Bovine Serum Albumin
BSCI	Broad Spectrum Chemokine Inhibitor
CAMs	Classically Activated Macrophages
CASP	Colon Ascendens Stent Peritonitis
cAMP	Cyclic Adenosine Monophosphate
cGMP	Cyclic Guanosine Monophosphate
CLAMS	Comprehensive Laboratory Animal Monitoring System
CLP	Caecal Ligation and Puncture
COX	Cyclooxygenase
CRH	Corticotrophin Releasing Hormone
CRISPLD2	Cysteine-rich Secretory Protein Containing LCCL Domain 2
DAP	Diastolic Arterial Pressure
DDAH	Dimethylarginine Dimethylamino Hydrolase
DMSO	Dimethyl Sulfoxide
DNA	Deoxyribonucleic Acid
DPP	Days Postpartum
DSI	Data Science International
E2	Oestradiol
E16	Embryonic Day 16
ELISA	Enzyme-linked Immunosorbent Assay
eNOS	Endothelial Nitric Oxide Synthase
ERα	Oestrogen Receptor-alpha
ERK	Extracellular Signal-related Kinase
ET-1	Endothelin-1
EtBr	Ethidium Bromide
FACS	Fluorescence-activated Cell Sorting
FasL	Fas Ligand
FGR	Fetal Growth Restriction
FIRS	Fetal Inflammatory Response Syndrome

FWB	FACS Wash Buffer
G-CSF	Granulocyte Colony Stimulating Factor
GAPDH	Glyceraldehyde 3-Phosphate Dehydrogenase
GC	Guanylate Cyclase
GLUT1	Glucose Transporter 1
hCG	Human Chorionic Gonadotropin
HIV	Human Immunodeficiency Virus
HPLC	High Pressure Liquid Chromatography
HR	Heart Rate
Hsp70	Heat Shock Protein 70
HUVECs	Human Umbilical Cord Endothelial Cells
i.p.	Intraperitoneal
i.v.	Intravenous
ICU	Intensive Care Unit
IFN-γ	Interferon-gamma
IIV	Inactivated Influenza Vaccine
IL	Interleukin
iNOS	Inducible Nitric Oxide Synthase
IRAK	IL-1 Receptor-associated Kinase
ITU	Intensive Treatment Unit
JNK	c-Jun N-terminal Kinase
KO	Knockout
KPSS	High Potassium Physiological Salt Solution
LC-MS/MS	Liquid Chromatography-Mass Spectrometry
L-NAME	L-NG-nitroarginine Methyl Ester
L-NMMA	N-monomethyl-L-arginine
LBP	Lipopolysaccharide Binding Protein
LPS	Lipopolysaccharide
LV	Left Ventricle
MAP	Mean Arterial Pressure
MC	Monocytes
MCP	Monocyte Chemoattractant Protein
MHC	Major Histocompatibility Complex
mPR	Membrane Progesterone Receptor
MRM	Multiple Reactions Monitoring
mRNA	Messenger RNA
NA	Noradrenaline
NF-κB	Nuclear Factor kappa B
NK	Natural Killer
NKA	Sodium Potassium ATPase
nNOS	Neuronal Nitric Oxide Synthase
NO	Nitric Oxide
NOS	Nitric Oxide Synthase
NOx	Nitrates and Nitrites
NP	Non-pregnant
nPR	Nuclear Progesterone Receptor
P4	Progesterone
PAMP	Pathogen-associated Molecular Pattern
PBMC	Peripheral Blood Mononuclear Cells
PBS	Phosphate Buffered Saline
PCR	Polymerase Chain Reaction
PE	Phenylephrine
PG	Prostaglandin

PGC1-α	Peroxisome Proliferator-activated Receptor-gamma Coactivator-1-alpha
PKG	Protein Kinase G
PLGF	Placental Growth Factor
PLN	Phospholamban
PMN	Polymorphonuclear Cells (or Neutrophils)
PPAR-γ	Peroxisome Proliferator-activated Receptor-gamma
PPL	Procedure Project Licence
PR	Progesterone Receptor
PRMT	Protein-arginine Methyl Transferase
PSS	Physiological Salt Solution
PTL	Preterm Labour
PWB	Permeablizing Wash Buffer
PXR	Pregnane X Receptor
RA	Rheumatoid Arthritis
RIPA	Radioimmunoprecipitation Assay
RNA	Ribonucleic Acid
RP	Ribosomal Protein
RT-PCR	Reverse Transcriptase PCR
SAMM	Serious Acute Maternal Morbidity
SAP	Systolic Arterial Pressure
SCID	Severe Combined Immunodeficiency
SEM	Standard Error of Mean
SERCA	Sarco/Endoplasmic Reticulum Ca^{2+}-ATPase
SIRS	Systemic Inflammatory Response Syndrome
SNP	Sodium Nitroprusside
TBE	Tris-EDTA Buffer
TBS	Tris-Buffered Saline with Tween-20
Tc	Cytotoxic T Cell
Th	Helper T Cell
TipDCs	TNF-α/iNOS Producing Dendritic Cell
TIR	Toll IL-1 Receptor Homology Domain
TIRAP	TIR Domain-containing Adapter Protein
TLR	Toll-like Receptor
TNF-α	Tumour Necrosis Factor-alpha
TRAIL	Tumour Necrosis Factor-related Apoptosis-inducing Ligand
Tregs	Regulatory T Cells
TSI	Time Spent Inactive
UTI	Urinary Tract Infection
UV	Ultraviolet
VEGF	Vascular Endothelial Growth Factor
WHO	World Health Organisation
WT	Wildtype

viii. Publications and Presentations

Publications

Howe, L., Zöllner, J., Leiper, J., and Johnson, M.R., (2015), Inflammation Causes Marked Hypotension in Pregnancy, (In Preparation)

Oral Presentations

Protection from Endotoxin-induced Hypotension in Pregnancy: Attenuation by CCR2 Deficiency or Pharmacological Inhibition
Howe, L., Zöllner, J., Leiper, J., Johnson, M.R.,
Society for Gynaecologic Investigation 62nd Annual Scientific Meeting; San Francisco, USA, March 2015

Elucidation of the Role of DDAH/ADMA/NO Axis in Pregnancy-related Haemodynamic Dysfunction
Howe, L., Zöllner, J., Boruc, O., Wang, Z., Johnson, M.R., Leiper L.,
7th International Symposium on Asymmetric Dimethylarginine; St. Petersburg, Russia, June 2014

Poster Presentations

Elucidation of the Role of the DDAH/ADMA/NO Axis in Pregnancy-related Haemodynamic Adaptation
Howe, L., Zöllner, J., Leiper, J., Johnson, M.R.,
Society for Gynaecologic Investigation 62nd Annual Scientific Meeting; San Francisco, USA, March 2015

Elucidation of the Role of Oestrogen on Cardiovascular Function in a Model of Endotoxaemia
Zöllner, J., **Howe, L.,** Leiper, J., Johnson, M.R.,
Society for Gynaecologic Investigation 62nd Annual Scientific Meeting; San Francisco, USA, March 2015

Caecal Ligation and Puncture in Pregnancy
Zöllner, J., **Howe, L.,** Leiper, J., Johnson, M.R.,
Society for Gynaecologic Investigation 62nd Annual Scientific Meeting; San Francisco, USA, March 2015

Modulation of Haemodynamic Adaptations in Pregnancy by Progesterone and Nitric Oxide
Howe, L., Wang, Z., Edey, L.F., Leiper, J., Johnson, M.R.,
Society for Gynaecologic Investigation 61st Annual Scientific Meeting; Florence, Italy, March 2014

Haemodynamic Profiling Throughout Pregnancy in Normal and Lipopolysaccharide-treated Mice
Howe, L., Wang, Z., Edey, L.F., Leiper, J., Johnson, M.R.,
Society for Gynaecologic Investigation 60th Annual Scientific Meeting; Orlando, USA, March 2013

ix. Abstract

Sepsis is the leading cause of direct maternal mortality in the UK, but also a leading concern worldwide. In the USA, severe maternal sepsis rates and the risk of sepsis-related death have doubled in the last decade. There appears to be an increased susceptibility to, and severity of, infections during pregnancy. However, the mechanisms behind the increased morbidity and mortality are not fully understood. Pregnancy is associated with acute physiological changes in most organ systems, in particular the cardiovascular and immune systems. In this thesis the haemodynamic response to infection and inflammation was investigated. It was hypothesised that there is an altered haemodynamic response to infection mediated by inflammatory pathways, and by targeting signalling pathways within the immune and cardiovascular systems maternal outcomes could be improved. In order to achieve to this, a murine model of endotoxaemia during pregnancy was employed to study the effects of inflammation on maternal haemodynamics, utilising a telemetric technique to monitor physiologic changes. Firstly, this model was used to demonstrate that inflammation in pregnancy can lead to marked hypotension and haemodynamic dysfunction that does not occur in non-pregnant controls. Supplementation with additional progesterone, a key hormone of pregnancy, did not exacerbate this hypotensive effect. Manipulation of the chemokine receptor CCR2 was able to reverse inflammation-induced hypotension in pregnancy, both by genetic knockout and pharmacological inhibition. Manipulation via genetic knockout of DDAH1, a component of the nitric oxide signalling pathway, whilst conferring an initial hypertension did not significantly impact the gestational haemodynamic profile. The marked fall in blood pressure in response to endotoxin may help to explain the greater susceptibility of pregnant women to sepsis. Maternal outcomes may be improved by modulating the immune response.

Chapter 1: General Introduction

1.1 Physiological Adaptations in Healthy Pregnancy

1.1.1 Cardiovascular Adaptations in Pregnancy

The physiological adaptations that occur within the maternal cardiovascular system have been studied since the late 19th century, where although investigators agreed that cardiac output was increased during human pregnancy, the onset, extent and the mechanisms behind this have been the subject of dispute [1]. The discrepancy in results was likely due to the lack of repeatability and accuracy of the methods of measuring haemodynamic parameters, alongside wide individual variation. Thus, since the availability of non-invasive techniques such as echocardiography in the 1960s and 1970s, understanding within the field has greatly improved. It is now commonly accepted that cardiac output is increased by approximately five weeks of gestation after the last menstrual period and this continues to increase until approximately 24 weeks, where it remains at 45% above the baseline level [1]. Both stroke volume and heart rate are thought to contribute to this rise; however the increase in heart rate begins before stroke volume increases.

These changes are also accompanied by physiological cardiac hypertrophy which resolves following pregnancy. In non-pregnant women, these changes would lead to hypertension, yet in pregnancy mean arterial pressure (MAP) usually declines. Systemic vasodilation and transient insensitivity to vasoactive substances are suggested gestational hypotensive mechanisms [2].

It is the general consensus that the first process to occur is a significant drop in vascular resistance, where by eight weeks gestation, peripheral resistance is already 30% lower than pre-conception values. This reduction is paralleled in a fall in systemic blood pressure which reaches a nadir at the mid-gestational point, not to increase again until after 32 weeks [3, 4]. The mechanisms behind these changes are still not fully understood. Likely, these haemodynamic alterations are underpinned by hormonal changes, suggesting a role for the actions of progesterone, oestrogen, prostaglandins, prolactin and relaxin, or the interplay between them, in haemodynamic control [5, 6].

In human pregnancy, a decrease in MAP of 5-15 mmHg during the first and second trimesters is considered to be normal due to decreased vascular resistance and vasodilation, secondary to the effects of progesterone on smooth muscle. This decrease in MAP is thought to reflect changes in diastolic, rather than systolic arterial pressure [7].

Further, these changes in cardiac output, blood pressure and the reduction in vascular tone result in a relative drop in renal perfusion pressure. This in turn stimulates the production of renin, which via the formation of angiotensinogen and angiotensin I, leads to an increase in circulating angiotensin II. During pregnancy, the pressor responsiveness to angiotensin II is reduced, however its effects on the kidney (and also to some extent the liver) lead to a 3-4 fold increase in the adrenal steroid aldosterone [8-10]. The result is a significant increase in blood volume from as early as 6 weeks gestation, where both sodium and water retention leads to the characteristic hyponatraemic hypervolemia of pregnancy [11]. The pivotal role of the renin-angiotensin-aldosterone system in the maintenance of blood pressure and salt/water retention is also aided by increased renal sympathetic nerve activity at this time [12]. Typically, blood volume increases by approximately 45% during pregnancy (higher in multifetal gestations) and at term is estimated to be 100mL/kg [13, 14]. Amongst other reasons, it has been postulated that one possibility for this large increase in blood volume is that it may be an adaptive mechanism to prepare the mother for inevitable blood loss during labour [14].

Integral to these changes, many structural and functional changes occur within the uteroplacental vasculature, including structural reorganisation of the uterine and spiral arteries, to accommodate the increased circulatory requirements of the growing fetus [15]. This is principally achieved by a profound increase in uteroplacental blood flow (approximately 10-fold by term) which constitutes up to 25% of cardiac output [16, 17] and a decrease in uterine vascular resistance. In fact, the uteroplacental circulation is a low resistance circulation and contributes approximately 20% of the total reduction of systemic vascular resistance in the second trimester [18]. Increased blood flow is accommodated by the enormous modifications that take place in the spiral arteries, namely a marked

increase in luminal diameter and the absence of musculoelastic tissue [17, 19], changes that are initiated by trophoblast invasion.

1.1.2 Hormonal Adaptations in Pregnancy

The hormonal changes that occur from conception through to the post-partum period have been well defined. In human pregnancy, dramatic changes in progesterone and oestrogen are accompanied by changes in the levels of human chorionic gonadotropin (hCG), prolactin, placental lactogen, relaxin, oxytocin, corticotropin releasing hormone (CRH) and human growth hormone amongst others. Here, the pattern of progesterone and oestrogens are discussed.

During pregnancy, the plasma levels of progesterone rise from 11ng/mL in the luteal phase of the menstrual cycle to 125-200ng/mL in the third trimester [20]. After the initial six weeks gestation, the major site of progesterone production is the placental trophoblast, before which it is the corpus luteum that maintains progesterone levels [21]. The conceptus is also the source of high levels of oestrogens in human pregnancy, both from the placental trophoblast and also the fetal adrenal [21]. The extended secretion of progesterone is critical for the initiation and maintenance of a successful pregnancy, as it is the functional withdrawal of progesterone that is thought to be the driving factor for the onset of labour. Progesterone acts on the uterus to stimulate and maintain uterine functions that are permissive to early embryonic development such as implantation, placentation and successful fetal and placental development to term [22].

As well as being important for stimulation of progesterone production in the placenta, oestrogen acts to stimulate the correct growth and function of the placenta; which in turn ensures the maintenance and control of steroid hormone production. Along with progesterone, oestrogen is necessary for the development of fetal organs and promotes maternal breast growth. Similarly to progesterone, oestradiol-17β and oestradiol conjugates rise from approximately 1.6ng/mL to 52ng/mL at 5 weeks and at 40 weeks of pregnancy, respectively [23]. However, it is oestriol, produced by the placenta,

that rises from undetectable levels in non-pregnant women to plasma concentrations of 270ng/mL [24]. Low levels of oestriol in the third trimester may be an indication of adverse outcome.

1.1.3 Hormonal Regulation of Cardiovascular Adaptation in Pregnancy

Hormonal control of blood pressure during pregnancy and the mechanisms behind this are still relatively unclear. As described previously, it is thought that the drop in systemic vascular resistance is one of the first cardiovascular adaptations in pregnancy and it is therefore likely that this is triggered by the rapid hormonal changes that occur following conception.

Progesterone plays an important role in the regulation of cardiovascular adaptation from the moment that fetal implantation occurs. In a population of Swedish pregnant women, an epidemiological study noted that when concentrations of the hormones progesterone and relaxin were highest in early pregnancy, this correlated with lower mean systolic blood pressure in later pregnancy suggesting that these hormones influence haemodynamic changes. However, the authors note that this observation was not able to infer causality [6]. *In vitro*, progesterone (P4) has been reported to have both vasodilatory and vasoconstrictive effects in the vasculature depending on location of the vessel and level of exposure [25, 26], yet in hypertensive subjects treatment with P4 was able to reduce blood pressure [27]. Earlier work conducted in pregnant ewes was able to show that P4 had a direct haemodynamic effects, decreasing resting blood pressure and increasing plasma volume. The investigators observed that whilst administration of P4 was able to increase plasma volume, this was in absence of a rise in renin and aldosterone concentrations. Furthermore, the addition of oestradiol (E2) did not lead to a differential effect on blood pressure or volume from treatment with P4 alone thus suggesting the effect is not propagated via oestrogen-induced or -facilitated progesterone pathways [5].

Of course oestrogen plays an important role as well, and research dating back to the 1970s using intact and ovariectomised rats suggested that oestrogens may alter vascular compliance by decreasing the ratio of arterial collagen to elastin. These data also showed that as well as altering the relative

concentrations of these proteins, administered oestrogens affected the rate of collagen and elastin accumulation in the aortic wall [28, 29]. Studies in ovariectomised non-pregnant ewes have shown that systemic oestradiol infusion increases heart rate (and therefore cardiac output) and decreases systemic vascular resistance [30, 31]. Whilst Pencins-Thompson *et al*., did not find any additional effect of E2 upon blood pressure and volume, other research has indicated that 17β-oestradiol increases nitric oxide synthase (NOS) expression and therefore increasing concentrations during pregnancy add to the powerful vasodilatory action of nitric oxide (NO) [5, 19, 32].

As well as the effects of progesterone and oestrogen on blood pressure control during pregnancy, animal studies have shown that relaxin plays a major role in pregnancy as a vasodilator, both in renal vasodilation and osmoregulation [11, 33, 34]. Relaxin is a 6-kDa peptide hormone in the insulin-relaxin superfamily of hormones. It is produced by the corpus luteum under the stimulation of hCG and circulates during pregnancy in humans and other mammalian species [33]. Although secretion of relaxin is known to increase throughout pregnancy, its ability to exert a direct vasodilatory effect or to decrease vascular sensitivity to angiotensin II has been contested [8, 35]. The vascular refractoriness to vasoconstrictors (including angiotensin II and noradrenaline) is known to contribute to vasodilation in healthy pregnancy and other suggested reasons include a decrease in angiotensin II receptors or the effect of increased progesterone and prostacyclin [30, 36, 37]. Albeit, relaxin has been shown to be an important mediator of maternal blood pressure; potentially through its effects on vascular compliance, connective tissue composition, regulation of water metabolism and production of NO [38-42]. Chronic administration of recombinant human relaxin to non-pregnant animals produced increased cardiac output and arterial compliance. More recently, studies designed to understand the mechanism behind both the rapid and sustained vasodilatory response to relaxin have observed the critical role of the angiogenic factors vascular endothelial growth factor (VEGF) and placental growth factor (PLGF) as intermediaries in the relaxin vasodilatory pathway [39].

1.1.4 Immunological Adaptations in Pregnancy

As human pregnancy progresses and hormone levels change dramatically, the interplay between sex hormones and the maternal immune system leads to complex and multifactorial immunological changes (see Figure 1.1). Receptors for progesterone and/or oestrogen are expressed on the majority of cells in both the innate and adaptive immune systems and T cells, B cells, neutrophils, dendritic cells, monocytes and natural killer (NK) cells all have been shown to be transcriptionally regulated by oestrogen [43, 44]. Several theories have been proposed aiming to explain the immunological changes that occur during pregnancy. We know that the maternal immune response to infection is uniquely regulated; where the balance between tolerance and suppression has often been referred to as 'the immune paradox of pregnancy' [45]. This immune adaptation acts to allow for antimicrobial defence and tissue repair whilst preventing damage to developing fetal organs via paternal antigen tolerance.

The classic theory first proposed in 1953 by Peter Medawar viewed the fetus as a semi-allogenic graft [46]. The theory proposed that non-specific systemic immunosuppression in pregnancy reduces the chances of an antigen-specific response against the immunologically 'immature' fetus, aided by the 'neutral barrier' function of the placenta and the immunologically privileged nature of the uterus. Although we now know that the fetus does express major histocompatibility molecules and is not in that sense allogenically immature, the exact mechanism of fetal tolerance is yet to be elucidated. This likely over-simplistic theory has been largely superseded by the pervasive theory of Th2 (T helper 2) bias. First published in the early 1990s based upon experimental research investigating antibody production at the fetomaternal interface, Lin *et al*., suggested that the continuous presence of the interleukins IL-4, IL-5 and IL-10, and the transient expression of interferon-γ (IFN-γ), supported the idea of a Th2-like bias driving the maternal immune response [47]. It is possible however, that whilst this is a phenotype strongly characterised at the fetomaternal interface, there is a paucity of evidence that supports a systemic Th2 shift [43, 48].

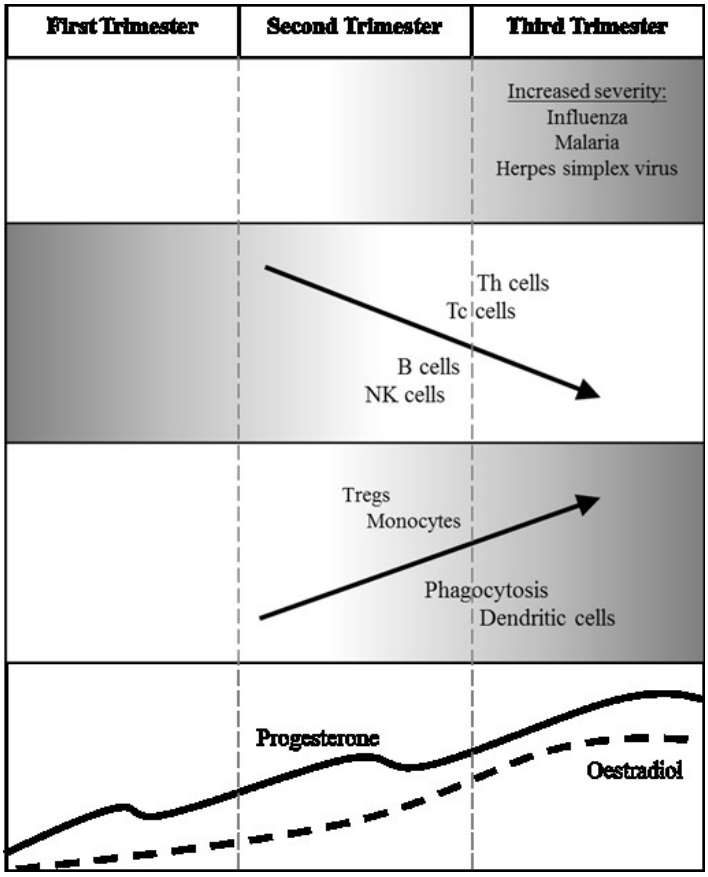


Figure 1.1: Changes in the principal hormone levels and corresponding immune system characteristics during pregnancy. As pregnancy advances and progesterone and oestrogen levels rise, T cell activity (T helper and cytotoxic T cells), natural killer cell activity, and possibly B-cell activity are reduced, whereas monocyte, dendritic cell, and other polymorphonuclear cell activity is increased. The severity of some infections increases with advancing pregnancy. Adapted from Kourtis *et al*., [49].

To ensure the tolerance of a semiallogenic fetus, it was initially thought that pregnancy confers broad immunosuppression. This idea was supported by the observation that during pregnancy, the symptoms of autoimmune diseases such as rheumatoid arthritis (RA) and multiple sclerosis (MS) are often suppressed. Klipple *et al*., hypothesised that the modulation of cell-mediated immunity coupled with alterations in immune complex generation during pregnancy may account for the partial or complete remission of RA symptoms in 70% of pregnant patients, even when coupled with almost complete cessation of medications. Additionally, the group observed that over 90% of patients relapsed by 6-8 months post-partum [50]. Similarly, in pregnant MS patients the rate of remission declines with

advancing gestation, and reverses in the 3 month post-partum period before returning to pre-pregnancy rates [51]. More evidence for the immunosuppressive hypothesis of pregnancy is found in the increased disease severity during pregnancy to some infectious pathogens including *Varicella zoster*, *Plasmodium falciparum* and *Listeria monocytogenes* [43]. Of considerable note is the apparent increased susceptibility of pregnant women to influenza (see Chapter 1.2.1.1).

Conversely, there is now a mounting body of evidence that challenges the notion of maternal immunosuppression. Data from studies of pregnant mice showing normal T cell development after lymphocytic choriomeningitis virus infection and data that indicated fetus-specific cytotoxic T cell (Tc cell) responses that could be generated in pregnancy without the occurrence of pregnancy loss; all contradict the idea of systemic immunosuppression in pregnancy [49, 52, 53]. Some have even gone on to suggest that pregnancy may in fact confer a 'hypersensitisation' to infection. For example, due to increases in CD14 expression (a cell-surface receptor that recognises endotoxin when a complex is formed with lipopolysaccharide-binding protein expression) in the third trimester and increases in the cytokine IL-12, there is an enhanced (and often fatal) monocyte cytokine response to endotoxin [54]. Furthermore there have been several reports presenting evidence of an adequate response to vaccines during pregnancy. Sperling *et al*., observed that in response to trivalent inactivated influenza vaccine, no diminution of immunogenicity was detected in the third trimester, which is a well-accepted time of increased clinical vulnerability to influenza [55]. Similar findings were reported for tetanus diphtheria and acellular pertussis vaccination [56].

It is now generally accepted that the view of pregnancy as a state of immunosuppression is outdated and probably oversimplified. In several recent review papers on the subject, many authors agree it may be better to view pregnancy as a "modulated immunological condition" [43, 49, 57]. This definition recognises that there is a change in the ratio and function (rather than a complete suppression) of the maternal leukocytes that occurs during pregnancy.

1.1.4.1. Innate Immune System Adaptations

Sacks *et al*., when discussing the idea that pregnancy is immunosuppressed, proposed a paradigm shift suggesting that suppression was confined to the maternal adaptive immune system. In this new concept, the authors suggested that the maternal innate immune system compensates for the adaptive, leading to monocyte-driven immunological response [58]. Cells of the innate immune system initiate a response by processing and presenting antigens to lymphocytes via association with major histocompatibility complex (MHC) class I and II molecules, described as 'signal 1'. The response to an immune challenge, such as endotoxin, instigates the production of co-stimulatory molecules and/or pro-inflammatory cytokines, described as 'signal 2'. Both of these mechanisms stimulate naïve T cells to become effector Th1 or Th2 cells; however in pregnancy, it is hypothesised that placental particulate and soluble products can stimulate cytokine release from macrophages, which occurs in the absence of antigen presentation (Figure 1.2) [58]. Furthermore, the hormones progesterone (the 'classic hormone of immune suppression') and oestrogen have been shown to promote Th2 bias [59-61].

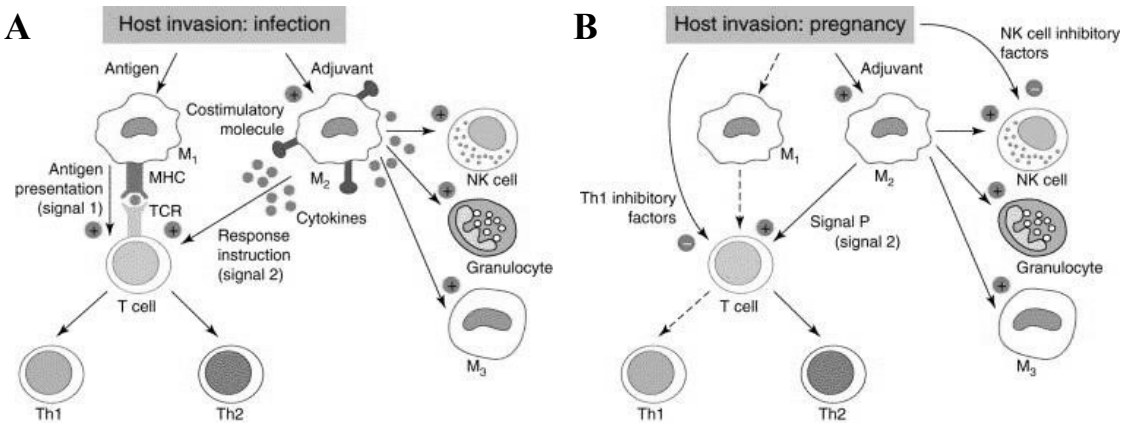


Figure 1.2: 'Signal 1' and 'signal 2' in an immune response to infection and how this is altered in pregnancy. (A) In an infection, monocytes/macrophages (M1) process and present antigen to T cells – signal 1. Monocytes/macrophages that might (M1) or might not (M2) be involved in antigen presentation are also activated by adjuvant (e.g. endotoxin) to produce costimulatory surface molecules or pro-inflammatory cytokines – signal 2. Signals 1 and 2 stimulate T cells to become effector Th1 or Th2 cells. (B) In pregnancy there is a bias to a Th2 response. However, adjuvant (e.g. deported fetal or placental products) activates monocytes and hence other innate cells. Adapted from Sacks *et al*., [58].

More recently however, two further paradigms have been proposed. The first of these is the idea of a complete absence of immune suppression [57, 62]. Two reviews written by Mor *et al*., outline the group's hypothesis that the maternal immune system is not suppressed, but functional and highly active. In pregnancy from the first trimester onwards, there is evidence to suggest that monocytes and granulocytes are already systemically activated without an infectious stimulus [63]. Moreover, monocytes are increased in number and have an activated phenotype and exhibit increased phagocytosis, production of certain cytokines and expression of CD14 [64, 65].

The second paradigm focusses on the addition of a further layer of complexity to the Th1/Th2 dichotomy model, where another subset of Th cells, Th17 cells, are introduced. The Th17 subset are a relatively recently characterised lineage that play a critical role in the induction and regulation of inflammation via the production of distinct cytokines such as the pro-inflammatory IL-17 [66]. Interestingly, these cells have been implicated in the pathogenesis of autoimmune disease and rejection [67]. In normal pregnancy, Th17 cells have been shown to be slightly decreased in peripheral blood, but increased in the uterus [68]. This indicates a role for Th17 cells in immune tolerance as a lack of IL-17 (or of Th17 cells) has been associated with neutrophil defects and increased incidence and severity of infections with *Staphylococcus aureus* or fungi [69].

1.1.4.2 Adaptive Immune System Adaptations

Whilst the innate immune response is a nonspecific reaction towards foreign antigens, the adaptive system (also known as the specific system) response forms a very specific reaction towards antigens. The adaptive immune system is exclusively present in higher multicellular organisms and consists of cellular (T and B cells) and humoral (antibodies) components. Although different immune components are involved in these systems, much overlap and cross-talk exists between the two [70]. In general, it is thought that the adaptive immune system response is decreased during pregnancy, especially in later stages [49].

Studies in mice have shown that upon presentation of fetal antigens to maternal T cells (which can begin as early as conception potentially via seminal fluid), they become aware of these antigens and actively protect them during pregnancy [71]. These cells are thought to contribute to the tolerogenic environment which allows the survival of the fetus. Regulatory T cells (Tregs) have shown to be elevated in normal pregnancy. Outside of pregnancy they are thought to be responsible for the maintenance of immunological self-tolerance by actively suppressing T cell proliferations and cytokine production [72]. They also play a major role in preventing autoimmunity and tolerating allogeneic organ grafts, potentially involving the promoting tolerance of dendritic cells [73, 74]. The importance of Tregs in the maintenance of pregnancy is demonstrated in a study by Jasper *et al*., where they propose that pregnancy is associated with reduced expression of the Treg cell transcription factor Foxp3 in endometrial tissue [75].

In addition to the T cell aspect of the adaptive immune system, B cells are the principal cells involved in the production of antigen-specific antibodies to target foreign antigens for phagocytosis; they are activated via signal from the Th cells. The role of B cells during pregnancy is not fully understood and previous studies have mostly concentrated on the production of antibodies in pathologic pregnancies [76]. However, in recent years, several other functions have been attributed to these cells showing that B cells can uptake, process and present antigens as well as produce several cytokines that further influence immunity [77].

1.1.4.3 Adaptations in Cytokine Production

Cytokines are small pleiotropic regulatory proteins that are released by cells to enable inter-cell interaction and communication, in either an endocrine or paracrine manner depending on the cytokine and location. The name ‘cytokine’ is a nonspecific term for several sub-groups including the interleukins (of which are made by one leukocyte and act on another), and the chemokines (cytokines which are chemotactic, that is the primary action involves leukocyte migration) [78, 79]. Cytokines are often produced in a cascade fashion, and although they are secreted by many cell types, they are

produced predominantly by activated macrophages and Th cells. Largely, cytokines can be thought of as belonging to one of three main categories: pro-inflammatory, anti-inflammatory and chemokine.

Levels of several cytokines are altered in pregnancy. Most notably, most pregnant women exhibit increased tumour necrosis factor-alpha (TNF-α), interleukin-10 (IL-10) and granulocyte-colony stimulating factor (G-CSF) and decreased IFN-γ and VEGF [43, 80]. More generally, levels of inflammatory cytokines are reduced and cytokines that induce macrophage recruitment and activity are increased. These alterations in cytokine profile do not follow a clear Th1 or Th2 phenotype [49]. These changes are summarised in Figure 1.3.

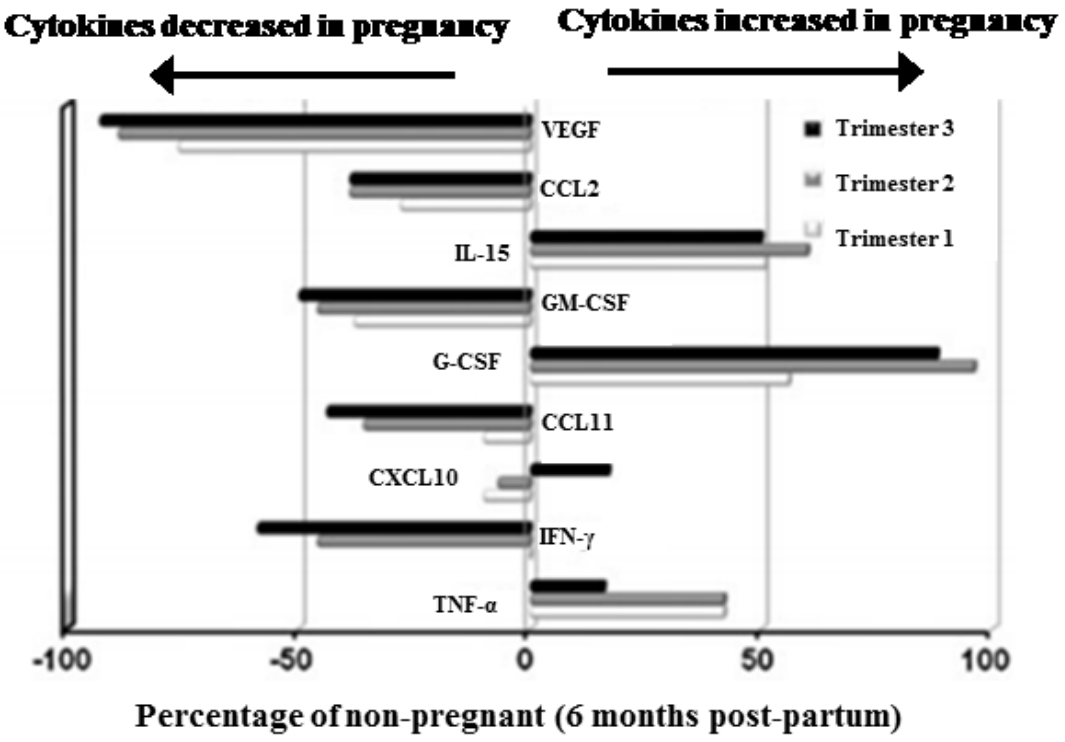


Figure 1.3: Cytokine alterations during pregnancy. Cytokines were measured by multiplex ELISA three times during pregnancy and compared to 6th month post-partum. Data were first published by Kraus *et al*., [80], figure adapted from Pazos *et al*. [43].

Broadly speaking, the Th2 cytokines are released from naïve Th0 cells under the influence of IL-4 and produce IL-4, IL-5, IL-13, IL-10 and IL-6. Whilst mainly these are considered to be anti-inflammatory drivers, IL-6 has pro-inflammatory properties. Additionally, although IL-10 and IL-6 are frequently associated with the Th2 phenotype, they are both produced by other cell types including Th1 cells, fibroblasts, macrophages and B cells [70, 81, 82]. IL-10 then acts to regulate Th1 differentiation in a negative feedback loop [48]. Th1 cytokines are released from naïve Th0 cells under the influence of IFN-γ and produce a broad spectrum of pro-inflammatory cytokines including IFN-γ and TNF-α. It is this phenotype that drives phagocyte-mediated host defence which is critical for defence against intracellular pathogens [83].

1.1.5 The Role of the Nitric Oxide Signalling Pathway in Pregnancy

NO is a physiological messenger, and major regulator within the cardiovascular, nervous and immune systems of the body [84]. It is synthesised through the sequential oxidation of L-arginine, catalysed by NOS enzymes of which there are three isoforms: neuronal (nNOS), inducible (iNOS) and endothelial (eNOS) [85]. In the circulation, NO through the second messenger cyclic guanosine monophosphate (cGMP), acts as a potent vasodilator that regulates vascular tone and tissue blood flow; it also inhibits platelet aggregation and leukocyte adhesion on the endothelial surface [86]. Further to this, NO also acts within the innate arm of the immune system as an antimicrobial and tissue-damaging effector molecule and in turn has been shown to strongly affect adaptive immune responses and exert cytoprotective effects [87].

1.1.5.1 The DDAH/ADMA/NO Pathway

NOS inhibition is largely achieved by the inhibitory L-arginine analogues N-monomethyl-L-arginine (L-NMMA) and N-nitro-L-arginine. They, via a competitive mechanism of inhibition, displace L-arginine from the substrate binding site of NOS [88]. Additionally, asymmetric dimethylarginine (ADMA) was identified as an endogenous inhibitor of NOS in 1992 [89]; and more recently, ADMA (specifically the ratio of ADMA to L-arginine) was observed to determine NOS activity at

physiologically occurring concentrations [90]. Both ADMA and L-NMMA are derived from the proteolysis of methylated arginine residues, a process which is catalysed by protein-arginine methyl transferases (PRMTs) [91]. The free methylarginines released can then be metabolised to L-citrulline through the activity of another group of enzymes, dimethylarginine dimethylamino hydrolases (DDAHs) [92].

1.1.5.2 DDAH Isoforms

DDAH is a predominantly cytoplasmic enzyme expressed as two isoforms: type 1 (DDAH1) and type 2 (DDAH2) [93]. The discovery of the second DDAH isoform by Leiper *et al.*, followed the observation that DDAH activity and protein expression did not always correlate [93, 94]. Initial experiments using cDNA cloning and northern blotting techniques as well as DDAH activity assays, led investigators to the conclusion that DDAH2 expression made a limited contribution to overall DDAH activity. However, this report plus subsequent other studies demonstrated a disparity in the organ and cellular distribution of the two isoforms. DDAH1 is principally expressed in the liver and kidney, major sites for the metabolism of ADMA [95, 96], as well as displaying strong expression in the pancreas and brain [97]. DDAH2 encoding mRNA is expressed in the vascular endothelium and immunohistochemical analyses have located DDAH2 in vascular smooth muscle cells, endothelial cells and vessel adventitia [98, 99]. Furthermore, DDAH2 is also expressed in heart, placenta, foetal tissues, peripheral leukocytes and various immune tissues known to express iNOS [97].

1.1.5.3 Role of Nitric Oxide in Pregnancy

NO is thought to contribute to maternal systemic vasodilation during pregnancy. In fact, several studies have supported the idea that NO is the principal mediator of arterial vasodilation in pregnancy, due to increased levels of NO in vascular beds in the pregnant guinea pig and increased NOS in the arteries of pregnant rats [100-102]. However, more recently it has been suggested that it is an orchestrated network of vasodilatory systems that control both local and systemic haemodynamic adaptations in pregnancy, including NO, prostacyclin, kallikrein, angiotensin-(1–7) and VEGF [103].

Other roles for NO during pregnancy include the regulation of uterine and fetal blood flow, and the relaxation of the myometrium [104]. One suggested mechanism for the regulation of NO-mediated uterine quiescence is the upregulation in DDAH expression levels and activity at mid-gestation accompanied by reduced ADMA levels which increase at term [105]. NO is also thought to play a central role in the remodelling of the uteroplacental vasculature, and it has been shown that eNOS is increased throughout pregnancy, leading to increased synthesis and release of NO from the endothelium [106].

1.2 Maternal Infection and Inflammation

1.2.1 Maternal Susceptibility to Infection

The link between bacterial infections (such as acute pyelonephritis and chorioamnionitis) and adverse pregnancy outcomes has been well established [107-109]. Additionally, viral infections such as influenza, malaria, human immunodeficiency virus (HIV), hepatitis E virus and herpes simplex virus amongst others, as well as bacterial sepsis, are more often fatal in pregnant women, with a positive correlation between disease severity and advanced gestation [110]. Furthermore, it is now generally accepted that pregnant women exposed to viral and bacterial infection risk potential harm to the fetus; even if placental transmission is not achieved, the fetus can be adversely affected by the maternal response to infection [57].

The maternal immune response to infection used to be described as blunted, where apparent increased maternal susceptibility to infection as indicated by epidemiological evidence was thought to indicate immunosuppression. Nonetheless, it must be considered that the evidence for pregnancy-induced increased susceptibility to infection is not clear-cut, as an increase in disease severity in pregnant women does not always imply increased susceptibility. Moreover, literature collated in a recent review by Sappenfield *et al*., suggests that the innate response may be boosted during pregnancy [43, 111, 112]. This led the authors' to suggest that this may represent a compensatory immune mechanism to protect the pregnant mother and the fetus, If this is so it would imply decreased susceptibility to infection [110].

1.2.1.1 Influenza

It was originally documented by Harris in 1919, that during the 1918 influenza pandemic, the mortality rate in pregnant women was as high as 27% (increasing to 50% when complicated by secondary pneumonia), compared to 1% in the general population [113]. Similarly, others observed that in the 1957 pandemic, 50% of all influenza deaths in reproductive-aged women occurred in those

who were pregnant [110, 114]. More recently during the 2009 H1N1 pandemic, 64.6% of the pregnant women diagnosed were hospitalised, and although pregnant women accounted for less than 1% of the population they accounted for 5-7% of deaths, hospitalisations and ICU admissions [110]. The highest proportion of ICU admissions during this time was in women in the third trimester, although severe illness was reported in women in all trimesters, which supports the finding that increased disease severity in third trimester pregnancies has been documented in the inter-pandemic periods also [49].

Interestingly, influenza-linked fatalities in pregnant and post-partum women have been documented in the developing world where mortality rates were more than three times higher in pregnant women than non-pregnant (25% in pregnant, 8% in non-pregnant) [115]. However, this has not been seen in western countries, possibly due to effective timely antiviral therapy and better medical facilities [110, 116, 117]. That being said, a three-fold greater risk of mortality is often quoted.

The mechanisms behind this increased morbidity and mortality are not fully understood, however it is likely that the immunological adaptations that occur during pregnancy that allow for fetal tolerance may affect outcome. Kay *et al*., were able to show that pregnant women have adequate antibody responses to the inactivated influenza vaccination (IIV), as they have increased NK and T cell responses after IIV when compared with non-pregnant women [118]. *In vitro*, NK and T cell mediated cytokine and chemokine production in isolated peripheral blood mononuclear cells (PBMCs) were also increased in pregnant women in response to influenza virus, indicating that there may be excessive immune cell recruitment and potentially a deleterious immune response [118]. This excessive innate immune system activation and consequent chemokine production has been shown to be a crucial factor in influenza-induced lethality, albeit in a non-pregnant mouse model [119]. To the author's knowledge there have been no direct comparisons of the production of chemokines in response to influenza virus between pregnant and non-pregnant animals.

Another possible mechanism underlying the increased lethality of influenza in pregnancy is that of respiratory adaptation and reduced capacity for repair. A recent study by Marcelin *et al.*, showed that

increased severity of the pH1N1 virus in pregnant mice was associated with increased pulmonary neutrophil and macrophage infiltration [120]. Their observation of disparity in the distribution of neutrophil infiltration within different lung tissues, and the alteration in macrophage populations driven by the Th2 shift and development of alternatively activated macrophages (AAMs), led to the hypothesis that an impairment in lung repair mechanisms is likely to contribute to the enhanced severity of H1N1 in pregnancy.

Despite these experimental and epidemiological data suggesting an increased severity of influenza infection in pregnancy, it must be addressed that an increase in susceptibility to infection has not been documented. This not only fits in well with the hypothesis of a decreased adaptive immunity in pregnancy, but that immune responses that are suppressed are likely to be those involved in recovery rather than the prevention of onset of infection [43].

1.2.1.2. Malaria

Malaria infection is a mosquito-borne infection transmitted by six species of *Plasmodium* parasite. It has been well documented that the greatest burden of disease is seen in young children and pregnant women [121]. The highest incidence is in sub-Saharan Africa, where approximately 25 million pregnant women are at risk of *Plasmodium falciparum* infection every year, and 25% have evidence of placental infection at the time of delivery [122]. In the Asia-Pacific region, malaria is the most common cause of maternal death during pregnancy, with a maternal mortality rate at 48% between 2004 and 2006 [123]. Several studies have shown that pregnant women have a 3-fold increase in risk of developing severe malaria (which is defined by the WHO as the presence of at least one clinical symptom, as opposed to asymptomatic malaria [124]), and analysis of eight studies (n=227) indicated that the median mortality rate for women with severe malaria in pregnancy was approximately 39% [123]. Furthermore, adverse outcomes including maternal anaemia, stillbirth, pre-term labour (PTL) and low birth weight have all been associated with maternal malaria infection [125], where in a meta-

analysis of 32 independent datasets Eisele *et al.*, estimated that maternal malaria was associated with 14% of low birth weight infants worldwide and 11% of infant mortality in sub-Saharan Africa [126].

Similar to influenza virus, the mechanism, or mechanisms, behind the increased mortality rates in pregnant women with malaria are not fully understood. Pregnant women are more susceptible to malaria in the first pregnancy than any subsequent pregnancies, which led researchers in the Gambia to conclude this may be due to the absence of antibodies that can target a subset of malaria-infected erythrocytes which can accumulate in the placenta [127, 128]. However, since this research was conducted, the idea that pregnant women have suppressed cell-mediated immune responses has been largely contradicted. A study that examined antimalarial T-cell responses in women in their first and second pregnancies, as well as postpartum women, found that IL-2 responses were suppressed but IL-4 and IFN-γ responses were either not affected or enhanced [129]. To add further complexity, a later study by the same group found that parasite type and strain also affected cytokine production [130]. The role of innate immune cells has also been examined in the placenta, where it is thought macrophages aid in direct parasite elimination as well as by indirectly enhancing the innate response through cytokine release [127]. Additionally, infected erythrocytes were observed to adhere to NK cells and initiate production of IFN-γ, as well as adhere to dendritic cells via CD36 which led to the modulation of dendritic cell function, likely through the parasite-produced pigment hemozoin [131-133].

1.2.1.3 Acute Pyelonephritis

Morphological and physiological changes to the genitourinary tract that occur during pregnancy mean that urinary tract infections (UTIs), both symptomatic and asymptomatic, are common [107, 134]. Asymptomatic bacteriuria, defined as the presence of actively multiplying bacteria without the symptoms of a UTI can be found in both pregnant and non-pregnant women, but the progression to symptomatic bacteriuria is enhanced in pregnancy [135]. In pregnancy, symptomatic bacteriuria leads to acute pyelonephritis (AP) in 20-50% of cases which in turn can lead to adverse obstetric outcomes

such as preterm birth, fetal mortality, and also sepsis and acute respiratory distress if left untreated [136, 137]. A retrospective analysis study by Wing *et al*., conducted in South Carolina found that almost 2% of pregnant women with AP developed septicaemia, which amounted to nearly 50 times that of women without AP [138].

One recent explanation put forward for the increased susceptibility of pregnant women to AP is the decreased presence of soluble tumour necrosis factor-related apoptosis-inducing ligand (sTRAIL) in maternal plasma. Chaemsaithonga *et al*., found that pregnant women with AP, especially those with bacteraemia, had a lower mean plasma concentration of sTRAIL than those with uncomplicated pregnancies; albeit pregnant women had lower plasma levels of sTRAIL than non-pregnant women to begin with [139]. These findings were consistent with previous studies which concluded that TRAIL is a protective cytokine against bacterial infection [140, 141].

1.2.2. The Effects of Maternal Infection and Inflammation

1.2.2.1 Maternal Sepsis

The term "sepsis" includes illnesses that range from minor through to multiple organ dysfunction and shock. It is often characterised first by a systemic inflammatory response syndrome (SIRS) followed by multiple organ failure and finally by immunosuppression [142]. The most severe form of sepsis, septic shock, is demarcated as sepsis with refractory hypotension despite adequate fluid resuscitation. The speed of progression from initial bacteraemia (or viraemia) through to SIRS, severe sepsis with organ dysfunction and septic shock, is determined by the balance between the virulence of the infecting organism and the host response. Co-existing conditions such as pregnancy and increased age have a major bearing on the effectiveness of the host response. Bacteraemia leads to SIRS and eventually sepsis via several mechanisms. The best known of which is the activation of the CD14/TLR4/MD2 complex by components of the invading organism, such as lipopolysaccharide (LPS). Consequently, activated inflammatory cells release cytokines, such as TNF-α, IL-1β and IL-6 which, amongst other effects, lead to increase capillary leakage, increased production of adhesion

molecules on endothelial cells and neutrophils and increased neutrophil-endothelial interaction [143]. It is the excessive production of these cytokines that can often be more dangerous than the original infection, overreaching the boundaries of normal immune response regulation.

This, alongside the simultaneous development of consumptive coagulopathy and other metabolic dysfunctions, promotes inflammation at the target site and at off-target systemic sites, thus to a lesser or greater extent affecting all organ systems (multiorgan failure) [144].

In the stages leading to multiorgan failure, severe sepsis is associated with depressed myocardial function; where approximately 50% of the patients who are diagnosed with sepsis exhibit signs of myocardial dysfunction [145]. Furthermore, reports have suggested that patients with sepsis who develop myocardial dysfunction have an increased risk of death compared to those without evidence of myocardial dysfunction [146, 147]. A critical inducer of this dysfunction is TNF-α, regulated by NO and calcium signalling mechanisms, and subsequent induction of the nuclear factor kappa-B (NFκ-B) pathway [148-150]. Animal studies have demonstrated that in septic heart models there is a decrease in left ventricular (LV) systolic and diastolic performance, and more recently a clinical study using echocardiography found that LV performance was altered in 44% of septic patients [145].

Cardiac troponins are regulatory proteins of the thin actin filaments of the cardiac muscle which are released upon myocardial cell injury. ver Elst *et al*., were able to demonstrate a positive correlation between LV dysfunction and cardiac troponin-I and troponin-T elevation in the first 48 hours of septic shock, although continuous electrocardiographic in patients who did not survive demonstrated that this elevation was not due to acute ischemia [151]. Both troponin-I and –T are now considered to be biomarkers that aid in the diagnosis and prognosis of myocardial dysfunction in severe sepsis [152]. Other such biomarkers are the peptide hormones atrial natriuretic peptide (ANP) and brain natriuretic peptide (BNP; also known as brain natriuretic factor, BNF) [153-155]. Both are secreted in response to atrial or ventricular volume expansion and pressure overload, respectively; however in the presence of inflammation, pro-inflammatory cytokines contribute to ANP and BNP release. Witthaut *et al*.,

found that in septic shock both ANP and BNP plasma levels were increased acutely in the early phases of septic shock, however increased BNP was more likely to be indicative of LV dysfunction, where elevation in ANP concentrations was more likely to be linked to a rise in IL-6 production [153]. In pregnancy, ANP and BNP play important roles in blood volume homeostasis and gradually increase throughout pregnancy and the peripartum period [156]. Elevated levels have also been noted in pre-eclamptic women where the degree of ANP and BNP increase has been correlated with the severity of maternal left ventricular dysfunction [157].

The cardiovascular consequences of sepsis may also be accompanied by respiratory symptoms, where lung infiltration by activated neutrophils increases capillary permeability leading to pulmonary oedema [158]. Gill *et al.*, showed that in an *in vivo* mouse model of sepsis, using pulmonary intravital videomicroscopy and histological assessment, pulmonary microvascular barrier dysfunction resulted in albumin hyperpermeability which was in turn associated with pulmonary microvascular endothelial cell death [159]. Pregnancy may exacerbate this as the oncotic pressure of blood is reduced [160], potentially increasing fluid leakage, alveolar collapse and the development of acute respiratory distress syndrome (ARDS). ARDS is a feature of many pregnant women who are admitted to ITU [161].

Clinically, pregnant women with sepsis can be more difficult to evaluate as pregnancy is associated with faster heart rate, lower blood pressure and altered respiratory capacity, all of which are clinical signs of sepsis [13]. Furthermore, the laboratory-based investigations to direct treatment and indicate prognoses such as white cells counts, creatinine levels and serum lactate levels are already altered in pregnancy [162, 163]. Barton and Sibai suggested that when taken together, there is the potential for early signs of overwhelming infection and sepsis to be masked, thus delaying the diagnosis and initiation of antibiotic (or other) therapies leading to a worsened outcome [162]. To the author's knowledge, there are no data comparing the outcomes of non-pregnant and pregnant septic patients.

In developed countries maternal sepsis is usually the result of urinary tract infections and instigating organisms originate from the polymicrobial flora of the genitourinary tract [108]. However, there is a plethora of both bacteria and viruses (see Table 1.1) and fungal infections that have been associated with maternal sepsis that make a significant contribution to infectious morbidity in pregnancy, exacerbated by the altered immune physiology during pregnancy. Other causes of severe sepsis in pregnancy include septic abortion, neglected endometritis, pelvic abscess or non-obstetric intraperitoneal aetiology such as appendicitis, bowel infarction or necrotising fasciitis [162].

Table 1.1: Organisms associated with maternal sepsis. Adapted from Morgan and Roberts [108]

Gram-positive cocci	Gram-negative rods	Gram-positive rods	Anaerobes	Viruses
Pneumococcus	*Escherichia coli*	*Listeria monocytogenes*	*Bacteroides spp*	Herpes and varicella
Streptococcus A and B	*Haemophilus influenza*		*Prevotella*	HIV
Enterococcus feacalis	*Klebsiella*		*Clostridium perprfringens*	Influenza A and B
Staphylococcus aureus	*Enterobacter spp*		*Fusobacterium spp*	
	Proteus spp		*Peptococcus*	
	Pseudomona spp		*Peptostreptococcus*	
	Serratia spp			

1.2.2.2 Role of Chemokines in Sepsis

Chemokines are a category of cytokine that can be classified into four further categories depending on the location of conserved cysteine residues: CC chemokines (such as CCL2, CCL5, CCL6) principally involved in the chemotaxis of mononuclear cells, CXC chemokines (CXCL1, CXCL2) principally involved in the chemotaxis of neutrophils, C chemokines (XCL1, XCL2) principally involved in the chemotaxis of T cells, and the CX_3C chemokine (CX_3CL1, also known as fractalkine or neurotactin) which is principally involved in the strong adhesion of leukocytes to endothelial cells where CX_3CL1 is primarily expressed [78]. Chemokines signal through chemokine receptors that largely correspond

to their respective ligand, although most are 'promiscuous' and bind structurally related chemokines but with differing affinity. Indeed, chemokines can bind to several different receptors, while chemokine receptors can bind more than one chemokine [164]. Of these families, the first two (CC- and CXC-motif) have been extensively studied over the past 20 years in the context of sepsis and endotoxaemia. For example, several studies have investigated the putative role of chemokines in pulmonary immunosuppression following experimental sepsis, proposing that it is, at least in part, a result of the activities of CCL2, CCL17 and CCL6; all of which are induced by IL-4 and IL-13. These studies concluded that the pulmonary immune response in septic patients may therefore be inappropriately tilted toward the Th2 cytokine pattern [165, 166]. This reflects the changes that are already apparent in pregnancy, where pregnancy is considered to shift the balance between Th1 and Th2 towards a Th2 phenotype (see Chapter 1.1.4). Specifically, the chemokine CCL2 (also known as monocyte chemotactic protein-1; MCP-1) and its receptor CCR2, have been shown to be involved in regulating Th1- and Th2-type immunity [167], and have been associated with pregnancy-specific responses such as driving CCR2-dependent monocyte homing to the uterus [168].

1.2.2.2a CCL2

Due to the regulatory effect on pro- and anti-inflammatory responses to infection, several studies have explored the potential protective role for CCL2 in sepsis. In mice systemically infected with *Pseudomonas aeruginosa* or *Salmonella typhimurium*, treatment with recombinant CCL2 increased bacterial clearance [169]. Similarly, Gomes *et al*., have demonstrated a crucial role for CCL2 in the clearance of bacteria by a mechanism that utilises increased iNOS expression and NO production via the extracellular signal-related kinase (ERK) signalling pathway [170]. Furthermore, in a model of peritoneal sepsis anti-CCL2 has been shown to lead to increased lethality and reduced leukocyte recruitment and bacterial clearance. CCL2-deficient mice have been shown to be more susceptible to sepsis induced by both LPS and caecal ligation and puncture (CLP), potentially due to the action of CCL2 in positively regulating the anti-inflammatory cytokine IL-10 [171]. However, other researchers utilising the CLP model of polymicrobial sepsis made the observation that inhibition of

CCL2/CCR2 signalling led to mice being significantly more resistant to CLP-induced mortality than their wildtype or vehicle-treated counterparts [172]. The explanation for this focussed on the role of CCL2/CCR2 signalling in neutrophil recruitment. Although CCR2 is principally expressed in monocytes, Toll-like receptor 2 (TLR2) and TLR4 have been shown to upregulate the expression of CCR2 in circulating neutrophils during sepsis leading to off-site neutrophil recruitment and systemic tissue damage [173]; and whilst increased survival in CCR2-deficient mice could not be attributed to improved migration of neutrophils to the target site of inflammation or enhancement of bacterial clearance, it could be attributed to a marked reduction of neutrophil infiltration in the lungs, liver, kidney and heart [172].

1.2.2.3 Role of Nitric Oxide in Sepsis

Since the original work in 1990 conducted by Thiemermann *et al.*, that showed enhanced formation of NO contributed to endotoxin-induced hypotension, there has been an ever increasing interest in the role of NO in the pathophysiology of sepsis and septic shock [174, 175]. Overproduction of NO is a known to occur in sepsis, where iNOS activity is upregulated as part of the host response [176]. When this is excessive, high levels of NO induce severe hypotension, partly through loss of vasomotor tone. As pregnancy is already associated with lowered vasomotor tone, potentially via increased NO production [177], the risk of severe hypotension is aggravated.

Trials of several non-selective NOS inhibitors have shown increases in MAP, but these were also accompanied by decreased cardiac output and increased pulmonary arterial pressure [178]. Furthermore, in a study utilising a model of sepsis in rats, pre-treatment with the non-selective inhibitor L-NG-nitroarginine methyl ester (L-NAME) improved glutathione concentration in the brain (beneficial due the involvement of glutathione in defence against reactive oxygen species) [179].

In 2004, a trial of the NOS inhibitor N(G)-methyl-L-arginine hydrochloride (546C88) resulted in resolution of shock at 72 hr by 40% and 24% of patients in the drug-treated and placebo cohorts respectively [180]. Whilst there was no initial indication that 546C88 had any major adverse effect on

pulmonary, hepatic or renal function, when the study entered an international phase III trial recruitment was discontinued due to the emergence of increased mortality in the drug-treated group [181]. Nevertheless, the data from this trial supports the idea that NOS-inhibition contributes to the improved vascular tone in septic patients which is likely to be the primary cause of the observed haemodynamic effects; that is, increased systemic and pulmonary vascular resistance as measured by systemic and pulmonary arterial pressure and cardiac output.

1.2.2.4 Preterm Labour

Infection and inflammation have been implicated in the aetiology of PTL and association between infection and spontaneous PTL is now thought to be responsible for preterm delivery in up to 40% of cases [182-184]. Maternal infection is the only process for which a causal relationship has been established. Current theories of PTL aetiology include the thought that intrauterine infection arises following an ascending intrauterine colonisation, which culminates into an infection of the choriodecidua, fetal membranes (chorioamnionitis), amniotic fluid (AF), and ultimately the fetus, resulting in activation of the inflammatory cascade and thereby triggering PTL [185]. It is important to consider, however, that only a minor proportion of PTL pregnancies exhibit clinical signs of chorioamnionitis [186, 187], yet elevated levels of inflammatory cytokines such as IL-1, IL-6, IL-8 and TNF-α in the AF of these women suggested an infectious background even when clinical signs of infection were lacking [188]. Elevations in AF levels of certain prostaglandins ($PGF_2\alpha$) have also been reported, however most AF eicosanoid concentrations (PGE_2 and PGD_2) are higher in term than in preterm births [189].

Normal parturition has been shown to involve the activation of a complex inflammatory cascade [190, 191]; and in both term and preterm labour, the production of pro-inflammatory cytokines induces the production of prostaglandins and chemokines which act to promote cervical ripening and allow the onset of uterine contractions [192-194]. Therefore, it is the aberrant and premature stimulation of these mechanisms, possibly by an intrauterine infection, which can lead to PTL [195]. Indeed,

evidence suggests that it is inflammation, rather than the infectious bacteria itself that leads to the onset of PTL [196, 197].

This may have bearing on the clinical strategies presently employed to combat PTL, as recent reviews of antibiotic therapies found no benefit and administration of currently available tocolytics has not been associated with an improvement in neonatal outcome [198]; therefore currently, immunomodulatory targets are being sought [195, 199]

1.2.2.5 Neonatal Sepsis

Whilst infections such as chorioamnionitis have been associated with the aetiology of preterm labour, maternal sepsis and preterm labour are also both risk factors for neonatal sepsis. In 30% of cases, bacteria responsible for maternal intra-amniotic infection can be detected in the fetal circulation leading to fetal inflammatory response syndrome (FIRS) [200, 201]. FIRS presents with systemic activation of the fetal immune system and eventually progresses to multi-organ failure where these neonates are at risk of developing chronic lung disease and cerebral palsy [202-204].

1.3 Animal Models

There are relatively few experimental models of bacteraemia and sepsis in pregnancy. One reason for this is that sepsis is notoriously difficult to model in animals. The models that have been developed follow one of three strategies: administration of endogenous toxins such as LPS; administration of viable pathogens such as bacteria; and alteration of the endogenous protective barrier of the animal [142].

1.3.1 The Endotoxaemic Model

LPS (which is also known as endotoxin) is an important structural cell wall component of Gram-negative bacteria. It is one of the best studied immunostimulatory components of bacteria and is known to induce systemic inflammation (which can lead to sepsis if the signals are great enough). The structure of LPS can be thought of in three parts: lipid A, a core oligosaccharide, and an O side chain [205]. It is the lipid A that is the key pathogen-associated molecular pattern (PAMP), considered by most to be the prototypical PAMP.

The principal mechanism by which LPS signals is via the TLR4/MD2 complex. LPS is sensed via the formation of a complex with LPS-binding protein (LBP) and the co-receptor CD14 [206]. LBP acts as a shuttle protein which directly binds and facilitates the association of LPS and CD14, and CD14 acts to facilitate the transfer of LPS to the TLR4/MD2 receptor complex and modulates LPS recognition. Upon binding, intracellular signalling relies on a signalling cascade involving the intracellular TLR domain (called Toll IL-1 receptor homology domain, or TIR) binding to IL-1 receptor-associated kinase (IRAK) which is facilitated by the adapter proteins myeloid differentiation protein 88 (MyD88) and TIR domain-containing adapter protein (TIRAP) [205, 207]. This pathway is outlined in Figure 1.4. The MyD88-dependant initiation of pro-inflammatory cytokines can be facilitated by the activation of NF-κB. This protein complex transcription factor is known to be activated in response to pro-inflammatory stimuli, but also regulates the transcription of inflammatory genes [208, 209].

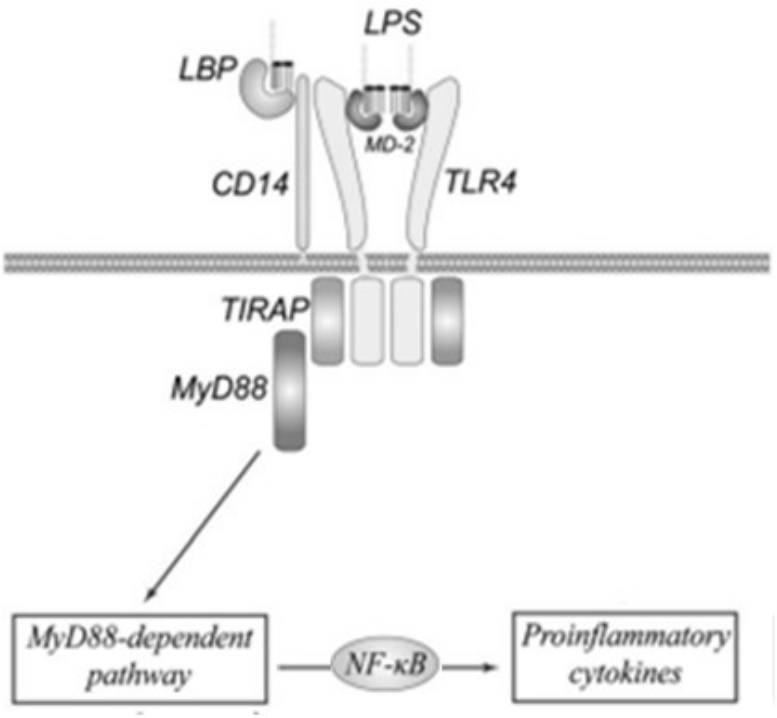


Figure 1.4: An overview of the LPS signalling pathway. LPS recognition is facilitated by LBP and CD14, and is mediated by the TLR4/MD2 receptor complex. Upon binding, the MyD88-dependent pathway mediates the activation of pro-inflammatory cytokines. This process can be intermediated by NF-κB driven transcription of pro-inflammatory genes. Adapted from Lu *et al*., [205].

Due to the key involvement of this cell wall component in the pathogenesis of sepsis, the effects of LPS have been extensively characterised over the past 50 years and it is widely used in inflammation, infection and sepsis research. The reason it is often preferred as an experimental tool is because of its stability and the ease of storage in its lyophilised form. Furthermore, it can be measured precisely and given to test animals as bolus or infusion [210]. For most sepsis models, LPS is administered via the intraperitoneal (i.p.), intratracheal or intravenous (i.v.) route, all of which result in increased concentrations of pro-inflammatory cytokines in the serum. However, i.p. injection of LPS has been shown to lead to a hyperdynamic cardiovascular response which does not occur if injected via the i.v. route [211, 212]. This is thought to more closely mimic the initial rise in cardiac output that occurs in human sepsis. Whilst the LPS model leads to increased serum cytokines that are clear markers of disease severity, the cytokine profile evoked in rodents shows several differences compared to

humans. The peaks of cytokine release can appear much earlier in LPS-challenged animals compared to other models of sepsis or in human sepsis [213-215]. Additionally, the dose of LPS used in most published *in vivo* sepsis studies in mice ranges from 1-80mg/kg which leads to a mortality rate of up to 50% [216]. This dose is between 10^3-10^4 times the dose required to induce septic shock in humans and 10^6 times the dose used in healthy volunteers to elicit pyrexia and elevated serum cytokines [217, 218].

Whilst the use of LPS challenge to model inflammation, infection and sepsis in non-pregnant animals is abundant, the vast majority of studies utilising LPS in pregnant animals do so to model PTL. Despite the lack of studies previously using this model to investigate sepsis during pregnancy, it is evident that LPS induces an inflammatory cascade which most consider to play a role in the onset of PTL.

1.3.2 Bacterial Inoculation Models

Following the strategy of administration of pathogens, some previous experiments have shown that pregnant mice (E14.5) inoculated with heat-killed *Escherichia coli* (*E. coli)* into the uterine horn or kidney delivered within 48 hours in a dose-dependent manner, equating to preterm birth [219, 220].

The literature describing animal models utilising live bacteria have demonstrated that there is an extremely variable phenotype depending on the type of bacteria used. For example, *Ureaplasma parvum*, a microorganism frequently associated with preterm birth and found in women presenting with chorioamnionitis, was found not to cause preterm delivery nor maternal mortality when injected via the intra-amniotic route in E13.5 CD1 mice [221]. Conversely, *Fusobacterium nucleatum* (gram-negative bacteria found in the oral cavity) injected intravenously into pregnant CD1 mice at E16 resulted in premature delivery, stillbirths and non-sustained live births. Interestingly, the *F. nucleatum* bacteria did not spread systemically, but were restricted to the uterus [222].

1.3.3 Models of Polymicrobial Sepsis

LPS endotoxaemia represents only one specific aspect of the immune response (signalling via TLR4) and not the complex interactions of multiple signalling pathways that occur during the progression of sepsis. Equally, both endotoxin injection and bacterial inoculum are followed by rapid elevations in cytokines which are much higher than observed in human sepsis [223]. Therefore, there is a need for a polymicrobial animal model of sepsis. The current gold standard animal model of polymicrobial sepsis is known as 'caecal ligation and puncture' (CLP) and is an example of a model that disturbs the endogenous intestinal barrier. In this model, the caecum of rodents is ligated and punctured with a needle, resulting in spillage of the intestinal contents into the peritoneum and the development of secondary bacterial peritonitis [216]. This model is one of the most stringent sepsis models in rodents and is considered to be crucial in preclinical testing of new therapies for sepsis in humans.

Despite the keywords 'caecal ligation puncture' bringing up over 2400 publications in NCBI PubMed, there have been no studies employing this procedure to study the effects of polymicrobial sepsis in pregnancy. This is surprising as one of the advantages of CLP is that it can recreate human sepsis progression with similar haemodynamic and metabolic phases, including both hyper- and hypo-inflammatory phases; also recreating the prolonged and lower elevation of cytokine release as in humans [142]. A mouse model of CLP in combination with radiotelemetry during pregnancy could be an ideal way to monitor and compare the normal cardiovascular adaptations that occur during pregnancy with the effects of polymicrobial sepsis. This method may also provide an opportunity to assess the potential adverse effects of new tocolytic and/or immunosuppressant therapies on the maternal ability to fight infection. However, it must be recognised, CLP does not exactly reproduce the clinical course of sepsis in humans.

Another model of polymicrobial sepsis was introduced in the late 1990s by Zantl *et al*., termed 'colon ascendens stent peritonitis' (CASP) [224]. The model involved the insertion of a small stent into the ascending colon of mice or rats leading to a continuous leaking of intestinal bacteria into the peritoneal cavity, resulting in peritonitis and systemic bacteraemia. The severity of the model can be

regulated by adjusting the diameter of the stent [225]. The CASP model is thought to be a reproducible model to enable investigations of peritoneal enterobacterial infection and sepsis progression. It has also been suggested that CASP is more representative of clinical sepsis, as opposed to a peritoneal abscess formation which is the main criticism of the CLP model. Although the prevalence of the CASP model in sepsis studies has only recently increased, the number of studies utilising the CLP sepsis model far exceed those using CASP [226].

There are several limitations of both CLP and CASP, including the large inter-study variations due to differences in protocols used between investigators (for example, the number of caecal punctures and sizes of needles or stents used to perforate the bowels) and inter-animal variability including differences in the amount of faecal content in the caecum at the time of surgery, the size of caecum of each animal, and bacterial flora in different animals. Most importantly however, there is no current animal model that can directly resemble complex human sepsis.

1.4 Clinical Relevance and Justification of Study

1.4.1 Sepsis in Pregnancy

Sepsis is now the leading cause of direct maternal mortality in the UK [227, 228]. Similarly, in developing countries, sepsis is one of the most important causes of maternal death [229, 230]. In the UK it is fortunately relatively rare with the rate of septic shock being 1.13 per 100,000 deliveries from 2006 to 2008 [231], however reports from Nigeria state that mortality related to maternal sepsis account for more than three times that number [229]. Furthermore, there is a higher incidence of pregnant women who suffer serious acute maternal morbidity (SAMM) as a result of sepsis, and although data are scarce, the reported incidence of SAMM in the western world is between 0.1 and 0.6 per 1000 deliveries [232, 233]. In 2011-2012, this equated to approximately 50 women for every maternal sepsis death in the UK [234].

A similar incidence of maternal sepsis has been reported in the USA, and worryingly, recent work has suggested an approximate doubling of the rate of severe maternal sepsis (since the period 1991-2003) and an increased risk of sepsis-related death [235, 236]. In 2014, Oud *et al.* found that in a population study in Texas, the rank of pregnancy-associated severe sepsis reported among hospital deaths had increased from sixth in 2001 to first (reported in up to 32.4% of cases) since 2008 [237]. These increases are expected to continue to increase in the future, and are thought to possibly be attributable to increasing maternal age that brings with it an increase in several co-morbidities [162]. These patients are more likely to require invasive diagnostic and therapeutic procedures that have been associated with an increased risk of septic complications [162, 238, 239]. It can be concluded therefore that maternal sepsis can be viewed as an infrequent but lethal complication of pregnancy that affects pregnant women on a global scale.

1.4.2 Maternal Infection and Preterm Labour

Premature delivery is one of the most important problems in obstetrics causing over 70% of neonatal death and handicap, where globally an estimated 15 million babies are born before 37 weeks of gestation annually [240, 241]. This translates to affecting between 5 and 18% of all pregnancies.

PTL is the leading cause and is often driven by maternal infection/inflammation. There is a correlation between gestational age and perinatal morbidity. Thus, whilst approximately 10% of all births are preterm, death and serious illness is most common in the 1-2% of infants delivered at less than 32 weeks of gestation [242]; furthermore, preterm pregnancies that are complicated by maternal infection are at greatest risk of cerebral palsy [243]. Infection and inflammation are now thought to account for PTL in over 40% of cases [182], and even subclinical infections can lead to severe neonatal morbidity and mortality [244-246].

1.5 Novel Hypotheses

It has been established that pregnancy is associated with an altered response to infection. Yet remarkably, there is little known about the effect of infection and sepsis in pregnancy on cardiovascular function, especially the adaptation and regulation of the peripheral vascular system that leads to the hypotension associated with severe sepsis.

In this thesis, the two main hypotheses are as follows:

- The haemodynamic response to infection and inflammation is altered in pregnancy.
- Agents targeting the chemokine and NO signaling pathways given in pregnancy could alter the maternal response to infection and inflammation.

1.5.1 Aims and Objectives

To explore these hypotheses, a telemetric method of measuring haemodynamic parameters during murine pregnancy in conscious mice need first be established, in which to investigate the cardiovascular response to inflammation in pregnancy. Further to this, the role of progesterone on inflammation-induced haemodynamic and immune alterations in pregnancy using progesterone supplementation will be determined. To try and understand the involvement of chemokines in these modulated responses, the role of chemokines (specifically CCL2/CCR2 signalling) in the inflammation-induced haemodynamic and immune responses in pregnancy using both CCR2-deficient mice and the pharmacological inhibition of CCR2 will be investigated. Finally, to try and understand the contribution of NO signalling to the altered responses in pregnancy to inflammation, focussing on the role played by the upstream endogenous ADMA inhibitor DDAH.

2. Materials and Methods

2.1 Materials

2.1.1 Reagents and Buffers

2.1.1.1 Chemicals and Solvents

Absolute Ethanol	VWR, Lutterworth, UK
Acetonitrile	Sigma-Aldrich, Poole, UK
ADMA	Merck Millipore, Billerica, MA, USA
Agarose (Iberose)	Web Scientific, Crewe, UK
D7-ADMA	Cambridge Isotope Laboratories, Cambridge, UK
Dithiothreitol	Sigma-Aldrich, Poole, UK
Ethidium bromide	Sigma-Aldrich, Poole, UK
Formic acid	Sigma-Aldrich, Poole, UK
Isopropanol	Sigma-Aldrich, Poole, UK
Methanol	VWR, Lutterworth, UK
Non-fat dried milk powder	Calbiochem, Millipore, Billerica, MA, USA
SYBR safe DNA gel stain	Life Technologies, Paisley, UK
Tween-20	Applichem, Darmstadt, Germany
Vanadium (II) chloride	Sigma-Aldrich, Poole, UK

2.1.1.2 Buffers

All chemicals used to make the following buffer recipes were purchased from Sigma-Aldrich, Poole, UK.

FACS Wash Buffer (FWB): 2% fetal calf serum (FCS), 0.1% NaN_3, 2mM EDTA

High Potassium Physiological Salt Solution (KPSS): 125mM KCl, 1.2mM $MgSO_4$, 1.2mM KH_2PO_4, 24.9mM $NaHCO_3$, 2.5mM $CaCl_2$, 11.1mM glucose. pH 7.4 when solution gassed with 95% O_2/ 5% CO_2 mixture.

NaOH Solution: 25mM NaOH, 0.2mM EDTA. pH 12.0.

Permeablizing Wash Buffer (PWB): 0.2% saponin, 0.5% bovine serum albumin (BSA), 0.1% NaN_3

Phosphate Buffered Saline (PBS): 140mM NaCl, 2.5mM KCl, 1.5mM KH_2PO_4, 10mM Na_2HPO_4. pH 7.2.

Physiological Salt Solution (PSS): 118.4mM NaCl, 4.8mM KCl, 1.2mM $MgSO_4$, 1.2mM KH_2PO_4, 24.9mM $NaHCO_3$, 2.5mM $CaCl_2$, 11.1mM glucose, 0.023mM EDTA. pH 7.4 when solution gassed with 95% O_2/ 5% CO_2 mixture.

Proteinase K Buffer: 1M Tris-HCl, pH8.5, 1M $MgCl_2$, 3M KCl, 1% Gelatine solution from porcine skin, Nonidet P-40, 0.45% Tween-20.

Tris-Buffered Saline with Tween-20 (TBS-T): 50mM Tris-HCl, 150mM NaCl, 0.01% (v/v) Tween-20. pH 7.5.

Tris-EDTA Buffer (TBE): 10mM Tris-HCl, 1mM EDTA. pH 8.0

Tris-HCl Buffer: 40mM Tris-HCl. pH 5.0.

2.1.1.3 PCR Reagents and Buffers

10mM dNTPs	Applied Biosciences, Foster City, CA, USA
10x NH4 Reaction Buffer	Bioline, London, UK
20U/µL RNase Inhibitor	Applied Biosciences, Foster City, CA, USA
25mM $MgCl_2$	Applied Biosciences, Foster City, CA, USA
2mM dNTPs	Bioline, London, UK
50mM $MgCl_2$	Bioline, London, UK
5nmoles Oligo d(T)	Applied Biosciences, Foster City, CA, USA
5U/µL Taq	Bioline, London, UK
Hyperladder I	Bioline, London, UK
Hyperladder III	Bioline, London, UK
Hyperladder V	Bioline, London, UK
MuLV 50U/ µL reverse transcriptase	Applied Biosciences, Foster City, CA, USA

PCR 0.1mL strip tubes	Qiagen, Crawley, UK
PCR Buffer	Applied Biosciences, Foster City, CA, USA
Power SYBR Green	Applied Biosystems, Warrington, UK
QiaShredder spin columns	Qiagen, Crawley, UK
Readymix Taq PCR reaction mix	Abgene, Thermo Scientific, MA, USA
RLT Lysis Buffer	Qiagen, Crawley, UK
TrackIt™	Invitrogen, Life Technologies, Paisley, UK

2.1.1.4 Protein Extraction and Western Blotting Reagents

DC Protein Assay Reagent A	Bio-Rad, Hemel Hempstead, UK
DC Protein Assay Reagent B	Bio-Rad, Hemel Hempstead, UK
DC Protein Assay Reagent S	Bio-Rad, Hemel Hempstead, UK
ECL-2 Plus	Pierce, Thermo Scientific, MA, USA
Halt Protease Inhibitor Cocktail	Thermo Scientific, MA, USA
Mini-PROTEAN TGX gels	Bio-Rad, Hemel Hempstead, UK
NuPAGE LDS sample buffer	Invitrogen, Life Technologies, Paisley, UK
Precision Plus™ Dual Colour Standard	Bio-Rad, Hemel Hempstead, UK
RIPA Buffer	Sigma-Aldrich, Poole, UK
SuperSignal Chemiluminescent Substrate	Pierce, Thermo Scientific, MA, USA
Trans-Blot Turbo™ PVDF membrane	Bio-Rad, Hemel Hempstead, UK

2.1.1.5 FACS Equipment and Reagents

40μM nylon cell strainer	BD, Falcon, Oxford, UK
AccuCheck counting beads	Invitrogen, Life Technologies, Paisley, UK
FACS lysing solution	BD, Falcon, Oxford, UK
gentleMACS M tubes	Miltenyi Biotex Ltd, Surrey, UK
IC fixation buffer	eBioscience, Hatfield, UK

Saponin	Sigma-Aldrich, Poole, UK
Sodium azide	Sigma-Aldrich, Poole, UK

2.1.1.6 Kits

Milliplex MAP Mouse Cytokine/Chemokine Magnetic Bead Panel	Merck Millipore, Billerica, MA, USA
Milliplex MAP Mouse Angiogenesis/Growth Factor Magnetic Bead Panel	Merck Millipore, Billerica, MA, USA
Mouse cGMP ELISA	Enzo Life Sciences, Farmingdale, NY, USA
Mouse PLGF2 ELISA	R&D Systems, Abingdon, UK
QIAgen RNeasy Mini Kit	Qiagen, Crawley, UK
QIAquick Gel Extraction Kit	Qiagen, Crawley, UK

2.1.2 Mice, Surgical Consumables and Drugs

25G 2.5cm needle	BD, Medisave, Weymouth, UK
4-0 Mersilk	MidMeds, Waltham Abbey, UK
Acetylcholine	Sigma-Aldrich, Poole, UK
Bovine serum albumin	Sigma-Aldrich, Poole, UK
Buprenorphine	Alstoe Animal Health, York, UK
CD1 mice	Charles River, Margate, UK
CD1 timed-mated mice	Harlan Laboratories, Bicester, UK
Dimethyl sulphoxide (DMSO)	Sigma-Aldrich, Poole, UK
Enrofloxacin	Bayer Animal Health, Newbury, UK
Evans Blue	Sigma-Aldrich, Poole, UK
Isoflurane	Abbot Laboratories, Maidenhead, UK
Lipopolysaccharide (O111:B4)	Sigma-Aldrich, Poole, UK
Microhaematocrit tubes	Sarstedt, Leicester, UK

Noradrenaline	Sigma-Aldrich, Poole, UK
PA-C10 Telemetry Device	Data Science International, Netherlands
Peanut Oil	Sigma-Aldrich, Poole, UK
Phenylephrine	Sigma-Aldrich, Poole, UK
Progesterone (P4)	Sigma-Aldrich, Poole, UK
RS504393	Tocris Bioscience, Bristol, UK
Sodium nitroprusside	Sigma-Aldrich, Poole, UK

2.1.3 Equipment

Agilent 6400 series LC-MS/MS	Agilent Technologies, Stockport, UK
AVerDiGi HYBRID Surveillance Platform	RF Concepts, Dundonald, UK
FACS CyAn ADP flow cytometer	Beckman Coulter, High Wycombe, UK
ND-1000 UV-Vis Spectrophotometer	NanoDrop Technologies, Labtech, UK
OPTImax tunable microplate reader	Molecular Devices, Wokingham, UK
RotorGene Sequence Detector	Corbett Research, Mortlake, Sydney, Australia
Sievers Nitric Oxide Analyser	GE Analytical Instruments, Manchester, UK
Tissue Tearor	BioSpec Products Inc, Bartlesville, OK, USA
Trans-Blot Turbo™ Transfer System	Bio-Rad, Hemel Hempstead, UK

2.1.4 Primer Sequences

Table 2.1: **Mouse primer sequences for use in PCR/ RT-PCR**. *Primers used for genotyping. [#]Sequence was provided by Jackson Laboratories. [##]Sequence obtain from Leiper laboratory. †Sequence obtained from Villanari *et al* (2013), [247].

Gene	Forward	Reverse	Ref Seq (NCBI/GenBank)
α-MHC	gaggaccaggccaatgagta	gctgggtgtaggagagcttg	NM010856
ANP	aacctgctagaccacctgga	tctctgaggtgggttgacct	AF460238
β-actin	aggctgtgctgtccctgtat	gctgtggtggtgaagctgta	NM007393
β-MHC	atgccaggattgaggatgag	ccagcctctcactgatctcc	NM080728
Bad	aggatcgctgtgtcccttta	gcagtccagaacaggagagg	NM_007522.2
Bax	tgcagaggatgattgctgac	gatcagctcgggcactttag	NM_007527.3
Bcl-2	yaatggaggagtcggtttgc	gctgctgctgcttcttcttt	NM_009741.3
BNF	cagctcttgaaggaccaagg	tccgatccggtctatcttgt	NM008726
CCR2 (WT)*	ccacagaatcaaaggaaatgg	ccaatgtgatagagccctgtg	[#]
CCR2 (KO)*	cttgggtggagaggctattc	aggtgagatgacaggagatc	[#]
COX-2	tgcagaattgaaagccctct	gctcggcttccagtattgag	NM_011198.3
Cre*	gcctgcattaccggtcgatgca	gtggcacatggcgcggaac	[##]
DDAH1 (floxed)*	cctcccattgctaatgaaacgg	tcagttggagtgtgagtgac	[##]
cTroponin-I	gaagcaggagatggaacgag	ttaaacttgccacggaggtc	NM_009406.3
CXCL1	gcctatcgccaatgagctg	aagggagcttcagggtcaag	NM_008176.3
CXCL2	agtgaactgcgctgtcaatg	ttcagggtcaaggcaaactt	NM_009140.2
CXCR1	gggtgaagccacaacagatt	tagggcagacaacagagcaa	NM_178241.4
CXCR2	atcttcgctgtcgtccttgt	agccaagaatctccgtagca	NM_009909.3
eNOS	aagacaaggcagcggtgg	gcaggggacaggaaatagtt	NM_008713.4
Endothelin-1	tcgtgactttccaaggagct	ccaggtggcagaagtagaca	NM_010104.3
FasL	catcacaaccactcccactg	gttctgccagttccttctgc	NM_010177.4
GAPDH	actccactcacggcaaattc	tctccatggtggtgaagaca	NM001001303
Hsp70	atgaaggagatcgctgag	tgagagtcgttgaagtagg	†
IL-1β	gctgcttccaaacctttgac	tgtcctcatcctggaaggtc	NM_008361
IL-4	tgacggcacagagctattga	ggtgttcttcgttgctgtga	M25892.1
IL-6	ccggagaggagacttcacag	ttctgcaagtgcatcatcgt	NM_031168
IL-10	ccaagccttatcggaaatga	gctccactgccttgctctta	NM_010548.2
iNOS	cagctgggctgtacaaacctt	atgtgatgtttgcttcggaca	NM_010927.3
NKAα1	ttcccttcaactccaccaac	cgtccttcagctcttcatcc	NM_144900.2
NKAα3	ccaagtgcgactgtgtgtct	cacgagagccatatgagcaa	NM_144921.1
NKx2.5	gctacaagtgcaagcgacag	gggtaggcgttgtagccata	NM_008700.2
PLN	tcgcctccttacctccacta	agcttcagcgtcacgtttct	NM_001141927.1
RP-L19	ggtgacctggatgagaagga	ttcagcttgtggatgtgctc	NM_009078.2
RP-S18	tgtggtgttgaggaaagcag	tcccatccttcacatccttc	NM_011296.2
SERCA	aagctatgggagtggtggtg	gcaatgcaaatgagggagat	NM009722
TNF-α	tggcagaagaggcactcc	gaggccatttgggaacttct	NM_013693
VEGF-A	atggcatgctttgtggatcc	taccaggcctcttcttccac	AF317892.1
VEGF-B	tggtgccatggatagacgtt	tgcattcggacttggtgttg	NM_011697.3

2.1.5 Antibodies

Table 2.2: **Antibodies used for FACS**

Antibody	Source
Ly6C (HK1.4)	BioLegend, Cambridge, UK
Gr1 (RB6-8C5)	BioLegend, Cambridge, UK
NK1.1 (PK136)	BioLegend, Cambridge, UK
F4/80 (Cl:A3-1)	BioLegend, Cambridge, UK
CD45 (30-F11)	BioLegend, Cambridge, UK
CD86 (B7-2)	eBioscience, Hatfield, UK
CD11b (M1/70)	eBioscience, Hatfield, UK
MHCII (AMS-32.1)	eBioscience, Hatfield, UK
F4/80 (BM8)	eBioscience, Hatfield, UK
COX-2 (M19)	Santa Cruz Biotechnology, Santa Cruz, CA, USA

Table 2.3: **Antibodies for use in Western Blotting.** *Antibodies were purified from goat serum in-house.

Antibody	Concentration	Source
Caspase-3 (ABIN125614)	1:500	Antibodies-online.com
DDAH1	1:4000	*
DDAH2	1:2000	*

2.2 *In Vivo* Methods

2.2.1 Animals

All animal procedures were carried out in accordance with the Home Office Animals (Scientific Procedures) Act, 1986, under project licenses 70/7372 (Imperial College) or 70/6096 (availability at UCL) and were previously approved by the Animal Welfare and Ethical Review Board (AWERB) at Imperial College London. All mice were housed in individually ventilated cages with access to normal rodent chow and water *ad libitum*, and maintained on a 12:12 light-dark cycle.

Unless otherwise specified, experiments were performed using female CD1 mice aged 7-9 weeks. Mice were purchased from Charles River (Margate, UK) aged 6-8 weeks and acclimatised for at least 1 week. CD1 stud males were used for timed mating with CD1 as well as $CCR2^{-/-}$ and $DDAH1^{-/-}$ female mice.

Mice lacking CCR2 ($CCR2^{-/-}$), originally from Jackson Laboratories [248], were maintained on an outbred CD1 background and bred in house using homozygous knockout breeding pairs. Experimental females were used aged 7-9 weeks. Wild-type (WT) controls were female CD1 mice purchased from Charles River (Margate, UK).

DDAH1 heterozygous floxed mice were generated by Genoway (Lyon, France) and mated to generate homozygous progeny. DDAH1 knockouts ($DDAH1^{-/-}$) were maintained on a mixed C57BL/6 background. Initial attempts to breed a DDAH1 knockout mouse were embryonic lethal [249], however deletion of exon one using the cre/lox-P system produced viable offspring. Cre was expressed under the control of α-actin which is expressed globally. DDAH1 heterozygous ($DDAH^{-/+}$ with cre negative female, cre positive male) matings produced experimental females. Litters therefore contained an approximate 1:1 ratio of DDAH1 cre positive and cre negative mice. Both homozygous $DDAH1^{-/-}$ and WT littermates were used aged 12-16 weeks.

For myography experiments, timed-mated female CD1 mice were purchased from Harlan Laboratories (Bicester, UK) so that mice would be of known gestation (E16) on consecutive working days.

2.2.2 Genotyping

Mice were weaned at 3-4 weeks and ear notched where necessary for identification. Tail clippings were taken for genotyping.

2.2.2.1 CCR2$^{-/-}$ Colony

To extract genomic DNA from CCR2 colony mice, tissue was submerged in 75µL NaOH solution and thoroughly vortexed. Samples were heated to 95^{o}C for 10 minutes before cooling to 4^{o}C by quickly plunging into ice. 75µL of Tris-HCl, pH 5.0 was then added to each sample before mixing by vortex and centrifugation. Polymerase chain reaction (PCR) was performed using heat stable DNA polymerase, Taq. Per reaction, 2µL 10x NH4 reaction buffer, 2µL 2mM dNTPs, 0.6µL 50mM $MgCl_2$, 0.1µL 5U/µL Taq (all from Bioline, London, UK), 1µL forward primer, 1µL reverse primer, 4µL DNA and 9.3µL dH_20 was used. Thermocycler conditions were as follows: hold for 5 minutes at 95^{o}C, 35 cycles of 30s at 95^{o}C, 60s at 65^{o}C, 120s at 72^{o}C, then a final extension for 10 minutes at 72^{o}C. Primer sequences are shown in Table 2.1. PCR products were separated by agarose gel (1.5%, containing 1x SYBR safe (Life Technologies, Paisley, UK)) and visualised under ultraviolet (UV) light using TrackIt™ (Invitrogen, Life Technologies, Paisley UK) loading buffer (Figure 2.1). Product sizes were confirmed through the use of the appropriate DNA ladder (Hyperladder; Bioline, London, UK) (Figure 2.1).

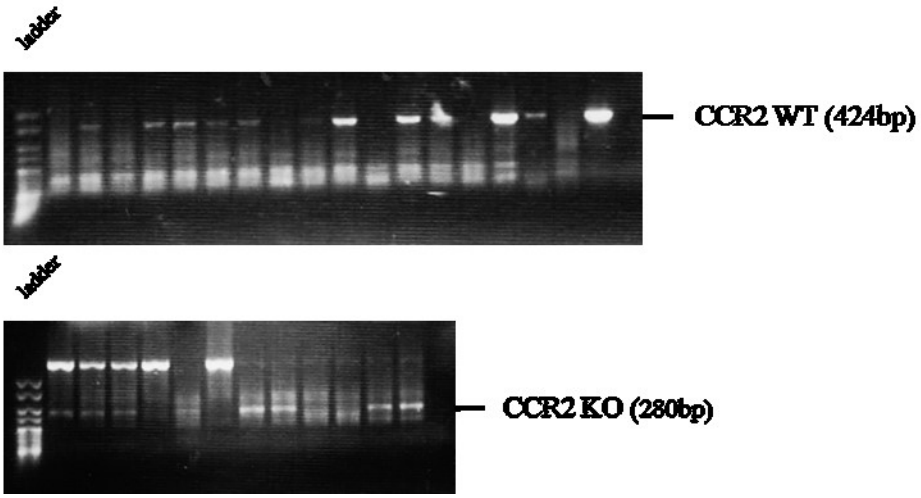


Figure 2.1: **Genotyping gels of CCR2 expression.** CCR2 genotype was identified due to either a single band at 424 base pairs (WT), a single band at 280 base pairs (homozygous knockout, KO), or the presence of both bands (heterozygote) (bp, base pairs).

2.2.2.2 DDAH1$^{-/-}$ Colony

This work was done by Mr. Matthew Delahaye (NOS Signalling Group).

To extract genomic DNA from DDAH1 colony mice, tail clippings were digested overnight at 53-55^{o}C in a digestive Proteinase K Buffer. After digestion the proteinase K was deactivated at 94^{o}C for 10 minutes. PCR was performed using 1x Readymix Taq PCR reaction mix which contained polymerase, dNTPs and loading dye (Abgene, Thermo Scientific, MA). Both DDAH1 floxed and Cre primer protocols utilised a hold of 2 minutes at 94^{o}C, then 20s at 94^{o}C, 40s at 60^{o}C and 60s at 72^{o}C for 40 cycles, before a final extension of 5 minutes at 72^{o}C. Primer sequences are shown in Table 2.1. PCR products were separated by agarose gel (1.5%, containing 0.01% ethidium bromide; EtBr) and EtBr-stained DNA bands were visualised under UV light (Figure 2.2).

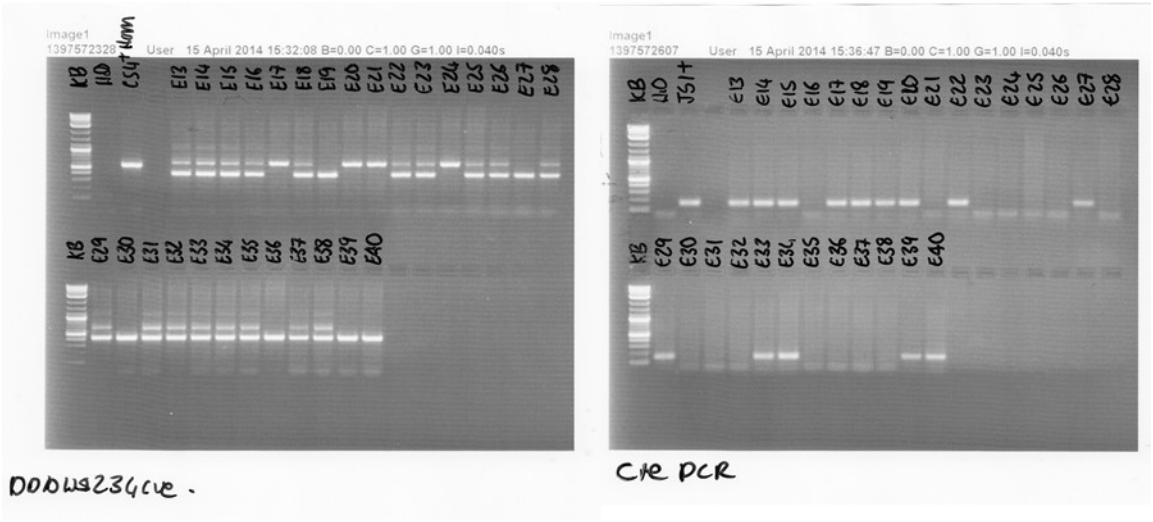


Figure 2.2: **Genotyping gels of DDAH1 floxed alleles and cre expression.** DDAH1 genotype was identified due to either a single band at 427 base pairs (WT), a single band at 568 base pairs (homozygous knockout), or the presence of both bands (heterozygote). Cre recombinase expression was verified through the presence of a single band at 720 base pairs.

2.2.3 Telemetry

Telemetry is a technology that allows the remote measurement of physiological and bioelectrical variables in freely-moving conscious animals. The absence of tethering, handling and restraint during measurement has provided the unique opportunity to study laboratory animals with reduced distress, discomfort and physiological disturbance over long periods of time in their normal housing. Long-term telemetric measurement of cardiovascular parameters such as blood pressure and heart rate in awake pregnant mice was a technique optimised by Butz and Davisson to study cardiovascular regulation during pregnancy [250], demonstrating the feasibility of radiotelemetric monitoring throughout pregnancy in mice. The advantages of this method include that it can reduce the numbers of animals used in each experiment. This is achieved by decreasing any variation due to stress and by enabling each animal to act as its own control.

2.2.3.1 Telemetry Device Implantation

Before surgery, mice received a subcutaneous injection of 5% enrofloxacin and 0.3mg/mL buprenorphine. Female CD1 mice were anaesthetised with isoflurane (5% induction, 2% maintenance,

2L/min O_2 flow rate) and the neck and chest were shaved and swabbed with povidone iodine. Animals were placed supine on the dorsal side on a heated mat, with the nose just inside a modified smaller sized coaxial Bain circuit nosecone for anaesthetic delivery. Forelimbs were loosely secured using tape and the nose held inside the anaesthetic tube by a loop of mersilk around the upper incisors and anchored to the surface. Surgical anaesthesia level was confirmed by a lack of pedal pinch reflex response. A ventral midline incision was made and the submandibular glands were gently separated before isolation of the left common carotid artery. The artery was tied off at the distal end to the aorta; temporarily occluded at the proximal end, and punctured with iris scissors or an adapted angled 25G needle (BD, Medisave, Weymouth, UK). The catheter tip of the transmitter was then advanced to the aortic arch and secured with two sutures (anterior and posterior) (Figure 2.3A). The transmitter body was then advanced subcutaneously to lie over the right flank (Figure 2.3B) before the incision was closed (4-0 Mersilk, MidMeds, Waltham Abbey, UK). Mice were then placed into a heated recovery chamber (30^{o}C). All mice were individually housed after implantation of the device.

Animal weights, surgical wound healing, general health and any signs of morbidity were observed daily for 5-7 days post-operatively to ensure good recovery. Over the course of this study, over 95% of mice survived surgery, with a further 90% surviving the post-operative recovery period. At the end of these experiments, mice were terminally anaesthetised before device removal. Device sterilisation was achieved using enzymatic detergent and cold sterilant.

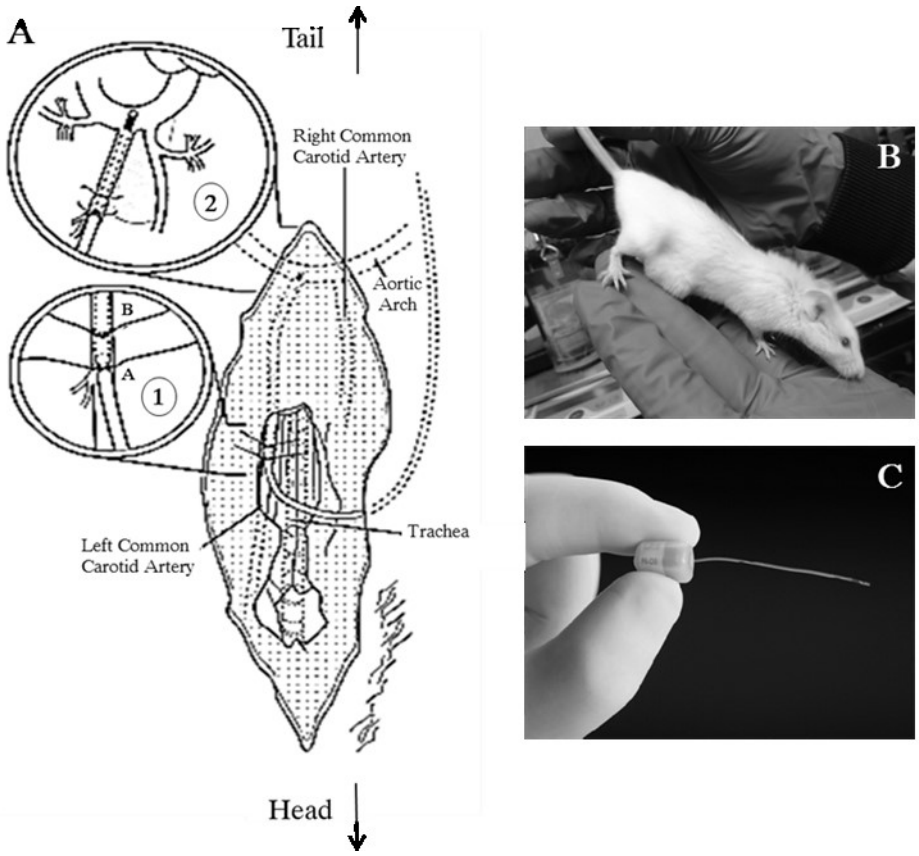


Figure 2.3: **Telemetry transmitter placement.** (A) Surgical procedure diagram for implantation of the telemetry device in the thoracic aorta via the left common carotid artery. Insets 1 and 2 are enlargements illustrating the catheter insertion site and tip placement (in the thoracic aorta). In Inset 1, A and B refer to the anterior and posterior ligatures, respectively. Adapted from Butz and Davisson [250]. (B) Subcutaneous placement of the transmitter body on the right flank. (C) DSI PA-C10 telemetry device before implantation (adapted from www.nc3rs.org.uk).

2.2.3.2 Telemetry Recording, Acquisition and Analysis

On day 8 after surgery, continuous 24 hour recording (data collection) began using the Dataquest ART Acquisition System (Data Sciences International, v4.1) for at least 48 hours to collect data in non-pregnant animals (non-pregnant baseline). These data allowed animals to act as their own controls. Radiotelemeters were magnetically activated and deactivated. Whilst recording, animals were kept in their home cages with access to food and water *ad libitum*; however these cages were placed in a separate room for recording. This environment was chosen to cause fewer disturbances from other facility users and staff.

For longitudinal studies which required recording throughout the course of gestation, data collection was resumed after evidence of a copulatory plug had been observed (E0) and continued up until 3 days post-partum; no data were collected during mating. For all other studies, data was collected during the following time points: E8-E9 (48hrs), E15-postpartum (48-120hrs).

Collected parameters included mean arterial pressure (MAP), systolic arterial pressure (SAP), diastolic arterial pressure (DAP), heart rate (HR), and activity. Haemodynamic data were collected for 10 seconds every 30 seconds. Labour time and litter sizes were also recorded. Accurate labour time was enabled by the use of infrared IP cameras in conjunction with the AVerDiGi (NV3000 Series) HYBRID Surveillance Platform (RF Concepts, Dundonald, UK).

2.2.4 PTL Model (Systemic Endotoxaemia) and Pharmacological Intervention

2.2.4.1 PTL Model (Systemic Endotoxaemia)

The administration of *E. coli* lipopolysaccharide (LPS) to rodents is a widely accepted technique which aims to model bacterial infection-induced PTL. However, the method of administration and dose of LPS previously used has been diverse [251]. Elovitz *et al*., reported a reproducible model using intrauterine administration of LPS that resulted in 100% PTL with no maternal mortality [252]. An adapted version of this model using 10μg LPS administered via the intrauterine route was subsequently established within our group; however the laparotomy required for intrauterine administration of LPS and the telemetry implantation surgery was not possible under the current Procedure Project Licence (PPL). Therefore we aimed to establish a systemic endotoxaemic model using the intraperitoneal (i.p.) route.

LPS endotoxin (serotype O111:B4; Sigma-Aldrich, Poole, UK) or sterile vehicle control (PBS) were administered systemically (i.p.). The dose of LPS was firstly determined using a dose-response study in CD1 females on E16 using a range of doses indicated by the intrauterine work in our group and current literature. A single injection of 10μg LPS per dam (in 100μL PBS) resulted in no maternal mortality and gave the most consistent outcomes in latency to labour and pup survival. All pregnant

mice were anaesthetised under isoflurane for i.p. injection to minimise potential harm to fetuses and were carried out between 8am and 10am.

2.2.4.2 Progesterone Treatment

In those experiments examining the role of progesterone, P4 (Sigma-Aldrich, Poole, UK) was dissolved in peanut oil (Sigma-Aldrich, Poole, UK) at a stock concentration of 250mg/mL. After initial dose-finding experiments, a final concentration of 10mg per mouse (in 40μL peanut oil) was injected subcutaneously (s/c) into the right flank. P4 or vehicle (peanut oil) injections were carried out once a day from E14 to E16 between 8am-10am.

2.2.4.3 CCR2 Antagonism

In those experiments using pharmacological inhibition of CCR2, the CCR2 antagonist RS504393 (Tocris Bioscience, Bristol, UK) was used at a final concentration of 2mg/kg per mouse. RS504393 was dissolved in dimethyl sulfoxide (DMSO; Sigma-Aldrich, Poole, UK) at a stock concentration of 4mg/mL and stored at -20^{o}C. One hour prior to use, stock solutions were thawed, diluted in sterile PBS and thoroughly vortexed so that the final DMSO concentration was 5%. RS504393 or vehicle (5% DMSO in PBS) was injected s/c into the right and left flank (half dose in each side) 30 minutes before LPS (on E16) and then every 12 hours until labour. Initial toxicity studies indicated that RS504393 alone did not confer any morbidity or alter labour times (n=3).

2.2.5 Tissue Collection

To record accurate haemodynamic data it is imperative to keep disturbances to a minimum. Therefore, blood, serum and other tissues were taken from separate groups of animals at two time points, 6 hours and 12 hours post i.p injection.

Mice were terminally anaesthetised using isoflurane (5% induction, 3% maintenance, 2L/min O_2 flow rate) and a cardiac puncture was performed to collect plasma or serum samples. Subsequent to schedule 1 culling, lung, heart, left ventricle, myometrium and placenta were collected and snap

frozen on dry ice. These samples were then stored at -80°C until needed for RNA and protein extraction.

For myography studies, thoracic aorta and uterine artery were dissected from a separate group of animals (see section 2.2.6).

Strips from left and right horn myometrium, lung, liver (sections from each lobe), placenta and blood (mixed with 5mM EDTA) were also temporarily stored (for up to 6h) in PBS for subsequent FACS analysis (see section 2.2.8).

In addition, Dr Bronwen Herbert gifted serum samples taken at extended time points (NP, E6, E11, E16, E18 and 36 hours post-partum) to be used to examine PLGF levels over the course of gestation.

2.2.6 Wire Myography

This work was done in collaboration with Anna Slaviero DVM (MRC Whole Animal Physiology team).

Vessel function and sensitivity to vasoactive substances was assessed by wire myography. Both aorta and uterine vessels were dissected from pregnant (E16) or non-pregnant CD1 mice. Animals received either vehicle (PBS) or 10µg LPS injected i.p. 12 hours before culling using schedule 1 procedure.

2.2.6.1 Preparation of Vessels

The thoracic aorta was dissected, extraneous connective tissue removed, and immediately placed in cold (4°C) physiological salt solution (PSS). The uterus was then dissected from below the ovaries to the upper cervix and the uterine artery identified and carefully dissected. Aortic sections (2mm), taken from the centre of the vessel, were mounted in parallel on the DMT vessel myograph (DMT, Aarchus, Denmark) using the pin mounting system. Vessels were gradually warmed to 37°C in PSS aerated with 95% O2, 5% CO2 for 30-60 minutes. Uterine vessels were mounted onto much thinner 20µm

tungsten wires. These were connected to an isometric force transducer which was then calibrated to zero.

2.2.6.2 Normalisation and Viability of Tissues

Once the myograph was at zero, tension was applied to the mounted vessels such that the force display was adjusted to 70 mmHg for aorta, and 45 mmHg for uterine artery. The vessels were then left to equilibrate for approximately 20 minutes before buffer was refreshed and the force adjusted to 10mN. Force was again adjusted to 10mN after two further 20 minute equilibrations; buffer was changed after every 20 minute period.

Viability of tissues was confirmed using a standard 'wake up' protocol. To obtain optimal data from vessels, it is important to ascertain that functional response is not compromised by the dissection, isolation and mounting of the vessels [253]. This was performed by testing contractile ability using the response to high potassium depolarisation and a standard vasoconstrictor, noradrenaline (NA). Briefly, vessels were stimulated with potassium physiological salt solution (KPSS) with 10μM noradrenaline (Sigma-Aldrich, Poole, UK) for 3 minutes (when contraction reaches plateau) before 4x washes with PSS. This was repeated twice more before stimulating with KPSS alone for 3 minutes twice. If vessels failed to contract to KPSS with NA, or KPSS alone they were excluded from the study.

2.2.6.3 Concentration Response Curves

Cumulative concentration response curves were performed for phenylephrine (PE; from 10^{-6} M to 10^{-2} M), acetylcholine (ACh; from 10^{-6}M to 10^{-2}M), and sodium nitroprusside (SNP; from 10^{-7} M to 10^{-3} M); all drugs were procured from Sigma-Aldrich, Poole, UK. After each dose, time was given for the response to reach a plateau before continuing with the next dose. After the final concentration had been added, vessels were washed 4 times with PSS and left for 5 minutes to rest. In order to allow

for a relaxation response, before ACh or SNP were added, a dose of PE corresponding to 80% of the maximum concentration obtained was added to contract each vessel.

2.2.7 Plasma Volume Determination

To determine any plasma volume differences between pregnant (E16) and non-pregnant mice, an Evans Blue dilution method was used, as previously described by Sena *et al*., [254]. A 0.08% (w/v) of Evans Blue dye (Sigma-Aldrich, Poole, UK) solution was made up in sterile PBS. 100µL was then injected intravenously (i.v.) into the tail vein of CD1 mice that had been placed in a warming chamber at 34^{o}C for up to 10 minutes prior to the procedure. At 10 and 30 minutes post-injection venous blood was collected in microhaematocrit tubes (Sarstedt, Leicester, UK) to measure disappearance kinetics. After centrifugation at 13,000 rpm, plasma was diluted 1:15 in water before samples were added in duplicate onto a 96-well plate. Evans blue concentration in the plasma was measured as optical density on a spectrophotometer (OPTImax tunable microplate reader; Molecular Devices, Wokingham, UK) at λ=620nm.

Concentrations were determined using a standard curve constructed using known amounts of Evans Blue made up in a bovine serum albumin (BSA, Sigma-Aldrich, Poole, UK) solution (Figure 2.4A). Data were analysed using a least-square line fitted to the data at 10 and 30 minutes from each individual mouse. Extrapolation of the regression line back to x=0 meant plasma volume could be calculated as the total quantity injected, divided by the y intercept (Figure 2.4B).

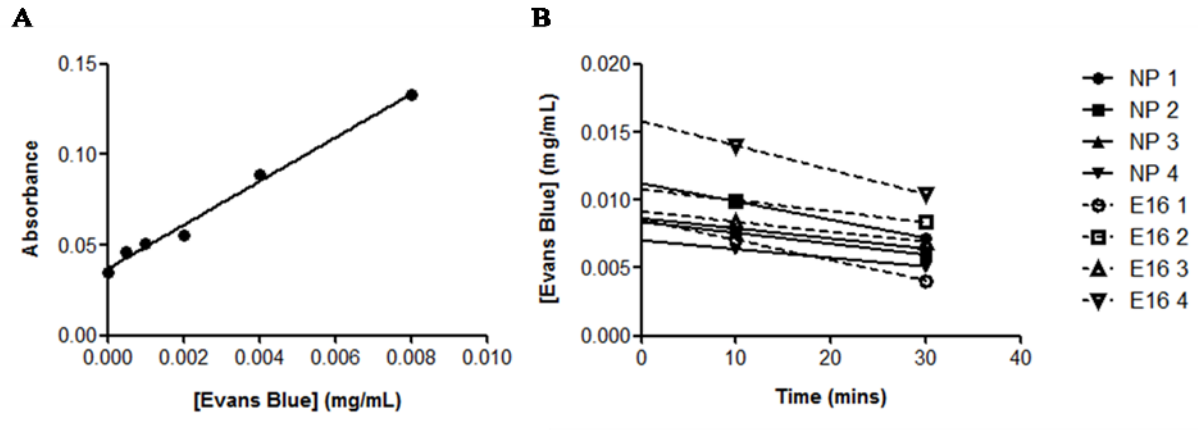


Figure 2.4: **Calculation of plasma volume using Evans Blue dilution method.** (A) Standard curve showing known amounts of Evans Blue against absorbance as determined by optical density at λ=620nm. (B) Extrapolation of the regression line back to x=0 determines the Evans Blue concentration as diluted by plasma volume. NP- non-pregnant, E16- pregnant.

2.2.8 Flow Cytometry

This work was performed in collaboration with Ms. Lydia Edey (Imperial Parturition Group).

Fluorescence-activated cell sorting (FACS) technique was employed to assess leukocyte cell densities in maternal blood and tissues. Lung and liver were homogenised using gentleMACS M tubes (Miltenyi Biotex Ltd, Surrey, UK) containing 1mL of IC fixation buffer (eBioscience, Hatfield UK) for 1 minute. After filtering through a 40µm nylon cell strainer (BD Falcon, Oxford UK), cell suspensions were centrifuged twice at 1450 rpm for 5 minutes to extract leukocytes. After the first centrifugation, cells were re-suspended in FACS wash buffer (FWB). After the final centrifugation cells were re-suspended in permeablizing wash buffer (PWB). The exact volume of the cell suspension was assessed and recorded. EDTA was added to blood samples at a 1:10 ratio and incubated at RT.

All cell samples were then incubated with the appropriate antibodies for 30 minutes at 4^{o}C. Fluorophore-conjugated rat anti-mouse monoclonal antibodies were used for staining (outlined in Table 2.2). Following the incubation, samples were re-suspended in 4mL PWB for tissue, and 4mL FWB for blood. All samples were then centrifuged at 2000 rpm for 5 minutes at 4 ^{o}C. Following this,

tissue samples were re-suspended in 400µL PWB. FACS lysing solution (BD, Falcon, Oxford UK) was used to lyse erythrocytes in blood samples before a final centrifugation and re-suspension in 400µL FWB.

Cell counts were determined using AccuCheck counting beads (Invitrogen, Life Technologies, Paisley UK). Samples were run using a CyAn ADP Beckman Coulter flow cytometer in conjunction with Cell Quest 3.3 software. Data were analysed using FlowJo version 7.6.5.

2.3 *In Vitro* Methods

2.3.1 Reverse Transcriptase Polymerase Chain Reaction (RT-PCR)

2.3.1.1 mRNA Extraction

mRNA was extracted from mouse tissue using the QIAgen RNeasy Mini Kit (Qiagen, Manchester, UK) according to manufacturer's instructions. Homogenisation was achieved using a RLT lysis buffer (Qiagen, Crawley, UK) with 2M DTT (Sigma-Aldrich, Poole, UK) added before mechanical homogenisation (Tissue Tearor, BioSpec Products Inc, Bartlesville, OK). The tissue lysate was put through QIAshredder columns (Qiagen, Crawley, UK) to eliminate DNA contamination prior to addition to the RNeasy spin columns. RNA yield was quantified using a ND-1000 UV-Vis spectrophotometer (NanoDrop Technologies, Labtech International, UK). RNA sample purity was assessed using $A_{260/280}$ ratio of approximately 2.0. Resulting RNA samples were stored at -80^{o}C.

2.3.1.2 cDNA Synthesis

Reverse transcription of RNA for cDNA synthesis was performed using 2µg RNA heated at 70°C for 5 minutes before incubation with 4µL PCR Buffer II (2x) (Applied Biosciences (AB) Foster City, CA), 8µL 25mM $MgCl_2$ (AB) 8µL 10mM dNTP (AB), 1µL 20U/µL RNase Inhibitor (AB), 1µL 5nmoles Oligo d(T) (AB), and 1µL MuLV 50U/µL reverse transcriptase (AB) at 42°C for 60 minutes, followed by 5 minutes at 95°C. Samples were then quickly chilled to 4°C, and the resulting cDNA stored at -20°C.

2.3.1.3 Primer design and Production of Standards

Paired oligonucleotide primers for amplification of genes of interest were designed using Primer 3 software (http://frodo.wi.mit.edu/cgi-bin/primer3/primer3_www.cgi) against the sequences downloaded from GenBank (Table 2.1). Standards were constructed using PCR (2uL mouse cDNA, 10uL Power SYBR Green (Life Technologies, Paisley, UK), 7uL water, 1uL primer F/R) where the

reaction conditions were 10min at 95°C followed by up to 60 cycles of 95°C for 20s, 60°C for 20s and 72°C for 20s followed by an extension at 72°C for 15s. Gel extraction of the PCR product was then performed using agarose gel electrophoresis (agarose gels were prepared using 1.5% agarose in 1x TBE buffer, plus SYBR safe (Life Technologies, Paisley, UK)) followed by extraction using QIAquick gel extraction kit (Qiagen, Crawley, UK) according to manufacturer's instructions. PCR product size was confirmed through the use of the appropriate DNA ladder (Hyperladder; Bioline, London, UK). Standards were prepared using 1:10 serial dilutions in distilled water. In subsequent reverse transcriptase PCR (RT-PCR) assays, standards 3-9 were used alongside a water blank (no-template control).

2.3.1.4 RT-PCR

2µL cDNA templates were combined with the 1uL of primer (mixed forward and reverse), 10µL Power SYBR Green (Applied Biosystems, Warrington, UK) and 7µL distilled water in PCR 0.1mL strip tubes (Qiagen, Crawley, UK). Amplicon yield was monitored during cycling in a RotorGene Sequence Detector (Corbett Research Ltd., Mortlake, Sydney, Australia). Pre-PCR cycle was 10min at 95^{o}C followed by up to 65 cycles of 95^{o}C for 20s, 60^{o}C for 20s and 72^{o}C for 20s followed by an extension at 72^{o}C for 15s. To determine amplicon purity, a melt curve was constructed over the temperature range of 72-99^{o}C rising by 1 degree steps with a wait for 15s on the first step followed by a wait of 5s for each subsequent step. One single peak alluded to a pure product without dimer contamination. The cycle at which the fluorescence reached a pre-set threshold (cycle threshold) was used for semi-quantitative analyses. The cycle threshold in each assay was set at a level where the exponential increase in amplicon abundance was approximately parallel between all samples.

By use of the comparison to standards, relative concentrations could be determined. These were then normalised to a housekeeping (or reference) gene. Four housekeeping genes, selected for their stability across all treatment groups, were used in this study: Glyceraldehyde 3-phosphate dehydrogenase (GAPDH), β-actin, ribosomal protein s18 (s18) and ribosomal protein L19 (L19)

[255]. In heart and left ventricular tissue, s18 was found to be the most consistently expressed, and in placenta GAPDH was found to be most consistently expressed and so these comparisons are shown in subsequent analyses.

2.3.2 Protein Expression Analysis

2.3.2.1 Protein Extraction

Protein was extracted from mouse tissue using mechanical homogenisation (Tissue Tearor, BioSpec Products Inc, Bartlesville, OK) in RIPA buffer (Sigma-Aldrich, Poole, UK) with added protease inhibitor (Halt Protease Inhibitor Cocktail, Thermo Scientific) and phosphatase inhibitor (Halt Phosphatase Inhibitor Cocktail, Thermo Scientific, MA) at 4^{o}C. Lysates were centrifuged at 4^{o}C at 13,300 rpm for 20 minutes and the supernatant aliquoted. Concentration of protein in each sample was determined by protein assay.

2.3.2.2 Protein Assay

To quantify protein concentrations in tissue homogenates, a DC protein assay (Bio-Rad, Hemel Hempstead, UK) was performed according to manufacturer's instructions. These reagents allow for concentration determination following detergent solubilisation, similar to the well-documented Lowry assay [256]. Briefly, in a 96-well plate 7 dilutions of BSA (Sigma-Aldrich, Poole, UK) in duplicate were used to construct a standard curve, made up in the appropriate buffer. 5µL of each sample were added in duplicate to the plate, previously diluted in the appropriate buffer 1:3 or 1:5. Reagent S was combined 1:50 with Reagent A (an alkaline copper tartrate solution) before added 25µL to each well. 200µL of Reagent B (a dilute Folin reagent) was then added to each well and the plate was gently mixed for 30s on a plate shaker. The plate was incubated at room temperature for 10-20 minutes before reading optical density on a spectrophotometer (OPTImax tunable microplate reader; Molecular Devices, Wokingham, UK) at λ=595nm.

2.3.2.3 SDS-PAGE and Western Blot

Electrophoresis was carried out on aliquots of protein samples that were denatured by adding NuPAGE LDS sample buffer (Invitrogen, Life Technologies, Paisley, UK) and DTT (Sigma-Aldrich, Poole, UK) at a final concentration of 20mM and heating for 10min at 70-80^{o}C. 40µg of protein sample was loaded into each well on pre-cast 15 well 4-15% Mini-protean TGX gels (Bio-Rad, Hemel Hempstead, UK). Proteins were separated by electrophoresis in 1x SDS running buffer for 40-60 minutes at 80-120V.

Western blotting was performed following a 7-minute electrophoretic transfer onto Trans-Blot Turbo™ PVDF membrane (Bio-Rad, Hemel Hempstead, UK) using the Trans-Blot Turbo™ Transfer System (Bio-Rad, Hemel Hempstead, UK). Membranes were blocked in blocking buffer (5% milk in 1x TBS-T) for 1 hour at room temperature, washed in 1×TBST and hybridized with the primary antibody over night at 4^{o}C in 1% milk. Antibody details are outlined in Table 2.3. Membranes were washed again and then incubated with secondary antibody at a dilution of 1:2000 in 1% milk for 2 hours at room temperature. SuperSignal West Pico Chemiluminescent Substrate (Pierce, Thermo Scientific, MA) or ECL-2 Plus (Pierce, Thermo Scientific, MA) was used for detection. Protein band size was determined using Precision Plus Protein™ Dual Colour Standard (Bio-Rad, Hemel Hempstead, UK).

DDAH1 and DDAH2 western blots were completed by MSc project student, Miss Stephanie Dowle.

2.3.2.4 Multiplex Assay

Tissue homogenates were prepared as described in section 2.3.2.2. Serum or tissue samples were prepared for analysis in a 96-well plate using a bespoke 9-, 7-, 5-, or 3-plex mouse cytokine/chemokine or angiogenesis/growth factor magnetic bead panel (Merck Millipore, Billerica MA, USA) according to manufacturer's protocol. Analytes were quantified using a Luminex MAGPIX instrument with xPonent 4.2 software (Luminex Corp., Austin TX, USA) or Bioplex Manager MP (Bio-Rad, Hemel Hempstead, UK).

Briefly, colour-coded microspheres were provided where each distinctly coloured bead set was coated with a specific capture antibody. Analytes in each test sample were then captured by the bead before a biotinylated detection antibody was introduced. This was followed by the addition of Streptavdidin-phyocoerythrin conjugate, which attaches as a reporter molecule. The microspheres were then passed rapidly through a laser in the MAGPIX instrument which excites the internal dyes denoting the specific bead set, whilst a second laser excites phyocoerythrin. Individual microspheres were identified from images captured on a cooled CCD camera and quantified by Milliplex Analyst Software (Merck Millipore, Billerica MA) or Bioplex Manager 6.1 (Bio-Rad, Hemel Hempstead, UK). In this way, multiple analytes within each test sample could be measured simultaneously. The concentrations of analytes were calculated by comparison to standard curves. Two company-provided quality controls, low level and high level, were run with each assay.

2.3.2.5 Placental Growth Factor (PLGF2) Enzyme-linked Immunosorbent Assay (ELISA)

This work was done in collaboration with Dr. Julia Zöllner.

Quantitative sandwich enzyme immunoassay ELISAs for mouse placental growth factor (PLGF2) was performed to investigate the circulating levels of PLGF occurring during normal CD1 mouse gestation. In humans, four isoforms of PLGF have been identified, PlGF1-4. However, only the PlGF2 transcript can be detected in mouse tissues [257, 258].

ELISA assay procedure was followed according to manufacturer's instructions (R&D Systems, Abingdon, UK). Serum samples were diluted 1:2 in Calibrator Diluent RD5-17 and mixed well. Calculation of concentrations was performed using standard concentrations for comparison fit with a 4-parameter logistic curve.

2.3.2.6 Cyclic Guanosine Monophosphate (cGMP) ELISA

This work was done in collaboration with Dr. Julia Zöllner.

NO is known to activate guanylate cyclase (GC) to stimulate cGMP synthesis; where *in vivo* evidence has suggested that cGMP plays a primary role in the mediation of the response to NO [259]. The contribution of cGMP to the vasodilator response is thought to be through a Ca^{2+}-dependent mechanism [260]. To quantify cGMP levels in the circulation and in a representative vascular tissue, serum and heart tissue were examined respectively. Frozen heart tissue was ground into a fine powder under liquid nitrogen and homogenised in 10 volumes of 0.1M HCl. Samples were then centrifuged at 13,000 rpm and the supernatant reserved for analysis.

ELISA assay procedure was followed according to manufacturer's instructions (Enzo Life Sciences, Farmingdale, NY). The acetylated format of the assay was run to increase sensitivity. Serum samples were diluted 1:10 in Assay Buffer 2. Calculation of concentrations was performed using standard concentrations for comparison fit with a 4-parameter logistic curve.

2.3.2.7 Soluble Fms-like Tyrosine Kinase-1 (sFlt-1) ELISA

This work was done by MSc project student, Miss Stephanie Dowle.

Quantitative sandwich enzyme immunoassay ELISAs for sFlt-1 were performed on placental homogenate according to manufacturer's instructions (R & D systems, Minneapolis, USA). 1µg of protein was loaded onto the pre-coated 96 well plate containing a specific sVEGFR1 monoclonal antibody. Correlation between sample dilutions and known measured sVEGFR1 were linear (R^2>0.99).

2.3.3 Nitric Oxide Analysis

NO production was determined from the concentrations of both nitrite and nitrate combined (NOx). The Sievers nitric oxide analyser (NOA, GE Analytical Equipment) was used to measure total NOx concentration in mouse serum and tissue homogenates [261]. The NOA is capable of detecting NOx within very small volumes of samples (down to 5µL with a lower limit of detection of 0.2µM). Samples were prepared by protein precipitation with four volumes of methanol and centrifugation at

16,000 rpm for 30 minutes. The supernatant was then used for analysis. Nitrates and nitrites in each sample were reduced back to NO through a reaction with VCl_2 (Sigma-Aldrich, Poole, UK) in 1M HCl (Sigma-Aldrich, Poole, UK) at 90^{o}C before passing into the system to react with ozone (O_3). This produced a chemiluminescent signal that was quantified by a photo-multiplier system. The concentration of NOx was calculated by comparison to a calibration curve of known nitrate samples.

2.3.4 Methylarginine Measurement

ADMA was identified and quantified by Liquid Chromatography-Mass Spectrometry (LC-MS/MS). Tissue samples were prepared as described in section 2.3.2.2. 2µL of 25µg/mL D7-ADMA (Cambridge Isotope Laboratories, Cambridge, UK) was added to 50µL of tissue homogenate, or 30µL of serum, as an internal standard. 5 volumes of 100% methanol were used to precipitate out protein. Samples were centrifuged at 13,000 rpm at room temperature for 20 minutes. The supernatant was removed and incubated at 95^{o}C to evaporate excess methanol. 100µL of 0.1% formic acid (mobile phase; Sigma-Aldrich, Poole, UK) was then added to each sample and thoroughly mixed before loading onto a 96-well plate. Standards were generated using a starting concentration of 100µM of ADMA (Merck Millipore, Billerica, MA) and 1:2 serial dilutions were made thereafter to a final concentration of 5.96×10^{-6} M. To later calculate extraction efficiency of ADMA, 2µL of D7-ADMA was added to 100µL of 0.1% formic acid (spiked sample).

Samples were then analysed by LC-MS/MS. The high pressure liquid chromatography (HPLC) system (Agilent, Stockport, UK) separates sample components based on their binding affinity to a silica-based column. 10µL of samples were injected onto the column and eluted using 1% formic acid, 1% acetonitrile (Sigma-Aldrich, Poole, UK), rising to 50% acetonitrile over 10 minutes, taking 15 minutes per sample. The column was washed clean in between each sample using 1% formic acid, 50% acetonitrile. After elution, samples were vaporised and ionised in the Agilent 6400 series triple quadrupole LC-MS/MS (Agilent Technologies, Stockport, UK). ADMA was detected using mass to charge ratio (m/z) 203.3 to 46.0 and d7-ADMA 210.0 to 46.0.

After extraction of chromatograms using the multiple reactions monitoring (MRM) method, analyses of ADMA values were performed by determination of the total ion count within the relevant peak. Concentrations were then calculated based on comparison to the standard curve accounting for extraction efficiency and normalised to the amount of protein in each sample where appropriate.

2.3.5 Data Handling and Statistical Analysis

In the longitudinal study using CD1 mice looking at haemodynamic parameters over the course of gestation, parameters were plotted as mean values ± standard error of mean (SEM) for each 12 hour light/dark period and as mean values ± SEM for each 24 hour period; or as change (Δ) from baseline. Longitudinal data collected using DDAH1$^{-/-}$ mice over the course of gestation were plotted as mean values +/- SEM for each 24 hour period as a change (Δ) from baseline. Data collected in the 24hr period after intraperitoneal injections were plotted as 1 hour averages ± SEM as a change (Δ) from baseline alongside area under the curve (AUC) analysis, maximum increase and maximum decrease (where appropriate).

Differences in the cardiovascular parameters at different time points throughout pregnancy were analysed by repeated measures ANOVA followed by Bonferroni correction for multiple comparisons between the means.

Multiple effects modelling (performed by Dr Fabiana Gordon, Imperial Statistical Advisory Service) was used to compare the response to LPS in pregnant and non-pregnant animals (Appendix 1). In all further haemodynamic data to assess the impact of progesterone or CCR2 deficiency, treatment groups were compared using a 2-way ANOVA followed by Bonferroni correction. Student's t-tests or Mann Whitney U tests (as appropriate) were used to compare haemodynamic data after AUC analysis and for comparisons of maximum increase and decrease.

Two-way ANOVA followed by Bonferroni correction was used to make comparisons between concentration-response curves (wire myography). All FACS data, multiplex data, RT-PCR data, NOx analysis, ADMA analysis, ELISA analysis and western blot densitometry, were statistically analysed

using pairwise analyses using t-tests or Mann Whitney U tests (as appropriate) unless indicated otherwise in the text.

Student's t-test was used to compare litter sizes, latency to labour, plasma volume and P4 dose response. Where data were found to be not normally distributed as determined by Kolmogorov-Smirnoff tests, non-parametric equivalent tests such as or Mann-Whitney U were employed.

Chapter 3: Longitudinal Telemetric Recording of Haemodynamic Parameters and Activity in Murine Pregnancy

3.1 Introduction

As previously discussed in greater detail, the cardiovascular changes that occur in normal pregnancy are well defined: where cardiac output, heart rate and blood volume are increased, vascular resistance and arterial pressure are decreased [2, 41]. The drop in vascular resistance is a consequence of peripheral vasodilation, which is reflected in a fall in systemic blood pressure (predominantly driven by diastolic pressure) [3, 4]. Accordingly, cardiac contractility and heart rate, and therefore cardiac output, are increased. Furthermore, blood volume increases during pregnancy by approximately 45-50% [14, 262]. Alongside the fall in vascular tone, increases in blood volume in early pregnancy trigger a decrease in preload to the heart which initiates the compensatory increase in heart rate [263]. These changes allow for implantation to occur.

In non-pregnant women the haemodynamic changes described above would lead to hypertension, yet in uncomplicated pregnancies MAP is maintained, or declines. Suggested hypotensive mechanisms behind these changes include systemic hormone-driven vasodilation and transient insensitivity to vasoactive substances [264, 265].

To measure long-term haemodynamic changes in a murine model, radiotelemetric monitoring was used throughout normal mouse pregnancy. This method provides several advantages over other techniques that can be employed to measure arterial pressures in the mouse, such as tail cuff plethysmography, or exteriorised implanted fluid filled catheters. Although a non-invasive technique, tail cuff systems require extensive animal handling and restraint. This can lead to inflated systolic pressure measurements and may affect accuracy and reproducibility. Vasoconstriction of the tail artery due to environmental temperature, increased sympathetic tone, hypotension or the action of vasoactive substances could further affect the accuracy of measurements taken using the tail cuff method [266]. Fluid filled catheter systems require that mice are tethered throughout the monitoring period, thus restricting movement and activity adding to stress. Additionally, the frequency of catheter obstructions could hinder long-term measurements. By using small radiotelemetric devices to chronically implant mice, the absence of tethering, handling and restraint allows for more accurate

long-term haemodynamic measurements. The initial surgical technique developed using these devices involved catheter placement into the abdominal aorta, which would obstruct blood flow to the lower extremities in mice weighing <30g, thus potentially compromising uterine blood flow [267]. Since this would not be feasible for the study of pregnant mice, the surgical procedure was subsequently adapted to a carotid placement of the catheter tip [250, 268], which is now by far the most widely used approach [269]. Butz and Davisson went on to show that haemodynamic and cardiovascular parameters could be monitored throughout gestation, and that the device did not interfere with conception, delivery or postnatal care of pups.

3.1.1 Aims and Objectives

To be able to further dissect the underlying impact of inflammation on the cardiovascular system during pregnancy, it was important to understand the haemodynamic changes that occur normally. Therefore, haemodynamic parameters and activity levels were studied using telemetry method in an outbred CD1 mouse strain over the course of normal gestation.

3.2 Results

3.2.1 The Haemodynamic Profile of Pregnancy in CD1 Mice

Continuous data collection across the gestational and post-partum period in the CD1 strain of mice enabled the composition of a haemodynamic and activity profile that included detection of subtle haemodynamic changes. All mice that were used in this experiment were recorded for at least 48 hours before mating and subsequent pregnancy (termed Baseline) which enabled the use of each individual mouse as their own control. Labour occurred at term (overnight between E18 and the morning of E19) in all mice.

We observed a gradual decline in MAP from 109.4 ± 1.86 mmHg at baseline to a mid-gestation nadir of 100.75 ± 1.3 mmHg at E8 ($p<0.01$; Figure 3.1). Pressure then gradually increased and returned to baseline levels by E14. Post-partum pressure did not differ significantly from baseline (Figure 3.1).

Similar trends were observed in systolic arterial pressures (SAP; Figure 3.2) where SAP fell to a mid-gestational nadir on E8 from 121.25 ± 1.23 mmHg to 109.88 ± 1.03 mmHg ($p<0.001$). However, the significant reduction in systolic pressure during mid-gestation occurred for a longer period of time (E7-E11). Furthermore, there was an additional drop in systolic pressure during the post-partum period. DAP was also reduced to a mid-gestational nadir of 88.17 ± 1.66 mmHg from baseline levels of 94.48 ± 2.8 mmHg (E8, $p<0.01$); however, when normalised to baseline this reduction was not significant (Figure 3.3). There was no change in diastolic pressure during the post-partum period.

There was no observed change in HR (Figure 3.4). There was an initial trend seen at E0 towards increased heart rate but this returned to baseline levels without reaching significance. This is likely to be due to the large variability seen between animals. Pulse pressure remained constant throughout the course of gestation (data not shown).

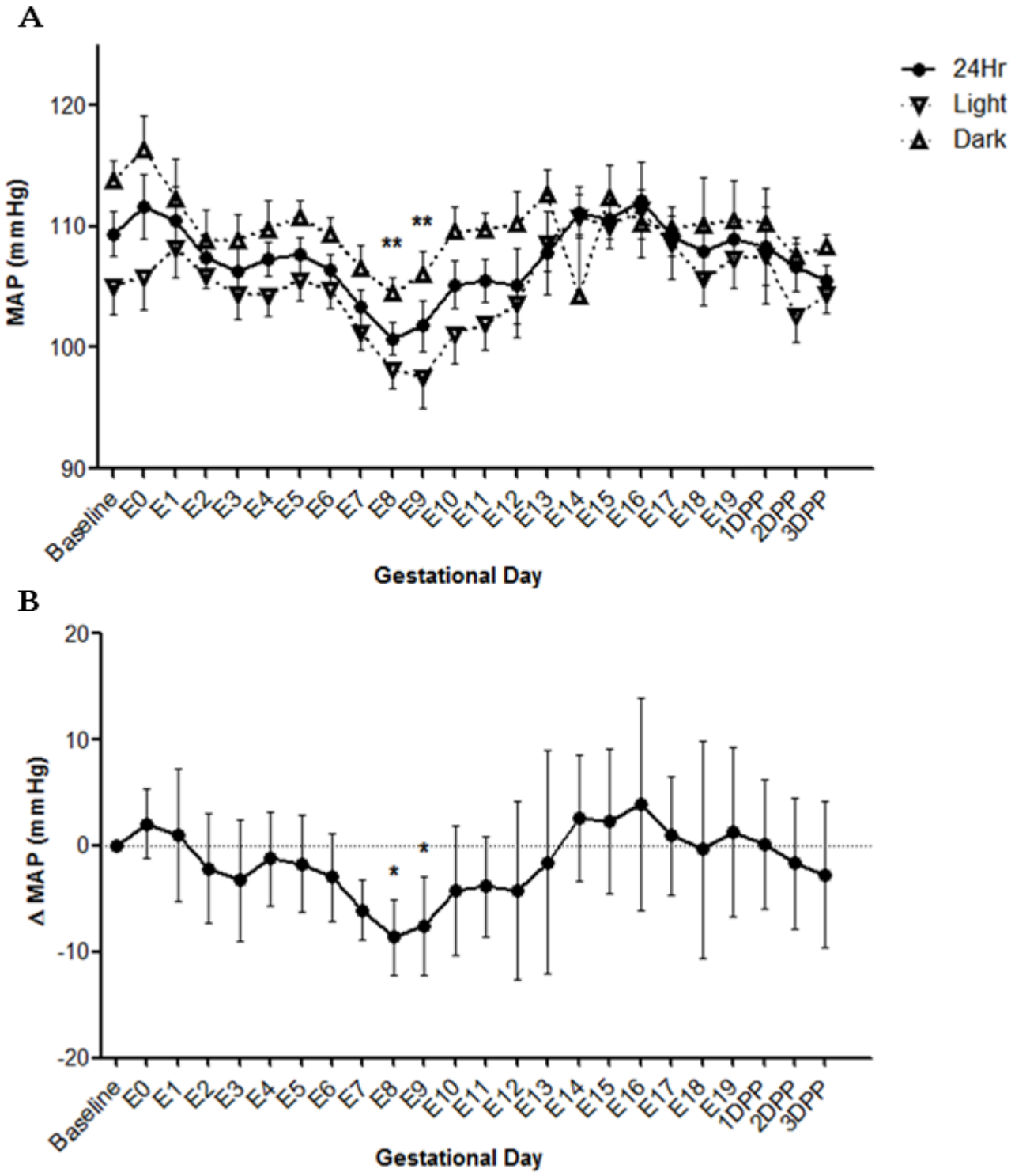


Figure 3.1: **Continuous measurement of mean arterial pressure (MAP) throughout pregnancy.** (A) MAP in CD1 mice whilst not pregnant (Baseline), throughout gestation, and for 3 days post-partum (1DPP-3DPP) shown as 24-hour, light-phase and dark-phase averages. **$p<0.01$, 1-way repeated measures ANOVA, Bonferroni post-test (n=7) compared to baseline for 24h average. (B) ΔMAP from baseline. *$p<0.05$, 1-way repeated measures ANOVA, Bonferroni post-test (n=7) compared to baseline.

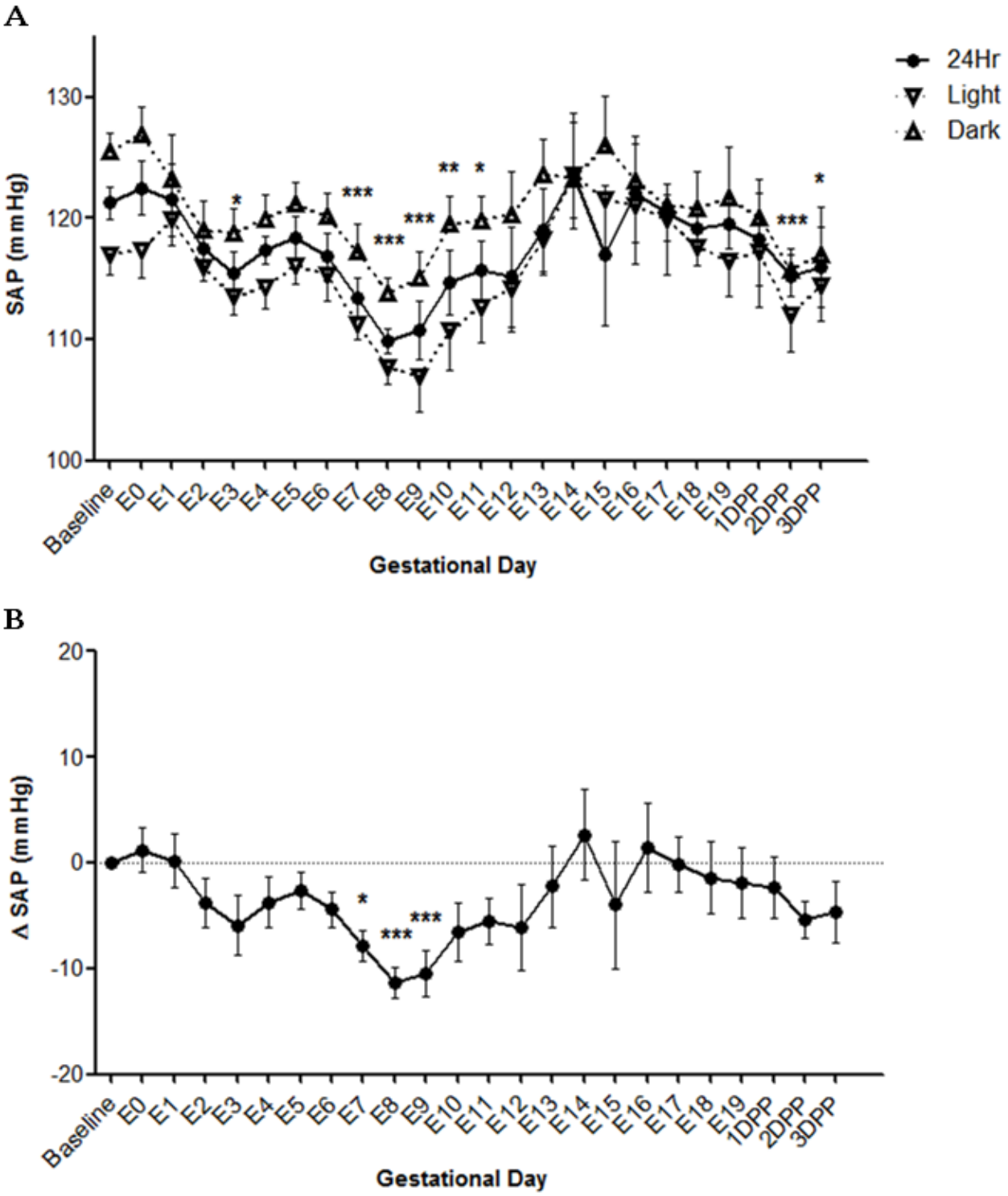


Figure 3.2: **Continuous measurement of systolic arterial pressure (SAP) throughout pregnancy.** (A) SAP in CD1 mice whilst not pregnant (Baseline), throughout gestation, and for 3 days post-partum (1DPP-3DPP) shown as 24-hour, light-phase and dark-phase averages. *p<0.05, **p<0.01, ***p<0.001, 1-way repeated measures ANOVA, Bonferroni post-test (n=7) compared to baseline for 24h average. (B) ΔSAP from baseline. *p<0.05, **p<0.01, 1-way repeated measures ANOVA, Bonferroni post-test (n=7) compared to baseline.

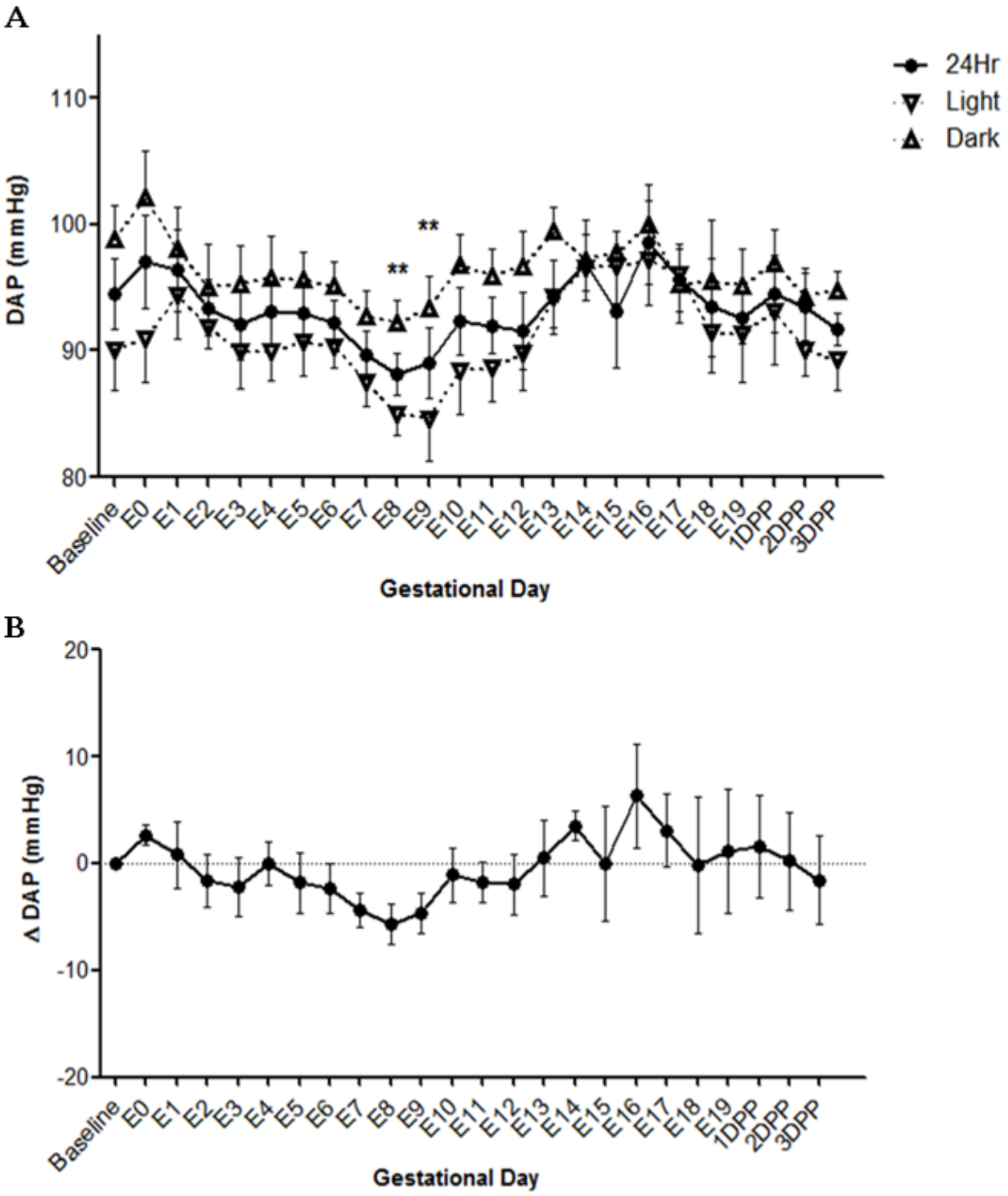


Figure 3.3: **Continuous measurement of diastolic arterial pressure (DAP) throughout pregnancy.** (A) DAP in CD1 mice whilst not pregnant (Baseline), throughout gestation, and for 3 days post-partum (1DPP-3DPP) shown as 24-hour, light-phase and dark-phase averages. **p<0.01, 1-way repeated measures ANOVA, Bonferroni post-test (n=7) compared to baseline for 24h average. (B) ΔDAP from baseline (n=7).

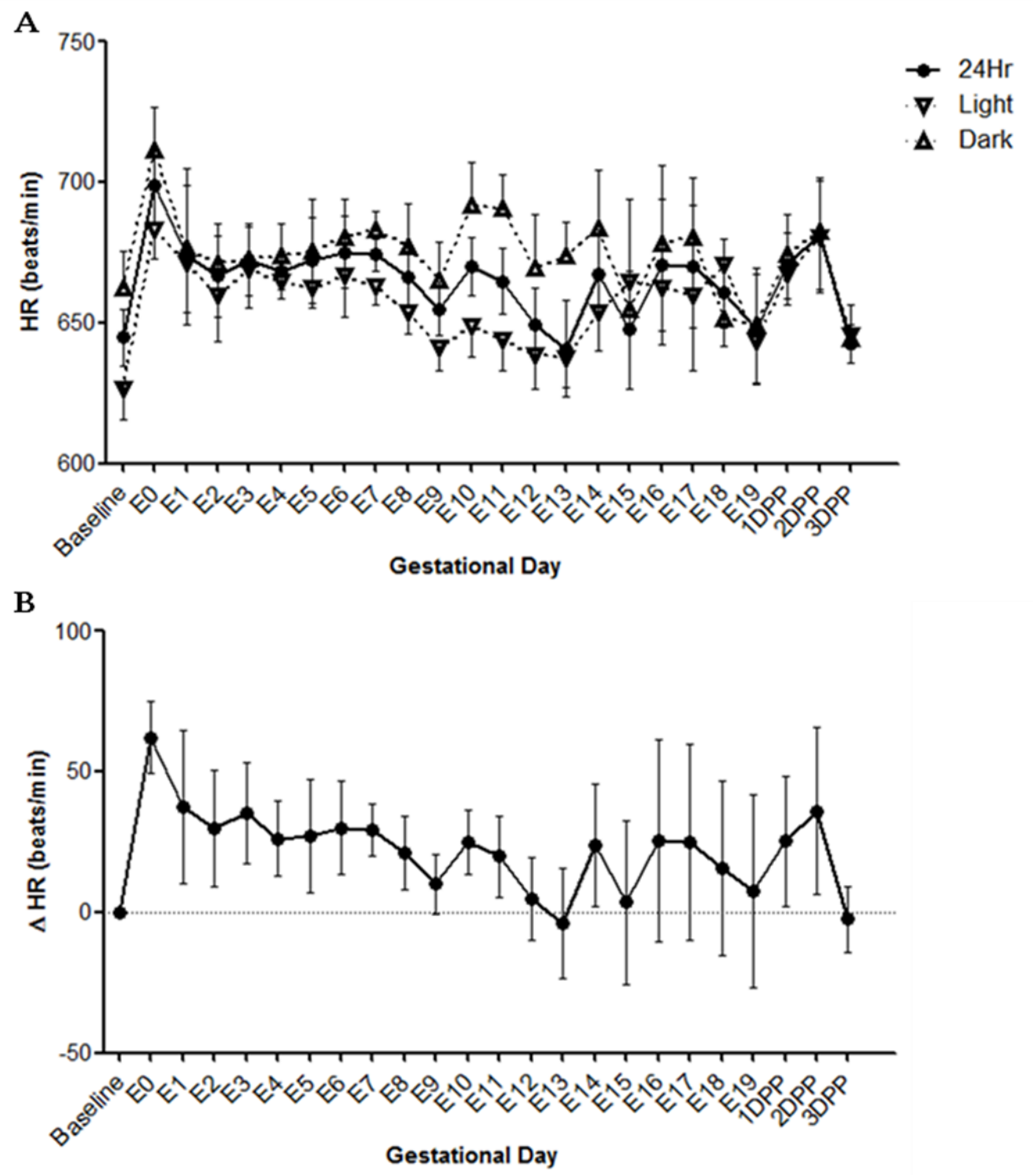


Figure 3.4: **Continuous measurement of heart rate (HR) throughout pregnancy.** (A) HR in CD1 mice whilst not pregnant (Baseline), throughout gestation, and for 3 days post-partum (1DPP-3DPP) shown as 24-hour, light-phase and dark-phase averages (n=7). (B) ΔHR from baseline (n=7).

3.2.2 Activity during Pregnancy in CD1 Mice

As well as measuring haemodynamic parameters, the telemetry system also produces an activity 'count' that represents an index of the animal's locomotor activity. These data show that the percentage of time spent inactive (%TSI) increased gradually over the course of gestation (Figure 3.5) with mice generally spending more time inactive during the light phase. The change in %TSI from baseline was significantly greater at E17 and E18; increasing to 85.15 ± 1.18% and 84.34 ± 1.19% respectively from baseline levels of 77.5 ± 1.69%.

Intensity of activity was shown to decrease towards labour, particularly during the generally more active dark phase (Figure 3.6). This decrease in activity was significantly reduced from baseline during labour and the post-partum period ($p<0.05$), likely to birthing and weaning behaviours. As expected, due to the nocturnal nature of mice, activity was generally observed to be greater during the dark-period than the light period at all time points until labour. Across the 24hr averages taken, activity remained relatively constant until E8, and then from E9 onwards until 3DPP there was a decline in activity to a nadir at E18. When eliminating inactive time points, mean activity >0 did not differ as much between light and dark periods (Figure 3.7A). Similar to overall activity, there was a gradual decrease in activity from E8 until 3DPP. This general decrease over the period of gestation was likely to result from the large size of the animal towards the end of pregnancy, and then weaning during 1DPP-3DPP.

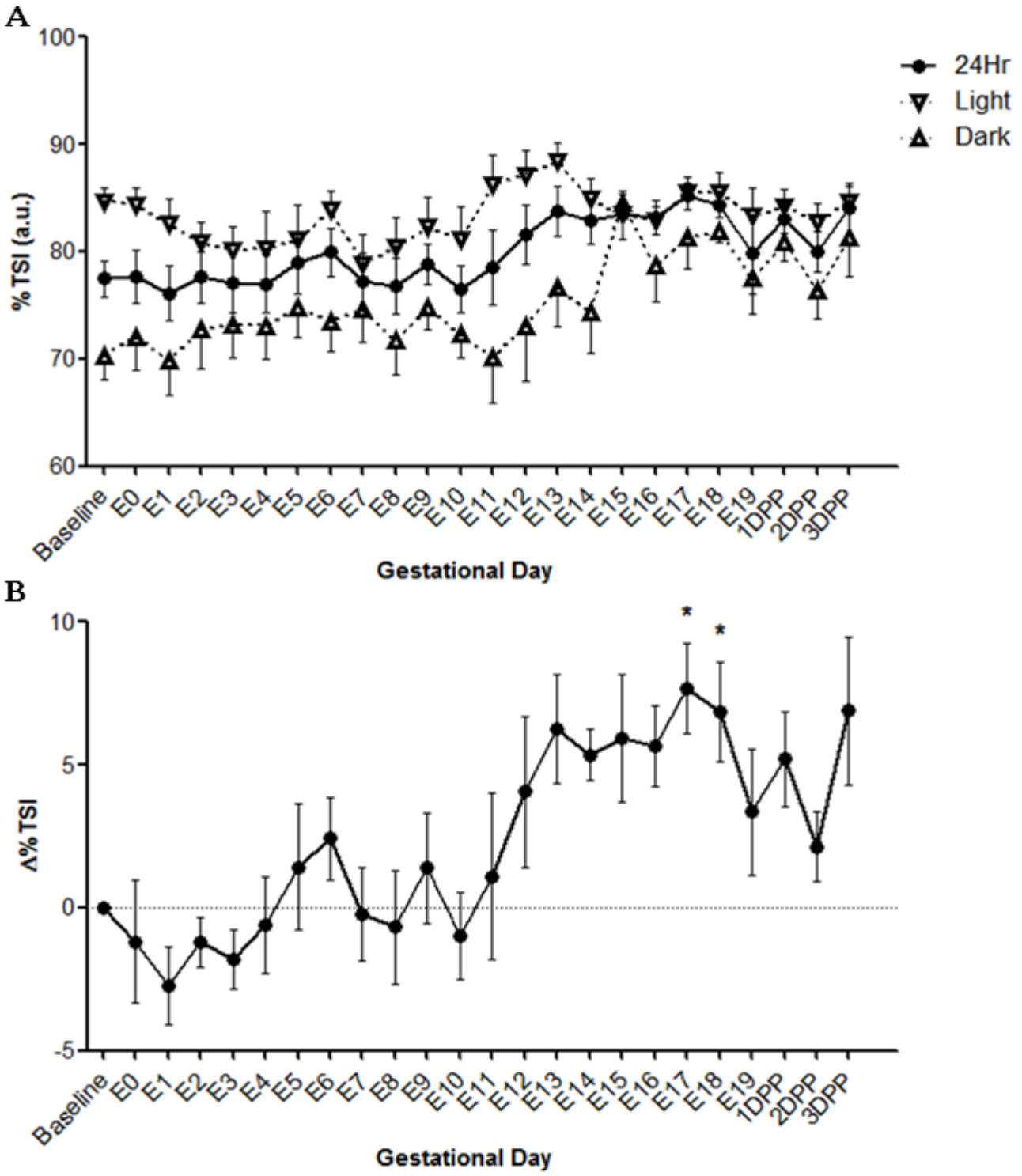


Figure 3.5: **Continuous measurement of the percentage of time spent inactive (%TSI) throughout pregnancy.** (A) %TSI in CD1 mice whilst not pregnant (Baseline), throughout gestation, and for 3 days post-partum (1DPP-3DPP) shown as 24-hour, light-phase and dark-phase averages (n=7). (B) Δ%TSI from baseline. *p<0.05, 1-way repeated measures ANOVA, Bonferroni post-test (n=7) compared to baseline.

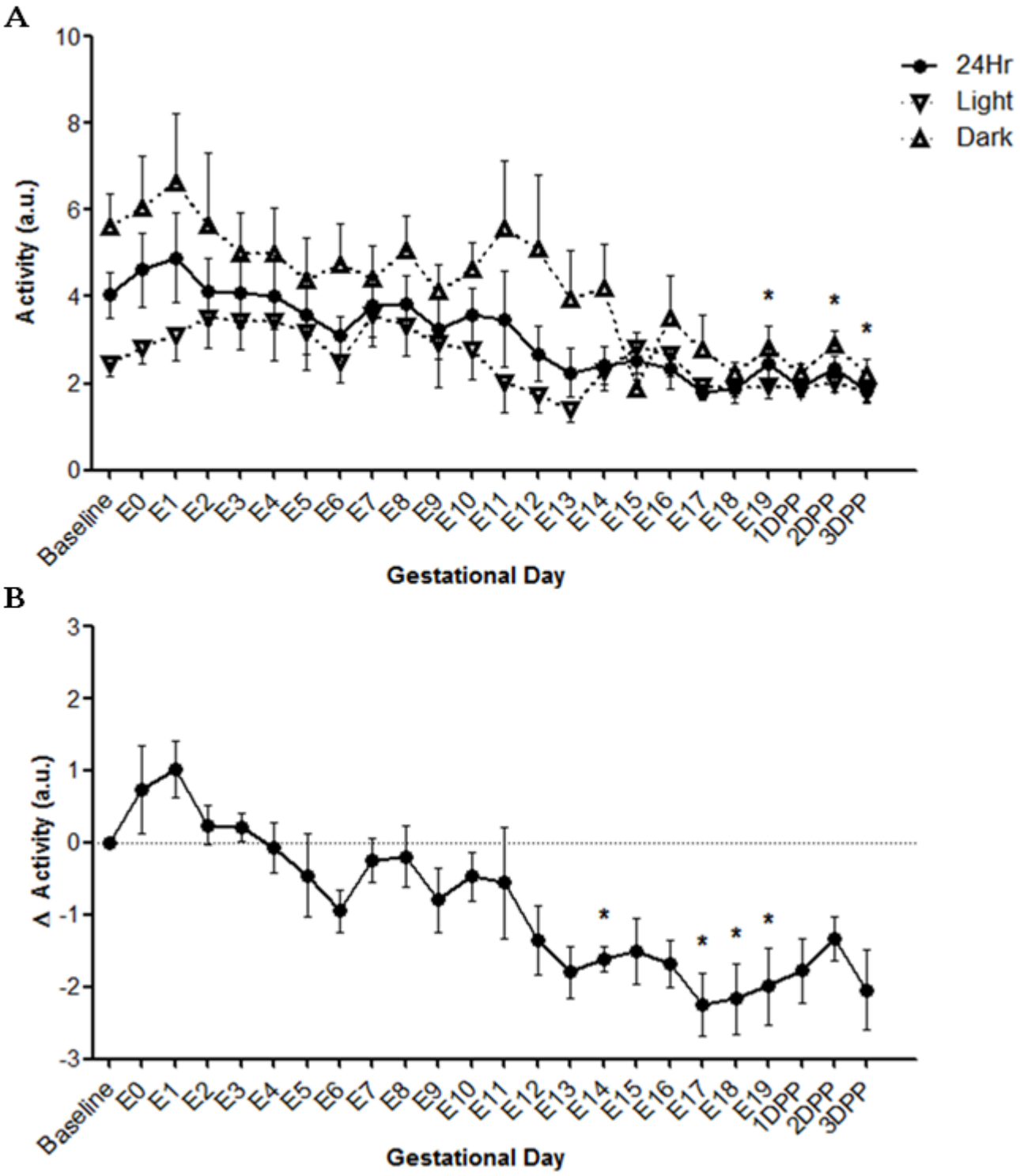


Figure 3.6: **Continuous measurement of activity throughout pregnancy.** (A) Activity (in arbitrary units) in CD1 mice whilst not pregnant (Baseline), throughout gestation, and for 3 days post-partum (1DPP-3DPP) shown as 24-hour, light-phase and dark-phase averages. *$p<0.05$, 1-way repeated measures ANOVA, Bonferroni post-test (n=7) compared to baseline. (B) Δ Activity from baseline. *$p<0.05$, 1-way repeated measures ANOVA, Bonferroni post-test (n=7) compared to baseline.

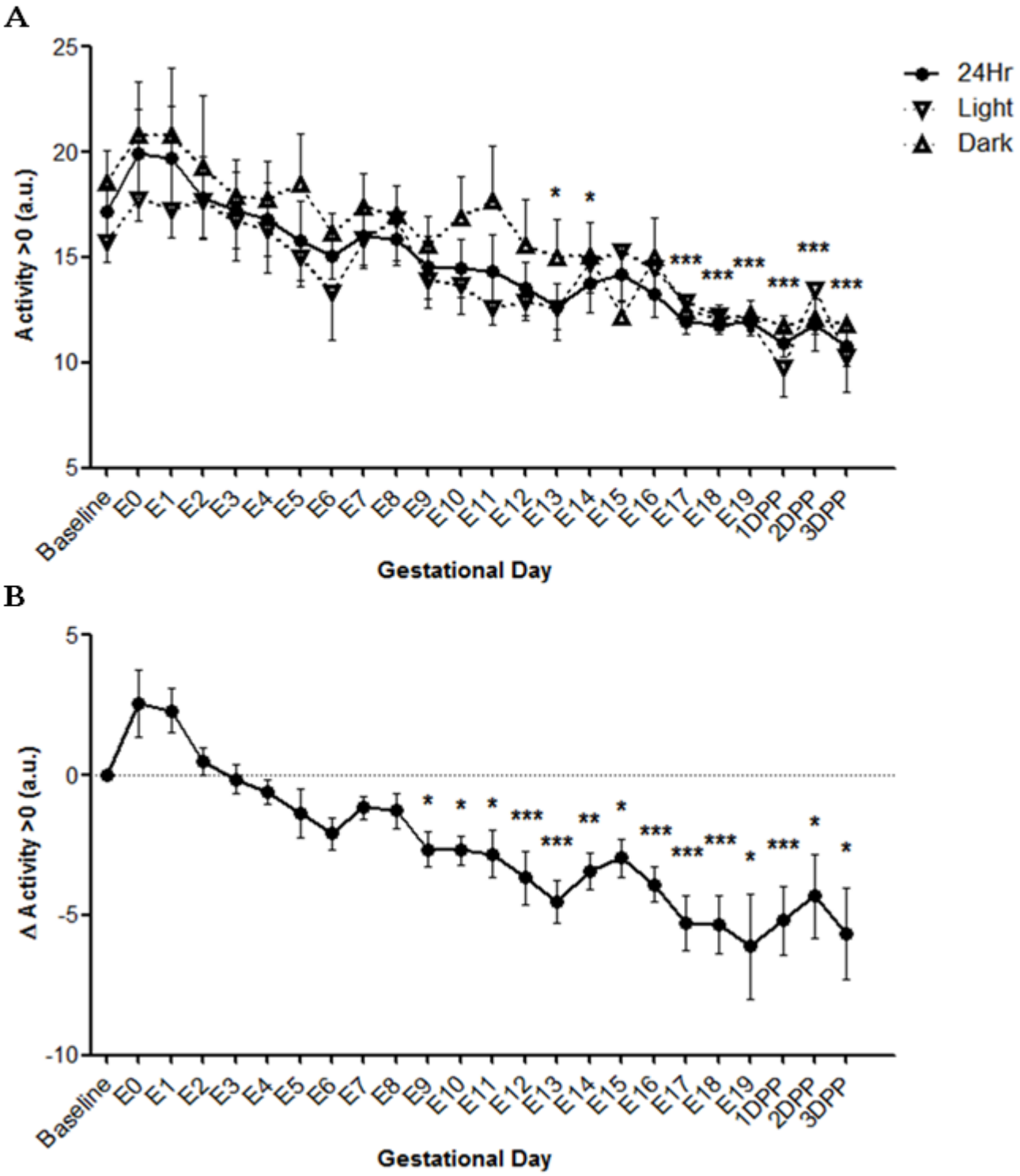


Figure 3.7: **Continuous measurement of activity >0 throughout pregnancy.** (A) Activity >0 (in arbitrary units) in CD1 mice whilst not pregnant (Baseline), throughout gestation, and for 3 days post-partum (1DPP-3DPP) shown as 24-hour, light-phase and dark-phase averages. *p<0.05, ***p<0.001 1-way repeated measures ANOVA, Bonferroni post-test (n=7) compared to baseline. (B) Δ Activity>0 from baseline. *p<0.05, **p<0.01, ***p<0.001 1-way repeated measures ANOVA, Bonferroni post-test (n=7) compared to baseline.

3.3. Summary and Discussion

MAP in CD1 mice decreased to mid-gestational nadir at E8 before rising back to baseline levels. This seems to be mainly driven by systolic rather than diastolic pressure. Heart rate did not change significantly over the course of gestation; however there was a trend to increase in the first days of pregnancy only to decline as the drop in blood pressure was reversed. Activity levels decreased gradually towards labour and the post-partum period where they remained low.

This first study demonstrates the feasibility of remote monitoring of cardiovascular parameters in conscious freely moving pregnant mice. Additionally, these mice were able to successfully conceive and carry a normal-sized litter to term (approximately 12 pups per litter [270]). The implants remained relatively undisturbed and fully functional over the course of the experiment.

The haemodynamic profile observed in CD1 mice was comparable to that observed by Burke *et al.,* in other mouse strains (BALB/c and B6) [2]. The general trend reported was that MAP remained constant until E5 and then declined, reaching a nadir at E9. Pressure then returned to non-pregnant baseline levels by E12 and remained stable until the peri-partum period. The authors identified a distinct pattern of arterial pressure which corresponded with gestational milestones such as implantation (E5), pre-placental conceptus development (E5-E9), placental growth and the opening of placental circulation (E9-E14), the fetal growth phase (E14-E18) and the peri-partum interval.

The decrease in MAP observed in CD1 mice, with a nadir approximately halfway through gestation, is comparable to the decline in blood pressure seen in human pregnancy where MAP reaches a nadir at approximately halfway through gestation at 16-20 weeks [271, 272]. However, whilst in human pregnancy the decline in blood pressure is thought to be predominantly due to a fall in DAP [3, 4, 273], in CD1 mice the decline in SAP was more pronounced and appeared to be the drive behind the decrease in MAP, rather than DAP. This difference may contribute to the limitations of using the mouse to model pregnancy-related haemodynamics. Due to the many differences in human and murine uterine anatomy, placental morphogenesis and endocrine function, the structural enlargement

of the uterine vascular tree which contributes to the initial drop in vascular resistance is likely to be different in the mouse. Greater numbers of uteroplacental implantation sites and developing placentae in the mouse may confer a larger drop in systolic arterial pressure [15, 274].

It has been proposed that the observed haemodynamic changes over the course of gestation are primarily due to systemic vascular resistance. Endogenous mediators of vasodilation, principally NO and its second messenger cGMP, have been shown to be increased in both human and animal pregnancy [275-277]. Other suggested key mediators include oestrogens, prostaglandins (particularly prostacyclin) and relaxin [33, 34, 278, 279]. Additionally, progesterone has also been implicated in the regulation of vascular tone, via locally produced NO [280].

Oestrogen is thought to exert protective effects on the vasculature through vasorelaxation; largely mediated by the generation of NO via modulation of eNOS through both genomic and non-genomic pathways [281], and by stimulation of hydrogen sulphide which induces vasodilation through the activation of protein kinase G (PKG) [282]. However, oestrogen may play a more important role in specific vascular relaxation and function in reproductive tissues [31, 283, 284]. Rosenfeld and Roy saw that exogenous oestradiol-17β led to a 79% decrease in ovine uterine vascular resistance and a 3-fold increase in uterine blood flow which did not result in a change in MAP [284]; although this may have been due to the compensatory increase in HR.

Furthermore, as haemodynamic changes in pregnancy are temporally defined, it has been suggested that because peripheral vasodilation occurs before placentation is complete this may be responsible for the fall in MAP. Chapman *et al*., proposed that maternal factors, possibly related to changes in ovarian function or extended function of the corpora lutea, are responsible for the initial peripheral vasodilation found in human pregnancy [265]. Studies in rodents have also shown that haemodynamic changes in pregnancy occur early without the contribution of the fetus or placenta, and this can be mimicked in pseudopregnancy [285].

Interestingly, decreased activity did not correlate with a decrease in HR. This is likely to be due to the overriding effects of maternal cardiovascular adaptation and changes in peripheral resistance. Moreover, in human pregnancy, maternal HR measured during physical activity was found to be lower than in post-partum controls [286]. This finding supports the concept that HR during pregnancy is less likely to be affected by activity level and more so by prevailing changes to vascular resistance and blood volume.

Chapter 4: The Response to Lipopolysaccharide-Induced Inflammation in Non-Pregnant and Pregnant Mice

4.1 Introduction

Once the normal haemodynamic profile of CD1 mouse throughout gestation was established, the next step was to evaluate the haemodynamic response to LPS-induced inflammation in pregnancy. It is well established that LPS administration in rodents causes marked hypotension. Yamashita *et al*., showed that 80mg/kg i.p. LPS, a dose shown to cause >90% mortality in WT (C57bl/6) male mice, triggered a severe and progressive drop in MAP, where blood pressure fell to ~60 mmHg equalling a 40% reduction from pre-treatment values [287]. Lower doses of LPS have also induced marked hypotension in WT mice over 6-12 hours using 40mg/kg, 10mg/kg and 3mg/kg i.p. respectively [288-290]. This effect has also been demonstrated in rats where a 5mg/kg intravenous dose of LPS led to a significant and sustained drop in MAP as early as 90 minutes post-administration [291, 292]. These haemodynamic responses were also associated with increased iNOS expression in the lung, as well as increased plasma levels of nitrates and pro-inflammatory cytokines.

Similar effects have also been seen in humans, where LPS induces a hypotensive response, associated with an increase in circulating cytokines. Interestingly, humans are more sensitive to the effects of LPS, requiring much smaller doses to achieve similar cytokine responses when compared to studies in rodents [293, 294]. There appears to be a dimorphism in the response to LPS with several studies showing that females are more resistant [295-297]. However, this is not consistent across all studies, as work by Van Eijk *et al.,* showed that females had a greater pro-inflammatory response to LPS in terms of a higher rise in C-reactive protein, more leukocyte sequestration and a more pronounced drop in blood pressure [298].

Although sex-steroid dependent modulation of the immune function in mammals is widely accepted, very few experiments have assessed the differences between the male and female murine response to systemic LPS. Female mice appear to be more resistant to LPS-induced inflammation as shown by the resistance to intra-tracheal administration of LPS in females, when the same dose in male mice results in increased albumin leakage, increased IL-1β and TNF-α levels in bronchoalveolar lavage (BAL) fluid, and airway hyperresponsiveness [299, 300]. These findings were independent of strain.

Additionally, several groups have demonstrated that oestrogen administration in animal models of trauma-haemorrhage can restore altered immune function and rescue adverse outcomes via prevention of androgen-induced immunosuppression [301, 302].

The administration of LPS has also been widely used in pregnant mice to model PTL [303]. Intraperitoneal administration of LPS provokes preterm delivery in pregnant females, often with marked maternal morbidity and even mortality [304-307]. However, more recent models have moved towards using the intrauterine route of administration to more closely approximate localised inflammation in order to allow for the investigation of specific PTL signal transduction pathways [252]. Furthermore, due to maternal morbidity, the i.p. route is thought to more closely resemble systemic maternal sepsis, including pyelonephritis or overwhelming pneumonia. Therefore, although the effects of pre-natal LPS on fetal cerebral hypoxia, brain injury and offspring haemodynamics have been previously investigated in both ovine and rodent models [308-311]; the effects of LPS-induced inflammation on maternal haemodynamics are not well understood.

In summary, being female appears to be protective in the context of inflammation and the response to LPS. However, it appears that pregnancy may reverse this and potentially exacerbate the response to LPS.

4.1.1 Aims and Objectives

The following studies were undertaken to test the hypotheses that infection and inflammation in pregnancy have a more marked effect on haemodynamic parameters than in non-pregnant animals, and that pregnancy is associated with an altered inflammatory response to LPS. Therefore, using telemetry, maternal haemodynamics were studied in both non-pregnant and pregnant populations after systemic administration of LPS. This novel application of telemetry in pregnant mice combined with the systemic LPS model of PTL aimed to optimise the information gained and reduce the numbers of animals needed, thus refining current models. Additionally, the inflammatory response was investigated by examining cytokine profiles of non-pregnant and pregnant mice after LPS exposure.

4.2 Results

4.2.1 Maternal Systemic LPS Administration

To enable an investigation into the changes in maternal haemodynamics in response to inflammation, an alternative to PTL model previously set up in our group which used LPS given via the intrauterine route, needed to be established. The intraperitoneal route was chosen as it was less invasive than intrauterine administration, could be used subsequent to telemetry probe implantation surgery and is thought to be a more representative model of systemic maternal sepsis.

A dose response curve was constructed to examine the effects of intraperitoneal administration of LPS (serotype O111:B4, Sigma) injected on E16, where measured outcomes were maternal morbidity and mortality, latency to labour and pup survival (Figure 4.1, Table 4.1). Pup survival was reported as the mean percentage survival for each litter. All mice injected with phosphate buffered saline (PBS) i.p. (vehicle control) carried their pregnancies to term and delivered 57.2 ± 6.6 hours post injection. Over 90% of these control litters survived to 3 days post-partum (3DPP), the chosen endpoint to assess survival. In subsequent experiments, 100% of litters born to PBS-treated dams survived labour. After the i.p. administration of 5μg LPS, latency to labour was reduced to 29.9 ± 2.6 hours ($p>0.05$). The i.p. administration of 10μg LPS led to a significant reduction in latency to labour to 23.07 ± 2.07 hours ($p<0.01$) accompanied by 18.8 ± 16.43% pup survival. At 15μg and 20μg LPS, both latency to labour and pup survival were highly variable. Maternal mortality was observed in a least one mouse when doses of 20μg LPS or higher were used (Table 4.1); for this reason, fewer animals were subject to high doses of LPS.

Due to consistent effects on (i) the interval to preterm delivery (significantly reduced latency to labour after injection), (ii) pup survival and (iii) maternal mortality, 10μg per dam LPS was chosen as the appropriate dose for all subsequent experiments.

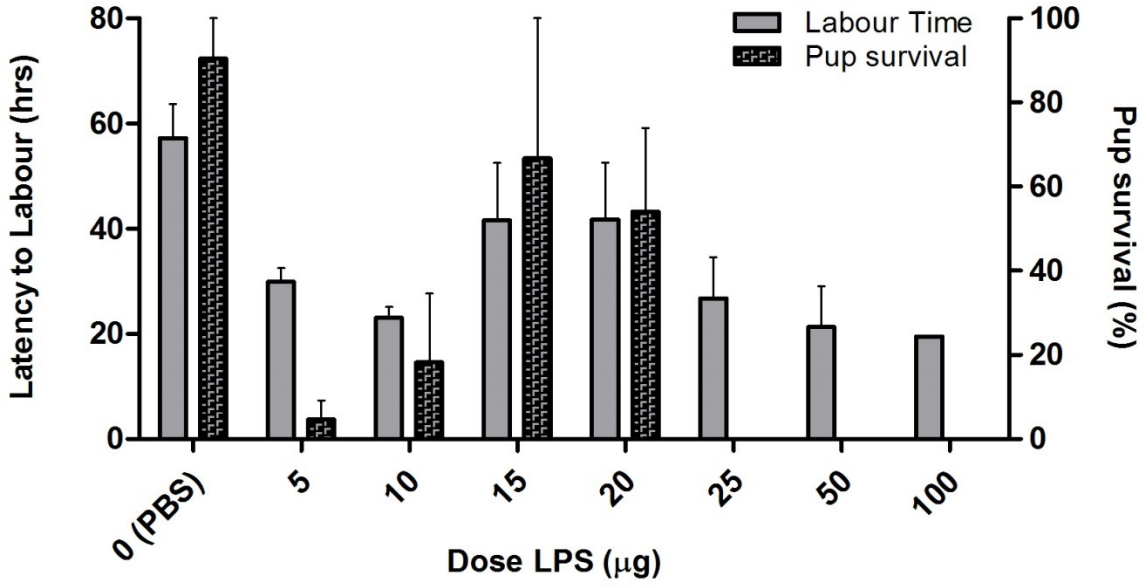


Figure 4.1: **Dose response to intraperitoneal administration of LPS in CD1 mice.** Intraperitoneal LPS or PBS (100μL) used as a vehicle control were administered on E16 of gestation between 8-10am. Both labour time (left y axis) and pup survival (right y axis) are reported. **p<0.01 compared to PBS control, Kruskal-Wallis followed by Dunn's multiple comparison test. Data shown as mean ± SEM (n=1-7; see Table 4.1).

Table 4.1: **Summary of LPS dose response outcomes.** Table describing mean labour times (hours), pup survival (% litter that survived labour) and number of animals that received each LPS dose. *Maternal mortality was observed in at least one mouse that received doses of 20μg LPS or higher.

Dose LPS (μg)	Labour Time (hours) ± SEM	Pup Survival (%) ± SEM	n number
0 (PBS)	57.2 ± 6.6	90.4 ± 9.6	7
5	29.9 ± 2.6	4.6 ± 4.6	5
10	23 ± 2.07	18.2 ± 16.4	6
15	41.6 ± 10.9	66.7 ± 33.3	3
20*	41.8 ± 10.8	54 ± 19.9	6
25*	26.8 ± 7.75	0	2
50*	21.3 ± 7.75	0	2
100*	19.5	0	1

4.2.2 The Haemodynamic Response to LPS-induced Inflammation in Non-Pregnant and Pregnant Mice

4.2.2.1 The Effect of LPS-induced Inflammation on Labour Time and Pup Survival

In the subsequent study of maternal haemodynamics, latency to labour was recorded in telemetered animals after systemic 10µg LPS or PBS (vehicle control) administration. In these mice, 10µg LPS reliably and significantly reduced latency to labour from 48.63 ± 6.1 hours to 19.31 ± 1.3 hours ($p<0.01$; Figure 4.2A). In a separate experiment, where tissue was taken at intermediate time points (6 and 12 hours post-LPS/PBS) and at the time of labour in telemetered animals, pup survival was recorded. In PBS-treated dams, there was 100% pup survival at 6 hours and 12 hours post-i.p., and at the time of labour (Figure 4.2B). Pups that were born to telemetered dams who laboured survived for at least 3 days until schedule 1. At 6 hours post-LPS, 70.4 ± 18.1% of pups survived which then decreased to 39.1 ± 16%, although this was not significant. Unlike the pup survival recorded in the dose-response (Figure 4.1), there was no pup survival at the time of labour.

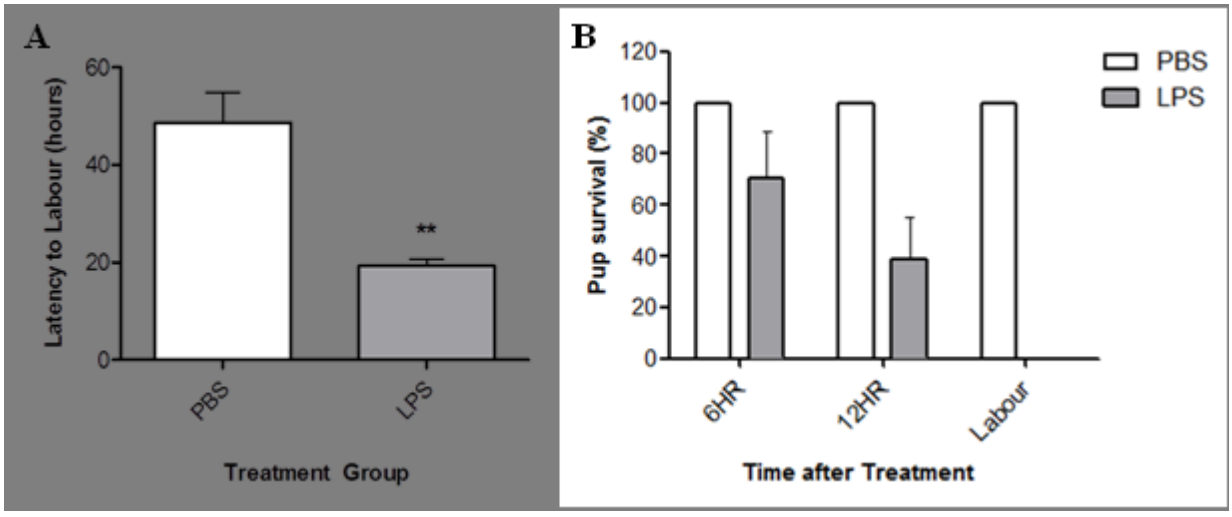


Figure 4.2: **Latency to labour and pup survival in CD1 mice administered 10µg LPS or vehicle.** (A) Latency to labour (time from LPS/PBS until labour) was observed in telemetered animals. *$p<0.01$ student's t-test (n=4). (B) Pup survival was recorded in those animals used for tissue collection at 6 and 12 hour time points or in telemetered animals (labour) after LPS/PBS (Labour, n=4; 6HR, 12HR, n=7).

4.2.2.2 The Effect of LPS-induced Inflammation on Maternal Haemodynamics

The haemodynamic response of pregnant mice to LPS administration was observed to be significantly different to the haemodynamic response in non-pregnant controls ($p<0.05$; Figure 4.3). After i.p. administration of 10μg LPS in non-pregnant mice, MAP remained stable for approximately 15 hours before peaking at Δ30.9 ± 5.8 mmHg at 21 hours post-LPS when compared to PBS-treated controls (Figure 4.3). Conversely, in pregnant mice MAP gradually declined after LPS administration before reaching a plateau at approximately 12 hours post-LPS. This resulted in a nadir of Δ-38.3 ± 12.67 compared to PBS-treated controls at 18 hours post-LPS. To compare the overall response between non-pregnant and pregnant mice to LPS, the trajectory of haemodynamic change was compared over the 24 hour period using mixed models statistics for longitudinal data. The overall difference in the response to LPS in MAP between non-pregnant and pregnant mice, allowing for any baseline differences, was significant ($p<0.05$). These statistical analyses are summarised in Table 4.2.

The maximum increase in ΔMAP was also significantly lower in pregnancy, Δ35.26 ±5.3 mmHg in non-pregnant mice vs. Δ-4.67 ± 15.4 mmHg in pregnant mice ($p<0.05$, Figure 4.3B). There was a drop from a maximum decrease in ΔMAP from Δ-19.24 ± 5.3 mmHg in non-pregnant mice to Δ-41.84 ± 11.9 mmHg in pregnant mice, but this did not reach statistical significance.

The same trend was also observed in the SAP and DAP recorded in non-pregnant and pregnant mice after LPS administration, although the overall ΔSAP and ΔDAP did not reach statistical significance. However, the maximum increase in ΔSAP and ΔDAP were significantly lower in pregnancy ($p<0.05$ and $p<0.01$ respectively; Figure 4.4B, 4.4D).

In both pregnant and non-pregnant mice, heart rate remained stable over the 24 hour period after LPS administration and did not significantly differ from HR in PBS-treated mice (data not shown). Furthermore, there were no significant differences in maximum change in HR between PBS- and LPS treated mice (Figure 4.4E).

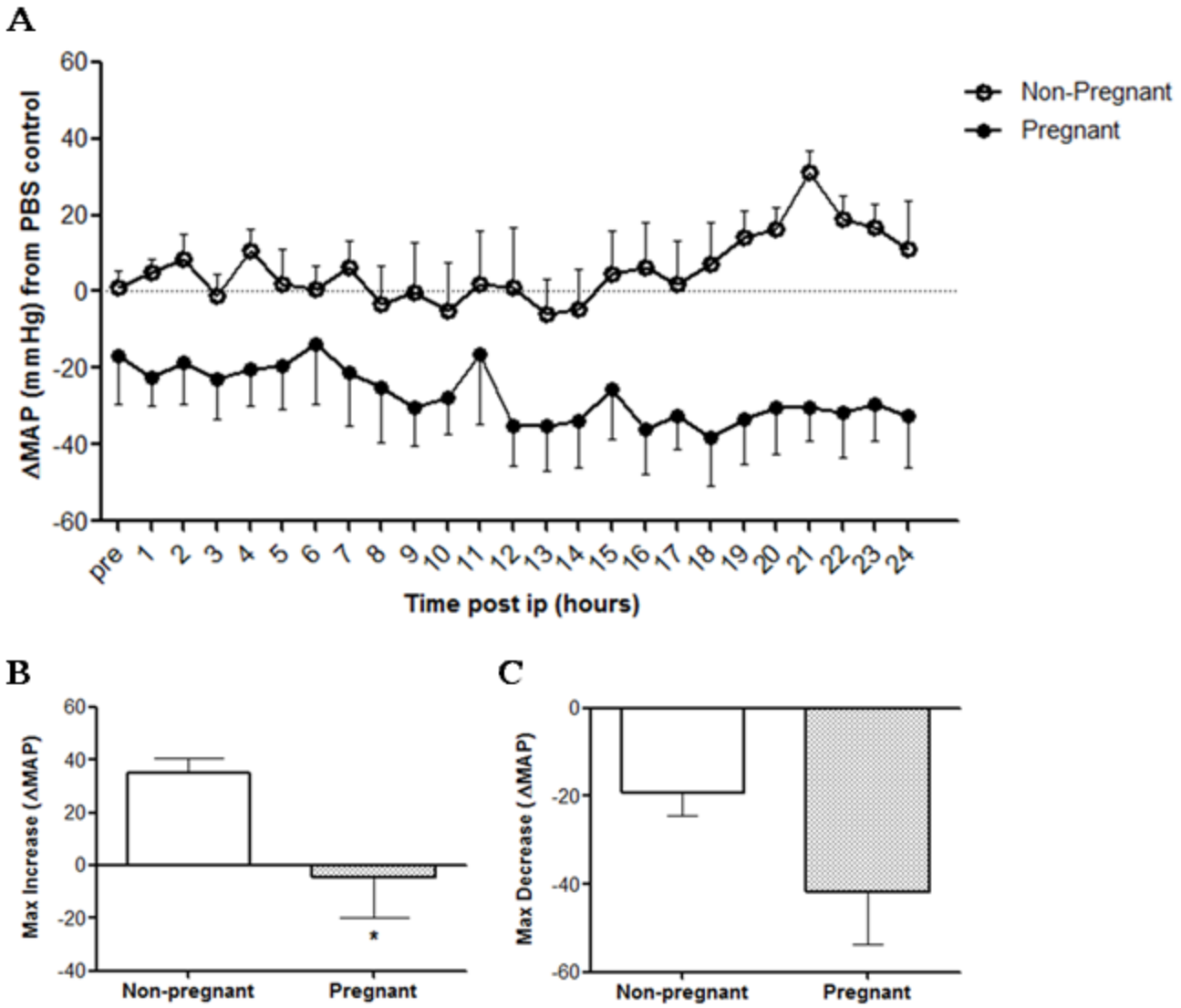


Figure 4.3: The haemodynamic response to LPS-induced inflammation in pregnant CD1 mice. The haemodynamic response was recorded in pregnant and non-pregnant female CD1 mice for 24 hours following LPS administration (on E16 in pregnant mice). (A) ΔMAP in LPS-treated mice compared to PBS controls. Data are expressed as a mean change from pre-LPS baseline (pre) compared to PBS controls ± SEM (n=4-5). (B) Maximum increase in MAP and (C) maximum decrease in MAP, observed during the 24 hours period. *P<0.05 student's t-test. Data are expressed as mean ± SEM (Pregnant, n=4; Non-pregnant, n=5).

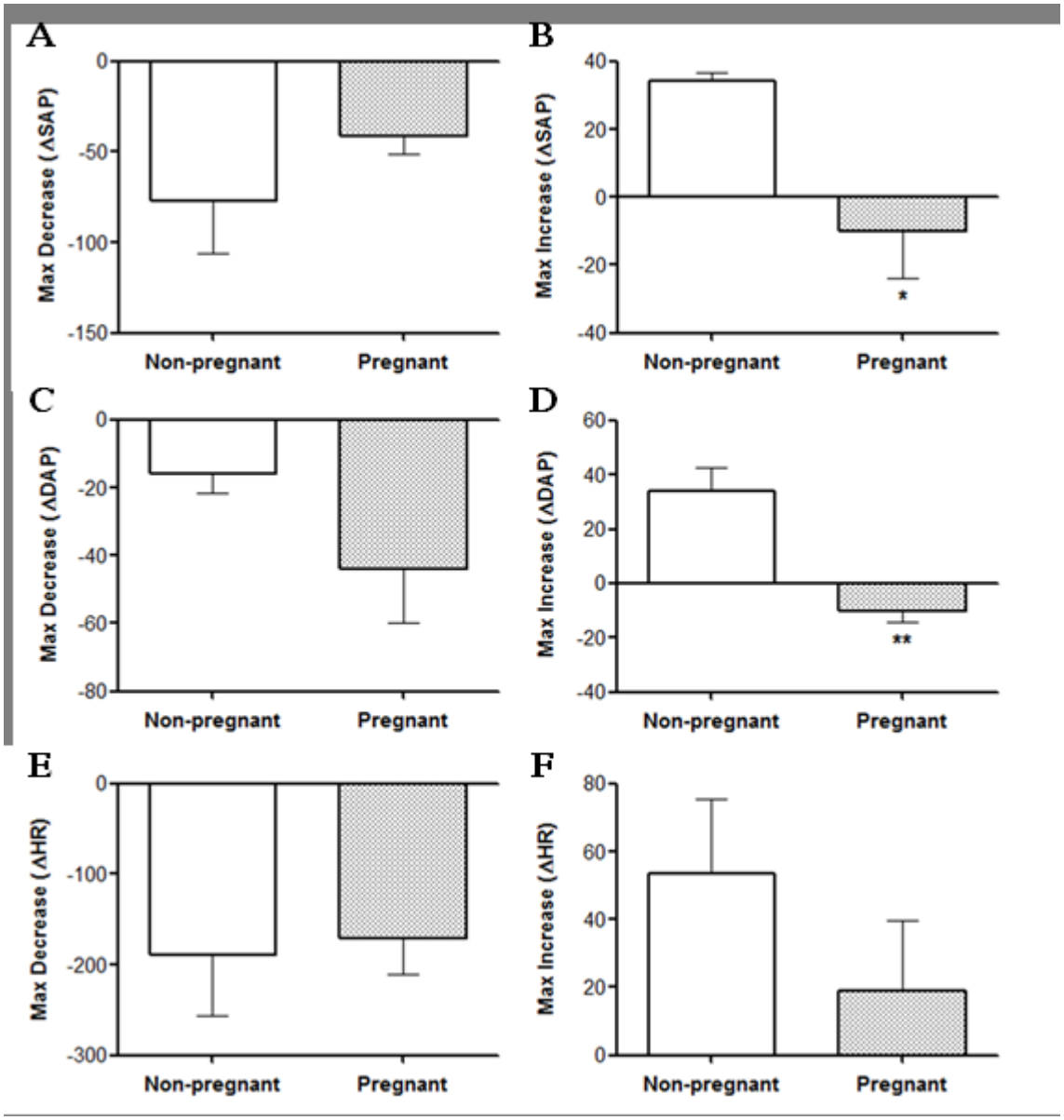


Figure 4.4: The haemodynamic response to LPS-induced inflammation in pregnant CD1 mice as assessed by maximum decrease and maximum increase. The haemodynamic response in pregnant and non-pregnant CD1 mice recorded during the period 24-hours after LPS administration. Maximum decrease was calculated for SAP (A), DAP (C) and HR (E). Maximum increase was calculated for SAP (B), DAP (D) and HR (F). *$p<0.05$, **$p<0.01$, student's t-test. Data are expressed as mean ± SEM (Pregnant, n=4; Non-pregnant, n=5).

Parameter	Comparisons	p-value			
		Overall	1 hour	12 hours	24 hours
MAP	**NP PBS vs. NP LPS**	**<0.001**	**ns**	**ns**	**ns**
	E16 PBS vs. E16LPS	**0.05**	**ns**	**0.016**	**0.035**
	NP LPS vs. E16LPS	**0.017**	**ns**	**ns**	**0.008**
SAP	**NP PBS vs. NP LPS**	**0.001**	**ns**	**ns**	**ns**
	E16 PBS vs. E16LPS	**0.047**	**ns**	**0.014**	**0.078**
	NP LPS vs. E16LPS	**ns**	**ns**	**ns**	**0.024**
DAP	**NP PBS vs. NP LPS**	**<0.001**	**ns**	**ns**	**ns**
	E16 PBS vs. E16LPS	**0.05**	**ns**	**0.009**	**ns**
	NP LPS vs. E16LPS	**ns**	**ns**	**0.027**	**0.012**
HR	**NP PBS vs. NP LPS**	**<0.001**	**0.014**	**ns**	**ns**
	E16 PBS vs. E16LPS	**ns**	**ns**	**ns**	**ns**
	NP LPS vs. E16LPS	**<0.001**	**ns**	**ns**	**ns**

en pregnant and non-pregnant haemo sponses to LPS. The overall trajectory of haemodynamic
PS (or PBS control) was compared betw t and non-pregnant CD1 mice (overall). Comparisons at
p-values are shown in this table. NP P gnant PBS-treated, NP LPS – non-pregnant LPS-treated,
t LPS-treated, ns- not significant.

4.2.2.3 The Effect of LPS-induced Inflammation on Maternal Activity

There were no statistically significant changes in the overall trajectory of Δ%TSI, ΔActivity or ΔActivity>0 between LPS-treated pregnant mice when compared to non-pregnant controls (Figure 4.5; Table 4.3).

In non-pregnant animals, compared to PBS-treated controls, LPS caused a significant increase in Δ%TSI ($p<0.001$) accompanied by a significant decrease in ΔActivity ($p<0.001$) and ΔActivity>0 ($p<0.001$). Conversely, in pregnant animals LPS did not cause any significant changes in activity parameters compared to PBS-treated controls (Table 4.3). As administration of 10μg LPS led to preterm birth in pregnant mice, it could be that in preparation for this event nesting behaviours prevented the LPS-treated mice from remaining sedentary. All statistical analyses are summarised in Table 4.3.

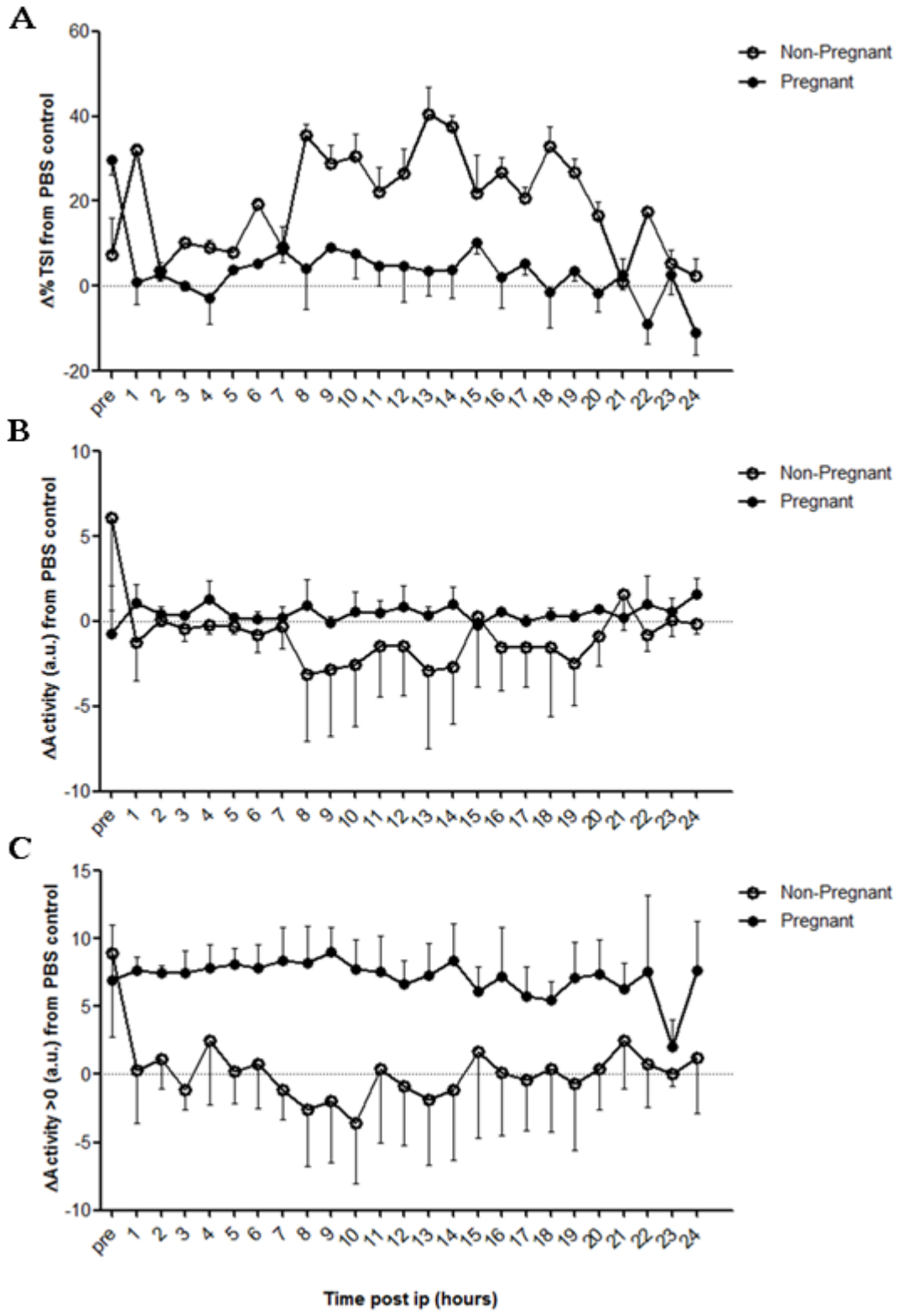


Figure 4.5: Activity in pregnant and non-pregnant CD1 mice after LPS administration. Activity levels in pregnant and non-pregnant mice were recorded for 24-hours following LPS administration (on E16 in pregnant mice). (A) Δ%TSI (B) ΔActivity (C) ΔActivity>0. Data are expressed as a mean change from pre-LPS baseline (pre) compared to PBS controls ± SEM (Pregnant, n=4; Non-pregnant, n=5).

Parameter	Comparisons	p-value			
		Overall	1 hour	12 hours	24 hours
TSI	NP PBS vs. NP LPS	<0.001	ns	<0.001	ns
	E16 PBS vs. E16LPS	ns	ns	ns	ns
	NP LPS vs. E16LPS	ns	ns	<0.001	ns
Activity	NP PBS vs. NP LPS	<0.001	ns	ns	ns
	E16 PBS vs. E16LPS	0.016	ns	ns	ns
	NP LPS vs. E16LPS	ns	ns	<0.001	ns
Activity >0	NP PBS vs. NP LPS	<0.001	ns	<0.001	ns
	E16 PBS vs. E16LPS	ns	ns	ns	ns
	NP LPS vs. E16LPS	ns	ns	ns	ns

n pregnant and non-pregnant activity se to LPS. The overall trajectory of activity was recorded as compared between pregnant and non D1 mice (overall). Comparisons at 1 hour, 12 hours and 24 is table. NP PBS- non-pregnant PBS-tr LPS – non-pregnant LPS-treated, E16 PBS- pregnant PBS- ficant.

4.2.3 LPS-induced Cytokine and Chemokine Production in Non-Pregnant and Pregnant Mice

Absolute concentrations of cytokines and chemokines in serum from pregnant and non-pregnant mice 6 and 12 hours after LPS/PBS were measured using the Millipore MAGpix multiplex assay system to evaluate the systemic inflammatory response. The 12 hour time point was chosen as the plateau in MAP was reached at a 12 hours post-LPS injection, and consequently 6 hours was chosen as an intermediary time point.

There was a marked increase in the concentrations of all of the pro-inflammatory cytokines examined in those mice treated with LPS compared to the corresponding time point PBS control (Figure 4.6). IL-1β and IL-6 and TNF-α increases were sustained over both 6 and 12 hours (Figure 4.6B, 4.6C and 4.6D). None of the pro-inflammatory cytokines were observed to be different in response to LPS in pregnant mice compared to non-pregnant mice.

There were also increases observed in the circulating levels of the anti-inflammatory cytokines IL-4 and IL-10 after stimulation with LPS (Figure 4.7). IL-4 was only significantly increased in pregnant mice, 12 hours post-LPS ($p<0.05$, Figure 4.7A). However, IL-10 was increased at both 6 and 12 hours following LPS administration in both non-pregnant and pregnant mice (Figure 4.7B).

The levels of several chemokines were also examined in serum from non-pregnant and pregnant mice (Figure 4.8). CCL2 (Figure 4.8A), CCL5 (Figure 4.8C), CXCL1 (Figure 4.8D) and CXCL2 (Figure 4.8E) were all significantly increased following LPS. CCL3 (Figure 4.8B) was significantly elevated 6 hours after LPS in non-pregnant mice from 75.01 ± 2.04 pg/mL to 286.2 ± 108.2 pg/mL ($p<0.01$). Interestingly though, CCL3 did not increase above basal levels (PBS-treatment) in the pregnant mice after LPS. Consequently, at 6 hours there was less CCL3 in LPS-treated pregnant mice than in non-pregnant controls ($p<0.001$).

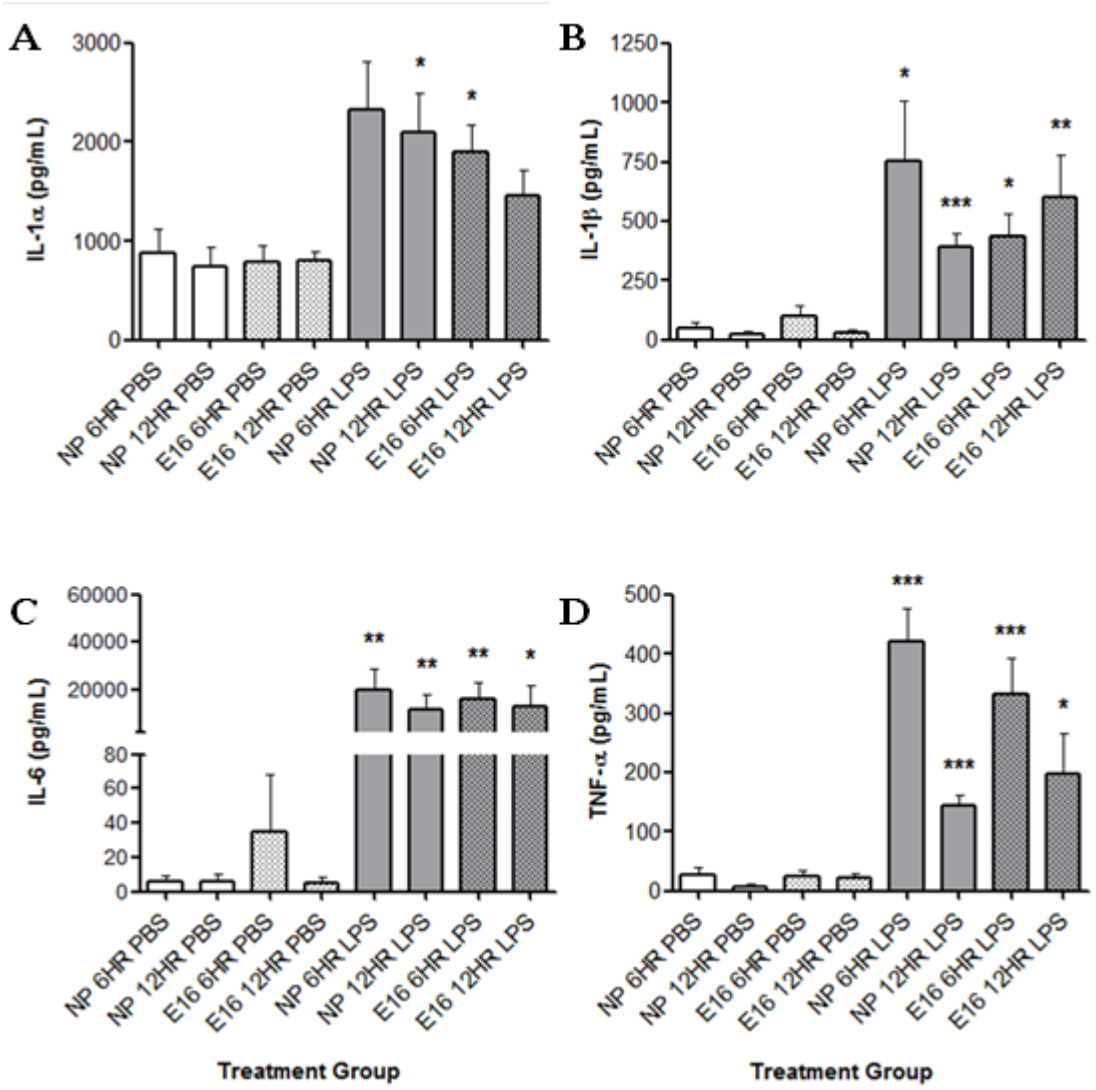


Figure 4.6: **Circulating concentrations of pro-inflammatory cytokines in serum of non-pregnant and pregnant mice treated with LPS or vehicle**. (A) IL-1α (B) IL-1β (C) IL-6 (D) TNF-α. *p<0.05, **p<0.01, ***p<0.001 compared to vehicle control, pairwise t-test comparisons or Mann Whitney U tests were used where appropriate. Data shown as mean ± SEM (LPS groups, n=6; PBS groups, n=4). NP- non-pregnant; E16- pregnant.

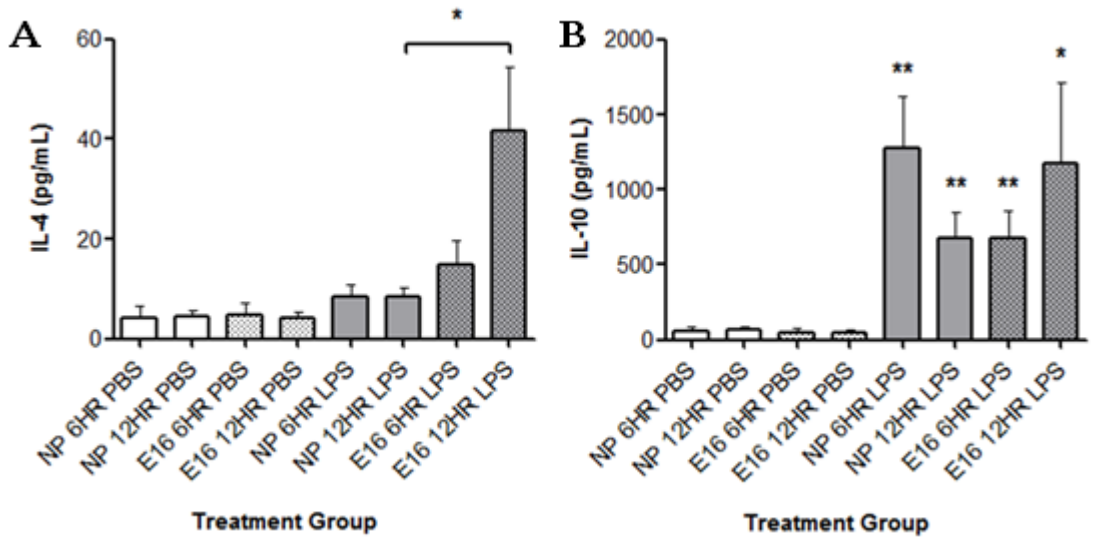


Figure 4.7: **Circulating concentrations of anti-inflammatory cytokines in serum of non-pregnant and pregnant mice treated with LPS or vehicle**. (A) IL-4 (B) IL-10. *p<0.05, **p<0.01 compared to vehicle control unless otherwise indicated, pairwise t-test comparisons or Mann Whitney U tests were used where appropriate. Data shown as mean ± SEM (LPS groups, n=6; PBS groups, n=4). NP- non-pregnant; E16- pregnant.

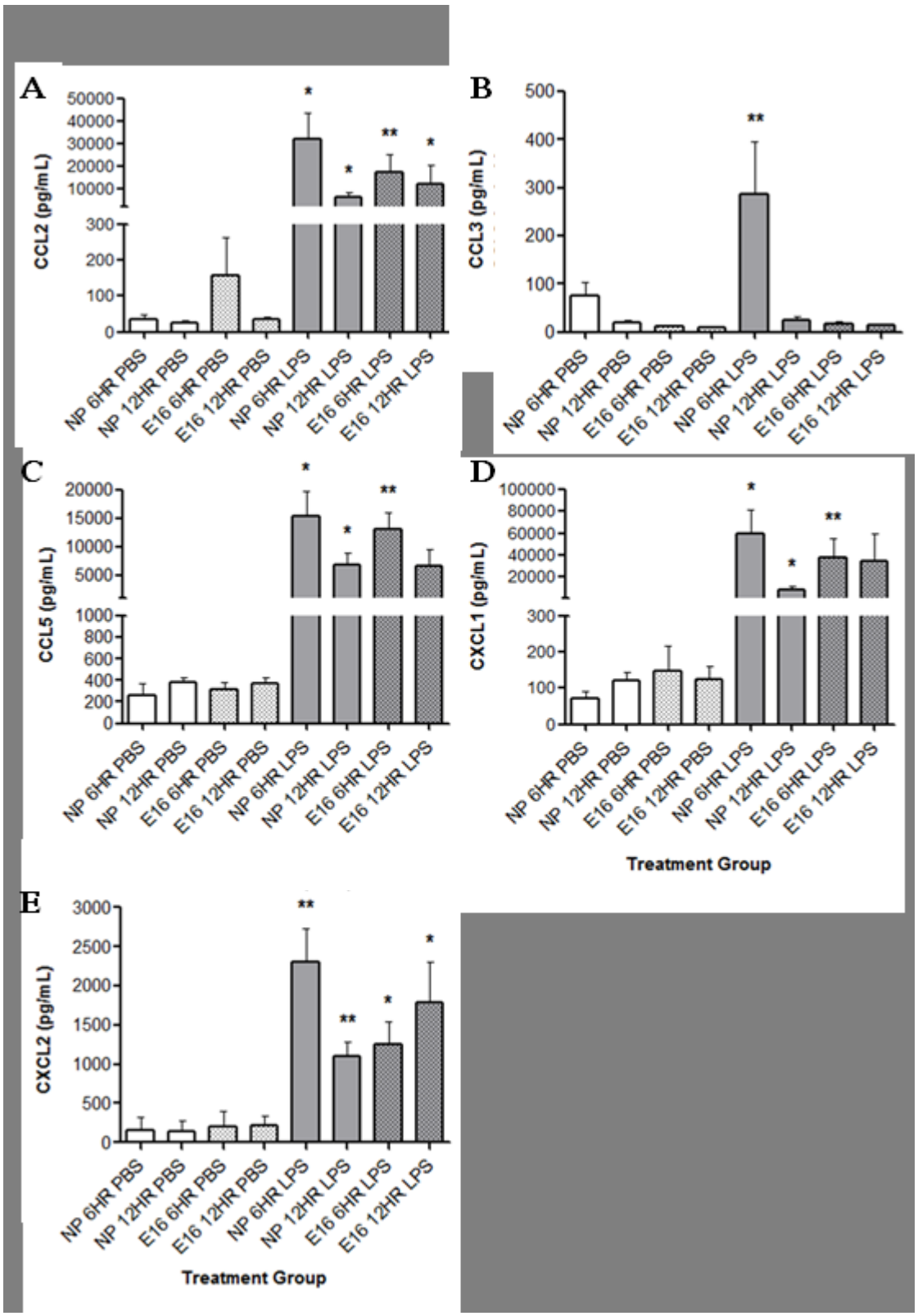


Figure 4.8: **Circulating concentrations of chemokines in serum of non-pregnant and pregnant mice treated with LPS or vehicle**. (A) CCL2 (B) CCL3 (C) CCL5 (D) CXCL1 (E) CXCL2. *p<0.05, **p<0.01, ***p<0.001 compared to vehicle control unless otherwise indicated, pairwise t-test comparisons or Mann Whitney U tests were used where appropriate. Data shown as mean ± SEM (LPS groups, n=6; PBS groups, n=4). NP- non-pregnant; E16-pregnant.

4.2.4 Circulating and Cardiac Expression of Vasoactive Factors in Response to LPS in Non-Pregnant and Pregnant Mice

NO, cGMP and ADMA concentrations in serum from pregnant and non-pregnant mice 6 and 12 hours after LPS/PBS were determined using the Sievers nitric oxide analyser, ELISA and mass spectrometry respectively. Absolute concentrations of vasoactive factors in serum from pregnant and non-pregnant mice 6 and 12 hours after LPS/PBS were measured using the Millipore MAGpix multiplex assay system to evaluate the systemic response. In addition, these factors were also analysed in whole heart homogenate to determine the local response. As the heart is an extremely vascular tissue, it was suggested that the presence or dysregulation of vasoactive factors here may indicate the response in systemic vascular beds.

At E16, circulating NO concentrations were not significantly different from non-pregnant controls (Figure 4.9A; 55.84 ± 12.43 μM and 54.2 ± 7.86 μM respectively at 6 hours). At 6 and 12 hours after LPS administration, NO was significantly increased in both non-pregnant and pregnant mice ($p<0.05$). However, at 6 hours post-LPS this effect was significantly attenuated in pregnant animals compared to non-pregnant (108.1 ± 13.51 μM and 191.1 ± 33.42 μM respectively, $p<0.05$). This result was surprising, and whilst initial thoughts were that NO concentrations may have been diluted due to an increased plasma volume in pregnant mice, when results were normalised to plasma volume (135% of non-pregnant mice; data not shown), NO levels in pregnant mice after LPS remained significantly reduced. These results could reflect increased sensitivity of pregnant mice to NO.

As many actions of NO are mediated by the downstream signalling molecule cGMP, we hypothesised that cGMP levels could be altered in pregnancy. cGMP was not found to be significantly increased in any of the groups treated with LPS. However, cGMP levels in pregnant mice 6 hours after vehicle (PBS) injection were increased compared to non-pregnant controls ($p<0.05$). This effect was not seen at 12 hours (Figure 4.9B). The endogenous inhibitor of NO, ADMA, was found to be increased in non-pregnant LPS treated animals at 6 hours ($p<0.05$), but no increase was observed in pregnant animals (Figure 4.9C).

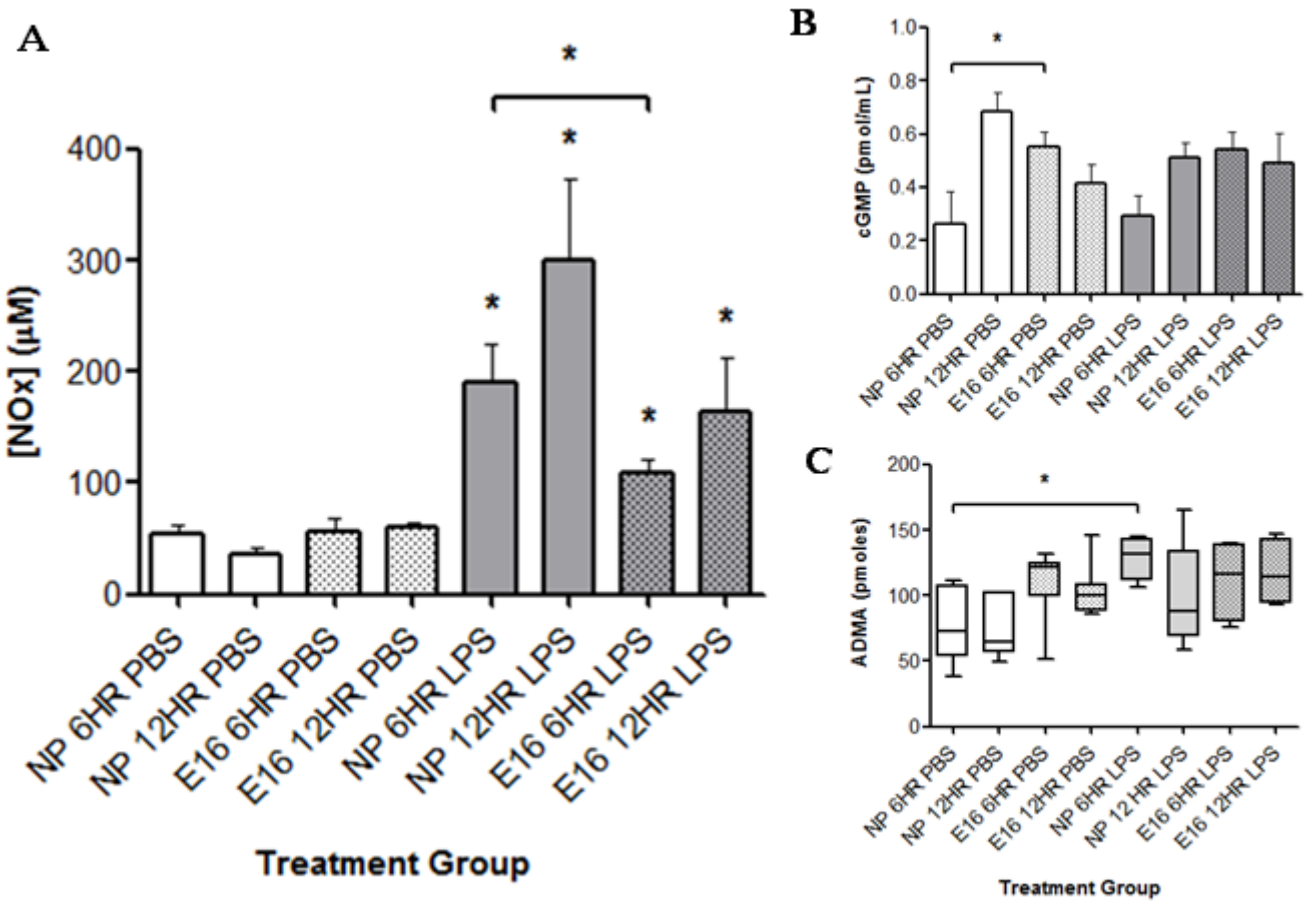


Figure 4.9: **Nitric oxide, cGMP and ADMA measurements in serum of non-pregnant and pregnant mice treated with LPS or vehicle.** (A) Concentration of total nitrates and nitrites (NOx) in serum samples taken 6 or 12 hours after LPS or PBS treatment in non-pregnant or pregnant mice. Values were adjusted to account for plasma volume. *p<0.05 pairwise analysis using student's t-test when compared to PBS control unless otherwise indicated. Data are shown as mean ± SEM (LPS groups, n=6; PBS groups, n=4). (B) cGMP levels in serum samples taken 6 or 12 hours after LPS or PBS treatment in NP or E16 mice. *p<0.05 pairwise analysis using student's t-test (LPS groups, n=8; PBS groups, n=4). (C) ADMA concentrations in serum samples taken 6 or 12 hours after LPS or PBS treatment in NP or E16 mice. *p<0.05 Mann-Whitney U test (LPS groups, n=8; PBS groups, n=4). NP- non-pregnant; E16-pregnant.

Circulating concentrations of VEGF-A (VEGF) were significantly increased at both 6 and 12 hours post-LPS in non-pregnant mice: 134.2 ± 51.82 pg/mL and 118.9 ± 31.3 pg/mL at 6 and 12 hours respectively up from 13.04 ± 1.04 pg/mL and 14.03 ± 2.7 pg/mL ($p<0.05$); this effect was almost completely abolished in pregnant mice ($p<0.05$; Figure 4.10A). Thus, in pregnant mice, LPS did not cause any increase in VEGF.

PLGF, a member of the VEGF family, is classically recognised as a pregnancy-related vasoactive factor due to its main site of production being the placental trophoblast [312]. However, there has been recent interest around its potential role in sepsis in non-pregnant animals [313, 314]. PLGF2 was increased in non-pregnant mice after LPS, significantly at 12 hours ($p<0.001$; Figure 4.10B). In pregnant mice, LPS did not cause any increase in PLGF2 and at 12 hours the response was very significantly attenuated compared to non-pregnant controls ($p<0.001$). The functional counterpart of NO in vascular function, endothelin-1 (ET-1) was found to be significantly decreased in pregnant mouse serum compared to non-pregnant, in both PBS and LPS-treated mice, although this was only statistically significant at the 6 hour time point ($p<0.05$ and $p<0.01$ respectively; Figure 4.10C). LPS did not cause any significant changes in ET-1 concentrations in non-pregnant mice, when compared to PBS-treated controls.

To further explore the PLGF response in view of the finding that PLGF levels were increased following LPS in the serum of non-pregnant mice compared to pregnant, serum taken from mice at gestational time points was examined using a PLGF2 ELISA to determine the normal PLGF profile throughout CD1 mouse pregnancy (Figure 4.11). Concentrations of PLGF2 were seen to rise through early pregnancy to reach a peak at approximately E11 (333.5 ± 35.79 pg/mL) before dropping again by E16 (101.1 ± 26.54 pg/mL) to levels similar to those seen in non-pregnant mice (95.06 ± 17.3 pg/mL). At E18, there was a large variability in PLGF2 levels (Figure 4.11A). This may possibly be due to the proximity of the progression of labour which may have fallen either on late E18 or early E19. Recent evidence has suggested that PLGF could play a role in the mediation of pro-inflammatory and pro-labour actions in mouse uterus [315], human cervix and placenta [316, 317].

PLGF2 levels then consistently fell to below non-pregnant levels in lactating post-partum mice (1.02 ± 1 pg/mL). This may be due to the anti-angiogenic effects of prolactin [318-320]. Circulating concentrations as determined by MAGpix multiplex assay and PLGF2 ELISA in untreated and PBS-treated CD1 mice at E16 were comparable (107.2 ± 16.97 pg/mL and 101.1 ± 26.54 pg/mL respectively).

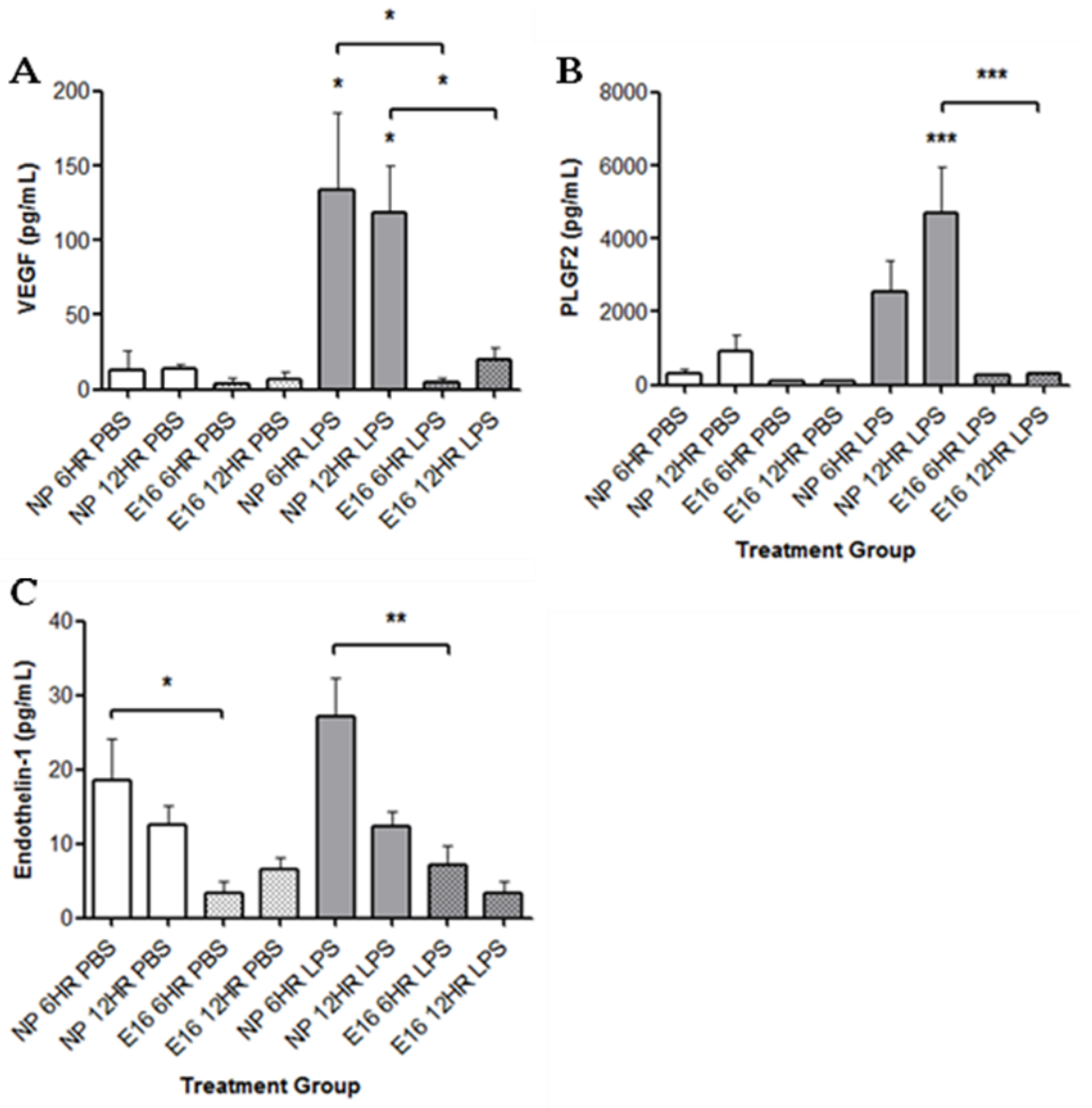


Figure 4.10: Circulating concentrations of vasoactive factors in serum of non-pregnant and pregnant mice treated with LPS or vehicle. (A) VEGF (B) PLGF2 (C) Endothelin-1. *p<0.05, **p<0.01, ***p<0.001 compared to vehicle control unless otherwise indicated, pairwise t-test comparisons or Mann Whitney U tests were used where appropriate. Data shown as mean ± SEM (LPS groups, n=8; PBS groups, n=4). NP- non-pregnant; E16-pregnant.

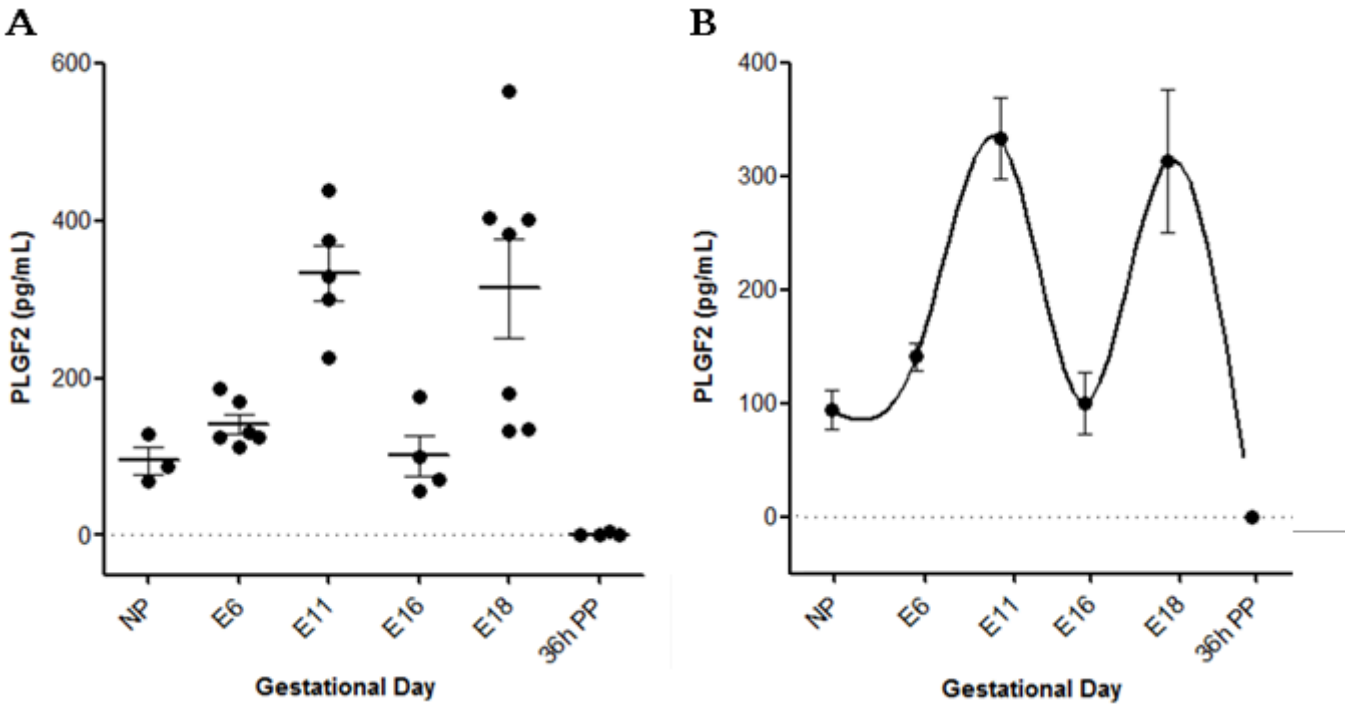


Figure 4.11: **Concentrations of circulating PLGF2 measured at gestational time points in CD1 mice.** PLGF2 as measured by ELISA at gestational time points in CD1 mice shown using data plotted as individual animals (A) and as a PLGF2 profile during pregnancy, data shown as mean ± SEM and LOWESS curve (B) (NP, n=3; E6, n=6; E11, n=5; E16, n=4; E18, n=7; 36h PP, n=4). NP – non-pregnant; E6 – gestational day 6; E11 – gestational day 11; E16 – gestational day 16; E18 – gestational day 18; 36h PP – 36 hours post-partum.

In whole heart homogenate, PLGF2 was increased in both non-pregnant and pregnant groups treated with LPS ($p<0.01$; Figure 4.12B). Concentrations of ET-1 remain unchanged between non-pregnant and pregnant, and between PBS- and LPS-treated mice (Figure 4.12C). Overall ET-1 concentrations in the heart were greater than those observed in the serum.

There was a trend observed where VEGF was decreased in PBS-treated mice 12 hours following injection compared to 6 hours in both non-pregnant and pregnant mice (Figure 4.12A), however this did not reach significance. This may indicate that the intraperitoneal injection itself may trigger increases in VEGF in the heart, but this speculation would need to be addressed by examining VEGF levels in naïve mice. Due to lower concentrations of VEGF in PBS-treated non-pregnant mice at 6

hours, this resulted in a significant increase after LPS at this time point alone. Absolute VEGF concentrations in the heart were also greater in PBS control mice than those observed in the serum.

To further investigate the serum VEGF response disparity in non-pregnant and pregnant mice, several VEGF isoforms were measured in serum and heart. It was found that VEGF-C was not significantly increased in any treatment group following LPS in the serum (Figure 4.13A). Although, pregnant mice had significantly lower VEGF-C concentrations at 12 hours after LPS than non-pregnant mice 12 hours after LPS ($p<0.05$), this was not significantly reduced from PBS control. VEGF-C in the heart and VEGF-D in both serum and the heart remained at consistent levels in all treatment groups (Figure 4.13B, Figure 4.13C, Figure 4.13D).

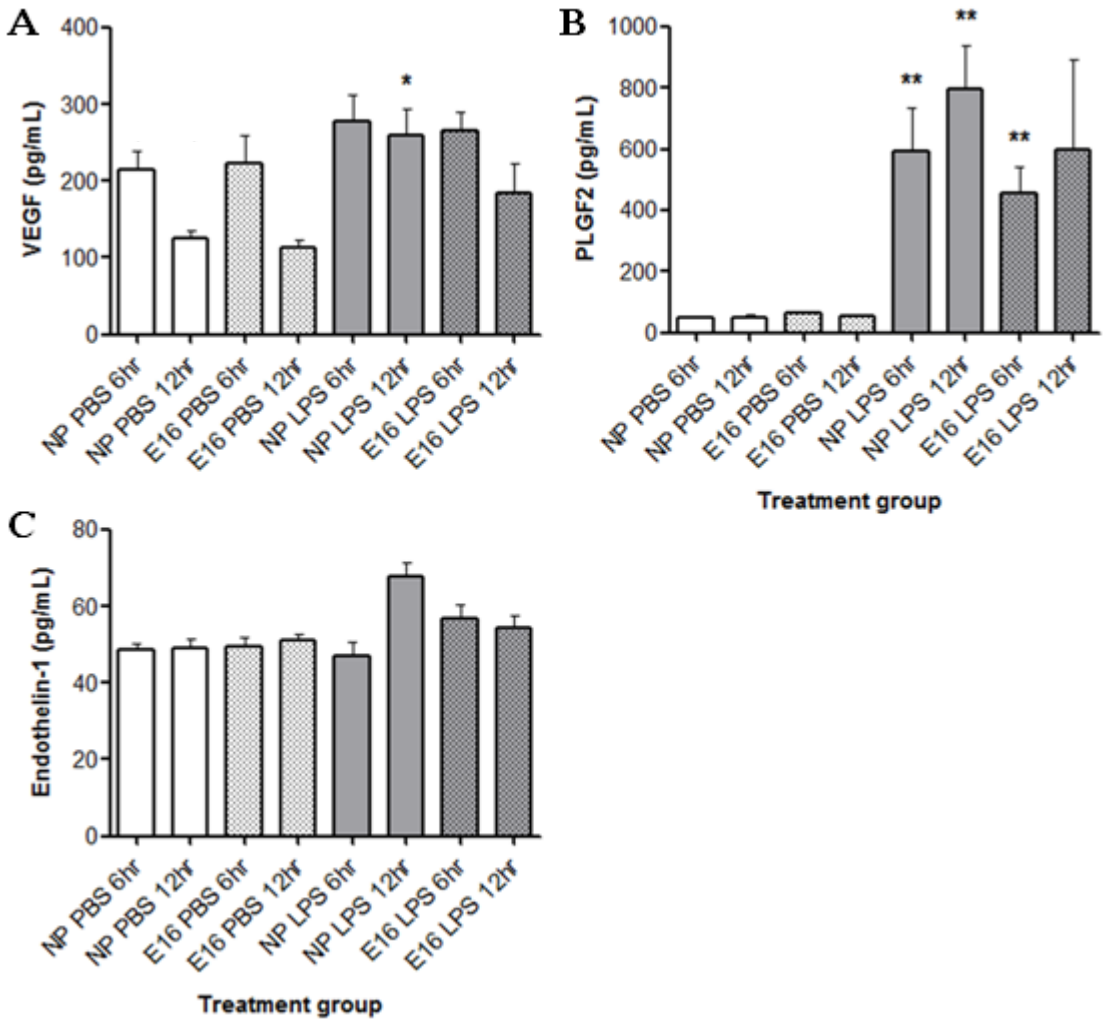


Figure 4.12: **Local concentrations of vasoactive factors in hearts taken from non-pregnant and pregnant mice treated with LPS or vehicle.** (A) VEGF (B) PLGF2 (C) Endothelin-1. **p<0.01 compared to vehicle control unless otherwise indicated, pairwise t-test comparisons or Mann Whitney U tests were used where appropriate. Data shown as mean ± SEM (LPS groups, n=6; PBS groups, n=4). NP- non-pregnant; E16-pregnant.

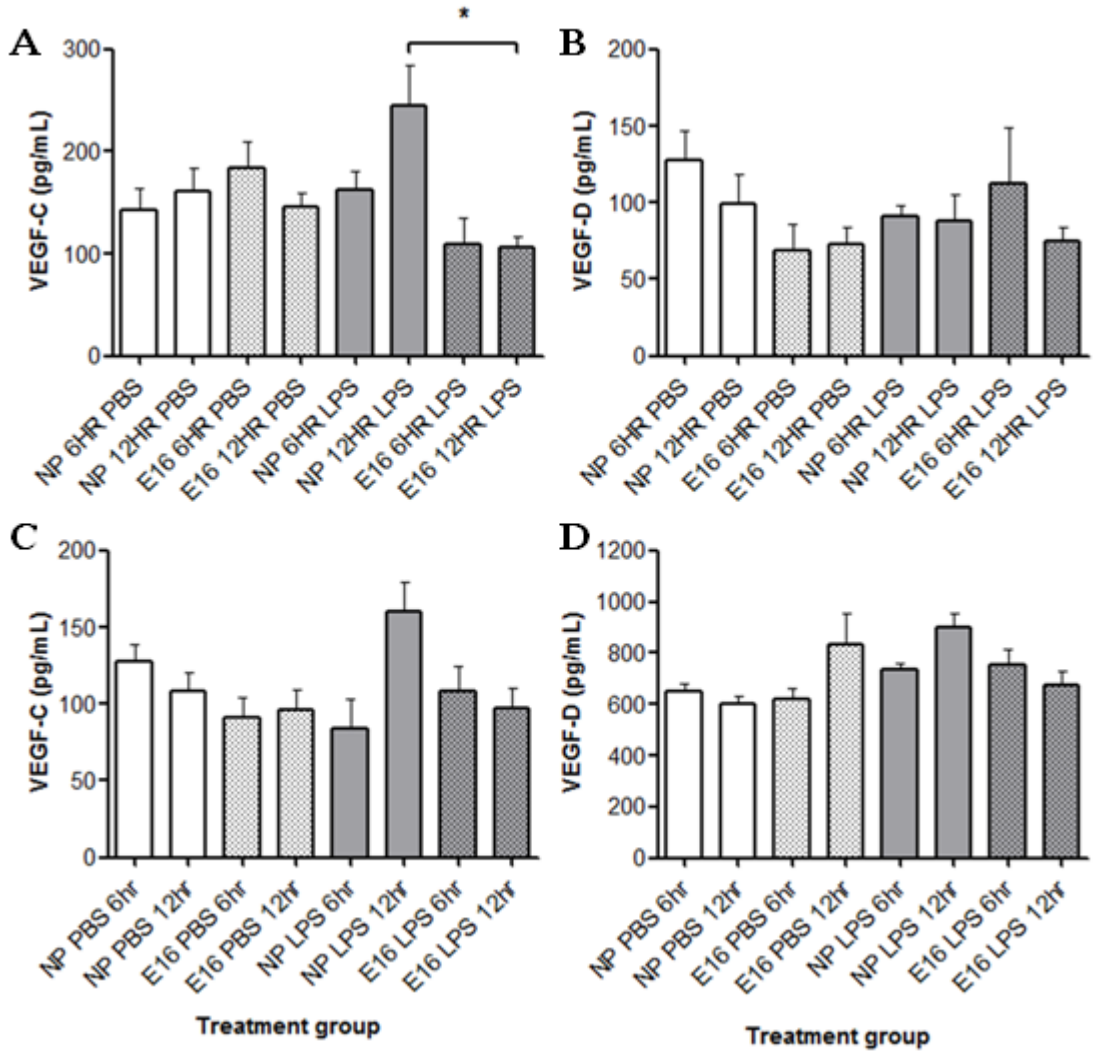


Figure 4.13: **Circulating and localised concentrations of VEGF isoforms in serum and hearts taken from non-pregnant and pregnant mice treated with LPS or vehicle.** (A) VEGF-C in serum (B) VEGF-D in serum (C) VEGF-C in heart (D) VEGF-D in heart. *$p<0.05$, pairwise t-test comparisons or Mann Whitney U tests were used where appropriate. Data shown as mean ± SEM (LPS groups, n=6; PBS groups, n=4). NP- non-pregnant; E16-pregnant.

4.2.5 LPS-induced Changes in Vascular Function in Non-Pregnant and Pregnant Mice

Despite the observed decline in MAP in pregnant mice in response to LPS, concentrations of circulating NO and VEGF were found to be attenuated in comparison to non-pregnant mice. It was hypothesised that this may be due to an increased sensitivity of the pregnant vasculature to the vasodilator action of NO. To further investigate this, vascular reactivity and vessel relaxation were examined using wire myography in both aorta (Figure 4.14) and uterine artery (Figure 4.15).

4.2.5.1 Aorta

Isolated aortic vessel sections were exposed to increasing doses of phenylephrine (PE) and the contractile response was recorded (Figure 4.14A, 4.14B). $LogEC_{50}$ values for PE were -3.84 M in non-pregnant and -3.19 M in pregnant mice ($p<0.01$). Vessel responses were significantly different at log[PE] -4 M and log[PE] -3.5 M as determined by Bonferroni post-tests. After LPS treatment, $logEC_{50}$ values for PE were -3.8 M for non-pregnant and -3.6 M for pregnant ($p<0.05$). The maximal contractions elicited by PE were the same in all treatment groups.

To test endothelial cell responsiveness to acetylcholine (ACh), vessels were first sub-maximally contracted with PE where the EC_{80} was used to yield an 80% contraction. There was no differential response to ACh in pregnant animals compared to non-pregnant (Figure 4.14C). When the response to ACh in PBS- and LPS-treated non-pregnant groups was compared, LPS was shown to significantly reduce vessel sensitivity ($p<0.001$, data not shown). However, when non-pregnant and pregnant groups after LPS administration were compared, the response in pregnant aorta was significantly decreased ($p<0.01$; Figure 4.14D). Because the data collected in response to ACh could not define a top and bottom plateau, EC_{50} values could not be calculated.

To investigate whether smooth muscle NO signalling is altered in pregnancy, an NO donor sodium nitroprusside (SNP) was used to relax vessels after initial pre-constriction with PE (EC_{80}). In both PBS- and LPS-treated groups, vessels from pregnant mice were significantly less responsive to SNP ($p<0.05$ and $p<0.001$ respectively; Figure 4.14E, 4.14F).

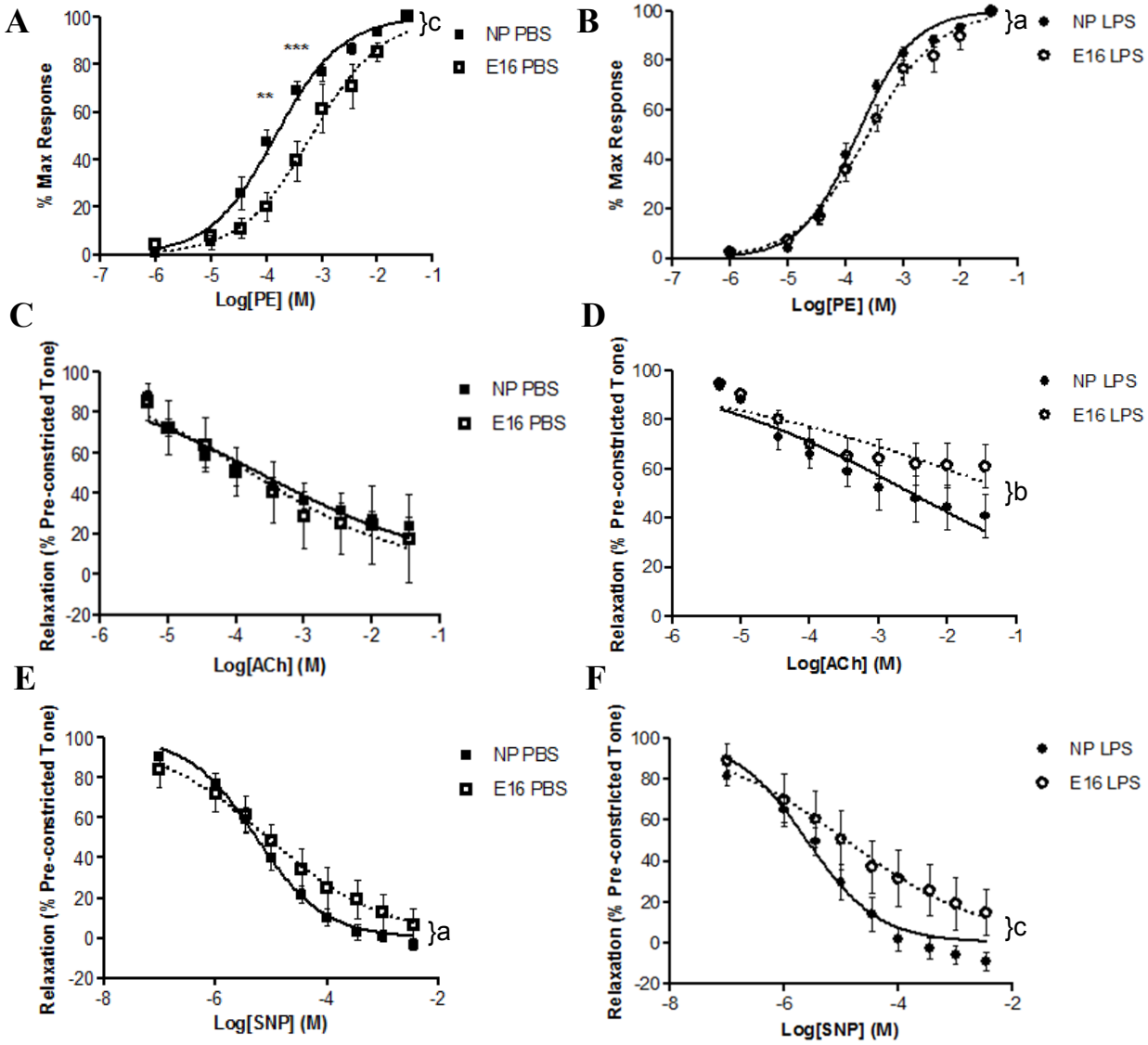


Figure 4.14: Ex–vivo measurement of aortic endothelial responses in non-pregnant and pregnant mice treated with LPS or vehicle. Responses to (A,B) phenylephrine (PE), (C,D) acetylcholine (ACh), and (E,F) sodium nitroprusside (SNP) in aorta from non-pregnant (closed symbols) or pregnant (open symbols) exposed to PBS (vehicle; square symbols) or 10µg LPS (circular symbols) for 12 hours. **p<0.01, ***p<0.001, 2-way ANOVA with Bonferroni post-hoc test at specific concentrations; overall comparisons were made using a 2-way ANOVA with Bonferroni post-hoc test, a p<0.05, c p<0.001. Data are presented at mean ± SEM (NP PBS, n=7; NP LPS, n=8; E16 PBS, n=8; E16 LPS, n=7[n=5 for SNP]). NP- non-pregnant; E16-pregnant.

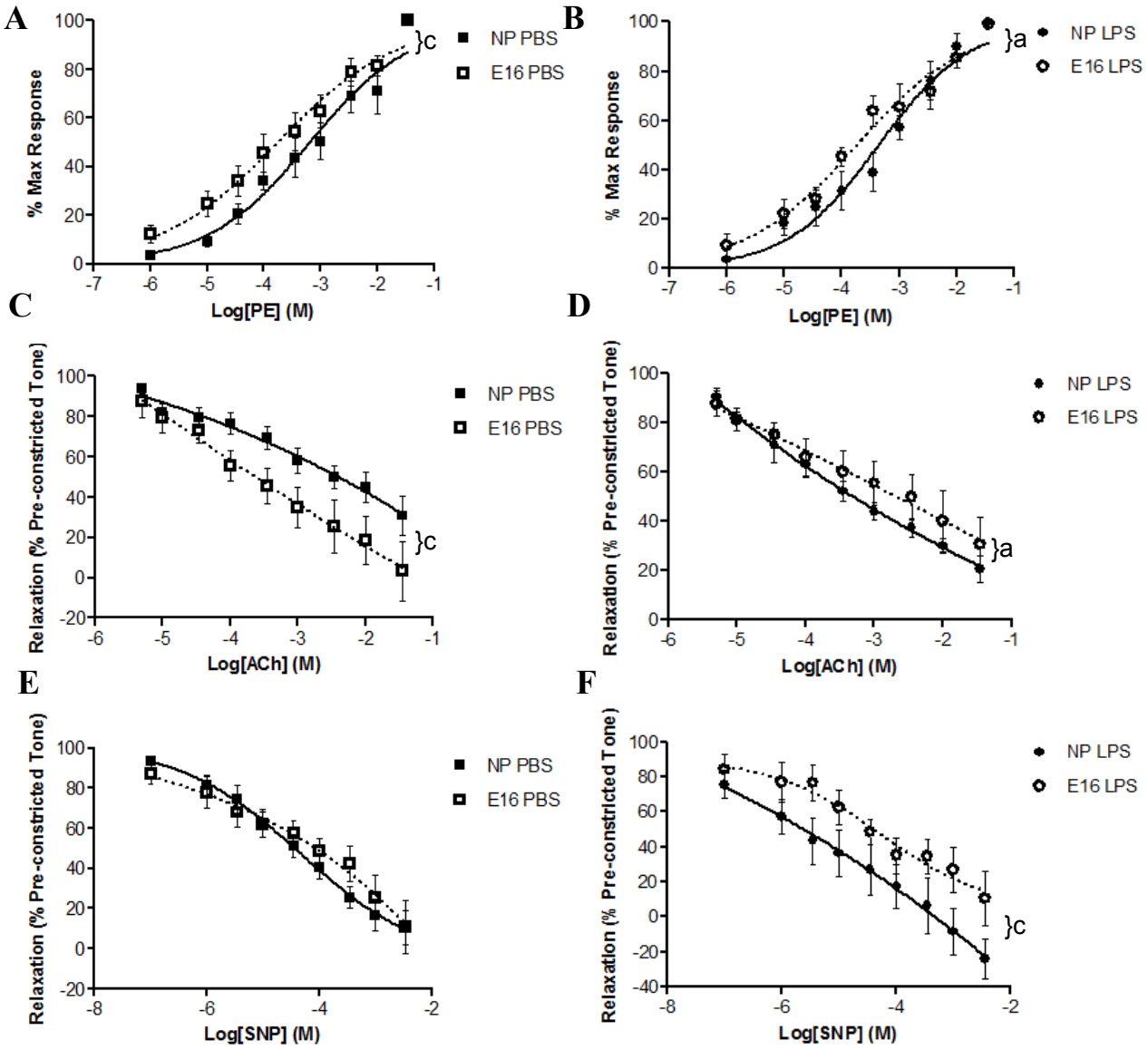


Figure 4.15: Ex–vivo measurement of uterine artery endothelial responses in non-pregnant and pregnant mice treated with LPS or vehicle. Responses to (A,B) phenylephrine (PE), (C,D) acetylcholine (ACh), and (E,F) sodium nitroprusside (SNP) in uterine artery from non-pregnant (NP; closed symbols) or pregnant (E16; open symbols) exposed to PBS (vehicle; square symbols) or 10µg LPS (circle symbols) for 12 hours. Overall comparisons were made using a 2-way ANOVA with Bonferroni post-hoc test, a $p<0.05$, c $p<0.001$. Data are presented at mean ± SEM (NP PBS, n=7; NP LPS, n=7; E16 PBS, n=8 [n=5 for ACh]; E16 LPS, n=8[n=5 for ACh and SNP]). NP-non-pregnant; E16-pregnant.

4.2.5.1 Uterine Artery

To more closely examine the altered uterine vasculature in pregnancy, uterine artery vessel sections were exposed to increasing doses of PE and the contractile response was recorded (Figure 4.15A, 4.15B). $LogEC_{50}$ values for PE were -3.19 M in non-pregnant and -3.75 M in pregnant mice ($p<0.001$). After LPS treatment, $logEC_{50}$ values for PE were -3.37 M for non-pregnant and -3.75 M for pregnant mice ($p<0.05$). The maximal contractions elicited by PE were the same in all treatment groups.

After pre-constriction with PE (EC_{80}) responses to ACh in the uterine artery were recorded. Unlike in the aorta, the uterine artery in pregnant animals was significantly more sensitive to ACh ($p<0.001$; Figure 4.15C). Interestingly, this effect was reversed in LPS-treated animals ($p<0.05$; Figure 4.15D). Again, after initial pre-constriction with PE (EC_{80}) responses to SNP in the uterine artery were not altered in pregnancy (Figure 4.15E), and after treatment with LPS, pregnant animals had significantly decreased sensitivity ($p<0.001$; Figure 4.15F).

Comparisons between treatment groups of both aorta and uterine artery responses to PE, ACh, and SNP have been summarised in Table 4.4. Analyses include comparisons between PBS- and LPS-treated responses in non-pregnant as well as pregnant mice.

Table 4.4: **Summary of changes in vascular function and sensitivity to vasoactive substances**. Comparisons were made between pregnant and non-pregnant mice in uterine artery and aorta from mice exposed to LPS or vehicle (PBS). P values were obtained from 2-way ANOVA analyses. NP- non-pregnant; E16-pregnant.

Aorta	Uterine Artery
E16 compared to NP	
Decreased sensitivity to PE (P<0.001)	Increased sensitivity to PE (P<0.001)
No difference in response to ACh	Increased sensitivity to ACh (P<0.001)
Decreased sensitivity to SNP (P<0.05)	No difference in response to SNP
E16-LPS, compared to NP-LPS	
Decreased sensitivity to PE (P<0.05)	Increased sensitivity to PE (P<0.05)
Decreased sensitivity to ACh (P<0.01)	Decreased sensitivity to ACh (P<0.05)
Decreased sensitivity to SNP (P<0.001)	Decreased sensitivity to SNP (P<0.001)
E16-PBS, compared to E16-LPS	
Increased sensitivity to PE (P<0.01)	No difference in response to PE
Decreased sensitivity to ACh (P<0.001)	Decreased sensitivity to ACh (P<0.01)
No difference in response to SNP	No difference in response to SNP
NP-PBS, compared to NP-LPS	
No difference in response to PE	No difference in response to PE
Decreased sensitivity to ACh (P<0.001)	Increased sensitivity to ACh (P<0.001)
Increased sensitivity to SNP (P<0.01)	Increased sensitivity to SNP (P<0.001)

4.2.6 Expression of Markers of Inflammation, Cardiac Dysfunction and Apoptosis in Non-Pregnant and Pregnant Mice

To assess the extent of cardiac sensitivity, the relative expression of various markers of inflammation, apoptosis and cardiac dysfunction were assessed in maternal heart tissue using RT-PCR and western blot.

In whole heart homogenate, IL-6 mRNA was significantly increased 6 hours after LPS treatment in non-pregnant mice ($p<0.05$), but there was no significant increase observed at 12 hours (Figure 4.16B). The same trend was observed in pregnant mice but levels were attenuated and significance was not reached. TNF-α mRNA was significantly increased 6 hours after LPS treatment in both pregnant and non-pregnant mice ($p<0.05$; Figure 4.16C). Cox-2 expression was significantly decreased in pregnant animals 12 hours after i.p. in both LPS and PBS groups ($p<0.05$). There were no observed changes between the treatment groups for IL-1β or IL-10 (Figure 4.16A, 4.16D).

There were no observed changes in markers of cardiac dysfunction in heart tissue after LPS treatment or between pregnant and non-pregnant mice (Figure 4.17). There was a trend towards increased BNF in pregnant mice treated with LPS at 6 hours, which was not seen at 12 hours, where comparatively in non-pregnant animals no increase was seen. However this observation did not reach statistical significance.

B-cell Lymphoma-2 (Bcl-2) family members and other apoptotic markers were examined to assess the extent of apoptosis in maternal heart, compared to those of non-pregnant animals. The anti-apoptotic Bcl-2 mRNA remained consistently expressed over all treatment groups, however the pro-apoptotic marker Bcl-2 associated X protein (Bax) mRNA was shown to be increased after LPS treatment in non-pregnant mice (significantly increased by 12hours, $p<0.05$) but not in pregnant animals (Figure 4.18B). Bcl-2 associated death promoter (Bad) and Fas ligand (FasL) were also unchanged after LPS and did not differ between heart tissue from pregnant and non-pregnant mice hearts (Figure 4.18C, 4.18D).

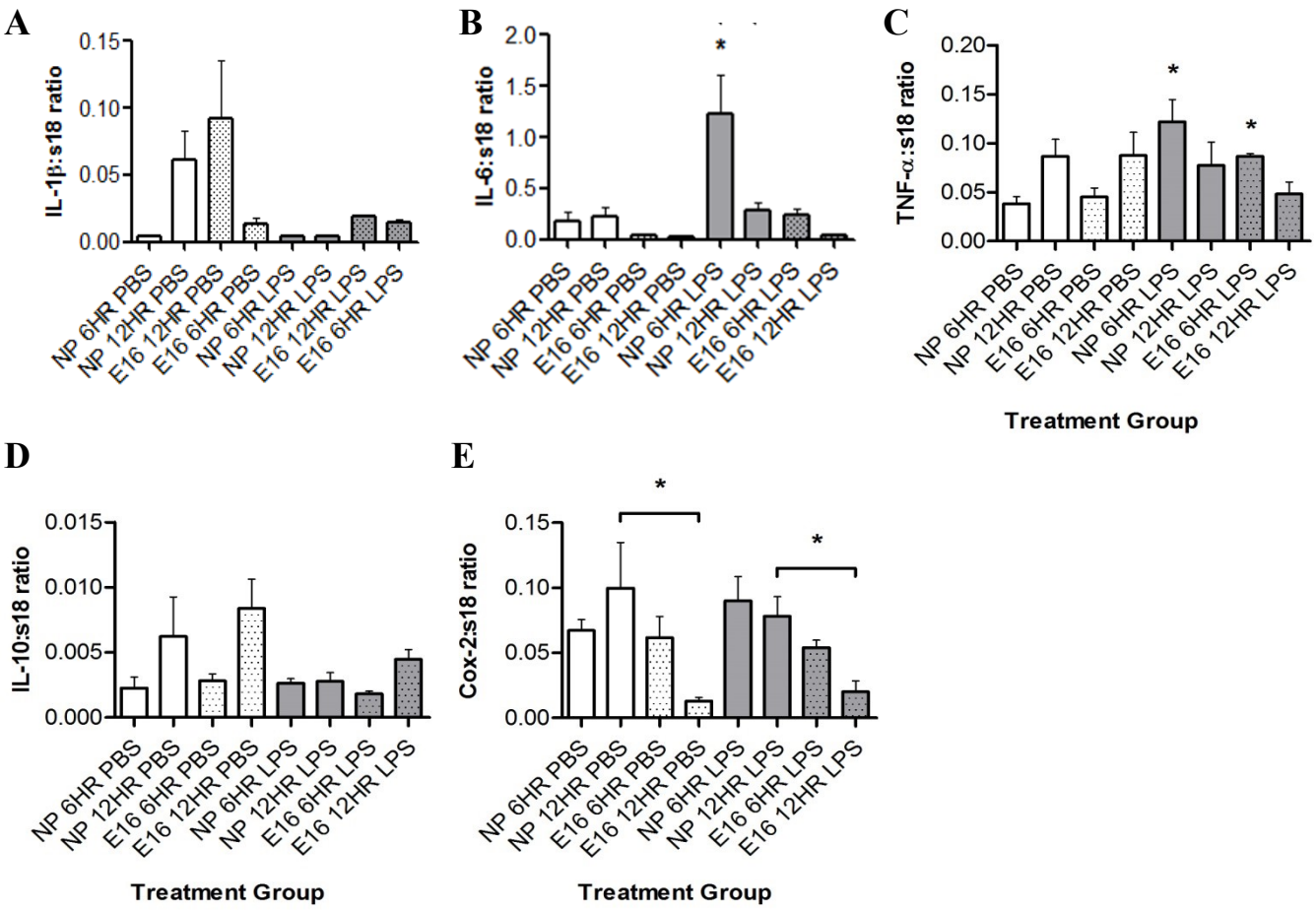


Figure 4.16: **mRNA expression of pro- and anti-inflammatory cytokines and inflammatory regulators in heart tissue taken from non-pregnant or pregnant mice treated with LPS or vehicle.** (A) IL-1β, (B) IL-6, (C) TNF-α, (D) IL-10, and (E) Cox-2. *$p<0.05$ compared to PBS control unless otherwise indicated, pairwise t-test comparisons or Mann Whitney U tests were used where appropriate. Data shown as mean ± SEM (LPS groups, n=6; PBS groups, n=4). NP- non-pregnant; E16-pregnant.

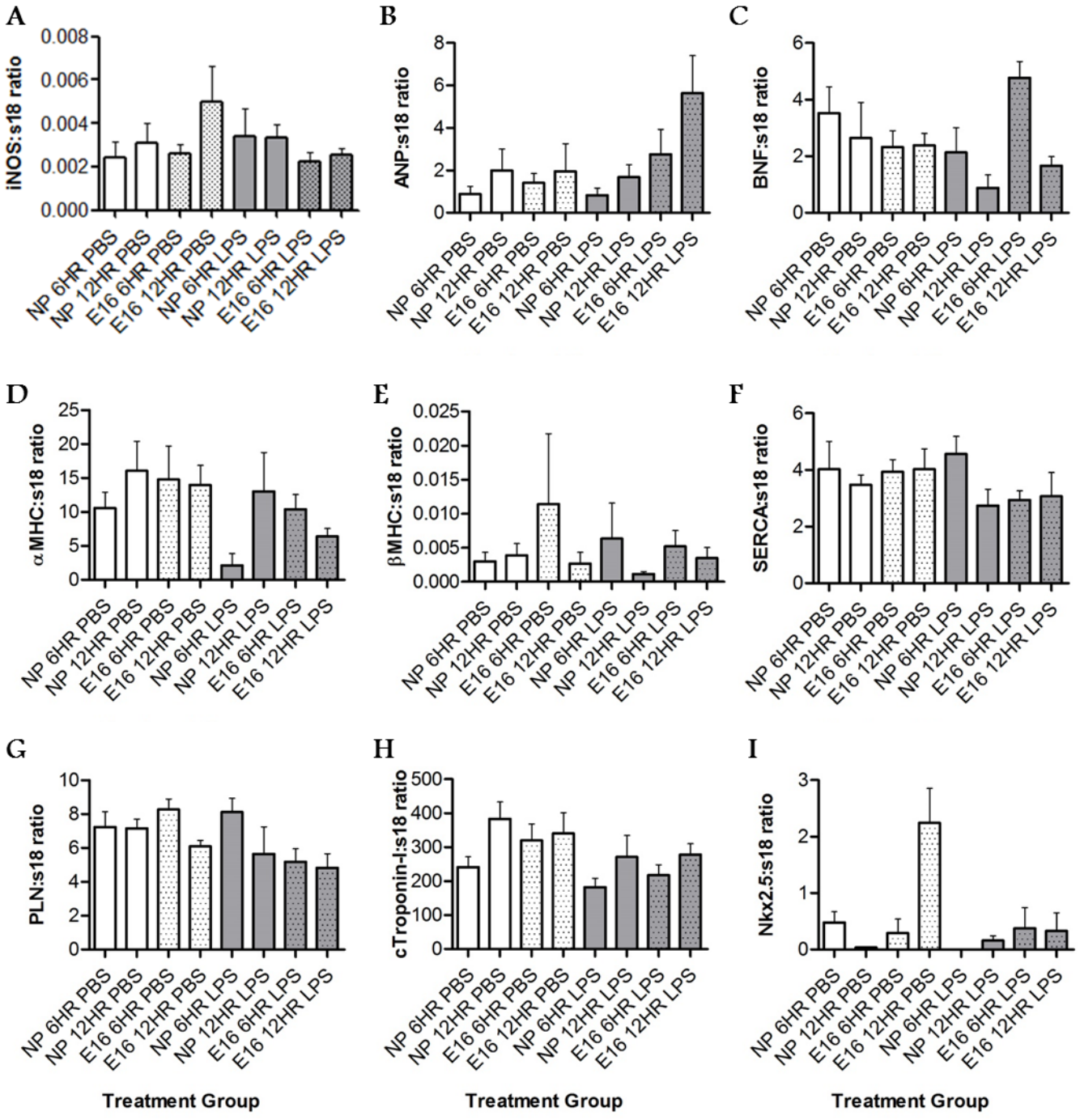


Figure 4.17: **mRNA expression of markers of cardiac dysfunction in heart tissue taken from non-pregnant or pregnant mice treated with LPS or vehicle**.(A) Inducible nitric oxide synthase (iNOS), (B) atrial natriuretic peptide (ANP), (C) brain natriuretic factor (BNF), (D) α-myosin heavy chain (α-MHC), (E) β-myosin heavy chain (β-MHC), (F) sarco/endoplasmic reticulum Ca^{2+}-ATPase (SERCA), (G) phospholamban (PLN), (H) cardiac troponin-I and (I) homeobox gene Nkx2.5. Pairwise t-test comparisons or Mann Whitney U tests were used where appropriate, no statistical significance was detected. Data shown as mean ± SEM (LPS groups, n=6; PBS groups, n=4). NP- non-pregnant; E16-pregnant.

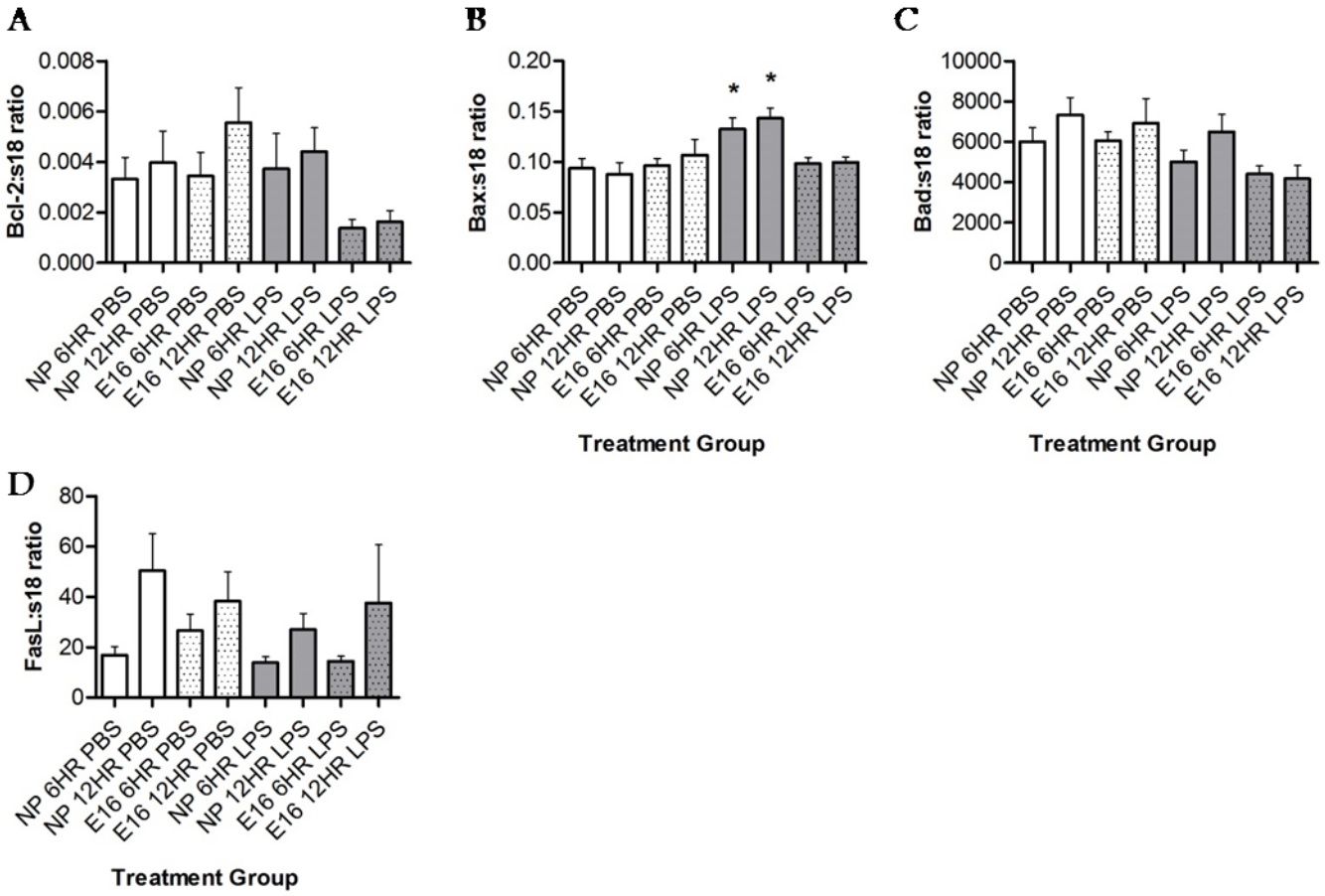


Figure 4.18: **mRNA expression of pro- and anti-apoptotic markers in heart tissue taken from non-pregnant or pregnant mice treated with LPS or vehicle.** (A) Bcl-2, (B) Bax, (C) Bad and (D) Fas ligand (FasL). *$p<0.05$ compared to PBS control, pairwise t-test comparisons were performed. Data shown as mean ± SEM (LPS groups, n=6; PBS groups, n=4). NP- non-pregnant; E16-pregnant.

To further examine the effects of LPS during pregnancy on apoptotic pathways, a series of western blots were performed to assess the abundance of caspase-3 protein (Figure 4.19A). As caspases are post-transcriptionally modified it was imperative to assess caspase activity at the protein level. Caspase-3 is formed from pro-caspase (approximately 32kDa) that cleaves into a 17kDa subunit (p17) and a smaller 12/14kDa subunit (p12/14) [321, 322]. It was shown by densitometry analysis in maternal heart samples that there were no significant changes in expression levels of either subunit in pregnant or non-pregnant mice 6 hours after LPS (Figure 4.19B) or 12 hours after LPS (Figure 4.19C).

Due to the somewhat dampened increase in pro-inflammatory cytokines observed in response to LPS, it was postulated that any systemic effect may have been masked by using whole heart homogenate. Therefore inflammatory markers, markers of cardiac dysfunction and makers of apoptosis were also assessed in isolated left ventricular tissue.

In left ventricular tissue, mRNA expression of IL-1β (Figure 4.20A), IL-6 (Figure 4.20B) and TNF-α (Figure 4.20C) were significantly upregulated 6 hours after LPS administration in both non-pregnant and pregnant mice ($p<0.01$). Expression levels of all pro-inflammatory cytokines were diminished by 12 hours. IL-10 expression was significantly increased 6 hours after LPS administration, but only in non-pregnant mice ($p<0.01$; Figure 4.20D). There were no observed changes in mRNA expression of Cox-2 (Figure 4.20E).

Similarly to mRNA expression levels in whole heart tissue, in left ventricular tissue there were few changes in markers of cardiac dysfunction. Of note, ANP was significantly decreased at 6 and 12 hours after LPS administration in both non-pregnant and pregnant mice ($p<0.01$; Figure 4.21B) and BNF was significantly increased 6 hours after LPS administration, but only in pregnant mice ($p<0.05$); however this increase was not significantly greater than expression 6 hours after LPS in non-pregnant mice. Further to this, unlike in whole heart tissue there were decreases in c-Troponin-I

and Nkx2.5 after LPS administration (Figure 4.21H, 4.21I). These decreases became significant in pregnant animals ($p<0.05$).

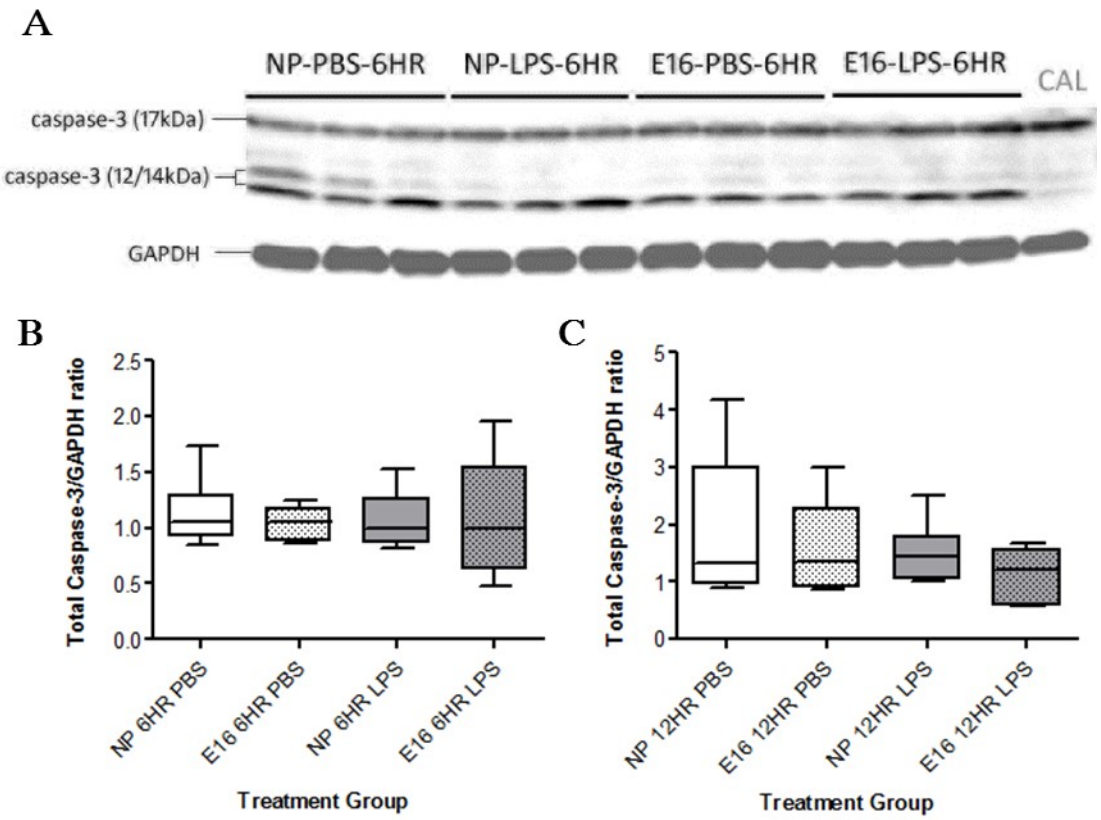


Figure 4.19: **Expression of caspase-3 in heart tissue taken from non-pregnant or pregnant mice treated with LPS or vehicle.** A representative western blot (A; n=6) showing p17 and p12/14 caspase-3 subunits for non-pregnant and pregnant heart tissue 6 hours after LPS/PBS treatment. Densitometry analysis was performed with ImageQuant software using GAPDH as loading control for heart tissue 6 hours after PBS/LPS (n=6) (B) and at 12 hours after PBS/LPS (n=6) (C). NP- non-pregnant; E16-pregnant.

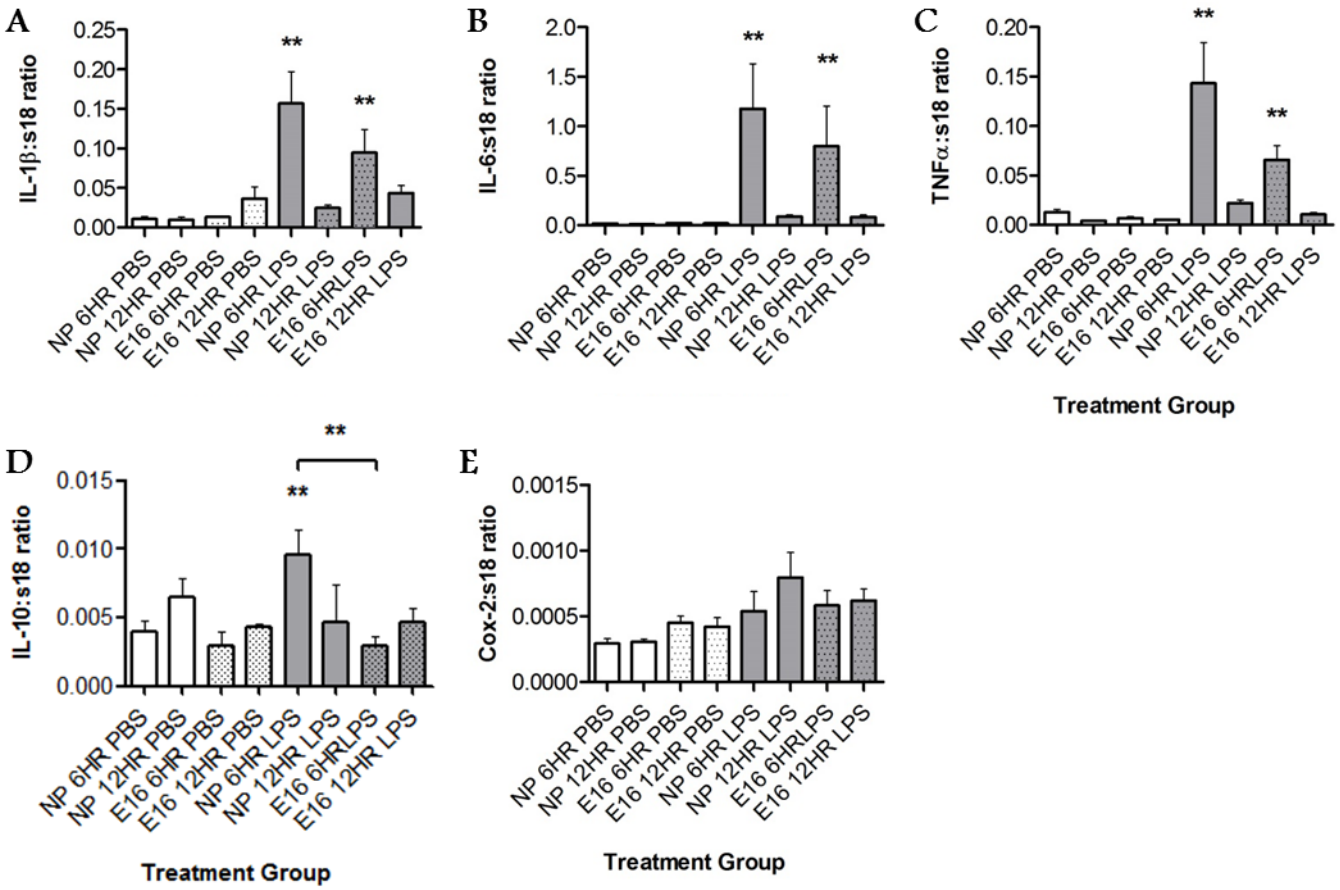


Figure 4.20: **mRNA expression of pro- and anti-inflammatory cytokines and inflammatory regulators in the left ventricle of non-pregnant or pregnant mice treated with LPS or vehicle.** (A) IL-1β, (B) IL-6, (C) TNF-α, (D) IL-10 and (E) Cox-2. **p<0.01 compared to PBS control unless otherwise indicated pairwise t-test comparisons or Mann Whitney U tests were used where appropriate. Data shown as mean ± SEM (LPS groups, n=6; PBS groups, n=5). NP- non-pregnant; E16-pregnant.

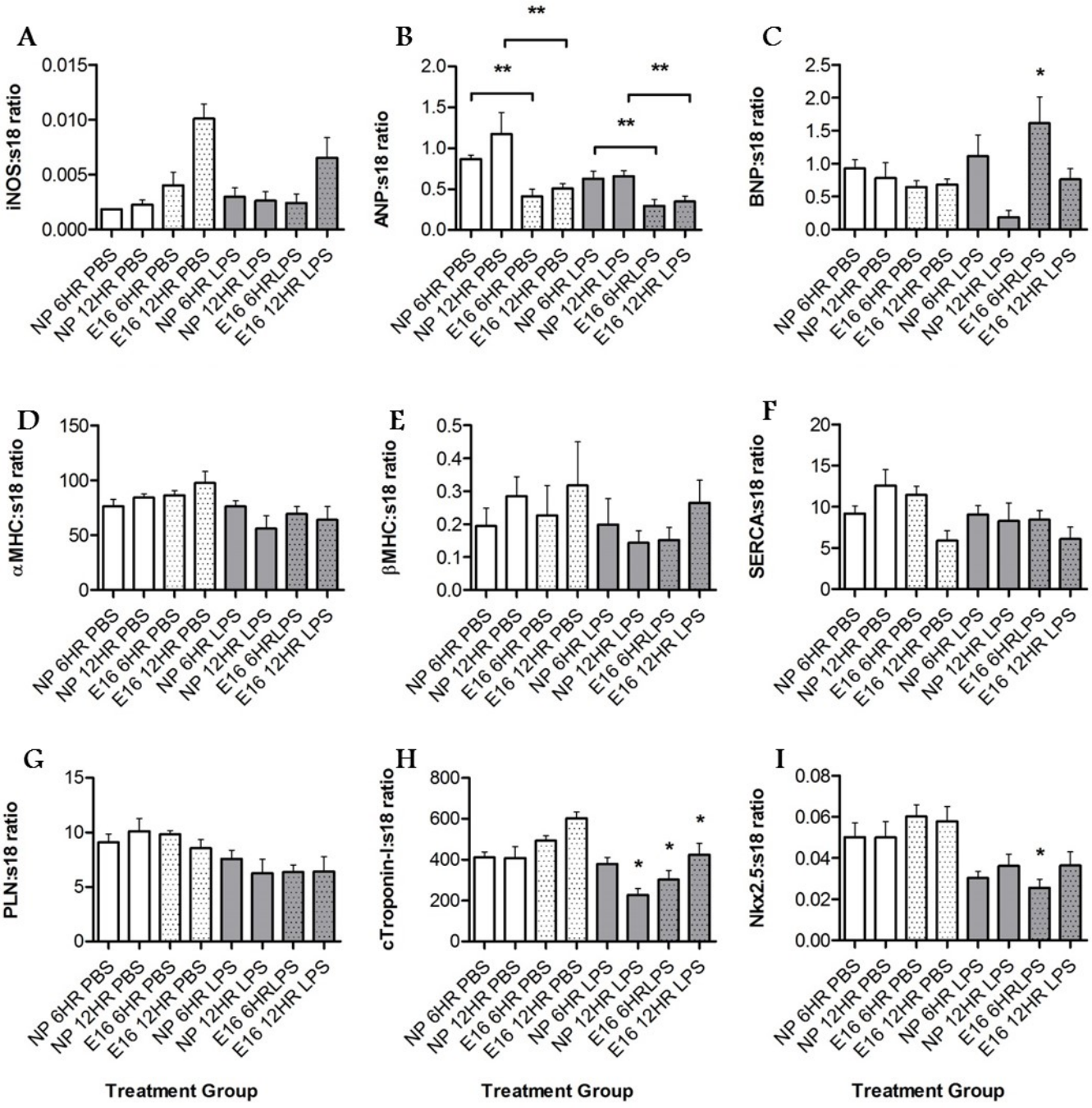


Figure 4.21: **mRNA expression of markers of cardiac dysfunction in the left ventricle of non-pregnant or pregnant mice treated with LPS or vehicle.** (A) Inducible nitric oxide synthase (iNOS), (B) atrial naturetic peptide (ANP), (C) brain naturetic factor (BNF), (D) α-myosin heavy chain (α-MHC), (E) β-MHC, (F) sarco/endoplasmic reticulum Ca^{2+}-ATPase (SERCA), (G) phospholamban (PLN), (H) cardiac troponin-I, and (I) homeobox gene Nkx2.5. *p<0.05, **p<0.01 compared to PBS control unless otherwise indicated, pairwise t-test comparisons or Mann Whitney U tests were used where appropriate. Data shown as mean ± SEM (LPS groups, n=6; PBS groups, n=4). NP-non-pregnant; E16-pregnant.

In contrast to the findings in whole heart tissue, Bcl-2 mRNA expression was significantly decreased in all mice treated with LPS, both at 6 and 12 hours in non-pregnant and pregnant mice ($p<0.01$ and $p<0.05$; Figure 4.22A). Furthermore, there were no changes observed in Bax or FasL levels (Figure 4.22B, 4.22D), but Bad was decreased after LPS ($p<0.05$; Figure 4.22C). Bad was downregulated in both non-pregnant and pregnant mouse left ventricular tissues after LPS, but only after 12 hours in non-pregnant mice; however the lack of significance at 6 hours may be reflected in the wider variability seen in the non-pregnant 6 hour PBS control.

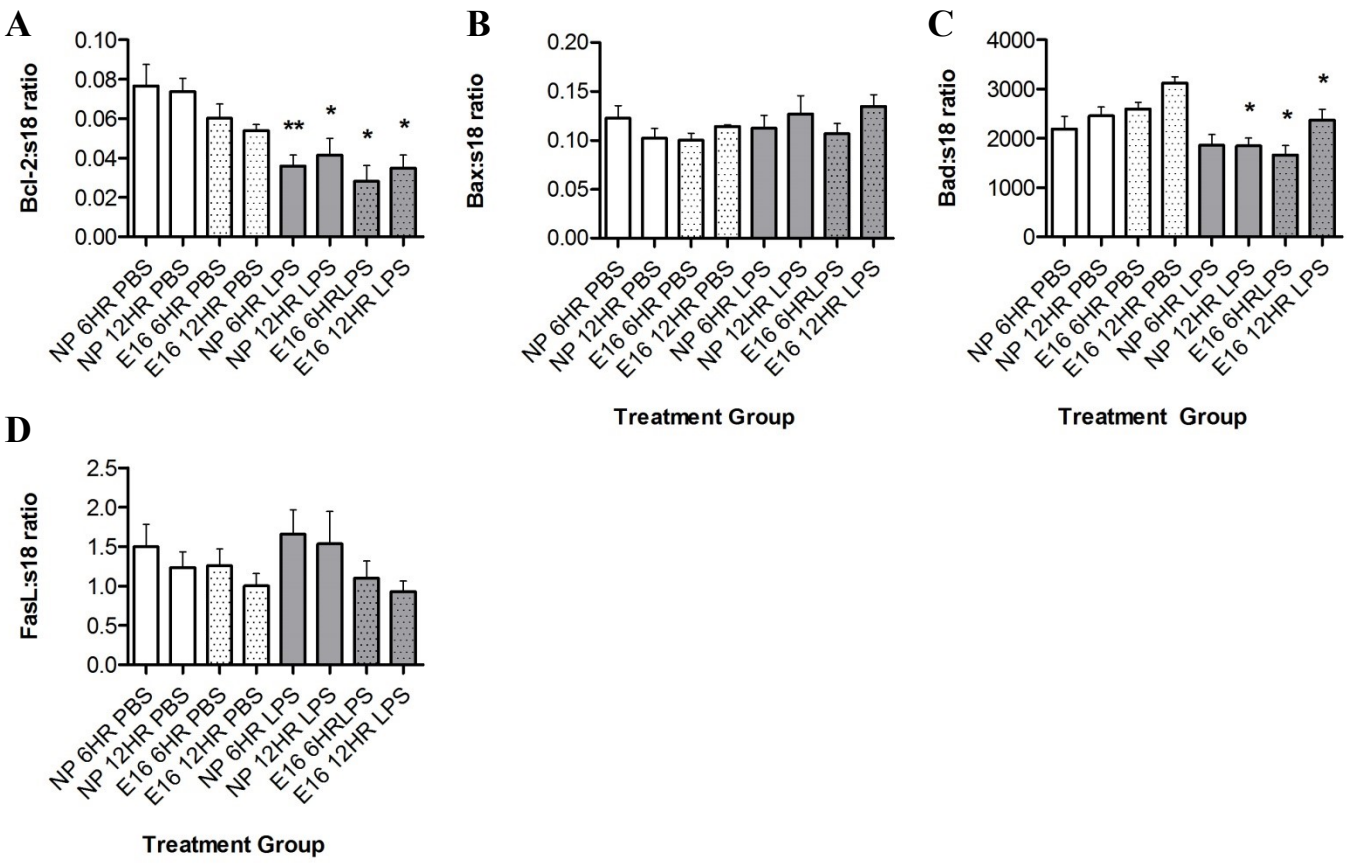


Figure 4.22: **mRNA expression of pro- and anti-apoptotic markers in the left ventricle of non-pregnant or pregnant mice treated with LPS or vehicle**. (A) Bcl-2, (B) Bax, (C) Bad, and (D) Fas ligand (FasL). *$p<0.05$, **$p<0.01$ compared to PBS control, pairwise t-tests comparisons or Mann Whitney U test were used where appropriate. Data shown as mean ± SEM (LPS groups, n=6; PBS groups, n=4). NP-non-pregnant; E16-pregnant.

4.2.7 LPS-induced Monocyte and Neutrophil Infiltration in Non-Pregnant and Pregnant Mice

It is known that there is an increase in systemic inflammation in pregnancy with a rise in numbers of circulating monocytes, granulocytes and NK cells from the first trimester onwards [58]. Here, data was collected using fluorescence-activated cell sorting (FACS) flow cytometry to investigate leukocyte infiltration in the blood, lung and liver of non-pregnant and pregnant mice exposed to LPS or vehicle (PBS), specifically focussing on monocyte and neutrophil populations.

There were significant changes in the acute response to LPS in pregnant animals compared to non-pregnant animals (Figure 4.23). The overall trend of monocyte presence in the blood was decreased 6 hours following LPS (compared to PBS) and then increased by 12 hours in both non-pregnant and pregnant mice. This likely represents the infiltration of monocytes from the blood into key tissues as an initial response to LPS.

There were significantly increased numbers of monocytes in lung tissue at 6 hours in pregnant mice compared to non-pregnant ($p<0.05$; Figure 4.23C), however these changes were attenuated by 12 hours. Accompanying this there was a decreased number neutrophils in lung in pregnant mice ($p<0.05$; Figure 4.23D). There were no changes in monocyte populations in the liver in response to LPS, but neutrophil infiltration was significantly reduced in pregnant mice compared to non-pregnant mice at 6 hours post-LPS ($p<0.05$; Figure 4.23F).

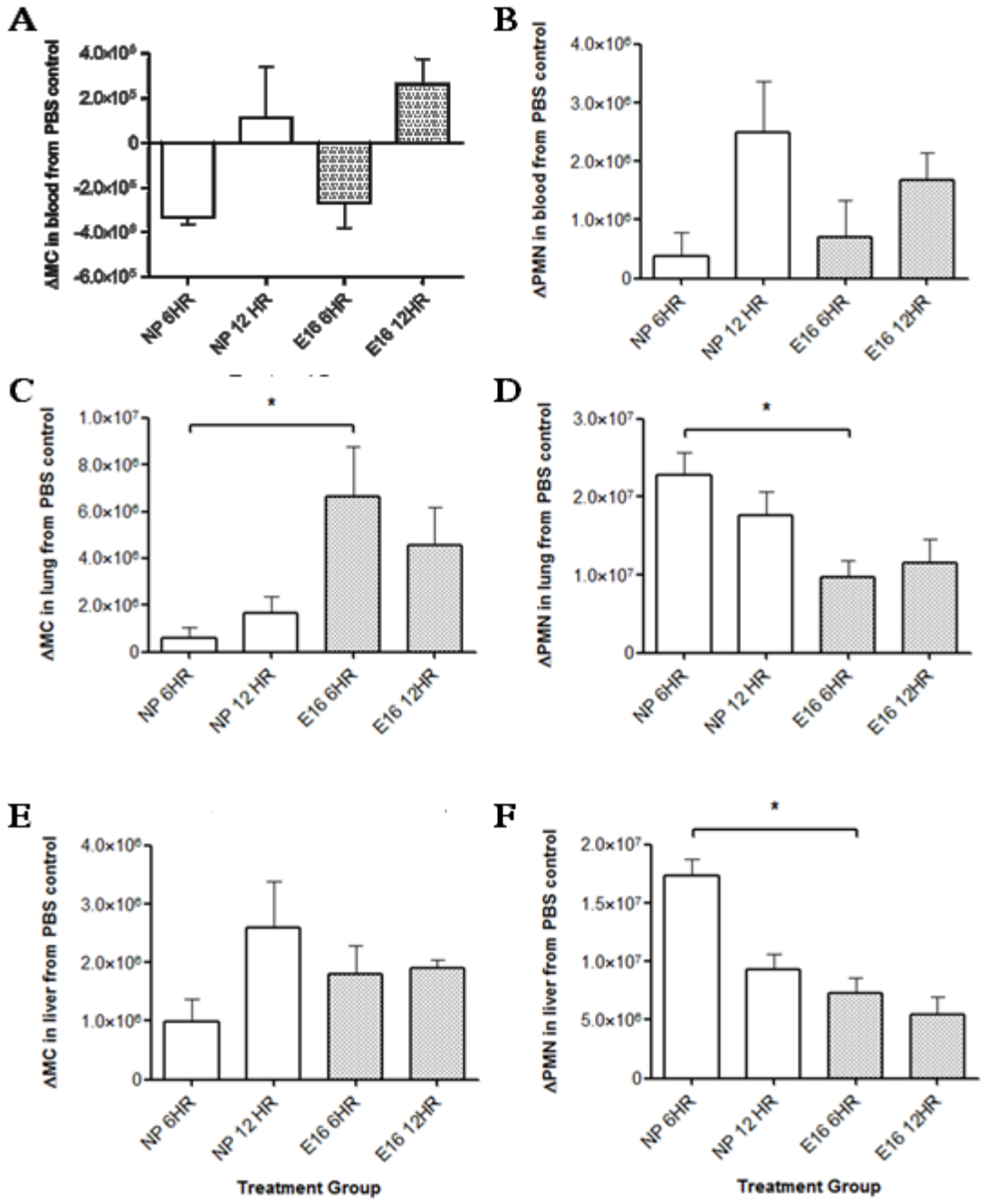


Figure 4.23: **Changes in infiltrating leukocytes in response to LPS in non-pregnant and pregnant mice.** The change in (Δ) cell counts after LPS treatment compared with vehicle controls (PBS) of both monocytes (MC; A, C, E) and neutrophils (PMN; B, D, E) in blood (A, B), lung (C, D) and liver (E, F) of non-pregnant or pregnant mice. *$p<0.05$, 2-way ANOVA, Bonferroni post-hoc test. Data shown as mean ± SEM (n=6). NP-non-pregnant; E16-pregnant.

4.3. Summary and Discussion

There was a marked hypotensive response to LPS in pregnant as compared to non-pregnant mice. Contrary to our hypothesis this was accompanied by a very similar systemic cytokine reaction, suggesting that the response of the innate immune system is not different in pregnancy. Further, the changes in levels of circulating vasoactive factors and the response of large vessels to the same vasoactive factors *in vitro* were similar in the two groups. Similarly, markers of cardiac dysfunction, cardiac apoptosis and cytokine levels were very similar. The most marked difference between the two groups was in the infiltration of the lungs, where pregnant animals had fewer neutrophils and more monocytes. If greater monocytic infiltration can lead to impaired arteriolar function as a result of an increase in inflammation and release of locally active vasoactive factors, this may contribute to the marked hypotension observed in pregnant animals. Taken together, these data suggest that during pregnancy, the cardiovascular system is more sensitive to inflammation and less able to maintain blood pressure in the face of an inflammatory stimulus.

Here we have shown that 10µg LPS led to a significant hypotensive effect which reaches a nadir at close to 12 hours, but had no effect on the haemodynamics of non-pregnant mice. Although systemic administration of LPS has been show to stimulate maternal systemic inflammation with an increase in pro-inflammatory cytokine production in maternal serum and cardiac tissue, the systemic response evoked does not appear substantial enough at this early time point to account for fetal demise. A recent study by Girsh *et al*., showed that an i.p. injection of a prostaglandin (PG)-$F_{2\alpha}$ analogue at E16 caused uteroplacental vasoconstriction and placental hypoxia in pregnant rats, mediated at least in part by elevated placental expression of the ET-1 gene and its receptor endothelin type A receptor [323]. Placental hypoxia as a result of increased LPS-induced prostaglandin and cytokine production may therefore lead to pup death as early as 6 hours post i.p. injection in the LPS model. However preliminary findings in the group (experiments conducted by MSc project student Miss Stephanie Dowle) have shown that LPS did not evoke any significant changes in the placental gene expression of several markers of hypoxia including peroxisome proliferator-activated receptor-γ (PPAR-γ),

peroxisome proliferator-activated receptor-γ coactivator-1-α (PGC1-α), glucose transporter 1 (GLUT1), or heat shock protein 70 (Hsp70), or in the expression of ET-1, eNOS or VEGF. There were also no significant differences in placental NO and ADMA after LPS i.p. [324]. These results imply that the fetal demise observed after LPS is not likely to be due to placental hypoxia and insufficiency; however this observation may be dependent on the timing of the investigation. Another explanation proposed by Silver *et al*, is that pup death could be caused by a LPS-induced maternal inflammatory response rather than a direct fetal one [305, 325]. They showed that a high dose of 1mg LPS led to no pup death in hypo-responsive dams (C3H/HeJ strain which are LPS resistant, thought to be primarily conferred by an LPS-specific impairment in TNF-α transcription and translation), and that co-administration of TNF-α could restore abortifacient activity and resulted in 65% fetal death; thus demonstrating a causal role for TNF-α possibly via the elaboration of prostaglandins (as demonstrated *in vitro* by Casey *et al*.,) or an ischemia and haemorrhagic necrosis in the decidua and trophoblast [325, 326].

In a recent study by Cotechini *et al*., low dose LPS was administered to pregnant rats on E13.5 followed by four high doses of LPS daily until E16.5 which resulted in increased MAP compared to vehicle controls. Non-pregnant rats given LPS on four separate occasions also demonstrated elevated MAP, but only after the second LPS injection. It was also noted that the LPS-induced increase in MAP was of a lower magnitude in non-pregnant rats. The authors postulate that the increases in MAP after LPS were the result of an inflammatory response triggered by LPS, namely an exaggerated TNF-α response as a consequence of an inadequately perfused placenta. This suggestion was supported by the observation that LPS did not cause an exaggerated inflammatory response in non-pregnant rats [327]. This seems contradictory to our results, as LPS administration in pregnant CD1 mice resulted in a marked hypotensive effect. However, as Cotechini *et al.*, delivered LPS to pregnant rats at an earlier time point in their pregnancy, and measured the response to LPS until 7 days post-partum, the pregnancy-related haemodynamic adaptations that would occur in normal pregnancy may have obscured the acute response to LPS. Thus, the immediate effect seen in the 24 hour period after

the initial dose of LPS in these rats was a decrease in MAP. Furthermore, as discussed above it seems unlikely that the results observed here are directly due to placental insufficiency and under-perfusion, however additional studies would be necessary to investigate this further.

In addition to an LPS-induced hypotension, pregnancy also conferred changes in activity after LPS administration. When compared to vehicle controls, non-pregnant animals treated with LPS spent more time inactive than pregnant animals treated with LPS. This may seem counter-intuitive when the LPS-treated pregnant animals were seen to have a greater hypotensive response to LPS indicating an increased sensitivity. However, as LPS administration led to PTL in the pregnant animals, the instinctive nature of these mice to create an environment for their offspring meant that nesting behaviours may have overridden the effects of LPS.

When the inflammatory response to LPS was investigated with the aim to determine any differences between the response in non-pregnant and pregnant mice after LPS exposure, it was observed that the circulating levels of pro- and anti-inflammatory cytokines and chemokines were increased in both groups after LPS with the exception of CCL3 and IL-4. CCL3 was found to be increased 6 hours after LPS administration in non-pregnant mice where IL-4 was higher in pregnant mice. This contrasts to the only other study to compare the response to LPS in non-pregnant and pregnant mice, where increases were observed for IL-6, IFN-γ and a reduction was observed in IL-10 in pregnant mice. These changes were associated with a greater mortality in pregnant mice and consequently the authors concluded that the greater cytokine response to LPS might explain the increased severity of some maternal diseases, including septic shock [328]. It must be considered that one explanation for the discrepancy may lie in that the dose of LPS used by Vizi *et al*., was much greater than used here, 1.6mg, compared with 10μg, and the serotype was not stated, meaning that it is difficult to make comparisons between the responses in the two studies. However, it seems likely that the potency of the LPS used was much greater, as they experienced a 75% maternal mortality [328].

In the current study, the circulating levels of ET-1 were not affected by LPS, consequently although they were higher in non-pregnant mice it is unlikely that ET-1 is solely responsible for the lower blood pressure observed in the pregnant animals. This conclusion is supported by a study by Iskit *et al.*, that showed in a mouse model of sepsis using CLP, the endothelin antagonist, bosentan, improved the outcome [329], suggesting that endothelin may play an active role in the outcome of sepsis. Following the observation that LPS administration led to hypotension in pregnant mice, it was hypothesised that this hypotension may be caused by a greater release of NO, as a critical role for NO has been demonstrated in septic shock [330, 331] and pregnancy is associated with higher NO levels [332]. Intriguingly, although LPS administration in this study was associated with a marked increase in NO, the increase was actually reduced in pregnant mice. Similarly, the levels of VEGF increased in the non-pregnant mice and were greater than those in the pregnant mice at both time points. The changes in NO and VEGF would be expected to result in a greater fall in blood pressure in the non-pregnant mice, again in contrast to the observations presented in this chapter.

One explanation may be that the vasodilation occurring during LPS-induced hypotension may lead to the increased oxygenation of tissues in pregnant mice, and thus in turn lead to a decrease in VEGF expression levels as part of a negative feedback loop. However, a decrease in VEGF in the maternal circulation was not paralleled in maternal heart tissue, where expression levels were similar to those in non-pregnant mice.

To investigate the hypothesis that pregnancy confers an increased vascular sensitivity to NO, we observed the responses of both non-pregnant and pregnant vessels to PE, ACh and SNP after treatment with LPS or vehicle. As pregnancy is associated with substantial increases in blood flow in the uterine artery, both aorta and uterine artery were used. The main findings from this particular experiment were that pregnancy conferred greater sensitivity to ACh in uterine arteries, albeit not in aorta. After LPS administration, the response to ACh was inverted leading to decreased sensitivity in both uterine artery and aorta.

Previous studies have demonstrated that in uterine and mesenteric vessels, pregnancy confers vascular adaptations that mediate enhanced NOS- and Cox-1-dependent vasodilation [333]. Moreover, studies have shown that in pregnant rats, uterine arteries display attenuated vascular smooth muscle relaxation in response to SNP [334], and that reduced vasoconstrictor sensitivity in the mesenteric bed of pregnant rats was associated with a greater inhibitory effect of nitric oxide [335]. However, a study conducted in rabbits showed that SNP could elicit similar responses in arterioles taken from non-pregnant and pregnant females, but administration of ACh led to greater dilation in pregnant arterioles. The authors concluded that this enhancement was primarily driven by enhanced release of NO, rather than from prostaglandins, as the NO inhibitor L-NAME was able to substantially reduce the ACh-induced dilation and eliminated the difference in response between non-pregnant and pregnant vessels [336]. It has been suggested that this may be due to altered endothelial signal transduction in pregnancy, where the sensitivity of eNOS to Ca^{2+} is associated with changes in ERK1/2 signalling [337].

Another study investigated venous adaptations in pregnancy and found that endothelium-dependent vasodilation markedly increased and smooth muscle response to NO decreased (primarily related to cGMP production) [338]. These results indicated a pro-vasodilatory state in the systemic venous system, thought to facilitate the accommodation to plasma volume expansion requisite for normal pregnancy. It could therefore be suggested that both venous and arterial vessel adaptations in pregnancy lead to a modified sensitivity to NO via altered signal transduction pathways in endothelial cells.

To understand whether cardiac dysfunction was responsible for the hypotension observed in this study, we assessed the mRNA expression of markers of impaired cardiac function, including ANP, BNF and cardiac troponin-I, in left ventricular tissue. ANP mRNA expression was consistently higher in the non-pregnant mice in all conditions, while the expression of LPS-induced BNF was higher in the pregnant mice at 6 hours only. Cardiac troponin-I was significantly decreased in pregnant mice at both 6 and 12 hours.

Circulating BNF and troponin have been reported to markedly elevated in patients with sepsis and septic shock [339], and to related to the prognosis. Circulating troponins have been related to cardiac dysfunction in sepsis [340], but in the case of BNF, levels have been found to be elevated in presence [341] and absence of cardiac dysfunction [342], suggesting that other factors may influence BNF circulating levels. Given that the expression of BNF mRNA was elevated, it seems plausible that some cardiac dysfunction was present in the pregnant mice in this study and may therefore contribute to the hypotension observed. Indeed, MAP observed in LPS-treated pregnant mice was normal at 6 hours and only started to decline at around 8 hours, consistent with the normal expression of BNF at 6 hours and an increase at 12 hours. Further work to determine BNF and troponin protein levels may help to better determine the role of these factors.

Sepsis-induced cardiac dysfunction may be caused by the local release of cardiac cytokines [343], but although the local levels of cytokines were greater in the mice treated with LPS, the levels in pregnant mice tended to be lower rather than higher compared to the non-pregnant mice. Intriguingly, the expression of both pro- and anti-apoptotic factors was lower in mice receiving LPS. This is counter to the existing literature, which is generally based on much higher doses of variable types of LPS administered to male rodents, from 250µg (in rats of unspecified sex) [344], to 3mg (male rats) [345]. Data from the mouse are equally variable, however one paper has reported increased Bax and reduced Bcl-2 expression in cardiac tissue from non-pregnant mice (sex not specified) after the injection of 30µg of LPS [346]. The findings presented here contrast to the existing data, but these data are derived predominantly from male rats and using higher doses of variable types of LPS; however, the reduction in apoptotic proteins may offer an explanation for the better outcome from sepsis observed in females [347]. Overall, the data suggest that cardiac function may be compromised in pregnant mice, but the aetiology is unclear, as there is little evidence of greater local cytokine levels or of increased apoptosis.

It is recognised that circulating monocytes, granulocytes and NK cells increase from the first trimester onwards in human pregnancy [58]. In response to LPS, there was no difference in the behaviour of the

circulating monocytes and neutrophils, yet in contrast to this monocyte infiltration into the lungs was higher and of neutrophils lower in pregnant mice. Lung inflammatory cell infiltration has been described in several mouse models of sepsis, but none have compared the impact of LPS in pregnant and non-pregnant animals. It was expected that both monocytes and neutrophils might show a greater lung infiltration, consistent with the greater mortality seen in pregnant women with flu epidemics [348], however, this was not the case. Lung cytokine levels were not assessed in this study; however future work in this area may help the understanding of the impact of the differential infiltration.

These data demonstrate that pregnant mice exhibit a marked hypotensive response to LPS and that this is associated with evidence of some cardiac compromise. The marked fall in blood pressure in response to LPS may help to explain the greater susceptibility of pregnant women to sepsis [349]. Understanding the mechanisms responsible will allow the development of a specifically targeted therapeutic response and an improvement in the management of severe infection in pregnant women.

Chapter 5: The Effect of Progesterone Supplementation on Maternal Haemodynamics

5.1 Introduction

Currently, the hormonal control of blood pressure during pregnancy is relatively poorly understood. During pregnancy, the primary role of progesterone is to inhibit uterine contractions and hence keep the uterus quiescent until term [350-352]. This is achieved both through a direct action on the myometrium and through the prevention of prostaglandin production in the uterus [353-356]. It is well known that gonadal steroids can regulate blood vessel functions and oestrogens, through binding to oestrogen receptor-α (ERα), are thought to play a role in the production of vasodilating agents such as NO, prostacyclin and PGE_2 [281, 357, 358].

During pregnancy, progesterone has also been shown to directly influence the shift in immunity to Th2-type responses at the maternal-fetal interface by suppression of T-cell differentiation into Th1 cells, thus contributing to the development of maternal immune tolerance of the fetoplacental unit [359]. Further experimental evidence suggests that progesterone exerts anti-inflammatory properties in LPS-treated human amniotic epithelium, likely via the reduction of LPS-induced TLR4 expression [360]. Furthermore, Anbe *et al*., demonstrated that LPS-induced IL-6 production, but not NO or PGE_2, in the pregnant murine myometrium was attenuated by progesterone, thus suggesting progesterone mediates an NO-independent anti-inflammatory effect via suppression of interleukin production [361].

However, progesterone also exerts effects on the cardiovascular system. *In vitro*, progesterone has been reported to have both vasodilatory and vasoconstrictive effects depending on the tissue and the level of exposure [25, 26, 362]. Furthermore, in hypertensive subjects, oral progesterone treatment reduces blood pressure [27]. Work done by Barbagallo *et al*., demonstrated that intravenous progesterone blunted MAP responsiveness to noradrenaline infusion in anaesthetised rats and blunted the pressor effects of noradrenaline in both in rat aorta and tail artery strips; a result of direct vascular action modulating calcium channel activity [363]. However, all these studies were conducted in non-pregnant animals/subjects, and it is possible that the higher concentrations of progesterone already

present in pregnant animals alter the response to LPS-induced inflammation through effects on both the cardiovascular and immune systems.

5.1.1 Aims and Objectives

Progesterone is a commonly used treatment for the prevention of PTL in high-risk women, despite the fact that its mechanism of action is largely unknown. Since progesterone alters the maternal immune response it is of critical importance to understand whether it may lead to changes the maternal response to infection. Consequently, if progesterone were to make women more susceptible to developing sepsis or septic shock, not only is this important information for women advised to take progesterone, but it may also suggest a potential therapeutic approach in these critically ill women.

To approach this problem, and to test the hypothesis that increased progesterone levels in pregnant mice modulate the haemodynamic response to LPS, the haemodynamics and immune responses of pregnant mice treated with supplementary progesterone prior to LPS administration were observed.

5.2 Results

5.2.1 The Effect of Progesterone Supplementation on Labour Time and Pup Survival

To explore the effects of progesterone on maternal haemodynamics and inflammatory pathways, a dose-response curve using increasing concentrations of progesterone (P4) administered on E14-E16 was constructed, in addition to the administration of 10μg LPS on E16.

Previous work in the group performed by Kaiyu Lei *et al*., (unpublished data) demonstrated that progesterone levels could be elevated 10-fold (from approximately 400nmol/L on E16) by daily subcutaneous administration of 10mg P4 in pregnant CD1 mice. This progesterone elevation was sufficient to prevent the mice from labouring if daily injections were continued through to E18. In this experiment, daily subcutaneous injections on gestational days E14-E16 of peanut oil (PO; vehicle), 5mg or 10mg P4 were given to raise P4 concentrations for 48 hours prior to LPS administration.

In initial dose finding experiments, 5mg/day P4 treatment delayed the onset of labour after LPS administration on E16 compared to PO treatment (52.92 ± 13.21 hours vs. 22.46 ± 1.47 hours respectively), however latency to labour was only significantly increased compared to PO using 10mg/day P4 (95.33 ± 7.76 hours, $p<0.001$; Figure 5.1A). Pup survival was increased using 5mg/day P4 compared to PO (61.54 ± 31.09 % compared to 0 % respectively) and then fell to 10 ± 10 % using 10mg/day P4 (Figure 5.1B). As 10mg/day was able to significantly delay latency to labour this dose was chosen for use in all subsequent experiments.

Latency to labour was recorded throughout the experiments using telemetered mice to monitor blood pressure after supplementation with P4 (Figure 5.1C). P4 supplementation reproducibly increased latency to labour after LPS ($p<0.001$, 98 ± 11.8 hours vs. 21.5 ± 2.07 hours). However, in this cohort of animals, no pup survival was recorded at labour in either PO or P4 treatment groups (Figure 5.1D). Pup survival significantly decreased from 56.9 ± 13.5 % and 50.5 ± 15.8 % for PO and P4

respectively at 6 hours, to 6.67 ± 6.67 % and 7.5 ± 7.5 % at 12 hours ($p<0.001$) . There were no significant differences in pup survival after P4 treatment.

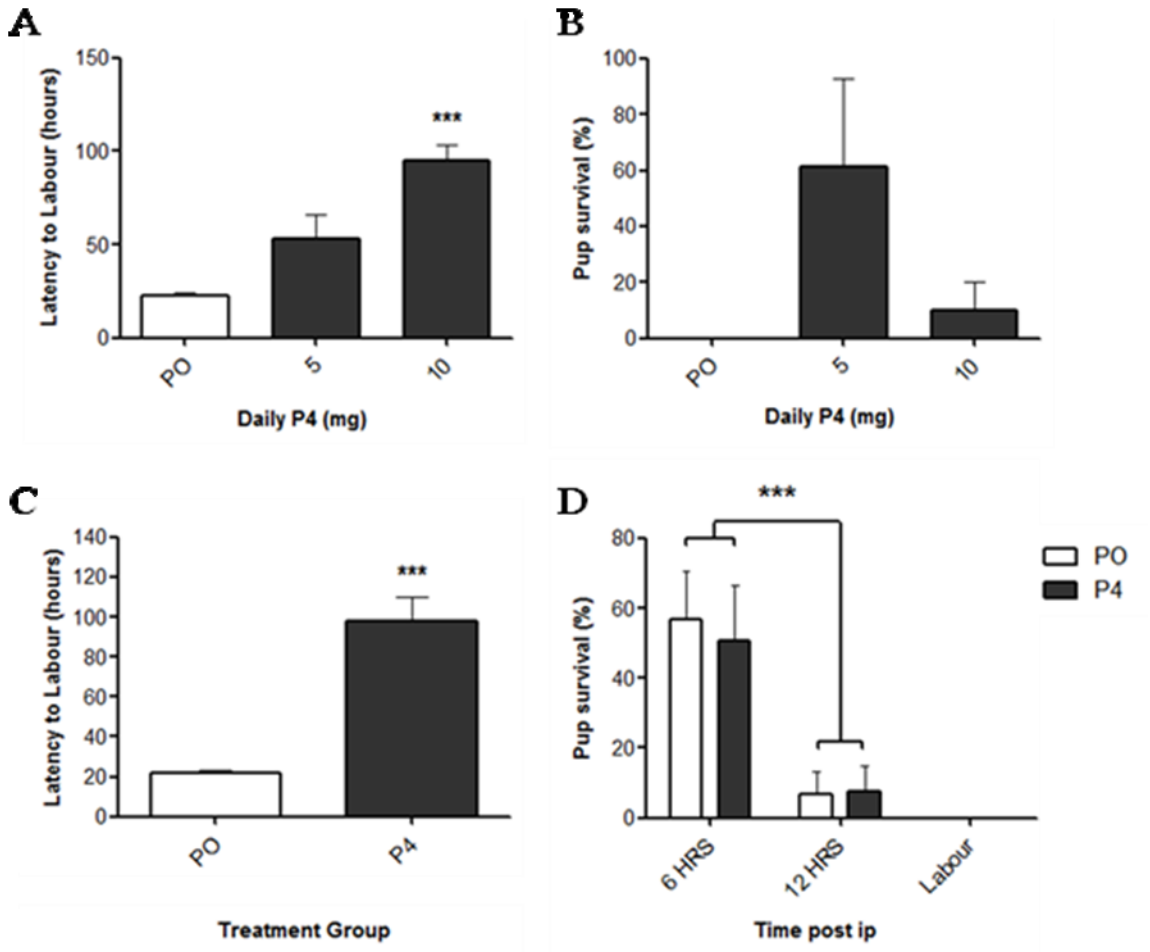


Figure 5.1: **Dose response to subcutaneous supplementation of progesterone in LPS-treated pregnant CD1 mice**. Initial dose response studies were carried out using increasing concentrations of P4, administered before LPS, where latency to labour (A) and pup survival (B) were observed as outcomes. ***P<0.001 compared to vehicle, student's t-test, (PO, n=6; 5mg, n=3; 10mg, n=9). (C) Latency to labour was then recorded for all telemetered animals receiving PO or 10mg/day P4 before LPS, ***P<0.001 student's t-test, (PO, n=4; P4 n=6). (D) Pup survival was also noted during tissue collections at 6 and 12 hours post-LPS and at labour in telemetered animals after PO or 10mg/day P4. ***P<0.001 2-way ANOVA, (6 HRS, n=6; 12 HRS, n=4; Labour, n=6). All data are expressed as mean ± SEM. PO- peanut oil; P4- progesterone.

5.2.2 The Haemodynamic Response to LPS-induced Inflammation in Mouse Pregnancies Supplemented with Progesterone

Haemodynamic and activity data was collected from telemetered CD1 mice. Mice were given 10mg P4 or PO (vehicle control) via the subcutaneous route daily from E14-E16 followed by i.p. LPS on E16.

A decline in MAP was observed in animals treated with PO in the first 12 hours post-LPS (Figure 5.2A). A nadir was observed at 9 hours post-LPS when MAP dropped to 101.09 ± 9.9 mmHg from a pre-LPS baseline of 115.54 ± 6.1 mmHg (Δ-14.5 ± 6.2). P4-treated animals maintained their MAP without any hypotensive response (Δ-1.56 ± 4.44 at 9 hours post-LPS). However, analysis using 2-way ANOVA did not indicate any significant differences between the treatment groups. Similar changes in blood pressure were also reflected in SAP (Figure 5.2B). In PO-treated animals a nadir was observed at 11 hours post-LPS when SAP dropped to 118.2 ± 15.7 mmHg from a pre-LPS baseline of 131.37 ± 13.9 mmHg (Δ-13.18 ± 7.9). No hypotensive response was seen in P4-treated animals (Δ-1.51 ± 4.47 at 11 hours post-LPS). Less marked changes were observed in DAP (Figure 5.2C). Between 12 hours and 24 hours post-LPS there appeared to be a gradual return to baseline in all three parameters in the PO-treated group, however P4-treated animals exhibited a slight trend towards hypertension above baseline pre-LPS levels. This was more pronounced in DAP where the peak pressure was 89.79 ± 2.8 mmHg compared to pre-LPS baseline of 76.78 ± 2.8 mmHg (Δ13.01 ± 3.39) at 19 hours post-LPS. No rise above basline was observed in the PO-treated group (99.3 ± 7.4 mmHg at 19 hours vs. 99.59 ± 1.1 at baseline).

The peanut oil vehicle itself was not thought to affect the haemodynamic profile of E16 mice as similar trends were observed in mice treated with LPS alone.

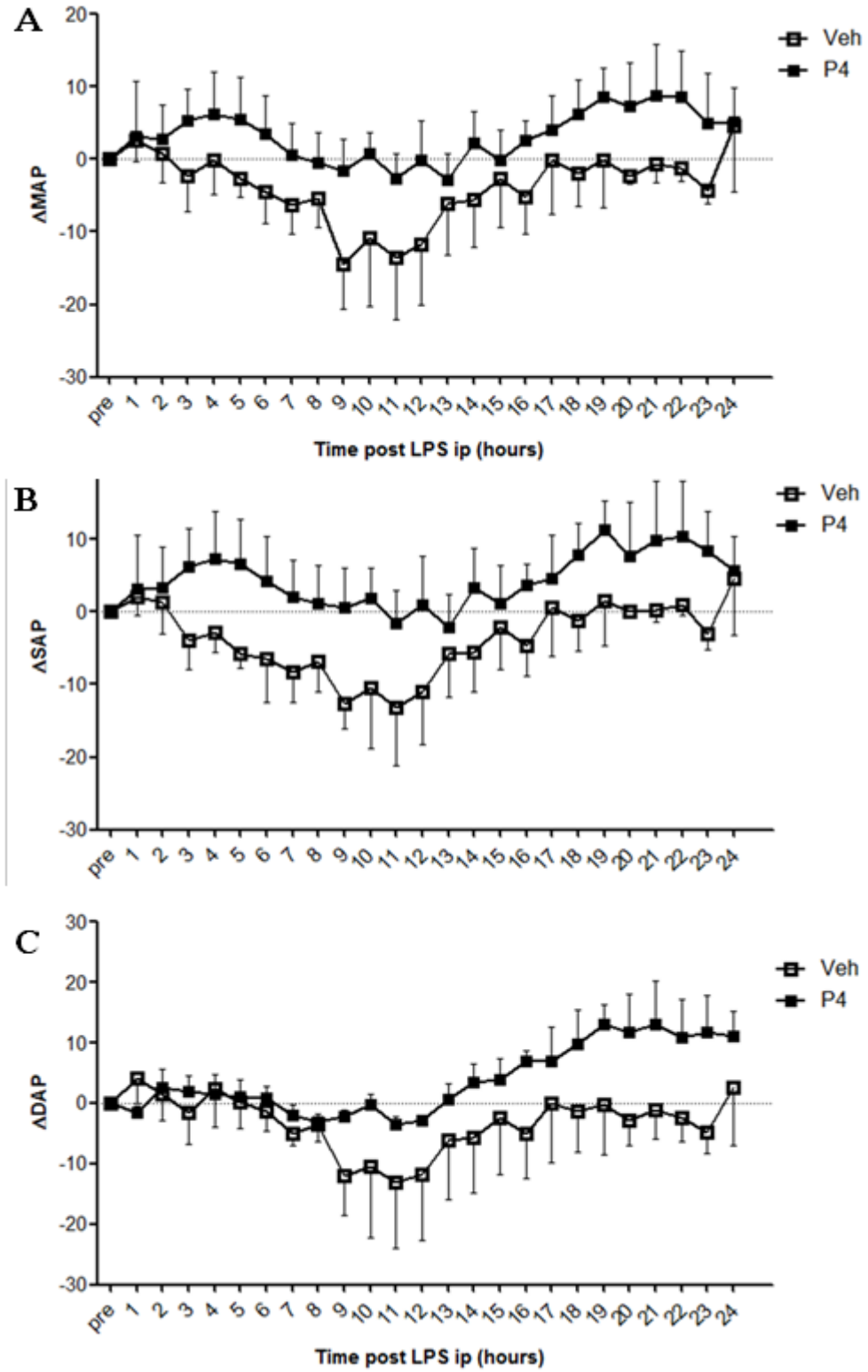


Figure 5.2: The haemodynamic response to LPS-induced inflammation after progesterone supplementation. The haemodynamic response in CD1 mice recorded 24 hours after LPS administration following either PO or P4 treatment daily from E14. (A) ΔMAP (B) ΔSAP (C) ΔDAP. Data are expressed as mean change from pre-LPS baseline (pre) ± SEM (Veh, n=3; P4, n=4). Veh- vehicle, peanut oil; P4- progesterone.

In the PO-treated group, there was a small reduction in HR, however due to the large variability of HR between animals this did not reach significance, therefore there was no signficiant change in heart rate in either treatment group after LPS (Figure 5.3).

Area under the curve (AUC) analyses showed no significant changes between P4- and PO-treated animals for either MAP, SAP, DAP or HR (Figure 5.5A, 5.5D, 5.5G, 5.5H). However, the maximum decrease in SAP was significantly reduced ($p<0.05$; Figure 5.5E).

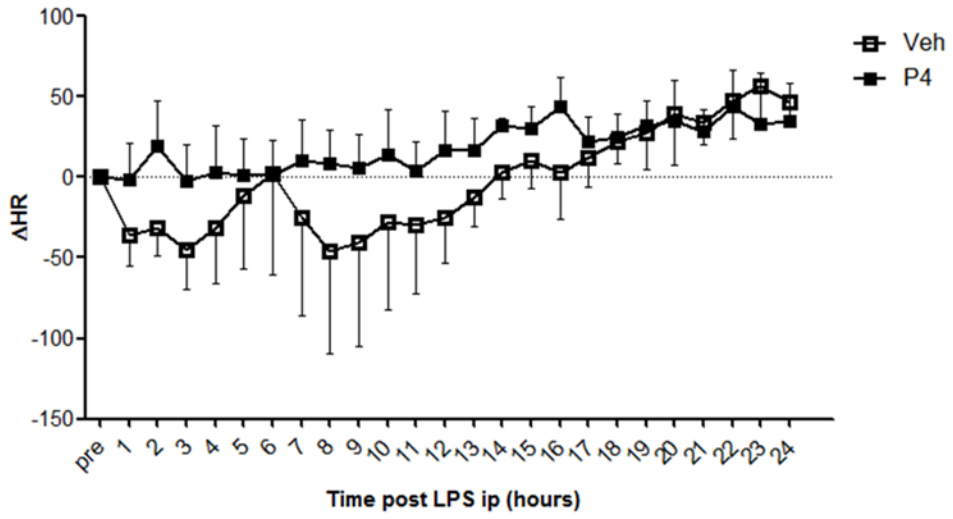


Figure 5.3: The heart rate response to LPS-induced inflammation after progesterone supplementation. Heart rate was recorded in the 24-hours after LPS administration following either PO or P4 treatment daily from E14. Data are expressed as a mean change from pre-LPS baseline (pre) ± SEM (Veh, n=3; P4, n=4). Veh- vehicle, peanut oil; P4- progesterone.

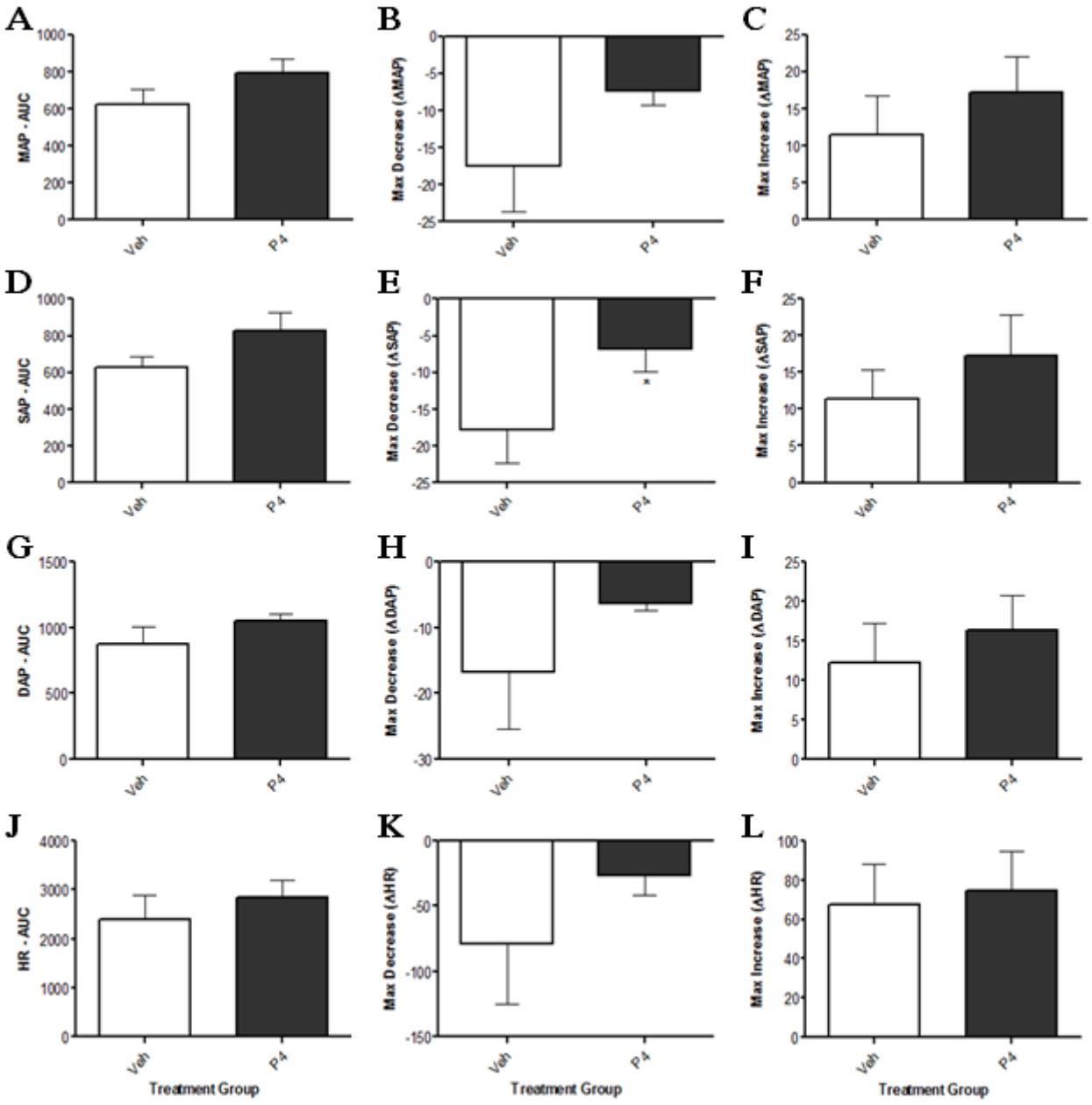


Figure 5.4: The haemodynamic response to LPS-induced inflammation after progesterone supplementation as assessed by AUC, maximum decrease and maximum increase. The haemodynamic response in CD1 mice recorded 24-hours after LPS administration following either PO (Veh) or P4 treatment daily from E14. AUC analysis was perfomed for MAP (A), SAP (D), DAP (G) and HR (J). Maximum decrease was calculated for MAP (B), SAP (E), DAP (H) and HR (K). Maximum increase was calculated for MAP (C), SAP (F), DAP (I) and HR (L). *P<0.05 student's t-test. Data are expressed as mean ± SEM (Veh, n=3; P4, n=4). Veh- vehicle, peanut oil; P4- progesterone.

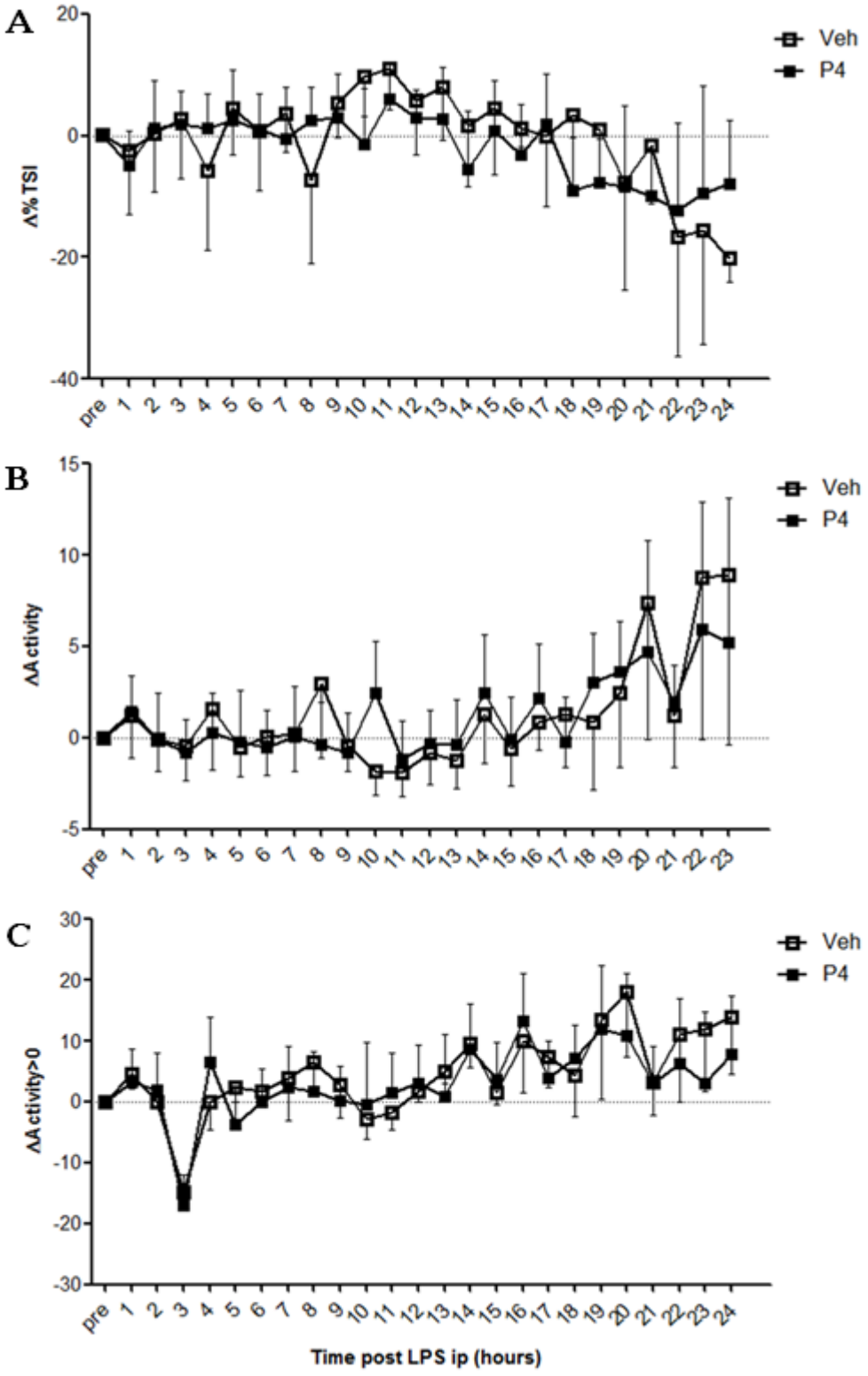


Figure 5.5: Activity in pregnant CD1 mice treated with LPS after supplementation with progesterone or vehicle. The change in activity in CD1 mice was recorded 24-hours after LPS administration following either PO or P4 treatment daily from E14. (A) Δ%TSI (B) ΔActivity (C) ΔActivity>0. Data are expressed as a mean change from pre-LPS baseline (pre) ± SEM (Veh, n=3; P4, n=4). Veh- vehicle, peanut oil; P4- progesterone.

P4-treatment had no significant effect on the %TSI and activity displayed by CD1 mice in the 24 hours after LPS administration. There was no significant change from baseline observed in either treatment group in the %TSI, although there was a slight reduction in the last three hours observed. As labour would have occurred in the PO-treated animals, this could account for the increase in activity at this point, however, as this was not true of P4-treated animals, it may be that the initial effects of LPS wear off with time as the LPS is cleared. These results are also reflected in a slight increase in activity at 18-23 hours post-LPS, although not significant. The intestity of activity, as described by activity >0, also remained unchanged from baseline despite a sharp and unexplained drop in activity >0 of both groups at 3 hours post-LPS. These results idicate that altered activity could not be responsible for any differences in blood pressure in P4-treated mice.

5.2.3 The Effect of Progesterone Supplementation on LPS-induced Cytokine, Chemokine, Nitric Oxide and Asymmetric Dimethylarginine Production in Pregnant Mice

Absolute concentrations of cytokines and chemokines in maternal serum from PO- or P4-treated mice 6 and 12 hours after LPS i.p. were measured using the Millipore MAGpix multiplex assay system to evaluate any effects of progesterone supplementation on the systemic inflammatory response.

There were no significant differences in any of the pro- or anti-inflammatory cytokines measured between P4-treated and PO controls (Figure 5.6). It can therefore be concluded that P4 supplementation did not suppress LPS-induced cytokine production in pregnant mice. Of note however, is that in PO controls, both IL-1β and TNF-α production significantly decreased between 6 and 12 hours post-LPS ($p<0.05$; Figure 5.6A, 5.6C). In P4-treated mice there was a trend towards decreased levels of IL-1β and TNF-α but this was not significant.

Similar results were found for the chemokines measured in these samples. There were no significant differences in any of the chemokines measured between P4-treated and PO controls (Figure 5.7). However, CCL2 and CXCL1 were significantly decreased between 6 and 12 hours post-LPS in PO controls ($p<0.05$; Figure 5.7A, 5.7C), yet there was no significant reduction in the P4-treated animals at 12 hours post-LPS.

Circulating NO concentrations were not significantly different between P4-treated mice and PO controls (Figure 5.8), neither were there any differences in circulating ADMA levels. Absolute concentrations were comparable of those measured in LPS-treated mice without PO indicating that injections of PO did not provide any additional nitrites. These results indicate that the maintenance of MAP in P4-treated animals after LPS was not due to suppressed NO levels.

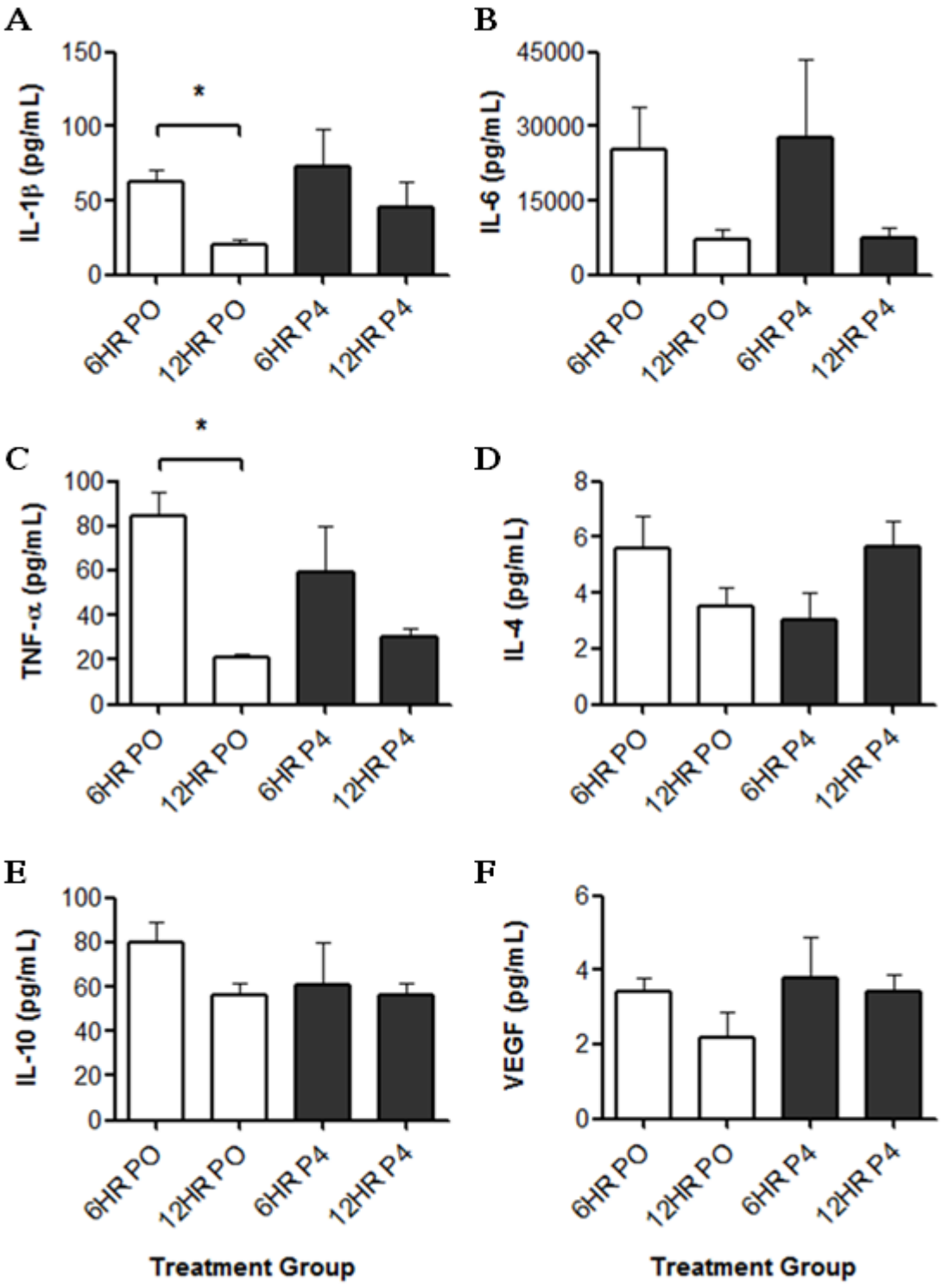


Figure 5.6: **Circulating concentrations of pro- and anti-inflammatory cytokines in the serum of pregnant mice treated with LPS after supplementation with progesterone or vehicle**. Measurements were made in serum samples taken 6 or 12 hours after LPS in PO- or P4-treated mice. (A) IL-1β (B) IL-6 (C) TNF-α (D) IL-4 (E) IL-10 (F) VEGF. *$p<0.05$ pairwise t-test comparisons or Mann Whitney U tests were used where appropriate. Data shown as mean ± SEM (n=6). PO- vehicle, peanut oil; P4- progesterone.

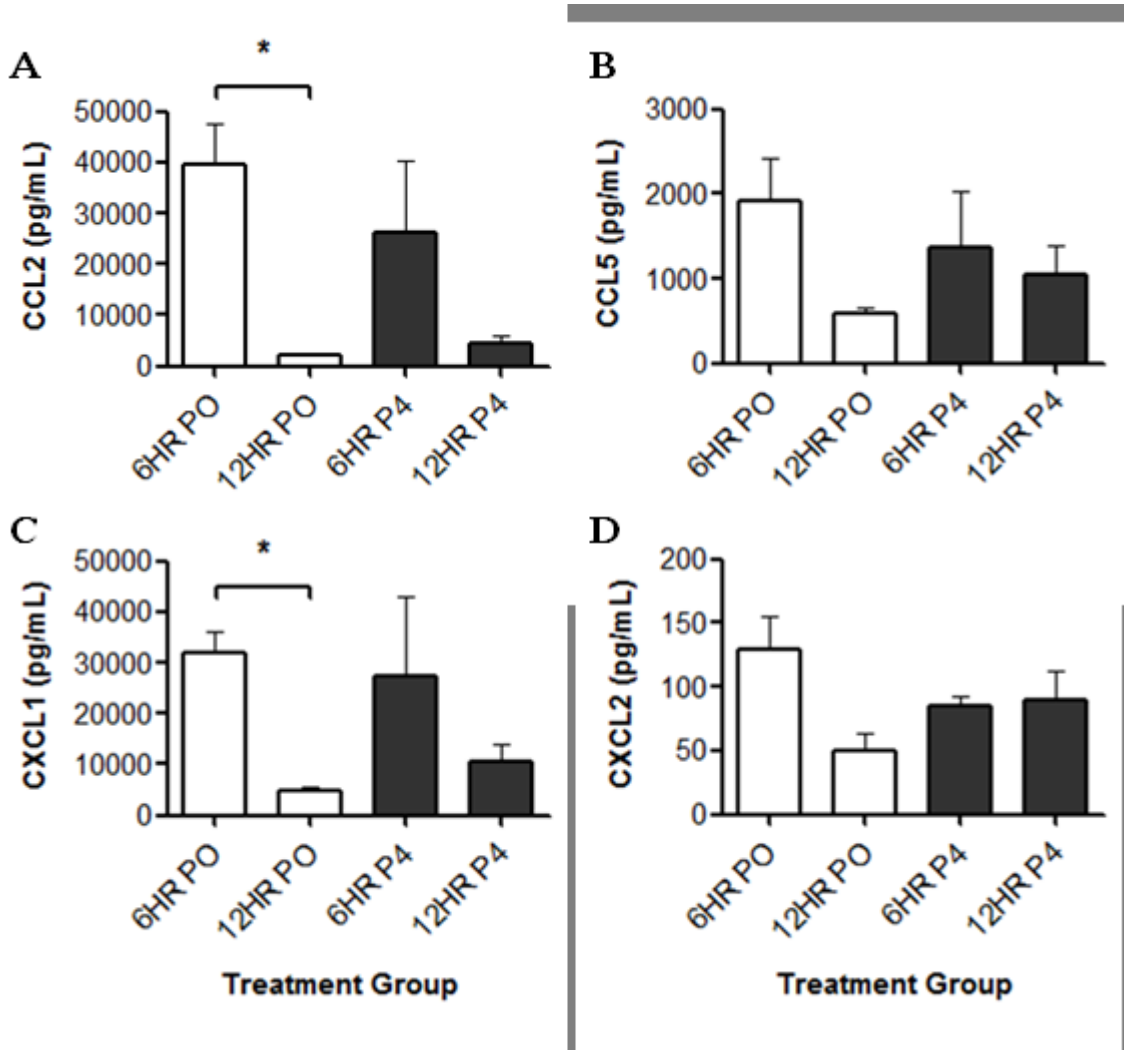


Figure 5.7: **Circulating concentrations of chemokines in the serum of pregnant mice treated with LPS after supplementation with progesterone or vehicle**. Measurements were made in serum samples taken 6 or 12 hours after LPS in PO- or P4-treated mice. (A) CCL2 (B) CCL5 (C) CXCL1 (D) CXCL2. *$p<0.05$ pairwise t-test comparisons or Mann Whitney U tests were used where appropriate. Data shown as mean ± SEM (n=6). PO- vehicle, peanut oil; P4- progesterone

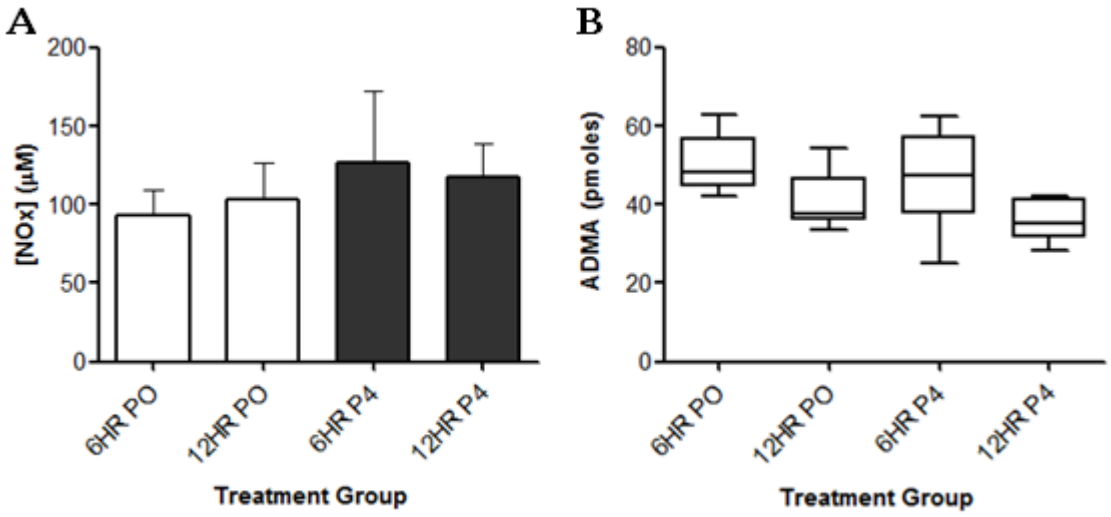


Figure 5.8: **Circulating concentrations of nitric oxide and asymmetric dimethylarginine in the serum of pregnant mice treated with LPS after supplementation with progesterone or vehicle**. Measurements were made in serum samples taken 6 or 12 hours after LPS in PO- or P4-treated mice. (A) Concentration of total nitrates and nitrites (NOx) as measured by nitric oxide analyser (B) ADMA as measured by mass spectrometry. Data shown as mean ± SEM, or as median ± interquartile range showing minimum and maximum (n=6). PO- vehicle, peanut oil; P4- progesterone

5.2.4 The Effect of Progesterone Supplementation on the Production of Inflammatory Markers, Markers of Cardiac Dysfunction and Apoptotic Markers in Left Ventricular Tissue

To assess the extent of cardiac sensitivity to LPS after P4 supplementation, the relative expression of various markers of inflammation, apoptosis and cardiac dysfunction were assessed in maternal left ventricular tissue using RT-PCR.

Similarly to circulating IL-1β levels, IL-1β mRNA expression in left ventricular tissue was not significantly reduced after P4-supplementation. However, in PO controls, IL-1β levels fell between 6 and 12 hours ($p<0.05$; Figure 5.9A), there was no change in P4-treated mice. There were no differences in IL-6 or IL-10 expression in any treatment group (Figure 5.9B, Figure 5.9D). Interestingly, unlike in the circulation, TNF-α was significantly reduced in the left ventricle of P4-treated mice 6 hours after LPS ($p<0.001$; Figure 5.9C).

As recent evidence suggested that upregulation of the LPS-binding protein cysteine-rich secretory protein containing LCCL domain 2 (CRISPLD2) protects mice from LPS-induced mortality and is also modulated by P4, we looked at CRISPLD2 expression in these samples [364-366]. We found that in P4-treated mice 6 hours after LPS, CRISPLD2 expression was significantly reduced compared to PO controls ($p<0.05$; Figure 5.9E). Upregulation of CRISPLD2 in PO controls 6 hours after LPS was also significantly reduced by 12 hours ($p<0.01$) but there was no change between 6 and 12 hours after LPS in P4-treated mice, suggesting that changes in CRISPLD2 are not responsible for the improved blood pressure responses to LPS induced by P4 supplementation.

Markers of cardiac dysfunction that were previously found to be altered after LPS administration in pregnant mice were also measured (see Chapter 4). The expression of ANP, BNF, c-Troponin I and Nkx2.5 were not significantly different after P4 supplementation (Figure 5.10). Similarly, the expression of apoptotic markers was unchanged after P4-supplementation (Figure 5.11). Bax expression was found to be significantly higher 12 hours after LPS compared to 6 hours, but this was true in both P4-treated mice and PO controls ($p<0.05$; Figure 5.11B).

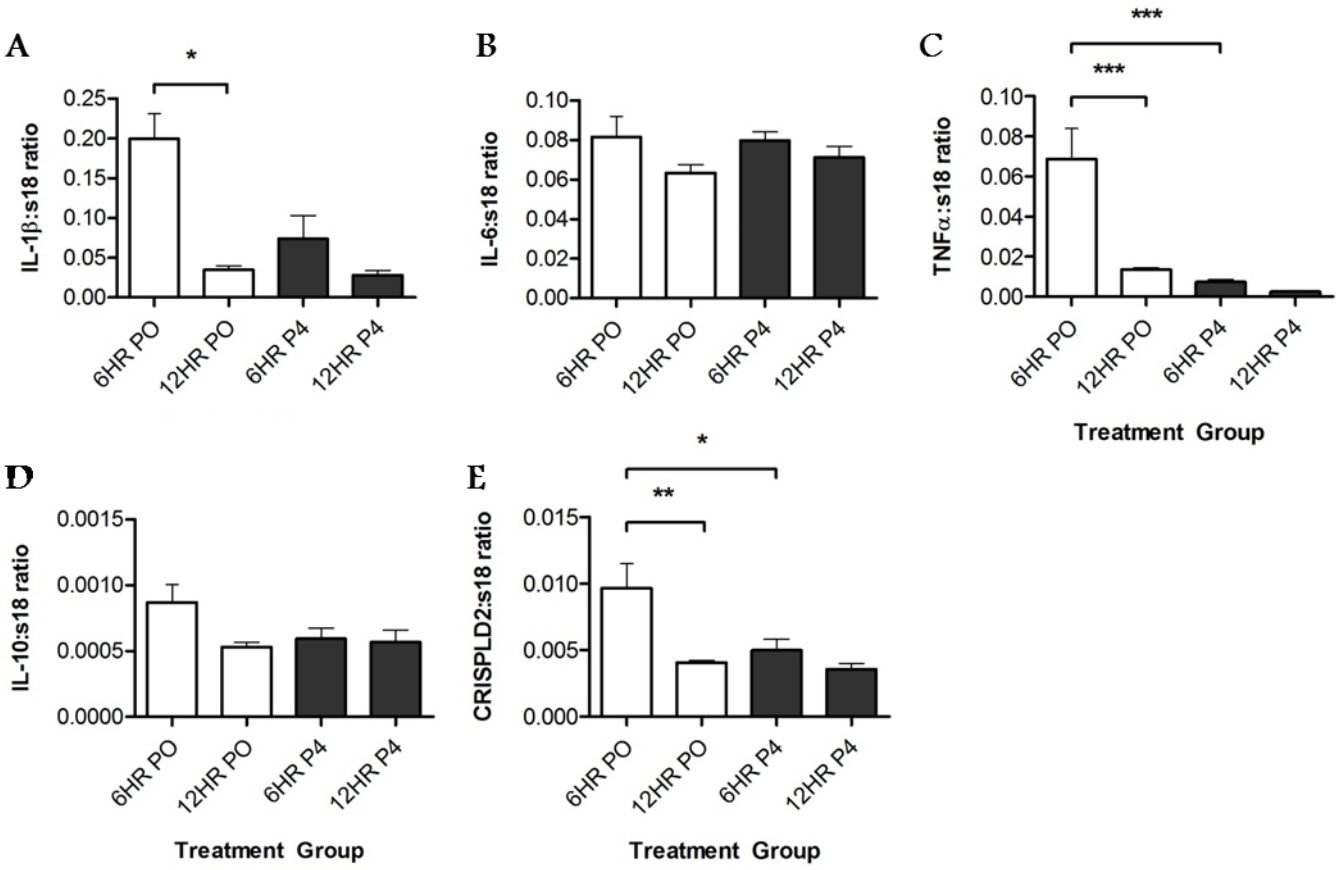


Figure 5.9: mRNA expression of pro- and anti-inflammatory cytokines and inflammatory regulators in left ventricular tissue taken from pregnant mice treated with LPS after supplementation with progesterone or vehicle. (A) IL-1β (B) IL-6 (C) TNF-α (D) IL-10 (E) CRISPLD2. *p<0.05, **p<0.01, ***p<0.001, pairwise t-test comparisons or Mann Whitney U tests were used where appropriate. Data shown as mean ± SEM (n=6). PO- vehicle, peanut oil; P4- progesterone.

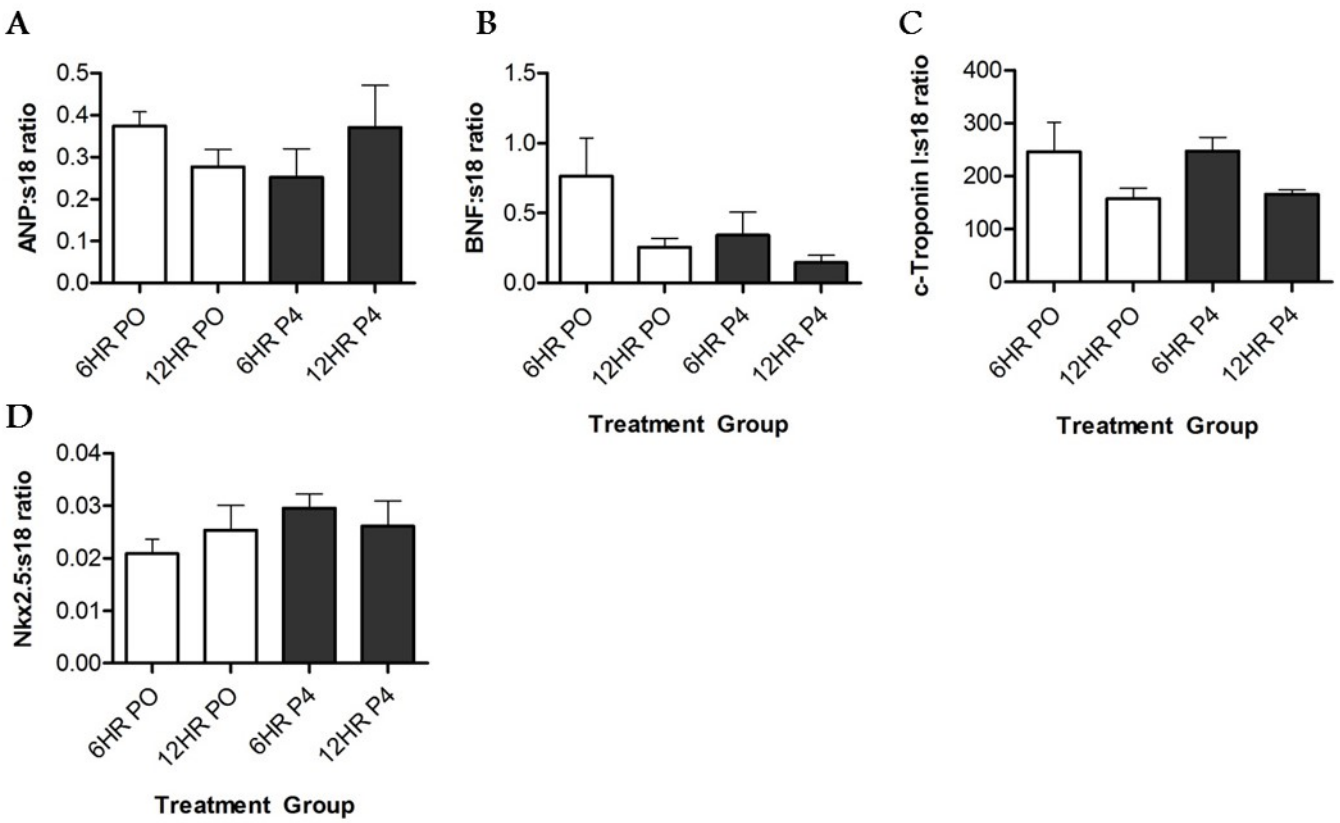


Figure 5.10: mRNA expression of markers of cardiac dysfunction in left ventricular tissue taken from pregnant mice treated with LPS after supplementation with progesterone or vehicle. (A) ANP (B) BNF (C) c-Troponin I (D) Nkx2.5. Data shown as mean ± SEM (n=6). PO- vehicle, peanut oil; P4- progesterone.

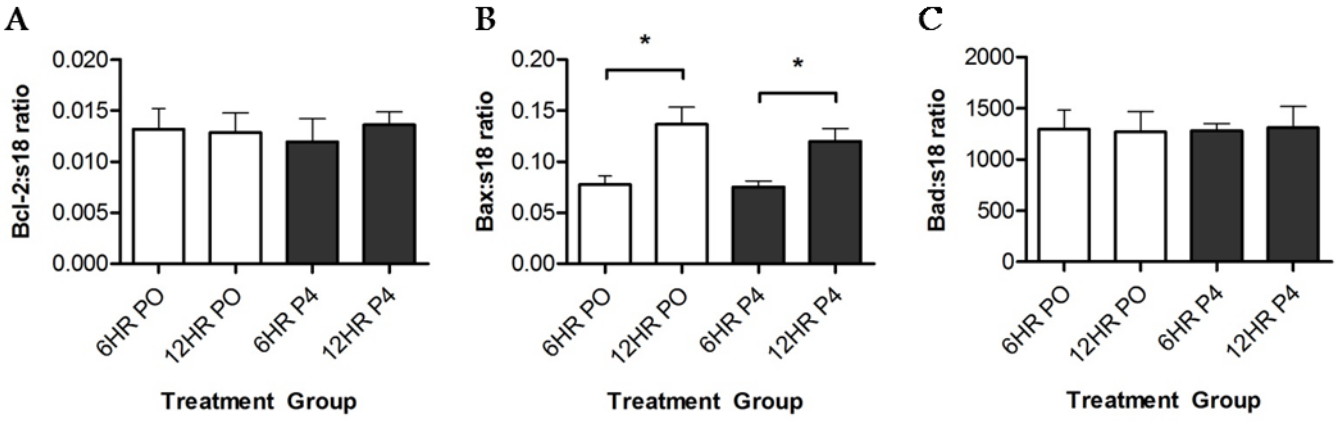


Figure 5.11: mRNA expression of markers of apoptosis in left ventricular tissue taken from pregnant mice treated with LPS after supplementation with progesterone or vehicle. (A) Bcl-2 (B) Bax (C) Bad. *$p<0.05$ pairwise t-test comparisons or Mann Whitney U tests were used where appropriate. Data shown as mean ± SEM (n=6). PO- vehicle, peanut oil; P4- progesterone.

5.3 Summary and Discussion

Daily supplementation of 10mg P4 was able to significantly delay the onset of labour after LPS administration in pregnant CD1 mice, but this did not lead to increased pup survival at intermediate time points or labour. After P4 supplementation, the LPS-induced hypotensive response observed in control animals was ameliorated and no hypotension was measured in P4-treated mice. P4-treatment led to a significantly reduced maximum decrease in SAP. Heart rate and activity levels were not affected. There were no significant differences detected in any of the circulating cytokines or chemokines measured after P4-treatment. Circulating VEGF, NO and ADMA concentrations were not altered by P4 supplementation. In the left ventricle, mRNA expression of TNF-α and CRISPLD2 were significantly down regulated after P4-treatment.

These data suggest that increased progesterone concentrations in pregnant mice do not drive the hypotensive response to LPS observed in pregnant animals. Actually, contrary to our hypothesis, that P4 may exacerbate the haemodynamic response to LPS, progesterone clearly plays a role in haemodynamic adaptation and may provide some protection against LPS-induced hypotension.

The mechanism of this action is still unclear, as increased progesterone did not exert an anti-inflammatory effect and decrease the levels of circulating pro-inflammatory cytokines and chemokines, nor did it increase the concentrations of anti-inflammatory cytokines such as IL-10. The absence of any impact on inflammation is surprising as progesterone plays a key role in the differentiation of Th cells and the shift from Th1 to Th2 dominance in pregnancy [367-371], but perhaps, as progesterone levels are high in E16 mice, the supplementation of further P4 may not induce any further increases in IL-10 or other Th2 cytokines.

Despite the improved blood pressure response to LPS after P4 supplementation, circulating NO concentrations were not altered. This result was unexpected, as Miller *et al*., showed that P4 treatement caused both time- and dose-dependent inhibition of NO production in macrophages [372]. Further experiments with LPS showed that P4 was able to inhibit the major effector system in

activated macrophages, reducing activation of the iNOS gene promotor, iNOS mRNA expression and synthesis of NO. However, these experiments were undertaken in macrophage cell lines and mouse bone marrow culture-derived macrophages, and NO levels were not measured in the circulation *in vivo*. Furthermore, these macrophages were activated with both LPS and INF-γ and therefore results could be an indication of the effects of INF-γ action.

Evidence from *ex vivo* vascular tension studies in endothelium-denuded tail artery and aorta helical strips showed that P4 blunted vasoconstriction in an NO-independent manner [363]. This work led to the suggestion that progesterone acts as a buffer in the vasculature against excessive calcium-dependent vasoconstrictor responses to a variety of hormonal stimuli. Therefore, progesterone may exert its effects on the vasculature via an NO-independent pathway, possibly prostacylin mediated.

Furthemore, since the discovery of membrane progesterone receptors (PRs) in 2003 [373], it could be that progesterone signalling in the vasculature is mediated through membrane PR activation and ERK1/2, p38 MAPKs activation, inhibition of cyclic adenosine monophosphate (cAMP) production and stimulation of intracellular Ca^{2+} mobilisation [374-378]. However, further work needs to be done to establish that this is a relevant pathway.

Additionally, progesterone metabolites have been shown to act upon the pregnane X receptor (PXR) which is known to be expressed in vascular tissue [379-381]. The PXR is a nuclear receptor and is important for the regulation of cytochrome P450 enzymes and consequently many aspects of xenobiotic metabolism [382]. Pregnancy-induced vascular adapatations were evident in arteries from WT but not PXR knockout mice, and these adaptations were exacerbated by treatment with exogenous progesterone metabolites [379]. Therefore P4 supplementation may have triggered further vascular adaptations via progesterone metabolite action at the PXR.

Although there were no significant differences in TNF-α measured in the serum, in the left ventricle TNF-α mRNA expression was signficantly downregulated in the P4-treated mice 6 hours after LPS administration. It has previously been shown that in LPS-stimulated macrophages, P4 downregulates

the production of intracellular TNF-α mRNA as well as released TNF-α protein [383], thought to be primarily achieved by increasing levels of IκBα. Similar results were also seen in BV-2 cells (a murine microglia cell line) where pre-treatement with P4 dose-dependently attenuated LPS-induced TNF-α secretion [384]. Progesterone also decreased LPS-induced iNOS and Cox-2 expression, NF-κB activation and p38, c-Jun N-terminal kinase (JNK) and ERK MAPKs phosphorylation in this model. The data collected from left ventricular tissue presented in this chapter, add to the emerging picture that progesterone exerts anti-inflammatory effects in a diverse range of tissues and cellular subsets. However, Jain *et al*., showed that TNF-α secretion was seen to increase two-fold following progesterone treatment in a human pro-monocytic cell line U937, albeit this was seen without LPS stimulation [385]. If increasing levels of progesterone can cause an elevation in TNF-α secretion in some inflammatory cells, the disparity between TNF-α levels measured in left ventricular tissue and the protein levels in the circulation could be explained by a counterbalance effect.

The expression of CRISPLD2 in P4-treated mice was signficantly decreased compared to in PO controls. This result was surprising, as previous experimental evidence had shown that in mice treated with P4 for 6 hours CRISPLD2 expression in the uterus was increased [366]. This group also demonstrated that P4 regulation of CRISPLD2 is regulated by the PR as CRISPLD2 was signficantly increased upon treatment with P4 only in WT mice and not in PR knockouts. However, expression of CRISPLD2 may be differently regulated in the heart, or secreted into the circulation leading to decreased expression in the tissue. Though this would need to be verified by determined protein levels of CRISPLD2. Interestingly, CRISPLD2 measured in the serum of human septic patients was highly variable in expression and levels did not correlate with increased sepsis severity, which may suggest that lower levels of CRISPLD2 expression indicate increased metabolism or reduced production of this protein [365]. An alternative explanation may be that excessive stimulation with P4 leads to a reduction in PR levels as well as positive PR chaperone proteins and mPRs in a negative feedback loop [386]. There is limited evidence to suggest that the classic nuclear PR (nPR) is downregulated at very high concentrations of P4, but tha the mPRα has been shown to undergo endocytosis after P4

stimulation via a clathrin-mediated pathway [373, 387]. Further work to define which PR are expressed in the heart would help to clarify P4 action on cardiac CRISPLD2 expression.

Taken together, these results indicate that progesterone plays an important role in the regulation of blood pressure in pregnancy, and is not responsible for the fall in blood pressure observed in pregnant animals after LPS challenge. Consequently, progesterone may afford some haemodynamic protection to pregnant animals but as these data suggest no overwhelming anti-inflammatory influence, the mechanism remains unclear.

Chapter 6: The Effect of C-C Chemokine Receptor Type 2 Deficiency on LPS-induced Hypotension in Pregnancy

6.1 Introduction

Characteristically, CCR2 is expressed in monocytes and in CCR2 deficient mice monocyte recruitment to sites of inflammation is impaired [388, 389]. CCR2 has also been found to be expressed in macrophages, subpopulations of T cells, basophils and DCs [390-392]. However, the chemokine CCL2 (also known as monocyte chemotactic protein-1; MCP-1) and its receptor CCR2 have been shown to play a crucial role in the inappropriate and excessive recruitment of neutrophils to multiple organs, often remote from the site of infection, causing tissue damage and organ dysfunction [172]. Additionally, although absent in resting neutrophil populations, chronic inflammation in adjuvant-immunised rats has been shown to induce the expression of CCR2 in circulating neutrophils [393]. This is thought to be driven by TLR2 and TLR4 signalling through the MyD88/NF-κB pathway, as neutrophils normally unresponsive to CCR2 chemotaxis acquired strong chemotactic responses to CCL2 and CCL7 after LPS administration, which was abolished in MyD88-deficient mice. Furthermore, in a mouse model of SIRS induced by cerulean-induced acute pancreatitis, CCL2 was found to be the key chemokine responsible for the polarised conversion of resident macrophages into alternatively activated macrophages (AAMs), which increased SIRS mouse susceptibility to CLP-induced sepsis [394]. IL-10 and IL-17 secreted from AAMs were also found to inhibit the antibacterial effector macrophages (classically activated macrophages, CAMs) to further perpetuate this effect.

In human pregnancy, chemokine receptors are expressed in both immune and myometrial cells and are thought to be important regulators of the inflammatory cell influx into the myometrium and cervix at term [395]. CCR2 has been also found in first-trimester decidual tissues, where CCL2 was shown to be upregulated by progesterone, oestrogen and hCG. He *et al*., suggested that this may suggest a key role for CCL2 at the maternal-fetal interface [396]. Gomez-Lopez *et al*., also demonstrated a further role of CCL2 in fetal membranes where membrane extracts from women who had experienced spontaneous labour exhibited increased CCL2-driven chemotaxis than in those from non-labouring women [397], thus amplifying the recruitment of monocytes and macrophages, and alongside CCL3,

co-ordinating the recruitment of monocytes into reproductive tissues [398, 399]. However, CCR2 expression is not required for successful pregnancy and labour [168]. Indeed, it is likely that compensatory mechanisms exist, and that CCR2-dependent leukocyte recruitment into the mouse uterus is superfluous for the initiation of labour.

In recent years, there has been a lot of attention paid to the role of inflammatory factors in the regulation of blood pressure, endothelial dysfunction and hypertension [400-403]. Chemokines are principally chemoattractants, but also thought to play other roles in angiogenesis and the promotion of cancer cell growth, haematopoiesis, embryogenesis and the maturation of several immune cells [400]. The involvement of chemokines in blood pressure regulation predominantly comes from control of inflammation in the vessels and heart, where inflammatory cell infiltration and oxidative stress in the vascular walls contributes to an increase in blood pressure [404, 405]. For example, Shen *et al*., were able to show that CCL2 deficiency was able to reduce CCL2-dependent macrophage recruitment and consequently reduce tissue inflammation and hypertension in a model of deoxycorticosterone and salt-induced hypertension cardiac fibrosis and hypertension [402].

To explore the role of CCL2/CCR2 signalling in the maternal hypotensive response to LPS, a CCR2 homozygous knockout mouse (Jackson Laboratories, strain name B6.129S4-Ccr2^{tm1Ifc}/J) was used. Originally crossed to C57BL/6 mice, the strain was backcrossed to a CD1 background as CD1 mice are a particularly fecund strain and typically have much larger litters than C57BL/6. The greater robustness and reproduction of the outbred strain was considered to be sufficiently advantageous to offset the heterogeneity of the background.

Preliminary data from our group has shown that in naïve E16 mice, CCR2 deficiency manifests in decreased monocyte and macrophage recruitment to various tissues including myometrium, placenta, liver and lung. In tissue collected during labour after intrauterine LPS administration, CCR2 deficiency did not cause a change in the accumulation of monocyte or macrophage cell densities. However, this work has shown that absence of maternal CCR2 reduces the adverse effects of

intrauterine administration of LPS, namely preterm labour and pup death, and improves neonatal outcome (unpublished data). Pup survival rates were improved from 0% at 7 hours post-LPS in CD1 dams, to over 90% in $CCR2^{-/-}$ mice which correlated with reduced pro-inflammatory cytokine production in $CCR2^{-/-}$ pup brain. These results were also accompanied by the finding that $CCR2^{-/-}$ placentas showed a reduced inflammatory response to LPS when compared to CD1 mice.

6.1.1 Aims and Objectives

As high levels of CCL2 are induced in response to inflammatory stimuli such as IL-1, TNF-α and LPS, modulation of CCL2/CCR2 signalling or expression could be beneficial in both treating and investigating inflammation in pregnancy. Therefore in this chapter, the role of CCR2 was examined to explore the potential effect on the maternal haemodynamic response to LPS. Taken together with the group's previous findings, it was hypothesised that manipulation of CCR2 may be protective in systemic LPS-induced inflammation during pregnancy.

6.2 Results

6.2.2 The Haemodynamic Profile of Non-Pregnant CCR2 Knockout Mice

To determine if there were any basal haemodynamic differences between CD1 (wild-type control) and $CCR2^{-/-}$ mice, non-pregnant recordings were taken before timed-mating. There were no differences in MAP, SAP or DAP in non-pregnant $CCR2^{-/-}$ mice (Figure 6.1A, 6.1B, 6.1C), however heart rate was significantly decreased from 662.1 ± 9.64 bpm in CD1 to 453.2 ± 26.2 bpm in $CCR2^{-/-}$ mice (Figure 6.1D). Changes in activity were also observed, where %TSI was significantly decreased and activity and intensity of activity (activity>0) were significantly increased in $CCR2^{-/-}$ mice ($p<0.001$; Figure 6.1E, 6.1F, 6.1G).

6.2.2 Latency to Labour and Pup Survival Outcomes after LPS administration in CCR2 Knockout Mice

After PBS i.p. on E16, $CCR2^{-/-}$ mice laboured spontaneously at term, approximately 58.0 ± 2.54 hours after injection, which was not statistically different from labour time in CD1 controls (48.63 ± 6.18 hours). Latency to labour after LPS was also not significantly different from CD1 as in both $CCR2^{-/-}$ and CD1 mice there was a very significant reduction in latency to labour after 10µg LPS administration on E16 to 16.99 ± 2.31 hours and 19.31 ± 1.34 hours respectively ($p<0.001$; Figure 6.2A).

There were also no differences between $CCR2^{-/-}$ and CD1 pup survival, with 100% survival after PBS and 0% survival at labour after LPS in both CD1 and $CCR2^{-/-}$ (Figure 6.2B, 6.2C). Surprisingly, after i.p. LPS administration we found that $CCR2^{-/-}$ pup survival was typically decreased compared to CD1 at 6 and 12 hour intermediate time points, although this did not reach statistical significance.

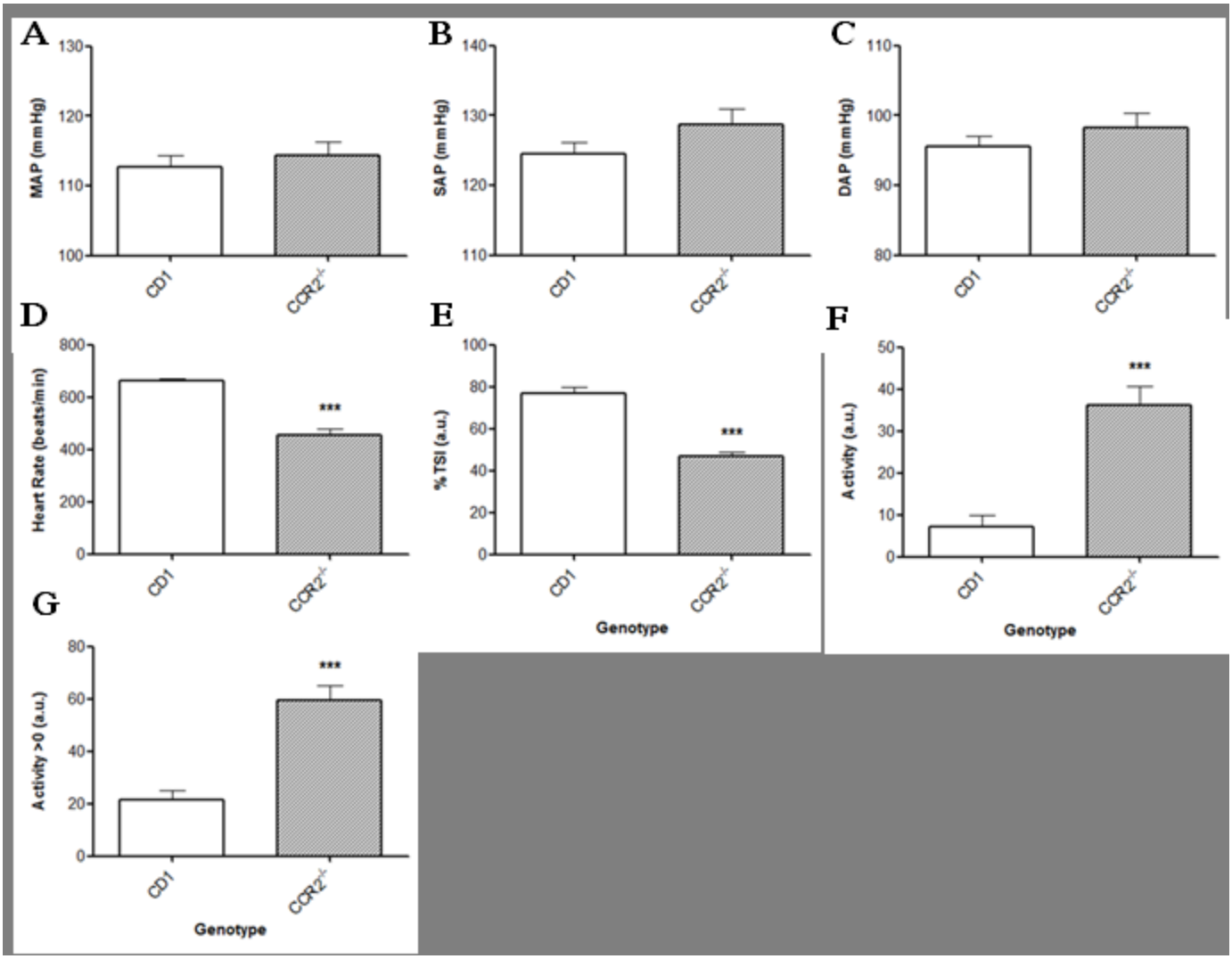


Figure 6.1: The haemodynamic and activity profile of non-pregnant CCR2$^{-/-}$ mice. Haemodynamic and activity parameters were recorded for 24 hours (prior to mating) in female virgin CD1 and CCR2$^{-/-}$ mice. (A) MAP (B) SAP (C) DAP (D) HR (E) %TSI (F) Activity (G) Activity >0. ***p<0.001 student's t-test or Mann-Whitney U test as appropriate. Data expressed as mean ± SEM (CCR2$^{-/-}$, n=14; CD1, n=20).

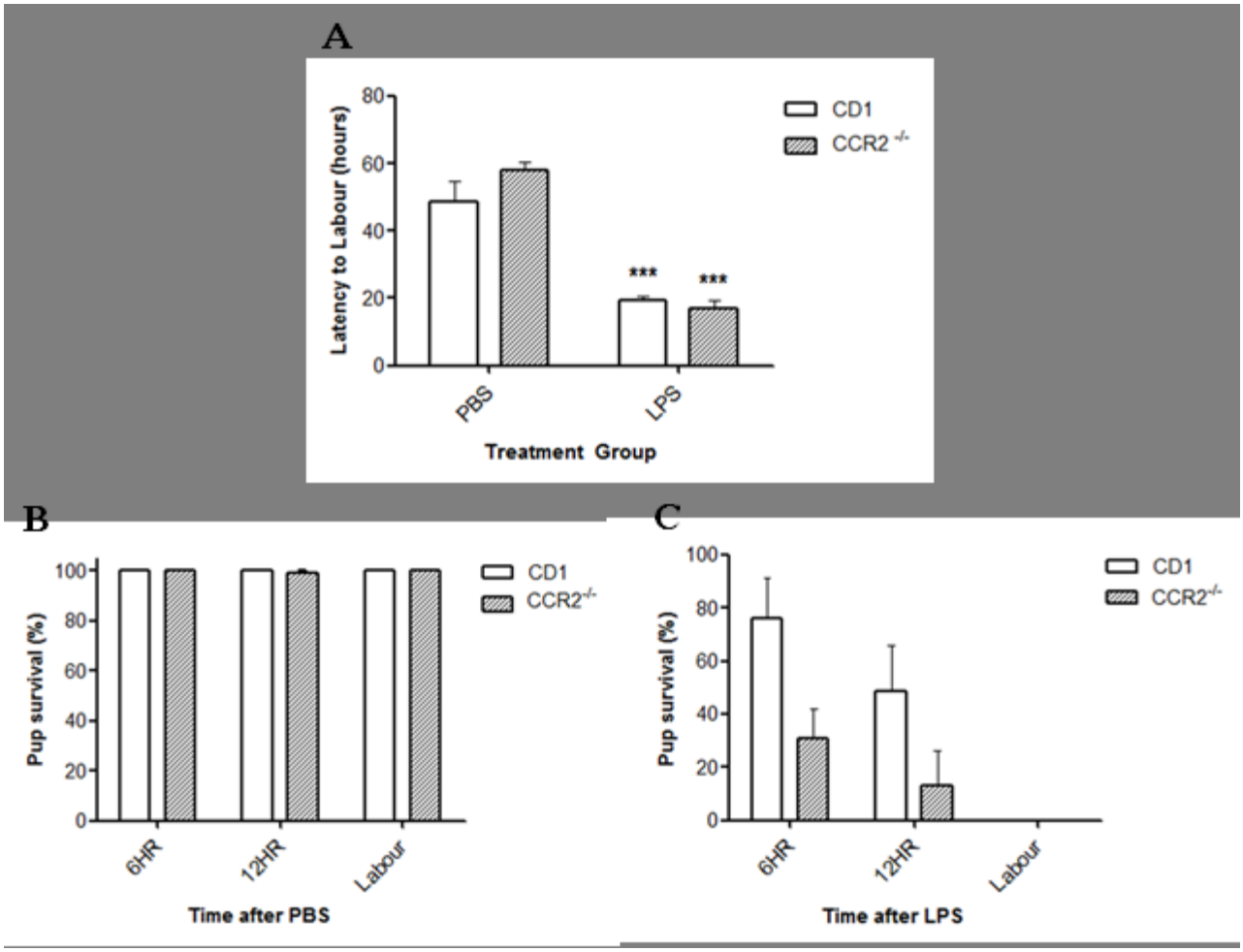


Figure 6.2: Latency to labour and pup survival outcomes after LPS administration in CCR2 knockout mice. (A) Latency to labour was recorded in telemetered mice (CD1 PBS, n=4; $CCR2^{-/-}$ PBS, n=7; CD1 LPS, n=6; $CCR2^{-/-}$ LPS n=5). (B) Pup survival was noted during tissue collections at 6 and 12 hours post-PBS and at labour in telemetered animals after PBS (vehicle) and (C) after 10µg LPS administration in CD1 and $CCR2^{-/-}$ mice (CD1 6HR, n=6 ; $CCR2^{-/-}$ 6HR, n=7; CD1 12 HR, n=6; $CCR2^{-/-}$ 12 HR, n=6; CD1 Labour, n=4; $CCR2^{-/-}$ Labour, n=4). ***P<0.001 compared to PBS control, 2-way ANOVA showing treatment but not genotype was significant. Data expressed as mean ± SEM.

6.2.3 The Haemodynamic Response to LPS-induced Inflammation in Pregnant CCR2 Knockout Mice

Experiments to assess the haemodynamic response of pregnant $CCR2^{-/-}$ mice to LPS showed that compared with pregnant CD1 controls, MAP was significantly elevated in $CCR2^{-/-}$ mice ($p<0.05$; Figure 6.3A). There was an initial hypertensive response to LPS in $CCR2^{-/-}$ mice when compared to CD1 controls which culminated in a peak elevation of $\Delta 28.24 \pm 8.5$ mmHg at 5 hours post-LPS administration ($p<0.01$; Figure 6.3A). This then gradually declined to reach pre-LPS baseline levels by 8 hours. MAP was then maintained at baseline levels which were higher than in CD1 mice. The difference in MAP during the last 8 hours measured was also markedly different between $CCR2^{-/-}$ and CD1 mice, where at 16, 17, 18 and 23 hours post-LPS there was a significant difference ($p<0.05$). As the Δ MAP above baseline at these time points were not as great as those seen earlier, the significance may reflects the gradual decline of MAP in CD1 mice rather than increases in $CCR2^{-/-}$. The nadir in MAP of Δ-31.1 ± 7.06 mmHg in CD1 mice was seen at 12 hours post-LPS, but this was then maintained and did not resolve.

These changes were also reflected in SAP and DAP (Figure 6.3B, 6.3C). The general trend in SAP was significantly increased in CCR2-/- mice ($p<0.05$) and SAP at 3, 4, 5, 6, 7, 12, 15, 16, 17 and 23 hours post-LPS were found to be significantly higher ($p<0.05$, $p<0.01$, $p<0.001$). The peak change in pressure at 5 hours post-LPS was $\Delta 35.43 \pm 12.6$ mmHg ($p<0.001$). Similarly, DAP was significantly elevated in $CCR2^{-/-}$ mice after LPS compared to CD1 ($p<0.05$) with a peak change in pressure at 5 hours ($\Delta 36.83 \pm 15.94$ mmHg, $p<0.001$). Interestingly, in $CCR2^{-/-}$ mice DAP remained above baseline throughout the 24 hour period in response to LPS. The nadir in DAP observed in CD1 mice also came much later than the nadir in MAP, where a Δ-27.91 ± 11.49 mmHg was recorded at 18 hours post-LPS.

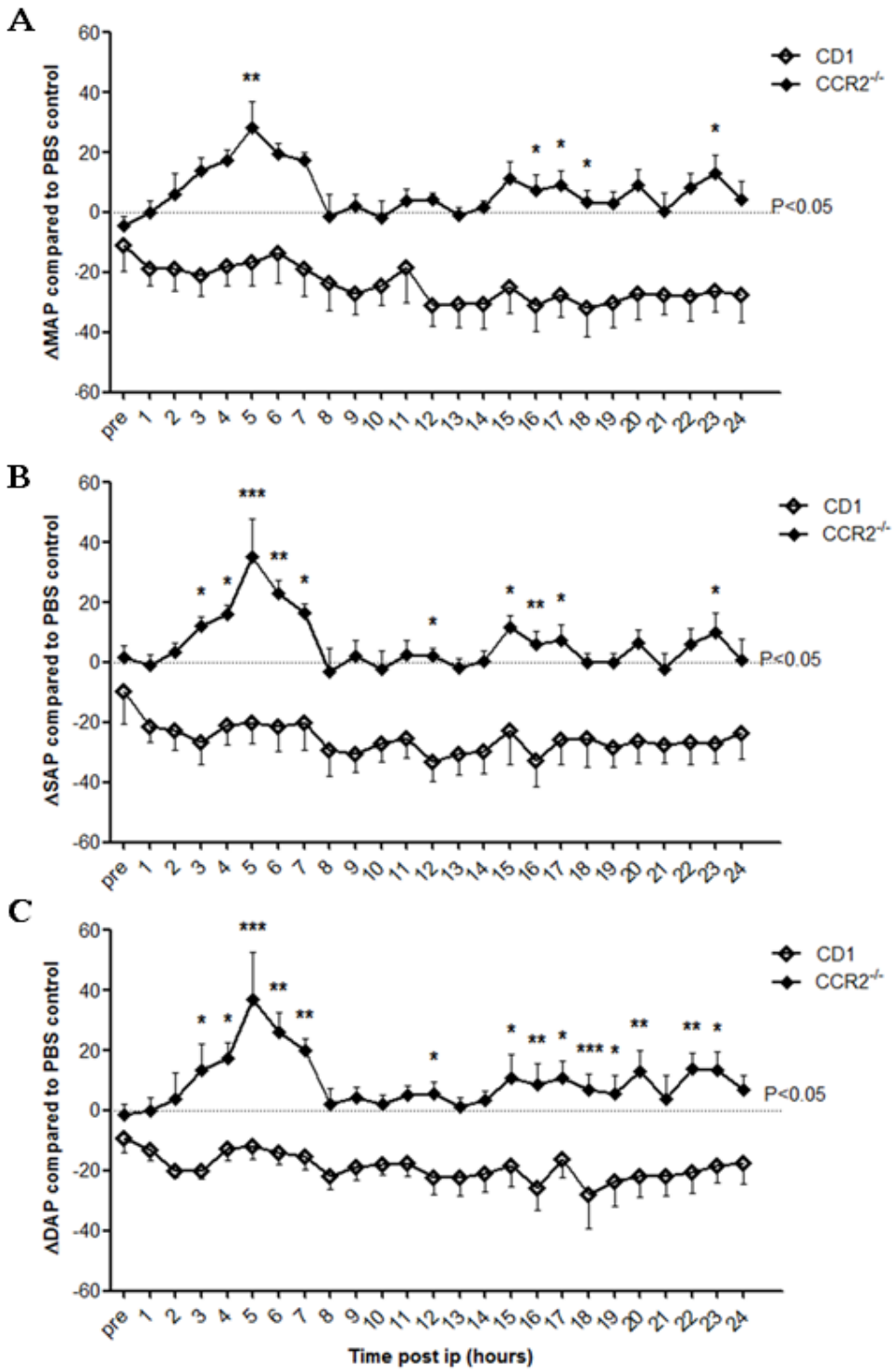


Figure 6.3: The haemodynamic response to LPS-induced inflammation in CCR2$^{-/-}$ mice. The haemodynamic response in CCR2$^{-/-}$ and CD1 mice was recorded for 24-hours following LPS administration on E16. (A) ΔMAP (B) ΔSAP (C) ΔDAP. *p<0.5, **p<0.01, ***p<0.001, trends were compared using 2-way ANOVA and individual time points were compared using 2-way ANOVA and Bonferroni post-hoc test. Data are expressed as a mean change from pre-LPS baseline (pre) compared to PBS controls ± SEM (CD1, n=7; CCR2$^{-/-}$, n=4).

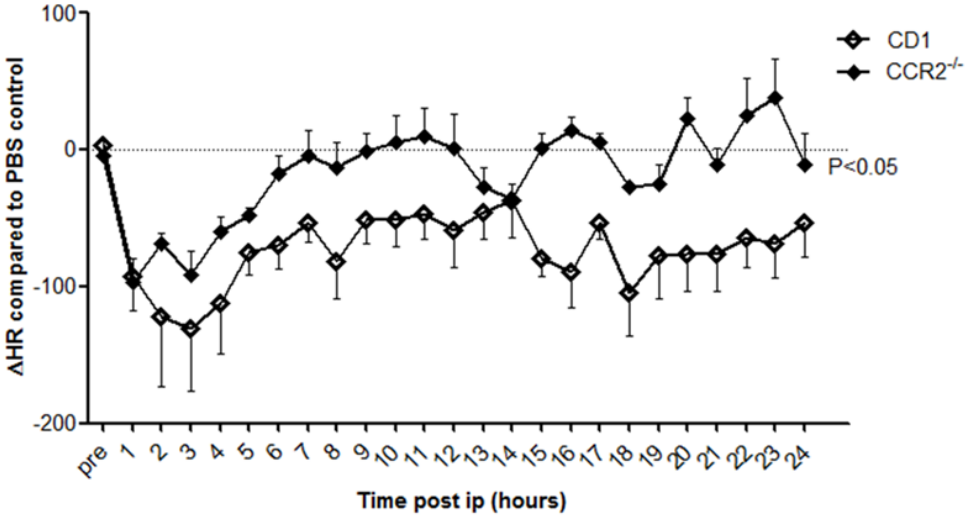


Figure 6.4: The heart rate response to LPS-induced inflammation in CCR2$^{-/-}$ mice. Heart rate in CCR2$^{-/-}$ and CD1 mice was recorded for 24-hours following LPS administration on E16. (A) ΔMAP (B) ΔSAP (C) ΔDAP. *p<0.5, **p<0.01, ***p<0.001, trends were compared using 2-way ANOVA and individual time points were compared using 2-way ANOVA and Bonferroni post-hoc test. Data are expressed as a mean change from pre-LPS baseline (pre) compared to PBS controls ± SEM (CD1, n=7; CCR2$^{-/-}$, n=4)..

HR was seen to decline immediately after LPS in CD1 and CCR2$^{-/-}$ mice. However in CCR2$^{-/-}$ mice HR returned to baseline by 7 hours post-LPS, whereas in CD1 mice HR remained significantly depressed ($p<0.05$; Figure 6.4).

AUC analyses showed that MAP was significantly increased in CCR2$^{-/-}$ mice after LPS ($p<0.05$; Figure 6.5A). The maximum decrease in ΔMAP in CCR2$^{-/-}$ mice was diminished but this did not reach statistical significance, and although the maximum increase in ΔMAP was greater in CCR2$^{-/-}$ mice this also did not reach statistical significance (Figure 6.5B, 6.5C). Very similar results were observed for SAP, where in CCR2$^{-/-}$ mice after LPS AUC was significantly increased ($p<0.05$; Figure 6.5D), maximum decrease in ΔSAP was significantly decreased ($p<0.05$; Figure 6.5E) and maximum increase in ΔSAP was significantly increased ($p<0.05$; Figure 6.5F). This was also reflected in changes in DAP, where AUC was significantly increased in CCR2$^{-/-}$ mice after LPS ($p<0.01$; Figure 6.5G) and the maximum increase in ΔDAP was significantly increased ($p<0.05$; Figure 6,5I).

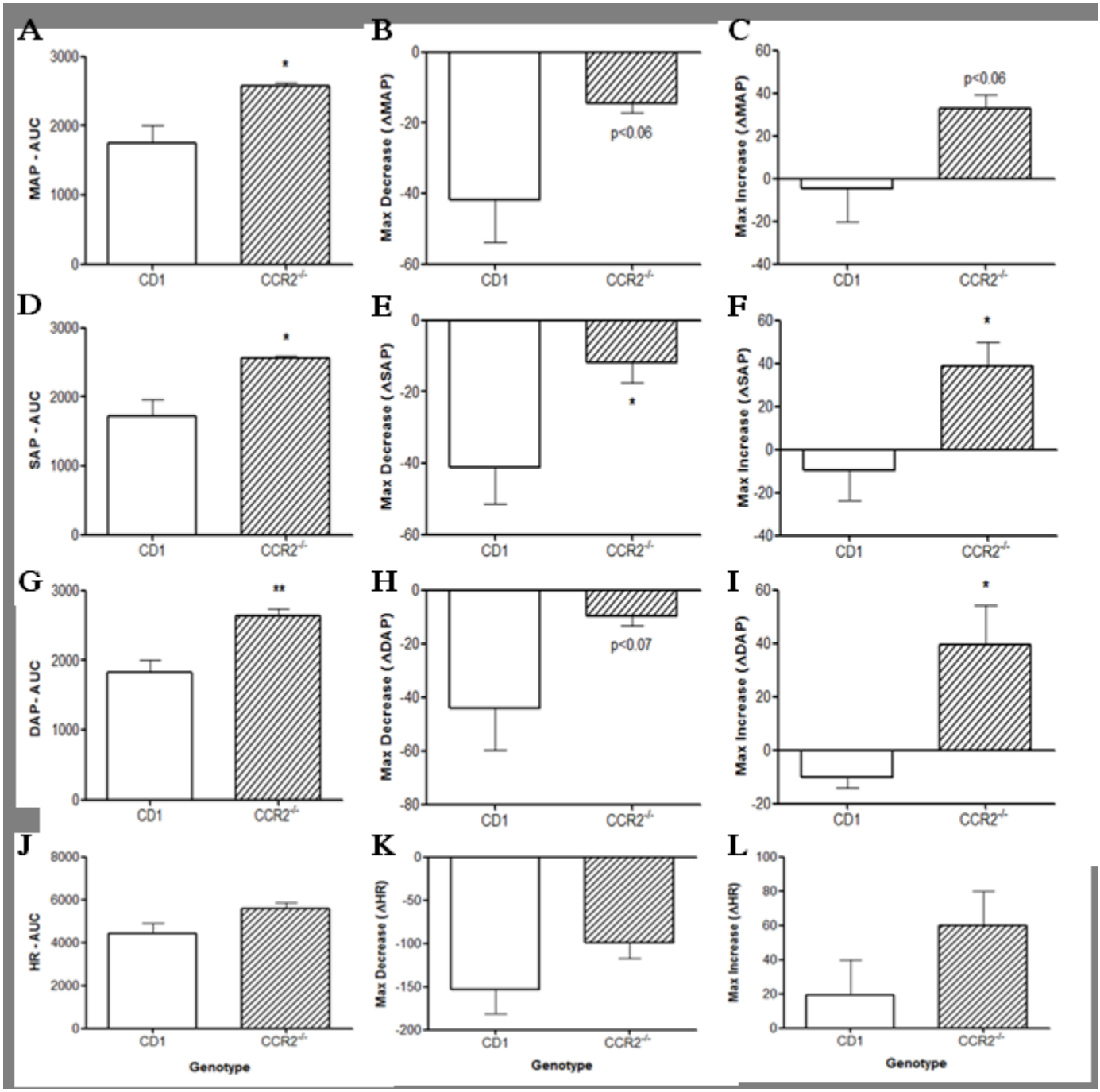


Figure 6.5: The haemodynamic response to LPS-induced inflammation in CCR2$^{-/-}$ mice compared to CD1 mice as assessed by AUC, maximum decrease and maximum increase. The haemodynamic response in CCR2$^{-/-}$ and CD1 mice recorded 24-hours after LPS administration. AUC analysis was perfomed for MAP (A), SAP (D), DAP (G) and HR (J). Maximum decrease was calculated for MAP (B), SAP (E), DAP (H) and HR (K). Maximum increase was calculated for MAP (C), SAP (F), DAP (I) and HR (L). *p<0.05, **p<0.01 student's t-test. Data are expressed as mean ± SEM (CD1, n=7; CCR2$^{-/-}$, n=4)..

Whilst the maximum decrease in ΔDAP was diminished in CCR2$^{-/-}$ mice after LPS this did not reach statistical significance (Figure 6.5H). There were no significant changes between CCR2$^{-/-}$ and CD1 mice after LPS in the AUC, maximum increase or maximum decrease of HR (Figure 6.5J, 6.5K, 6.5L).

There were no statistically significant differences between activity levels in the 24 hours after LPS between CCR2$^{-/-}$ and CD1 mice (Figure 6.6A, 6.6B, 6.6C). However, CCR2$^{-/-}$ mice generally had much more variable activity levels where the Δ%TSI was initially decreased after LPS and ΔActivity was increased in the first 8 hours. It is important to note that where activity in CD1 mice remained at baseline throughout the 24 hour period after LPS, activity in CCR2$^{-/-}$ mice did increase above baseline, to a peak of Δ60.76 ± 37.07 at 7 hours post-LPS. The highest peak in CD1 mice was Δ0.41 at 24 hours post-LPS (Figure 6.6B). It should be considered that these initial high levels of activity seen in CCR2$^{-/-}$ mice could account for the increased MAP observed at 5 hours post-LPS. However, as MAP remained elevated in CCR2$^{-/-}$ compared to CD1 after LPS in the 16 to 23 hour period where activity levels had remained at or below baseline, this is unlikely to be the only reason for elevated MAP but may be a contributing factor. As observed previously in pregnant animals, the reason for no change in activity after LPS administration may be due to overriding nesting behaviours.

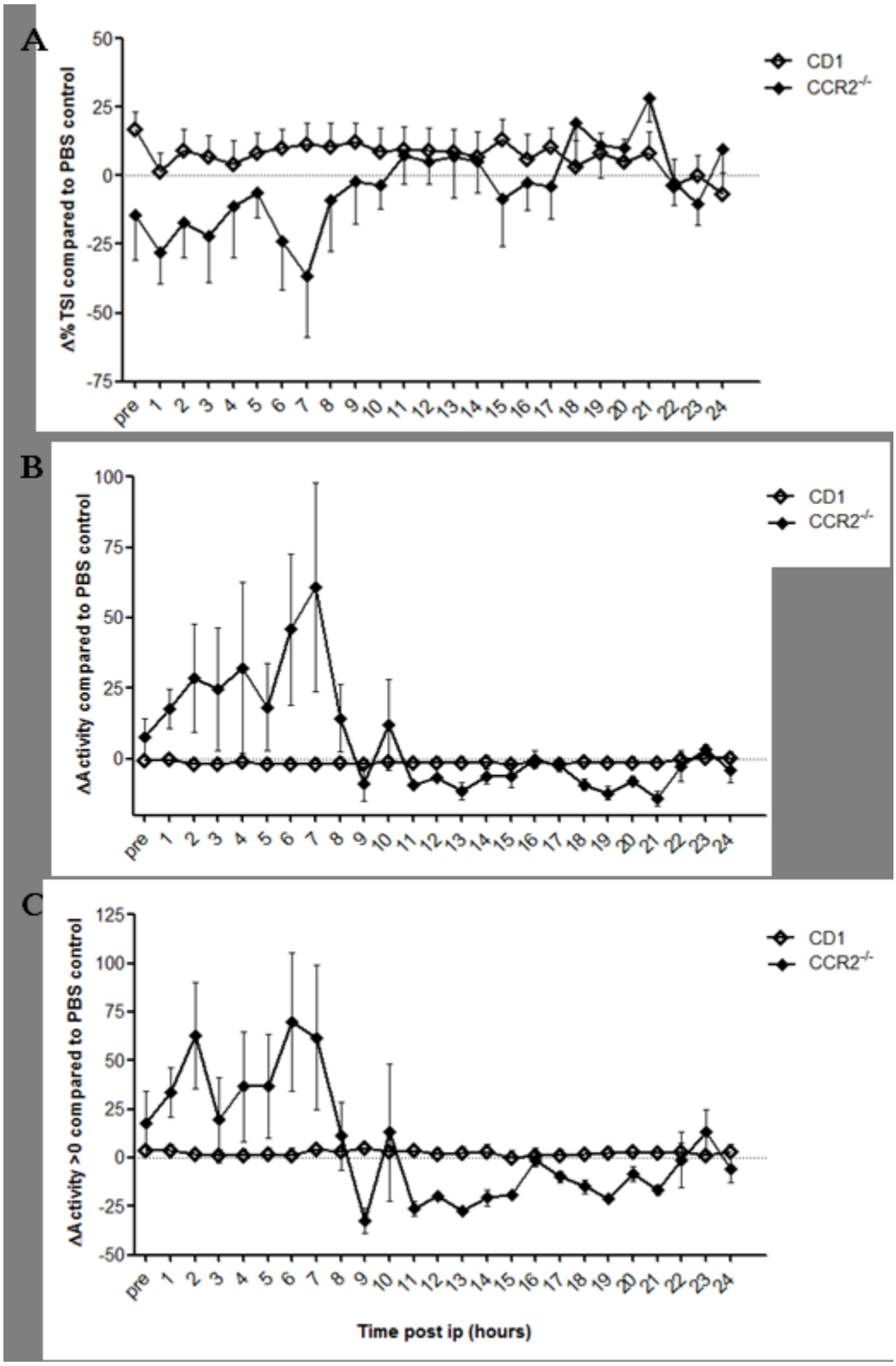


Figure 6.6: Activity in pregnant CCR2$^{-/-}$ and CD1 mice after LPS administration. Activity levels in CCR2$^{-/-}$ and CD1 mice were recorded for 24-hours following LPS administration on E16. (A) Δ%TSI (B) ΔActivity (C) ΔActivity>0. Data are expressed as a mean change from pre-LPS baseline (pre) compared to PBS controls ± SEM (CD1, n=7; CCR2$^{-/-}$, n=4)..

6.2.4 The LPS-induced Inflammatory Response in Pregnant CCR2 Knockout Mice

Absolute concentrations of cytokines and chemokines in maternal serum from CD1 and CCR2$^{-/-}$mice 6 and 12 hours after LPS i.p. were measured using the Millipore MAGpix multiplex assay system to evaluate any effects of CCR2 deficiency on the systemic inflammatory response.

There were numerous differences between the responses of CD1 and CCR2$^{-/-}$ mice to LPS when circulating pro- and anti-inflammatory cytokines were examined. In response to LPS, IL-1β was not significantly increased in CD1 or CCR2$^{-/-}$ mice (Figure 6.7A) and IL-6 was significantly increased in both strains ($p<0.05$, $p<0.01$; Figure 6.7B). Intriguingly, circulating concentrations of TNF-α were only significantly increased in CD1 mice ($p<0.01$), as at 6 hours post-LPS this increase was significantly attenuated in CCR2$^{-/-}$ mice ($p<0.001$; Figure 6.7C). Also of note, is that in PBS-treated CCR2$^{-/-}$ mice there was a trend towards decreased levels of TNF-α in the circulation (15.14 ± 4.3 pg/mL and 19.69 ± 5.5 pg/mL at 6 and 12 hours respectively in CCR2$^{-/-}$ mice compared to 346.7 ± 62.4 pg/mL and 502.8 ± 83.4 pg/mL at 6 and 12 hours respectively in CD1 mice), although this did not reach statistical significance. Conversely, IL-4 and IL-10 concentrations were significantly increased in CCR2$^{-/-}$ but not in CD1 mice. IL-4 was significantly increased after LPS compared to PBS control in CCR2$^{-/-}$ mice but only 12 hours post-LPS ($p<0.05$; Figure 6.7D). Where there was a trend towards increased IL-10 levels in CD1 mice in response to LPS, due to high inter-animal variability this was not significant; however there were significantly increased concentrations of IL-10 in CCR2$^{-/-}$ mice 6 hours ($p<0.05$) and 12 hours ($p<0.01$) post-LPS (Figure 6.7E).

There were no differences between the responses of CD1 and CCR2$^{-/-}$ mice to LPS when circulating chemokines were measured. CCL2 was increased after LPS administration in CD1 and CCR2$^{-/-}$ mice, although only at 6 hours post-LPS in CD1 mice ($p<0.05$) and at both 6 hours ($p<0.001$) and 12 hours ($p<0.01$) post-LPS in CCR2$^{-/-}$ mice (Figure 6.8A).

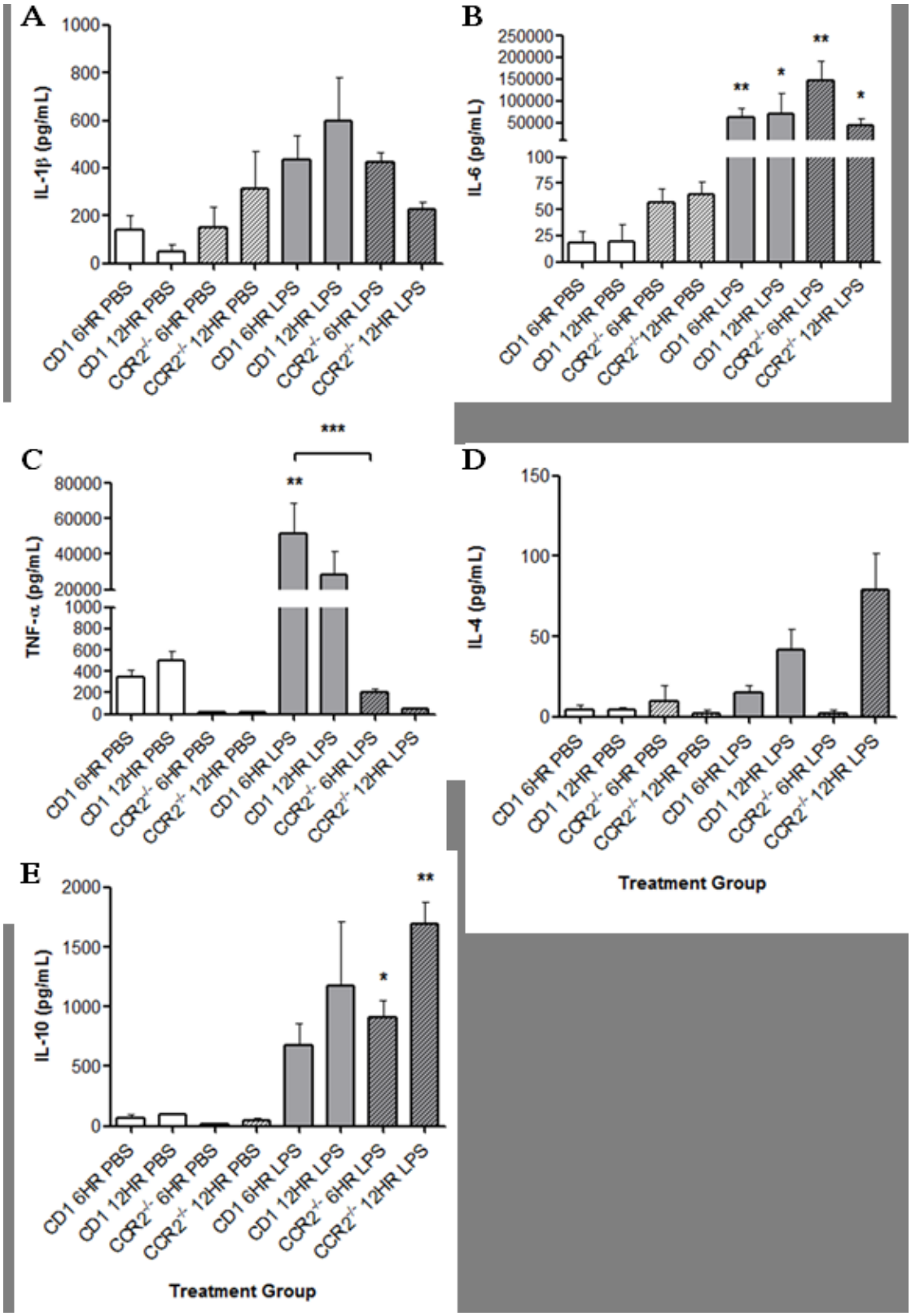


Figure 6.7: **Circulating concentrations of pro- and anti-inflammatory cytokines in the serum of pregnant CD1 and CCR2$^{-/-}$ mice treated with LPS or vehicle.** Measurements were made in serum samples taken 6 or 12 hours after LPS in CD1 and CCR2$^{-/-}$ mice. (A) IL-1β (B) IL-6 (C) TNF-α (D) IL-4 (E) IL-10. *p<0.05, **p<0.01, ***p<0.001 pairwise t-test comparisons or Mann Whitney U tests were used where appropriate. Data shown as mean ± SEM (CD1, n=7; CCR2$^{-/-}$, n=4).

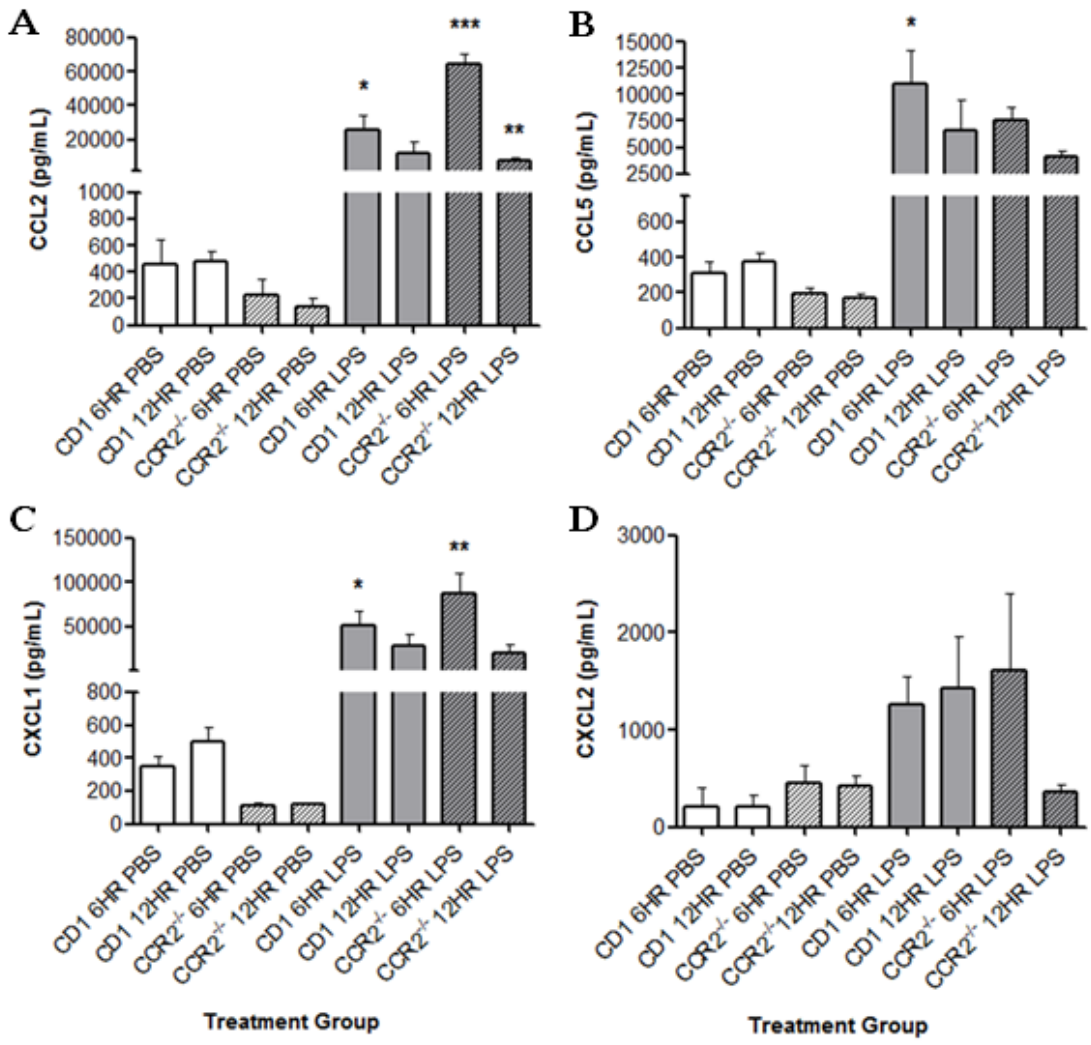


Figure 6.8: **Circulating concentrations of chemokines in the serum of pregnant CD1 and CCR2$^{-/-}$ mice treated with LPS or vehicle**. Measurements were made in serum samples taken 6 or 12 hours after LPS in in CD1 and CCR2$^{-/-}$ mice. (A) CCL2 (B) CCL5 (C) CXCL1 (D) CXCL2. *p<0.05, **p<0.01, ***p<0.001 pairwise t-test comparisons or Mann Whitney U tests were used where appropriate. Data shown as mean ± SEM (CD1, n=7; CCR2$^{-/-}$, n=4).

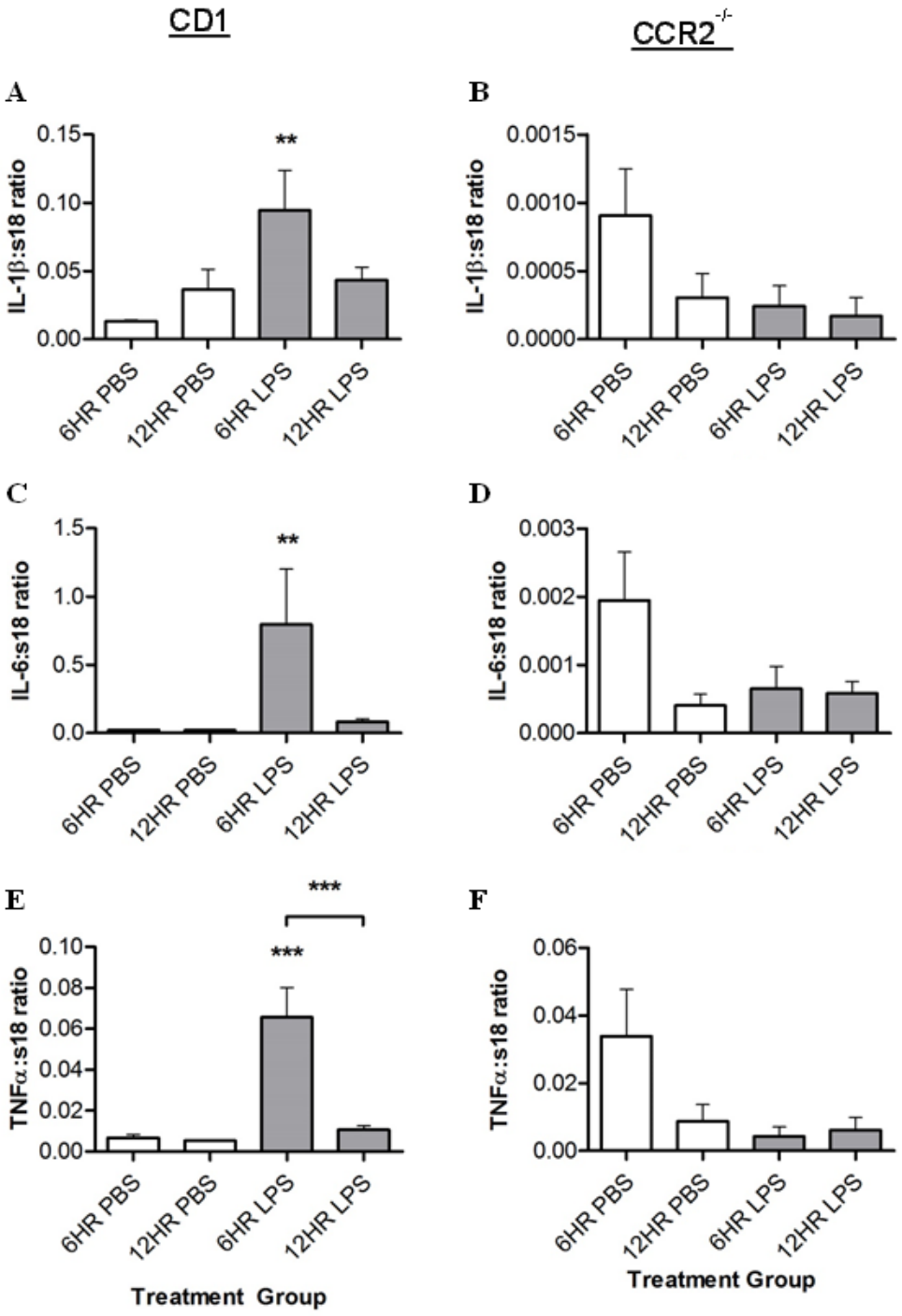


Figure 6.9: mRNA expression of pro-inflammatory cytokines in left ventricular tissue taken from pregnant CCR2$^{-/-}$ and CD1 mice treated with LPS or vehicle. (A) IL-1β in CD1 mice (B) IL-1β in CCR2$^{-/-}$ mice (C) IL-6 in CD1 mice (D) IL-6 in CCR2$^{-/-}$ mice (E) TNF-α in CD1 mice (F) TNF-α in CCR2$^{-/-}$ mice. Data for CD1 mice is shown in the left panels and CCR2$^{-/-}$ mice in the right panels. CD1 data is taken from Figure 4.6 showing here only pregnant responses. **p<0.01, ***p<0.001, pairwise t-test comparisons or Mann Whitney U tests were used where appropriate. Data are expressed as mean ± SEM (all CD1 groups, n=6; CCR2$^{-/-}$ 12HR PBS, n=5; all other CCR2$^{-/-}$ groups, n=6).

CCL5 was found to be increased in CD1 and CCR2$^{-/-}$ mice in response to LPS but this only reached significance in CD1 mice at 6 hours post-LPS ($p<0.05$; Figure 6.8B). There was no difference in the overall trend. Similarly, CXCL1 was increased at 6 hours but not 12 hours after LPS in CD1 and CCR2$^{-/-}$ mice ($p<0.05$; Figure 6.8C). CXCL2 was not found to be increased after LPS in either strain. This was surprising, as CXCL2 had previously been found to be significantly increased in pregnant CD1 mice in response to LPS ($p<0.05$; Figure 4.8E). It may be that in this cohort of mice, greater inter-animal variability prevented statistical significance from being achieved.

The inflammatory response to LPS in CCR2$^{-/-}$ mice was also studied in left ventricular tissue, where relative mRNA expression levels of pro- and anti-inflammatory cytokines and chemokines were measured. No direct comparisons could be made between CD1 and CCR2$^{-/-}$ left ventricles in response to LPS, but it was evident that three of the key pro-inflammatory cytokines were supressed in CCR2$^{-/-}$ mice (Figure 6.9). In CCR2$^{-/-}$ mice IL-1β (Figure 6.9A), IL-6 (Figure 6.9C) and TNF-α (Figure 6.9E) were not upregulated 6 or 12 hours after LPS administration. In CD1 mice 6 hours after LPS, IL-1β expression was significantly increased ($p<0.01$; Figure 6.9B) and similarly IL-6 ($p<0.01$; Figure 6.9D) and TNF-α ($p<0.001$; Figure 6.9F) were also significantly increased. Further to this, in CCR2$^{-/-}$ mice LPS caused no upregulation in mRNA expression of any of the markers of inflammation, cardiac dysfunction or apoptosis that were measured including Cox-2, ANP, BNF, Bcl-2, Bax and Bad (data not shown).

6.2.5 Circulating Expression of Vasoactive Factors in Response to LPS in Pregnant CCR2 Knockout Mice

NO and ADMA concentrations in serum from pregnant CD1 or $CCR2^{-/-}$ mice 6 and 12 hours after LPS or vehicle control (PBS) were determined using the Seivers nitric oxide analyser and mass spectrometry respectively. Absolute concentrations of vasoactive factors in serum were measured using the Millipore MAGpix multiplex assay system to evaluate the systemic response.

Serum NO concentrations were comparable with those seen previously in pregnant mice. Compared to CD1 mice, $CCR2^{-/-}$ mice had significantly lower circulating NO, where concentrations were found to be 22.88 ± 1.7 μM and 21.66 ± 4.6 μM at 6 and 12 hours post-PBS respectively in $CCR2^{-/-}$ mice compared to 44.67 ± 9.9 and 47.6 ± 4.5 μM at 6 and 12 hours post-PBS respectively in CD1 mice ($p<0.05$; Figure 6.10A). At 6 hours post-LPS, NO was significantly increased in CD1 mice to 86.49 ± 10.8 μM ($p<0.05$) and although there were increases in NO at 12 hours post-LPS due to high variability these were not significant. As well as lower basal NO, $CCR2^{-/-}$ mice also had significantly reduced circulating NO 6 hours after LPS compared to CD1 mice ($p<0.05$) which was not significantly increased from PBS controls. At 12 hours after LPS there were increases in NO in $CCR2^{-/-}$ mice, but like in CD1 mice this did not reach statistical significance.

To explore the differences in NO concentrations further, circulating ADMA levels were measured in serum of CD1 and $CCR2^{-/-}$ mice. In PBS-treated $CCR2^{-/-}$ mice, significantly reduced ADMA concentrations were found compared to those in CD1 mice ($p<0.001$; Figure 6.10B). No difference in ADMA was observed in CD1 mice after LPS treatment at either 6 or 12 hours post-LPS. Likewise, LPS did not alter AMDA levels in $CCR2^{-/-}$ mice and thus ADMA was significantly decreased at both 6 and 12 hours post-LPS compared to CD1 mice ($p<0.001$).

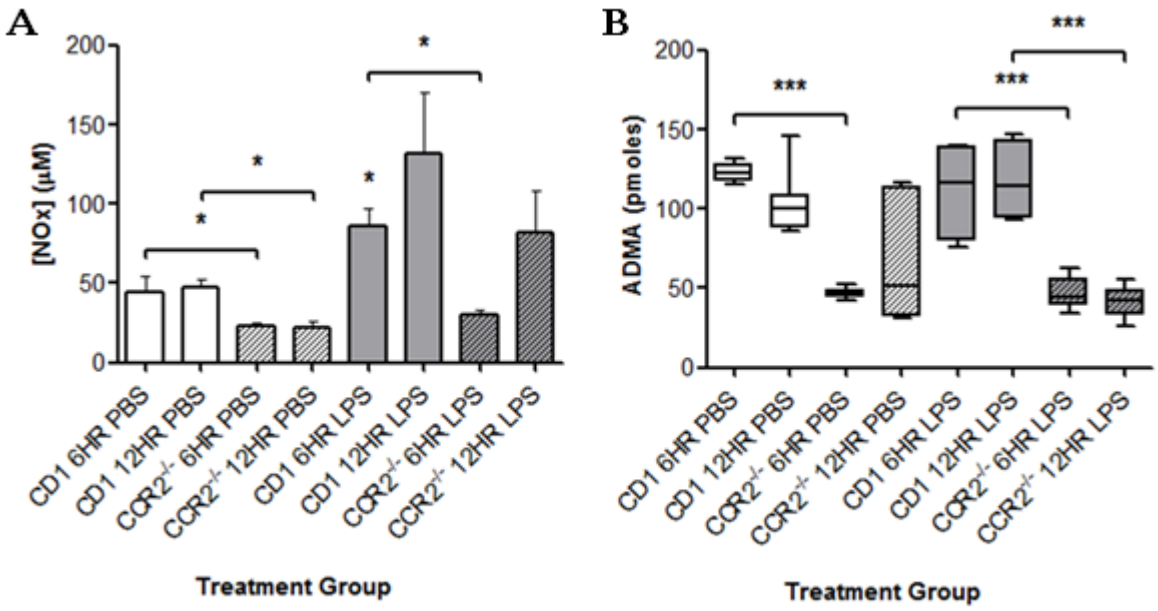


Figure 6.10: **Circulating concentrations of nitric oxide and asymmetric dimethylarginine in the serum of pregnant CD1 and CCR2$^{-/-}$ mice treated with LPS or vehicle**. Measurements were made in serum samples taken 6 or 12 hours after LPS or vehicle in CD1 and CCR2$^{-/-}$ mice. (A) Concentration of total nitrates and nitrites (NOx) as measured by nitric oxide analyser (B) ADMA as measured by mass spectrometry. *p<0.05, **p<0.01, ***p<0.001 compared to PBS control unless otherwise indicated, pairwise t-test comparisons or Mann Whitney U tests were used where appropriate. Data shown as mean ± SEM, or as median ± interquartile range showing minimum and maximum (CD1 6 HR PBS, n=7; CD1 12 HR PBS, n=5; CCR2$^{-/-}$ 6 HR PBS, n=4; CCR2$^{-/-}$ 12 HR PBS, n=6; CD1 6 HR LPS, n=4; CD1 12 HR LPS, n=4; CCR2$^{-/-}$ 6 HR LPS, n=6; CCR2$^{-/-}$ 12 HR LPS, n=6)

VEGF was not altered by CCR2 deficiency or the administration of LPS in these animals (Figure 6.11A). This was not surprising as previous data had suggested that LPS did not significantly increase VEGF in pregnant animals. LPS administration caused PLGF2 to be significantly increased in both CD1 mice as previously seen (p<0.05; Figure 6.11B) and in CCR2$^{-/-}$ mice (p<0.01, p<0.05 at 6 and 12 hours post-LPS respectively). Levels of PLGF2 were diminished in CCR2$^{-/-}$ mice, although this was not significant in PBS-treated animals. However, after LPS the increase in PLGF2 was significantly diminished in CCR2$^{-/-}$ mice (p<0.05). There were no differences in ET-1 between PBS- treated CD1 and CCR2$^{-/-}$ mice (Figure 6.11C). Additionally, there were no increases in ET-1 in CD1 mice after LPS. However at 6 hours post-LPS, ET-1 was significantly increased in CCR2$^{-/-}$ mice (p<0.05).

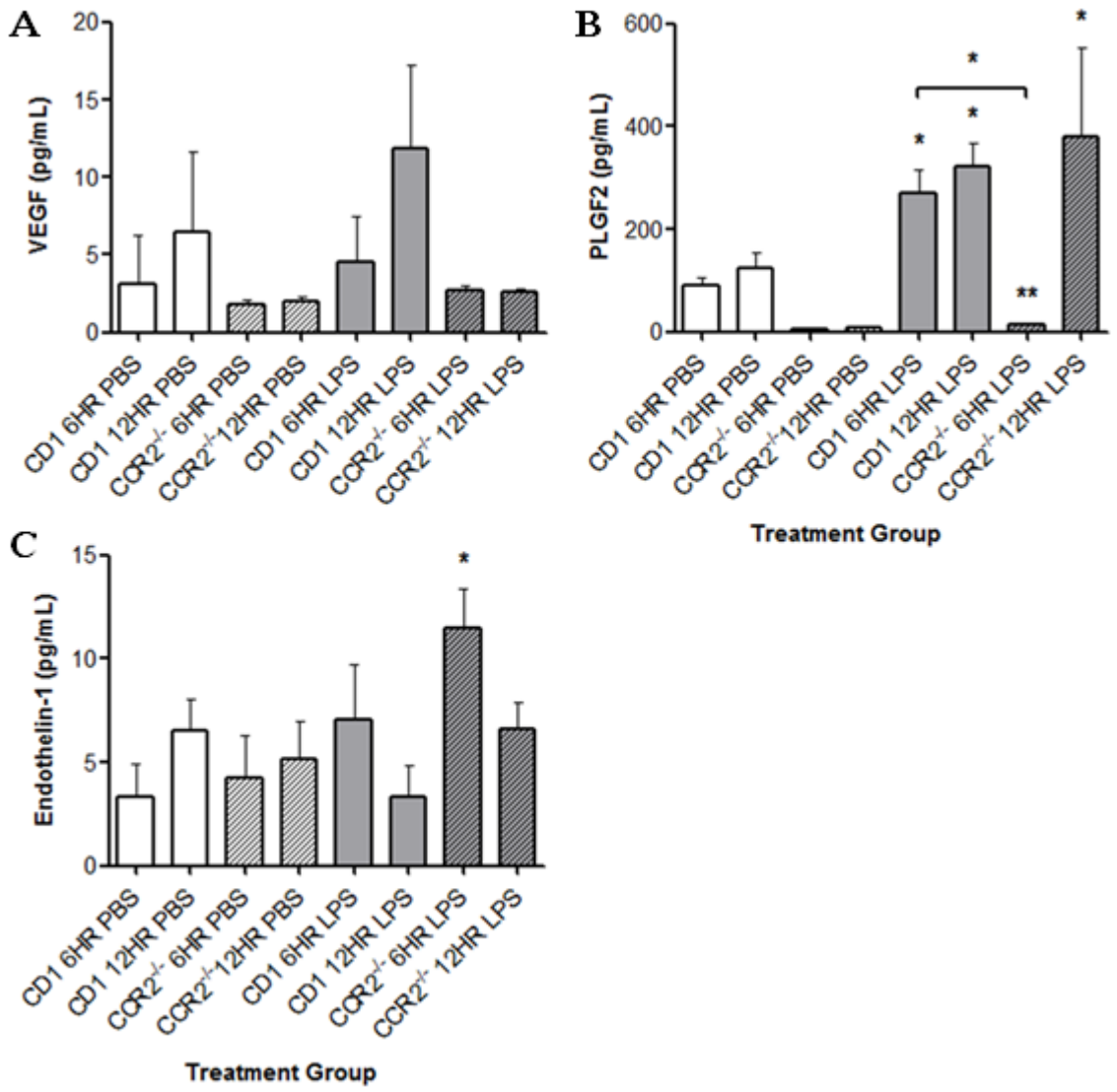


Figure 6.11: Circulating concentrations of vasoactive factors in serum of pregnant CD1 and CCR2-/- mice treated with LPS or vehicle. (A) VEGF (B) PLGF2 (C) Endothelin-1. *p<0.05, **p<0.01, compared to vehicle control unless otherwise indicated, pairwise t-test comparisons or Mann Whitney U tests were used where appropriate. Data shown as mean ± SEM (CD1, n=7; $CCR2^{-/-}$, n=4).

6.2.7 The Haemodynamic Response to LPS-induced Inflammation after Pharmacological CCR2 Inhibition in Pregnant Mice

To further explore the effects of CCR2 inhibition on LPS-induced hypotension in pregnancy, the CCR2 antagonist RS504393 was used in CD1 mice. RS504393 was chosen for its high specificity to CCR2 (approximately 700-fold better binding than at CCR1 with no binding at CXCR1 or CCR3 [406]) and due to recent evidence that suggested blockade of CCR2 using this receptor antagonist may be protective in murine sepsis [172]. Based on the experimental model of Souto *et al*., and others, RS504393 was given 2mg/kg subcutaneously in PBS (5% DMSO in PBS was given as vehicle) 30 minutes prior to LPS on E16 and every 12 hours thereafter until the onset of labour [172, 407-410].

Preliminary studies showed that RS504393, given to pregnant mice from E16 onwards, caused no maternal morbidity and that animals laboured spontaneously at term and birthed live litters (data not shown, n=3). After LPS administration, latency to labour in RS504393-treated mice did not significantly differ from vehicle-treated mice, however, labour time was much more variable (32.22 ± 7.98 hours compared to 28 ± 2.65 in vehicle-treated mice; data not shown, n=4-8). Pup survival was improved in RS504393-treated mice (19.79 ± 12.4 % survival, compared to 0% in vehicle-treated; data not shown, n=4-8), although again, the data were highly variable.

Experiments to assess the haemodynamic response of pregnant mice to LPS after pharmacological CCR2 inhibition with RS504393 showed that compared with pregnant vehicle (PBS/DMSO) controls, MAP was maintained at pre-LPS baseline levels (Figure 6.12A). Vehicle-treated mice exhibited a nadir in MAP of Δ-24.23 ± 10.04 mmHg at 19 hours post-LPS and MAP did not return to baseline within the 24 hours period, where in RS504393-treated mice MAP dropped to Δ-7.6 ± 5.97 mmHg at 12 hours post-LPS but this drop below baseline recovered by 14 hours (Δ2.62 ± 2.87 mmHg).

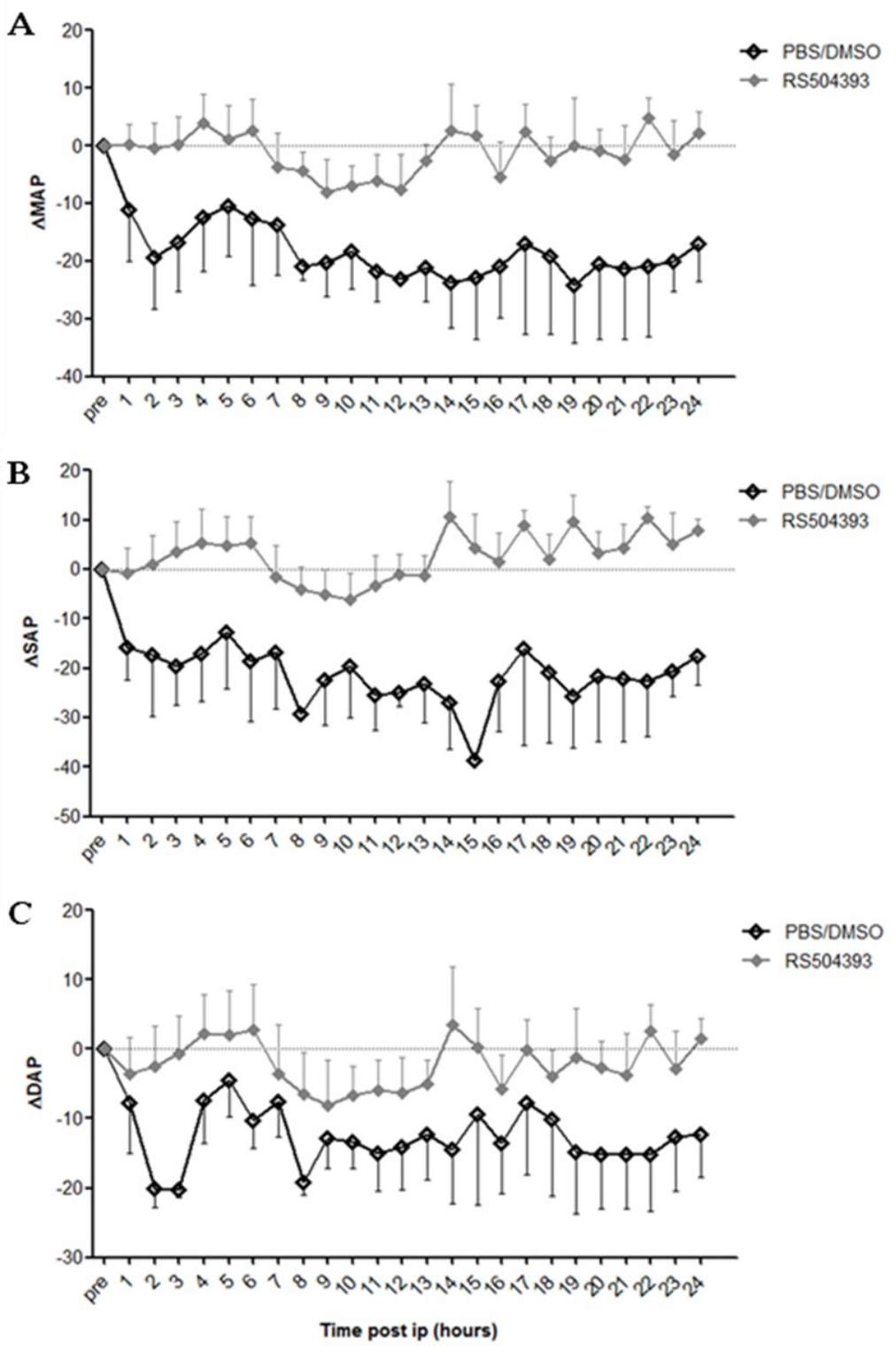


Figure 6.12: The haemodynamic response to LPS-induced inflammation in mice pre-treated with CCR2 inhibitor. The haemodynamic response in mice pre-treated with CCR2 inhibitor RS504393 or vehicle (PBS/DMSO) were recorded for 24-hours following LPS administration on E16. (A) ΔMAP (B) ΔSAP (C) ΔDAP. Data are expressed as a mean change from pre-LPS baseline (pre) ± SEM (PBS/DMSO, n=2; RS504393, n=6).

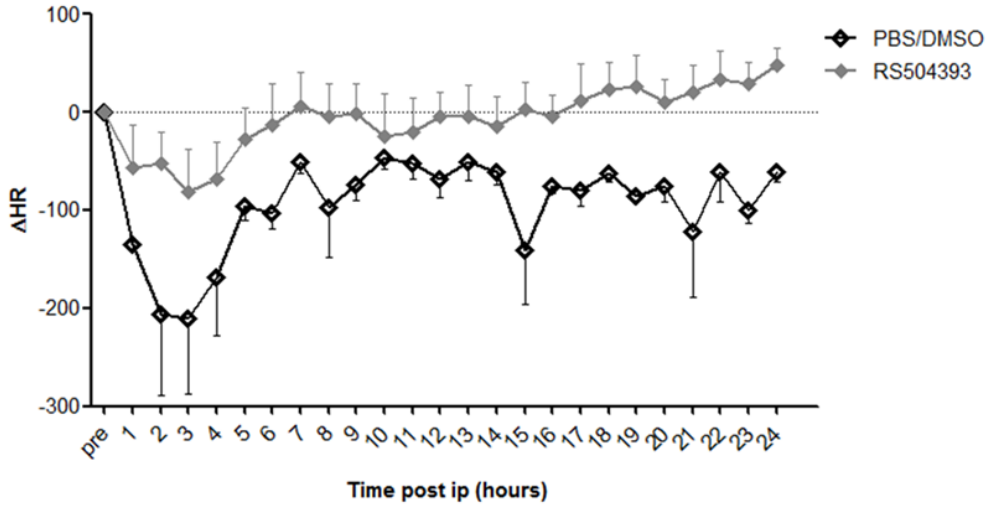


Figure 6.13: The heart rate response to LPS-induced inflammation in mice pre-treated with CCR2 inhibitor. Heart rate in mice pre-treated with CCR2 inhibitor RS504393 or vehicle (PBS/DMSO) were recorded for 24-hours following LPS administration on E16. Data are expressed as a mean change from pre-LPS baseline (pre) ± SEM (PBS/DMSO, n=2; RS504393, n=6).

There was no statistical significance between treatment groups as assessed by 2-way ANOVA followed by Bonferroni correction for multiple tests. Unfortunately there were some time points between 8-24 hours at which no data could be collected which led to this statistical test only being carried out between pre-LPS baseline and 8 hours post-LPS. This, and the small n number for vehicle control, may be the reason for a lack of significance.

Similar results were obtained for SAP and DAP (Figure 6.12B, 6.12C) where a comparable trend was observed. The nadir in SAP in vehicle-treated mice was measured to be Δ-38.6 ± 0 at 15 hours post-LPS compared to Δ4.25 ± 7.01 mmHg in RS504393-treated mice. A much earlier drop in DAP was seen in vehicle-treated mice after LPS where a ΔDAP of Δ-20.3 ± 1.07 mmHg was seen at 3 hours post-LPS. DAP then recovered to some extent but dropped to Δ-19.1 ± 1.88 mmHg by 8 hours and did not return to baseline levels. Despite these trends, there was no statistical significant difference between treatment groups.

As seen in previous experiments, HR in the vehicle-treated mice dropped in response to LPS to a nadir of Δ-211.02 ± 76.8 bpm by 3 hours (Figure 6.13). There was also an initial drop in HR in RS504393-treated mice but of much smaller magnitude (Δ-81.73 ± 44.59 bpm at 3 hours post-LPS). HR in RS504393-treated mice then remained at baseline but the HR of vehicle-treated animals did not return to baseline within the 24 hour period of recordings. There was no statistical significant difference between treatment groups.

Following a similar trend to the results obtained from $CCR2^{-/-}$ mice, where CCR2 was blocked by pharmacological antagonism AUC analyses showed that MAP was significantly increased after LPS compared to vehicle ($p<0.05$; Figure 6.14A). The maximum decrease in ΔMAP in RS504393-treated mice was diminished but this did not reach statistical significance, and although the maximum increase in ΔMAP was greater, statistical analysis was not possible (Figure 6.14B, 6.14C). Correspondingly, the AUC for SAP was significantly increased in RS504393-treated mice after LPS ($p<0.05$; Figure 6.14D) and the maximum decrease was significantly decreased ($p<0.05$; Figure 6.14E). Likely due to the large variability in maximum increase in vehicle-treated mice, there was no difference between treatment groups (Figure 6.14F). Unlike the significant differences in DAP between $CCR2^{-/-}$ mice and CD1 controls, RS504393 treatment did not cause significant increases in the AUC for DAP, nor a significant increase in maximum increase in ΔDAP (Figure 6.14G, 6.14I). There was no overall difference in HR as assessed by AUC analysis (Figure 4.16J), however the maximum increase in ΔHR was significantly increased in RS504393-treated mice ($p<0.05$; Figure 4.16L).

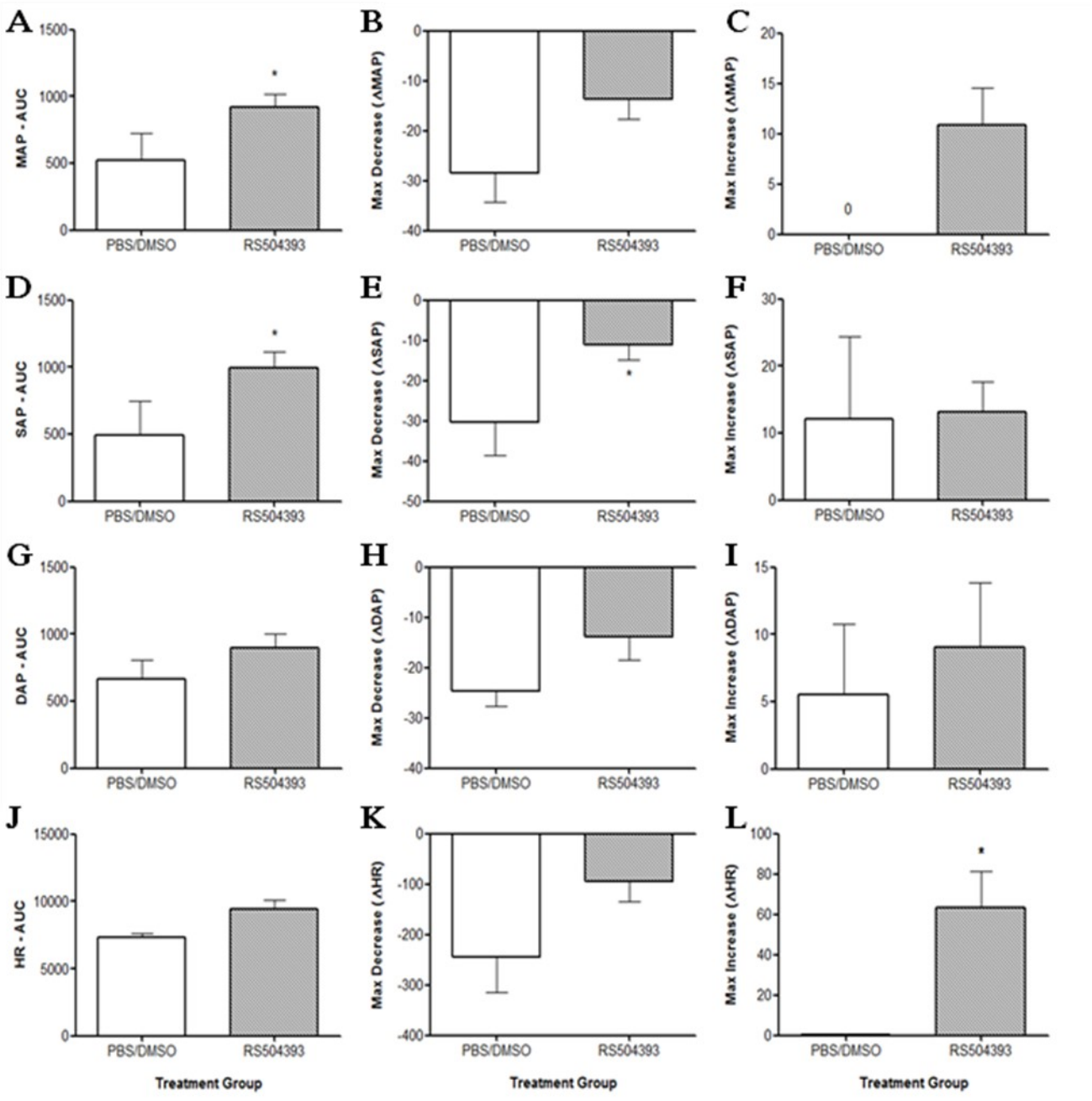


Figure 6.14: The haemodynamic response to LPS-induced inflammation in in mice pre-treated with CCR2 inhibitor or vehicle control as assessed by AUC, maximum decrease and maximum increase. The haemodynamic response in mice pre-treated with CCR2 inhibitor RS504393 or vehicle (PBS/DMSO) were recorded 24-hours after LPS administration. AUC analysis was perfomed for MAP (A), SAP (D), DAP (G) and HR (J). Maximum decrease was calculated for MAP (B), SAP (E), DAP (H) and HR (K). Maximum increase was calculated for MAP (C), SAP (F), DAP (I) and HR (L). *P<0.05 Mann-Whitney U test. Data are expressed as mean ± SEM (PBS/DMSO, n=2; RS504393, n=6).

To explore the possibility of altered activity levels contributing to changes in haemodynamics between treatment groups, activity levels were considered (Figure 6.15). There were no significant differences in the Δ%TSI, ΔActivity or ΔActivity>0 after LPS in either the vehicle- or RS504393-treated groups. However, it is important to note that both groups had an increased %TSI and decreased activity after LPS compared to pre-LPS baseline, which was not true of CD1 mice (Figure 6.6). Therefore the possibility of the DMSO in the vehicle affecting activity should be considered. In the design of this experiment, care was taken to reduce DMSO levels to 5% in solution and the animals showed no typical signs of DMSO-induced morbidity (piloerection, porphyrin staining and hunched posture).

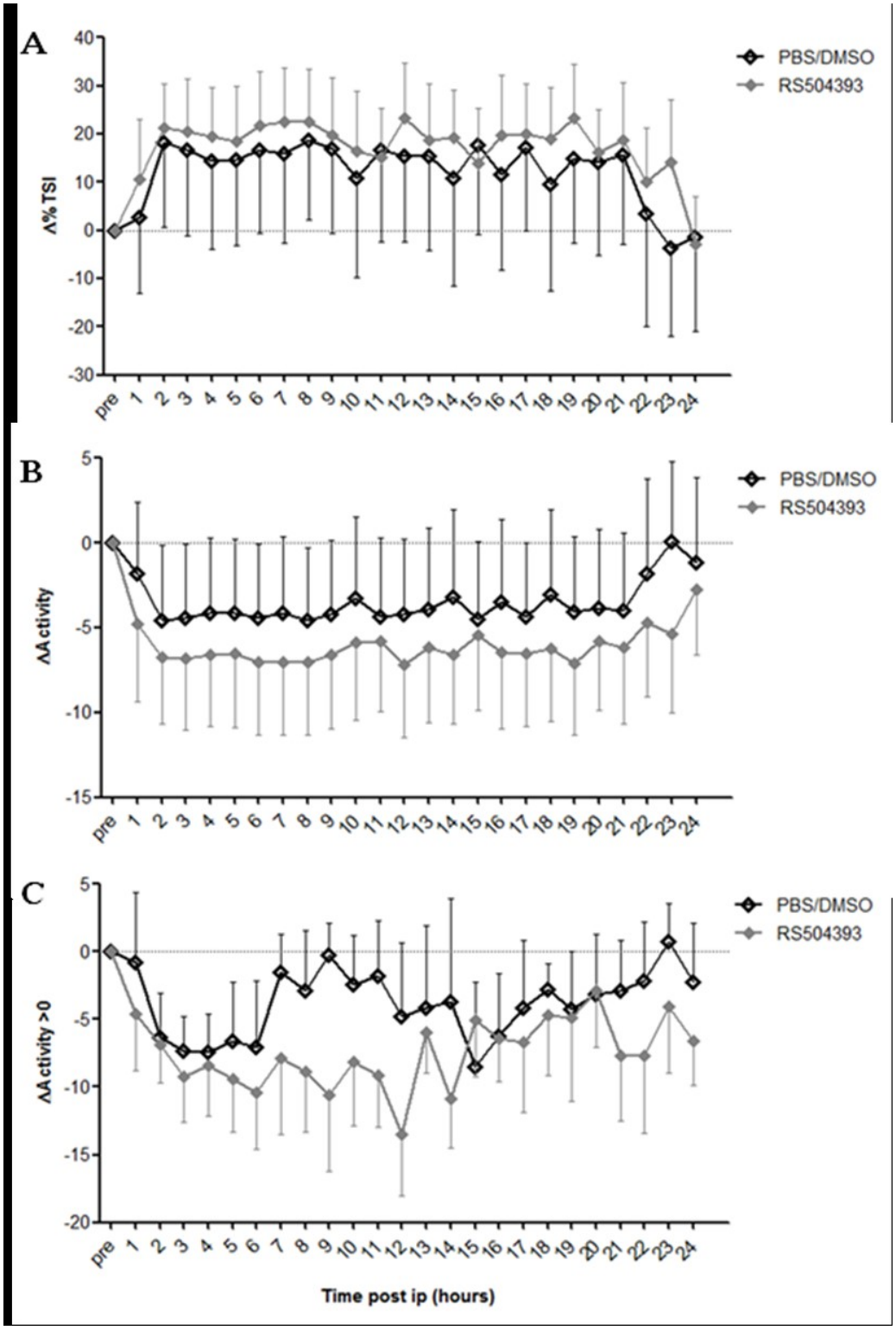


Figure 6.15: Activity in pregnant mice pre-treated with CCR2 inhibitor after LPS administration. Activity levels in mice pre-treated with CCR2 inhibitor RS504393 or vehicle (PBS/DMSO) were recorded for 24-hours following LPS administration on E16. (A) Δ%TSI (B) ΔActivity (C) ΔActivity>0. Data are expressed as a mean change from pre-LPS baseline (pre) compared to PBS controls ± SEM (PBS/DMSO, n=2; RS504393, n=6).

6.3 Summary and Discussion

Non-pregnant CCR2$^{-/-}$ mice did not have significant alterations in blood pressure but HR was decreased compared to CD1 mice. Accompanying this, CCR2$^{-/-}$ mice were found to be significantly more active. Latency to labour and pup survival after LPS administration (10μg) and vehicle control in CCR2$^{-/-}$ mice were not significantly different to CD1 mice. Compared with CD1 controls, the haemodynamic response to LPS in CCR2$^{-/-}$ mice was markedly augmented. Compared to the LPS-induced hypotension in CD1 mice, in CCR2$^{-/-}$ mice MAP was increased to a peak at 5 hours post-LPS and then returned to baseline. A very similar pattern was seen in SAP and DAP. There were no differences in %TSI which was as expected, as both groups of mice were pregnant and nesting. At intermediate time points between LPS administration and labour, circulating concentrations of TNF-α were found to be significantly reduced and IL-4 and IL-10 were significantly increased in CCR2$^{-/-}$ mice compared to CD1. The increase in expression of pro-inflammatory cytokines (IL-1β, IL-6 and TNF-α) in CD1 left ventricle at 6 hours post-LPS were not upregulated in CCR2$^{-/-}$ mice. Both circulating NO and ADMA concentrations were significantly reduced in CCR2$^{-/-}$ mice both basally and after LPS challenge. Additionally PLGF2, but not VEGF, was reduced in CCR2$^{-/-}$ mice at 6 hours post-LPS and this was accompanied by a significant increase in ET-1. By administering a CCR2 antagonist (RS504393) to CD1 mice, CCR2 blockade prevented LPS-induced hypotension; however greater numbers may be needed in addition to this preliminary work to potentially achieve statistical significance.

In this study CCR2 deficiency did not alter the timing of LPS-induced PTL. This result has been previously observed in our group (intrauterine LPS) and others [168]. The onset of LPS-induced PTL is in part, triggered by premature myometrial and decidual activation which cannot be overcome by blockade of CCR2 alone. Recently a broad spectrum chemokine inhibitor (BSCI) has been shown to delay systemic LPS-induced inflammatory PTL in the mouse [411]. The BSCI was thought to have more efficacy as a tocolytic agent as previous therapies targeting specific chemokines failed to mount the redundancy of the inflammatory pathway.

ET-1 was seen to be significantly increased at 6 hours post-LPS in $CCR2^{-/-}$ but not in CD1 mice. A potent vasoconstrictor, this may help to explain the significant increase in MAP observed in $CCR2^{-/-}$ 5 hours post-LPS. There is evidence to support an interplay between ET-1 and CCL2/CCR2 signalling, as CCL2 can be synthesised in the endothelium, cardiac myocytes and renal cells in response to haemodynamic (shear stress and blood flow) and hormonal stimuli (angiotensin II and ET-1) [400]. In blood vessels chemokines also play a role in the control of inflammation in blood vessel walls where infiltrating inflammatory cells and oxidative stress at the vascular wall can cause hypertension [400, 412]. Oxidative stress triggers signalling cascades that result in increased wall rigidity and narrowing of the vessel lumen [404]; however this mechanism has been contested by Kvist *et al*., who showed that in a model of renal artery stenosis induced-hypertension, removal of the stenosis resulted in alleviated hypertension but resistance vessel morphology regressed either slowly or not at all [413].

In this mouse model, we supposed that a lack of CCL2/CCR2 signalling caused decreased monocyte and neutrophil recruitment to off-target sites and thus prevented excessive macrophage infiltration and subsequent release of NO and other pro-inflammatory cytokines. This explanation could account for the decrease in circulating TNF-α and NO concentrations seen in pregnant $CCR2^{-/-}$ mice after LPS challenge. In turn, the reduction in NO could account for the failure of LPS to elicit hypotension in these animals. It is likely that the reduced TNF-α levels could also contribute to this effect as TNF is known to induce vasodilation and a loss of vascular permeability [414].

Previous work has demonstrated that a lack of functional CCR2 receptors may be associated with the emergence of hypertension in humans [415, 416]. However, other studies showed that CCR2 blockade in a L-NAME induced model of hypertension in rats caused a reduction in blood pressure by the inhibition of TNF-α and NF-κB [417]. Taken together with the findings presented here, these data suggest that an attenuation of the excessive pro-inflammatory cytokines can ameliorate subsequent effects on blood pressure.

At both 6 and 12 hours post-LPS, TNF-α was reduced in the serum of CCR2$^{-/-}$ mice. Likewise, there was also an absence of LPS-induced TNF-α mRNA upregulation in CCR2$^{-/-}$ left ventricle. In mice, CCR2 is expressed in immature DCs [392]. Peters *et al*., demonstrated that trafficking of these cells, as well as other antigen presenting cells (APCs) is impaired in CCR2 deficient mice [418]. This mechanism has been shown to be responsible for diminished INF-γ production and could provide an explanation for decreased TNF-α production, possibly from DCs or macrophages, in pregnant CCR2$^{-/-}$ mice after LPS exposure.

Furthermore, CCR2 has been shown to regulate TNF-α/iNOS producing dendritic cell (tipDC) emigration into the circulation from bone marrow [419] where CCR2 deficiency prevented tipDC trafficking, although this was not seen to correlate with decreased morbidity or mortality after influenza virus challenge [420]. This mechanism may also contribute to decreased levels of TNF-α and NO measured in the circulation of pregnant CCR2$^{-/-}$ mice after LPS.

Alongside decreases in TNF-α, the significant increases in circulating IL-4 (at 12 hours post-LPS) and IL-10 (at 6 and 12 hours post-LPS) suggest that in these pregnant CCR2$^{-/-}$ mice there is a modulated inflammatory response, where the balance between pro- and anti-inflammatory cytokine release is dysregulated. Alternatively, another explanation could be that in these mice there is an impaired adaptive immune response that is characteristic of dominating Th2 responses, although by 12 hours it may be too early to truly determine the involvement of the adaptive immune response. However, aside from the role of CCL2/CCR2 signalling in innate immune responses, there are several lines of evidence that CCR2 has been shown to be involved in regulating Th1- and Th2-type immunity [167, 421]. *In vitro*, CCL2 expression has been shown to enhance secretion of IL-4 by naïve T cells as well as Th2-differentiated cells [422]. However *in vivo,* mice lacking CCR2 are more susceptible to infection from pathogens including *Leishmania major* and *Listeria monocytogenes* at least in part due to impaired adaptive immune responses by way of an early development of Th2 responses demonstrated by high IL-4 levels [419, 423]. Taken together with the CCR2-dependency of tipDCs,

these results support the concept that increases in IL-4 and Th2 cytokines are in part caused by the paucity of DC migration [423-425].

It should be taken into consideration that the majority of published data discussed here were collected from studies using non-pregnant animals. As it has been established that the immune response is already altered in pregnancy, it cannot be disregarded that the actions of systemic CCL2/CCR2 signalling in pregnancy are also altered. However, our earlier finding that systemic CCL2 levels were not altered in pregnancy compared to levels in NP mice (see Chapter 4), would suggest that the effects of CCL2 deletion on the response to LPS are not likely to be specific to pregnancy.

When the CCR2 antagonist RS504393 was administered, the haemodynamic response to LPS reflected what had been observed in the knockout mouse, where LPS-induced hypotension was ameliorated. After AUC analyses, MAP and SAP were seen to be significantly increased compared to vehicle-treated mice, however no hypertension was observed and MAP remained at levels close to pre-LPS baseline. These data suggest that although CCR2 inhibition was achieved, it may have been only partial antagonism. This could be due to greater doses needing to be administered during pregnancy secondary to altered drug metabolism and/or haemodilution, or that a dose regimen should have been begun at an earlier time point to achieve maximum drug efficacy. The effects on the inflammatory response would need to be studied in greater detail to allow for further comparisons to be made to the genetic deletion of CCR2. What this study demonstrates, however, is that the compensatory mechanisms and promiscuity of the chemokine pathways are not able to surmount the effects of genetic manipulation of CCR2 in this model.

Chapter 7: The Effect of Dimethylarginine Dimethylaminohydrolase-1 Deficiency in Pregnancy

7.1 Introduction

Currently, methods of targeting NO include the manipulation of NO regulators, including the NO synthase enzymes and the DDAH enzymes which hydrolyse ADMA. To try and explore the role of NO in LPS-induced hypotension in pregnancy, we employed a mouse model of DDAH1 deficiency.

Studies that employed genetic eNOS deficiency to investigate the effects of altered NO levels demonstrated that the eNOS knockout mouse ($eNOS^{-/-}$) had significantly elevated MAP [426-428]. Investigations into the role of eNOS in blood pressure regulation in pregnancy showed that elevated blood pressure persisted throughout pregnancy in $eNOS^{-/-}$ mice [429], and continuing from this Kusinski *et al*., demonstrated that in $eNOS^{-/-}$ mice, pregnancy resulted in fetal growth restriction (FGR) which was associated with impaired uterine artery function (greater vasoconstriction and impaired vasodilatory capacity) that consequently led to placental hypoxia [428]. However, contrary to these findings, Shesely *et al*., had investigated the haemodynamic profile of $nNOS^{-/-}$, $eNOS^{-/-}$, and $iNOS^{-/-}$ mice throughout gestation and found that pregnancy did not increase blood pressure in any of the three strains of NOS deficiency [430]. Despite that $eNOS^{-/-}$ mice were hypertensive before pregnancy, blood pressure reverted to be no different from control during pregnancy.

Work that examined the role of eNOS in blood pressure regulation in sepsis and inflammation showed that in a endotoxaemic model of sepsis, $eNOS^{-/-}$ mice were resistant to LPS-induced hypotension and the authors comment that mortality was markedly reduced [427]. Further to this, Connelly *et al*., saw that LPS administration led to a time-dependent increase in the expression of iNOS in multiple organs, but in $eNOS^{-/-}$ mice there were significantly lower levels of iNOS protein expression. This led the authors to conclude that eNOS derived NO plays a crucial role in facilitating iNOS expression in LPS-induced endotoxaemia [427].

NO inhibition has also been studied by pharmacological inhibition using exogenous L-NMMA or L-NAME, inhibitors that target all three NOS isoforms. Several studies have shown that in rodent models, L-NMMA and L-NAME were able to significantly elevate blood pressure [431-434]

although, Pullamsetti *et al*., suggested that selective iNOS inhibitors were superior to non-specific NOS inhibitors for the treatment of both macro- and microcirculatory abnormalities in septic shock [433].

These data along with the results from genetically targeted NOS depletion suggested that NOS inhibition could be beneficial in treating septic shock, but several clinical trials proved unsuccessful with the intervention groups showing at best no significant improvement and at worst increased mortality [181, 435, 436]. Therefore an alternative approach in the modulation of NO production is to target DDAH. Inhibition of DDAH increases the endogenous NOS inhibitor ADMA [437]. Furthermore, as DDAH isoforms are tissue-specific [97], this would enable a more controlled approach to NOS inhibition, rather than the global effect achieved by exogenous administration of L-NMMA.

Pharmacological DDAH1 inhibition using the DDAH1 selective compound L-257 has been shown to inhibit LPS-stimulated NO production in aorta but not in macrophages [437]. Additionally, L-257 and genetic alteration of DDAH1 by way of a DDAH1 heterozygous mouse ($DDAH1^{+/-}$) led to an increase in endogenous ADMA. Consequently, the haemodynamic changes that occurred in response to LPS were attenuated, namely there was a significant improvement in the minimum systolic and diastolic blood pressure recorded in the 40 hour period after LPS administration [437]. These data are supported by evidence showing that by using gene silencing techniques, disruption of DDAH1 but not DDAH2 induced an increase in ADMA levels [98, 438].

Therefore to study the effects of NO modulation in the response to LPS in pregnancy, and with pharmacokinetic/pharmacodynamic data lacking for L-257 in pregnancy, the DDAH1 knockout mouse was used. Initial attempts to generate a global $DDAH1^{-/-}$ mouse through the replacement of exon 1 with a neomycin cassette through homologous recombination were unsuccessful and proved to be embryonic lethal [249, 439]. However more recently, Hu *et al*., were able to generate a global $DDAH1^{-/-}$ mouse through deletion of DDAH1 in the sperm of male double heterozygote protamine-

cre/DDAH1$^{flox/+}$ mice to produce homozygous knockout offspring. Further generations could then be produced via inbreeding of the heterozygotes [440]. Genomic DNA PCR analysis showed that exon 4 of the DDAH1 gene was deleted in these mice. In this study, a new global knockout mouse was generated in the Leiper laboratory (MRC CSC, Imperial College) where deletion of DDAH1 exon 1 was driven by actin cre, using the cre/lox P system.

7.1.1 Aims and Objectives

As there have been no studies published that have examined haemodynamic data in female DDAH1$^{-/-}$ mice, it was important to firstly assess whether there were any basal non-pregnant differences to their male counterparts. Secondly, as the DDAH1$^{-/-}$ mice were on a different background to previous telemetry experiments undertaken throughout pregnancy in CD1 mice, it was imperative to examine both the haemodynamic profile of DDAH1 WT (C57BL/6) and DDAH1$^{-/-}$ mice throughout pregnancy and to investigate the cardiovascular changes and adaptations in DDAH1$^{-/-}$ mice compared to WT controls throughout pregnancy, labour and the post-partum period. Continuing from this, we aimed to examine the effects of LPS-induced inflammation in pregnant DDAH1$^{-/-}$ mice on haemodynamic function and NO modulation.

7.2 Results

7.2.1 The Haemodynamic Profile of Non-Pregnant DDAH1 Knockout Mice

To determine if there were any basal haemodynamic differences between DDAH1 WT and DDAH1$^{-/-}$ females mice, non-pregnant recordings were taken before timed-mating. MAP was significantly elevated from 108.6 ± 0.98 mmHg in DDAH1 WT mice to 116 ± 2.8 mmHg in DDAH1$^{-/-}$ ($p<0.05$; Figure 7.1A) over 24 hours. SAP was significantly elevated from 120.8 ± 1.6 mmHg in DDAH1 WT mice to 131.1 ± 2.38 mmHg in DDAH1$^{-/-}$ ($p<0.01$; Figure 7.1B). DAP was more subtly elevated from 96.18 ± 1.3 mmHg to 100.5 ± 3.4 mmHg in DDAH1$^{-/-}$ mice, but this was not significant (Figure 7.1C). Additionally DDAH1$^{-/-}$ mice had a significantly elevated basal heart rate ($p<0.05$; Figure 7.1D) which increased to 605.5 ± 9.79 bpm from 562.1 ± 20.36 bpm in DDAH1 WT mice. There were no differences observed between DDAH1 WT and DDAH$^{-/-}$ activity levels including the %TSI or intensity of activity (Figure 7.1E, 7.1F, 7.1G).

7.2.2 The Haemodynamic Profile of Pregnancy in DDAH1 Knockout Mice

In DDAH1 WT mice, the trend in MAP throughout pregnancy can be described as a decrease in pressure from E0 to E9 before returning to baseline by E13, followed by a subsequent decrease in pressure at E15 which returned to baseline by E18 (labour) which was followed by a final fall in the post-partum period (Figure 7.2A). The trend observed however, was highly variable with large SEM and the ΔMAP values may be skewed by a marked increase in MAP from baseline to E0 (Figure 7.2B). The nadir in MAP of Δ-5.2 ± 9.5 mmHg at the mid-gestational point (E9) was not significantly reduced from baseline in these mice, which is in contrast to our previous findings in CD1 mice. The increase in MAP at E0 could be explained by heightened stress due to the animal cage being moved from the holding room to the recording room following evidence of a copulatory plug. This was also seen in CD1 mice, although the increase was not as marked.

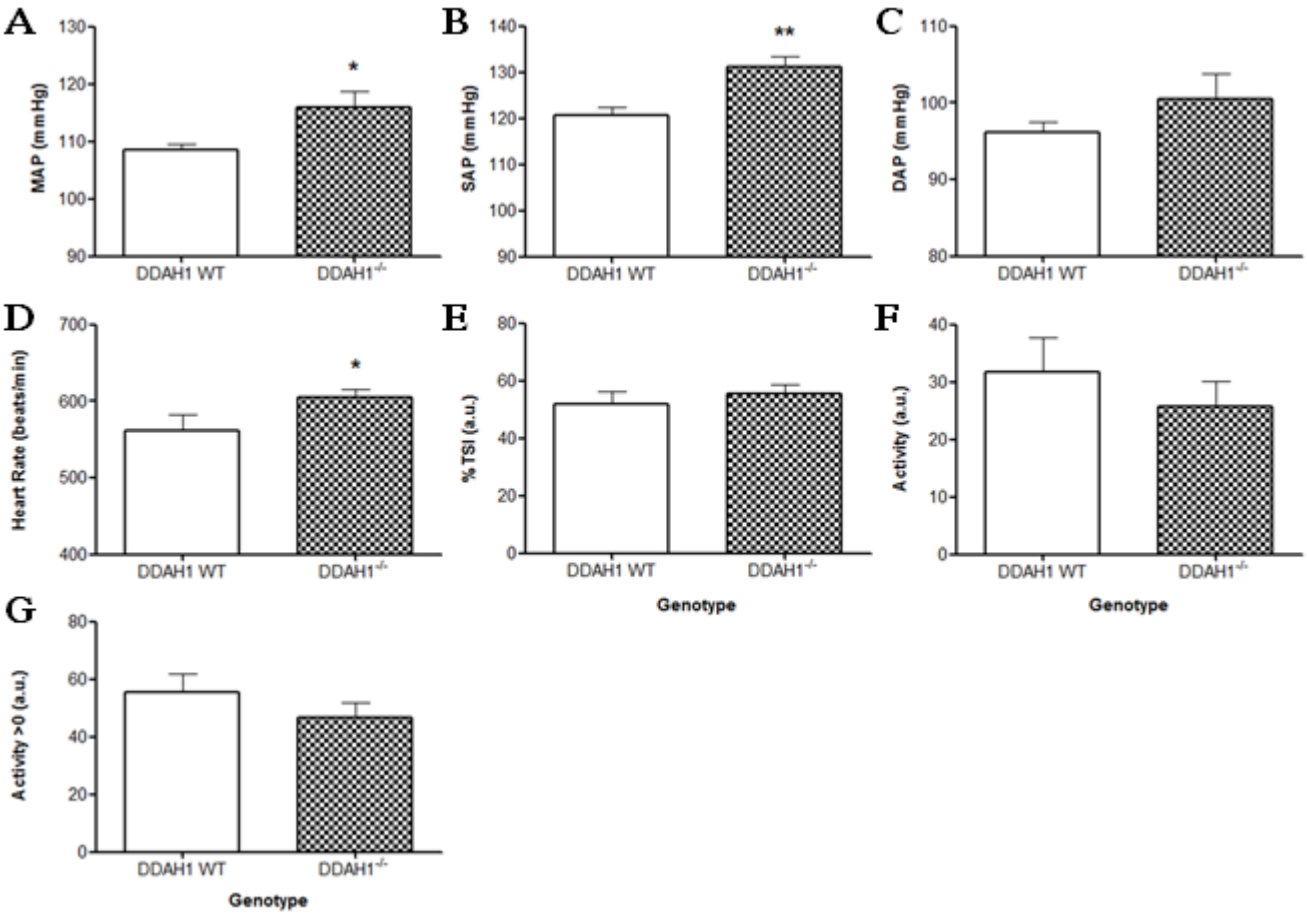


Figure 7.1: The haemodynamic and activity profile of non-pregnant female DDAH1 WT and DDAH1$^{-/-}$ mice. Haemodynamic and activity parameters were recorded for 24 hours (prior to mating) in female virgin DDAH1 WT and DDAH1$^{-/-}$ mice. (A) MAP (B) SAP (C) DAP (D) HR (E) %TSI (F) Activity (G) Activity >0. *p<0.05, **p<0.01 student's t-test or Mann-Whitney U test as appropriate. Data expressed as mean ± SEM (DDAH1 WT, n=9; DDAH1$^{-/-}$, n=11).

In DDAH1$^{-/-}$ mice, the trend in MAP throughout pregnancy was not significantly different to WT (Figure 7.2). Aside from increased MAP at baseline, there are two main observations that are of note. Firstly, there is a subtle increase in MAP in DDAH1$^{-/-}$ mice over the period between E3 and E8 where MAP is elevated. At its peak (E5), MAP was 115.14 ± 4.9 mmHg in DDAH1$^{-/-}$ compared to 106.9 ± 6.49 mmHg in DDAH1 WT. This elevation could be considered to be a conservation of baseline high blood pressure, as the ΔMAP did not elevate significantly above baseline. Secondly, MAP fell slightly further towards the end of gestation to a nadir at E14 of 99.83 ± 5.9 mmHg in DDAH1$^{-/-}$ compared to 105.6 ± 7 mmHg in DDAH1 WT mice, but interestingly this was followed by a discernible increase in MAP after labour (115.96 ± 4 mmHg on 1DPP, Δ14.2 mmHg from E18).

Similar trends were observed in SAP and DAP, where again there were no significant statistical differences between DDAH1 WT and DDAH1$^{-/-}$ mice (Figure 7.3, 7.4). The trend in SAP between E3 and E8 was more pronounced than DAP, which may indicate that the MAP on these days is a reflection of SAP. However, this is not true for the post-partum rise in pressure.

There were no significant differences in HR between DDAH1 WT and DDAH1$^{-/-}$ mice over the course of gestation. HR in DDAH1$^{-/-}$ mice remained higher than in WTs, (Figure 7.5A) but this was not as pronounced as in the non-pregnant state until the post-partum period. Therefore during pregnancy, DDAH1 WT and DDAH1$^{-/-}$ mice followed a similar trend. Interestingly, there was a peak in HR at approximately E7 in both genotypes (Δ61.15 ± 35.42 bpm and Δ71.8 ± 9.2 bpm in DDAH1 WT and DDAH1$^{-/-}$ respectively) rising from E5 and returning to baseline on E9-10 (Figure 7.5B). This trend was not observed in CD1 mice, although this could be considered reflective of the normal increase in cardiac output in early pregnancy that resolves upon placental development.

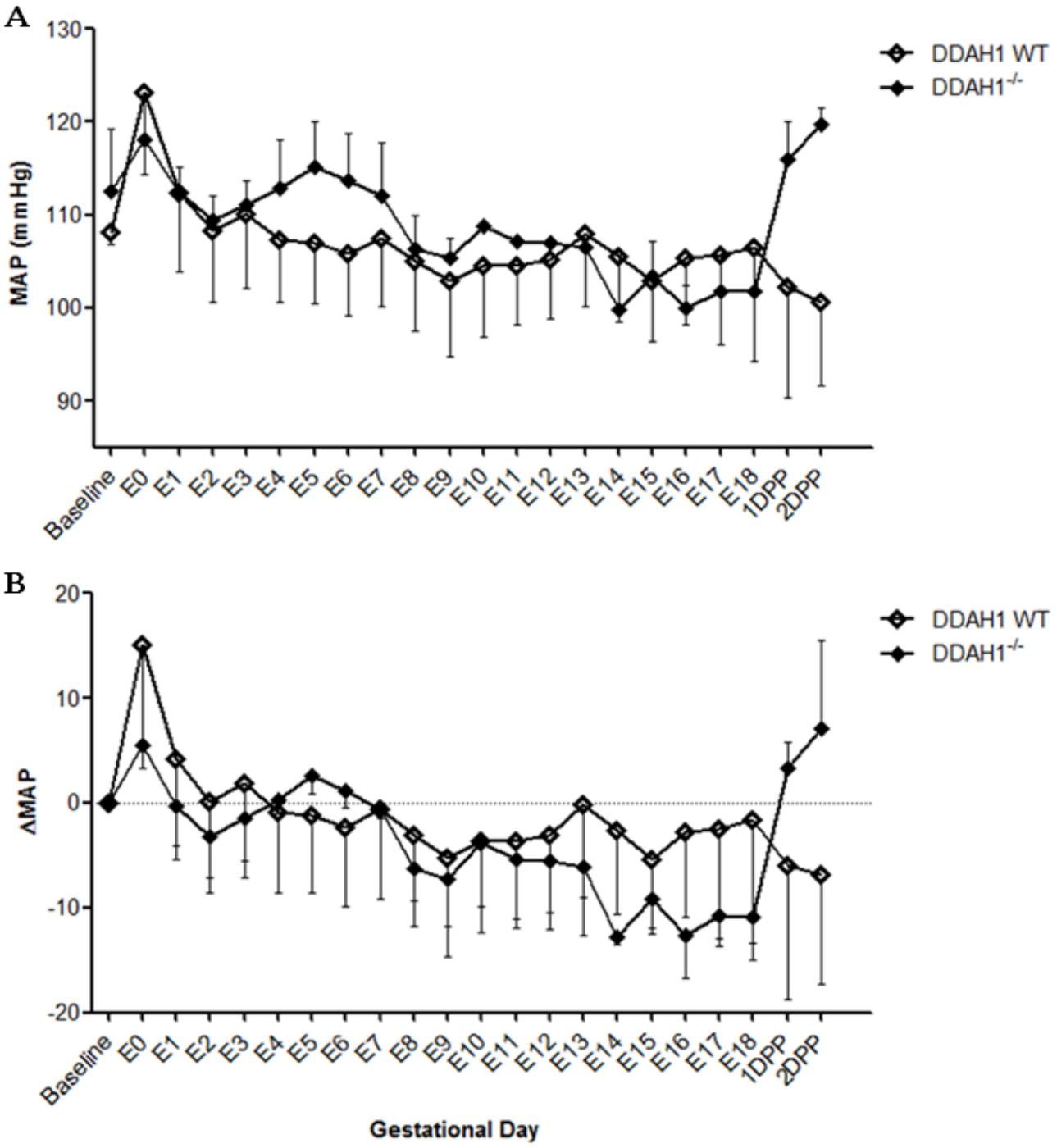


Figure 7.2: **Continuous measurement of mean arterial pressure (MAP) throughout pregnancy in DDAH1 WT and DDAH1$^{-/-}$ mice.** (A) MAP in DDAH1 WT and DDAH1$^{-/-}$ mice whilst not pregnant (Baseline), throughout gestation, and for 2 days post-partum (1DPP-2DPP) data shown as 24-hour mean average ± SEM (n=2-4) (B) ΔMAP from baseline in DDAH1 WT and DDAH1$^{-/-}$ mice. Data shown as 24-hour mean average ± SEM (DDAH1 WT, n=4; DDAH1$^{-/-}$, n=4).

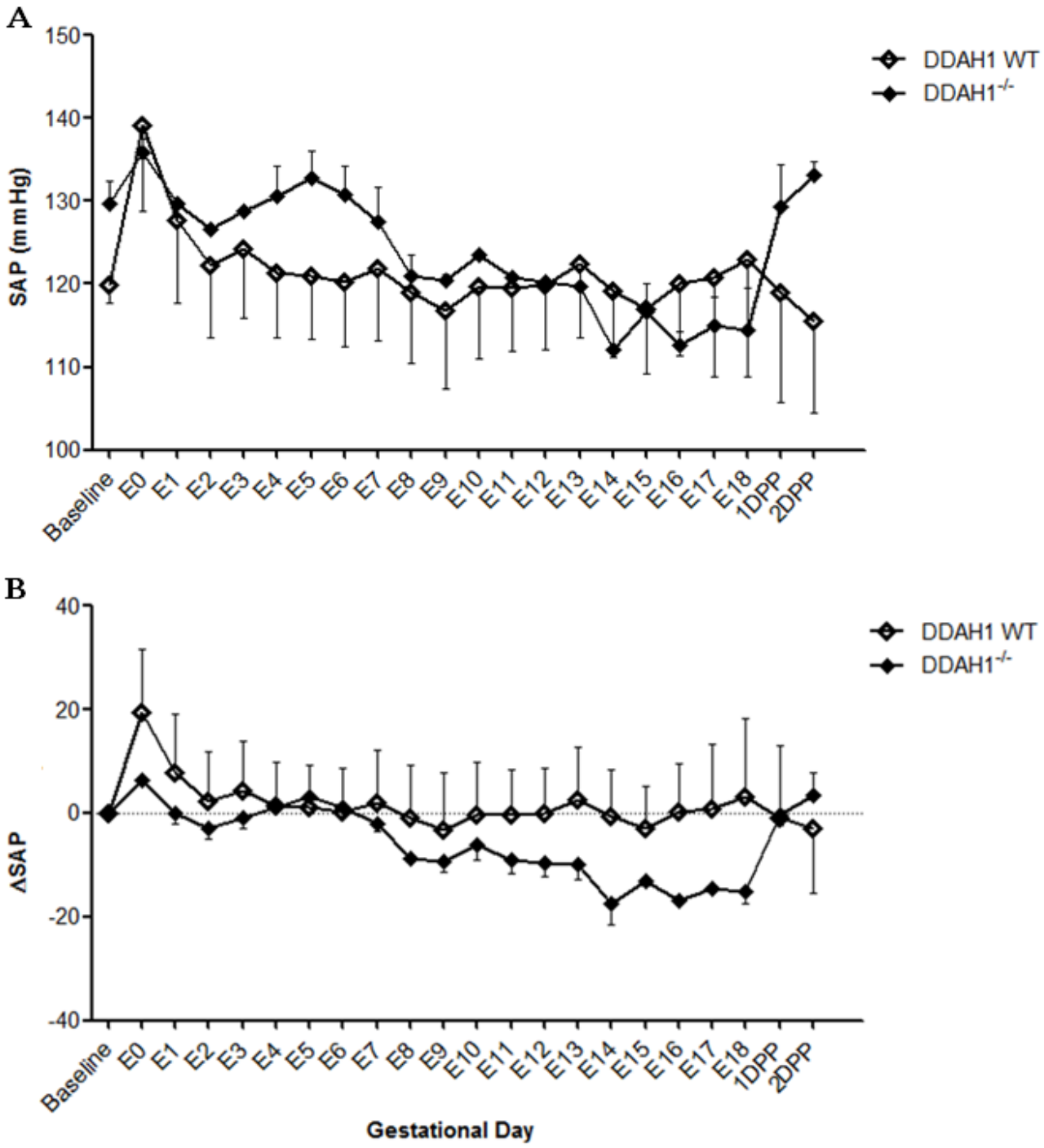


Figure 7.3: Continuous measurement of systolic arterial pressure (SAP) throughout pregnancy in DDAH1 WT and DDAH1$^{-/-}$ mice. (A) SAP in DDAH1 WT and DDAH1$^{-/-}$ mice whilst not pregnant (Baseline), throughout gestation, and for 2 days post-partum (1DPP-2DPP) data shown as 24-hour mean average ± SEM (n=2-4) (B) ΔSAP from baseline in DDAH1 WT and DDAH1$^{-/-}$ mice. Data shown as 24-hour mean average ± SEM (DDAH1 WT, n=4; DDAH1$^{-/-}$, n=4).

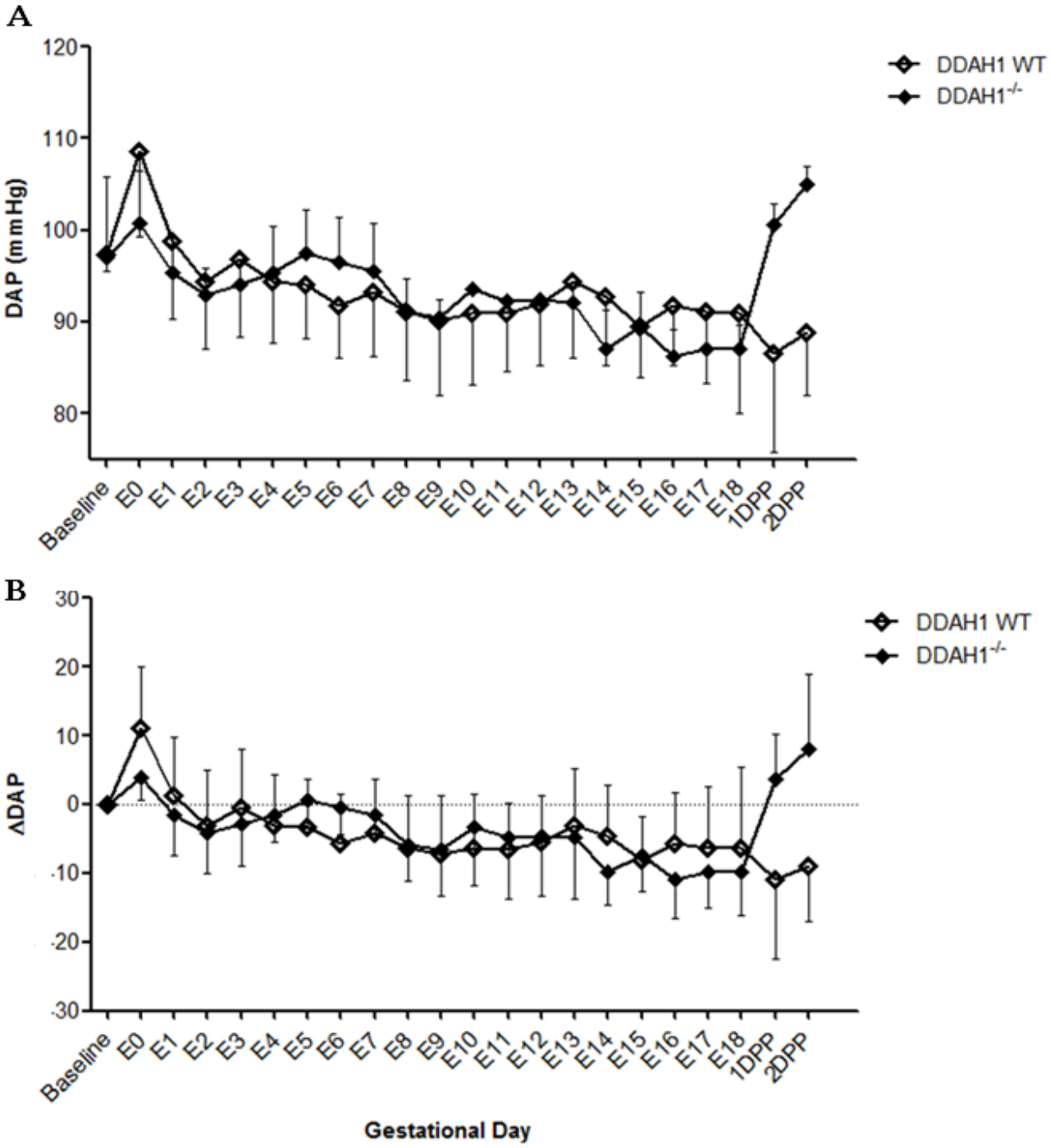


Figure 7.4: Continuous measurement of diastolic arterial pressure (DAP) throughout pregnancy in DDAH1 WT and DDAH$^{-/-}$ mice. (A) DAP in DDAH1 WT and DDAH1$^{-/-}$ mice whilst not pregnant (Baseline), throughout gestation, and for 2 days post-partum (1DPP-2DPP) data shown as 24-hour mean average ± SEM (n=2-4) (B) ΔDAP from baseline in DDAH1 WT and DDAH1$^{-/-}$ mice. Data shown as 24-hour mean average ± SEM (DDAH1 WT, n=4; DDAH1$^{-/-}$, n=4).

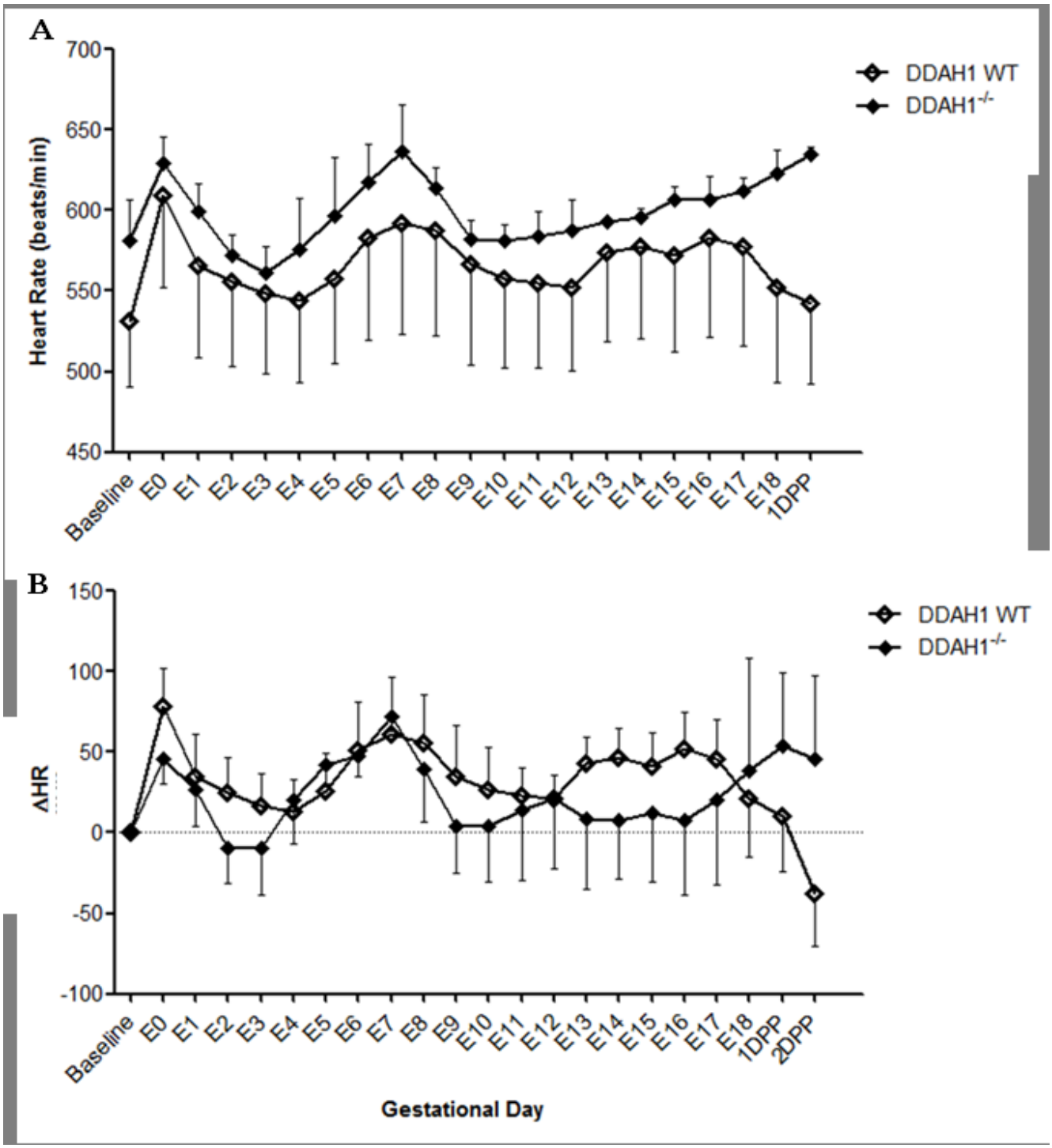


Figure 7.5: Continuous measurement of heart rate (HR) throughout pregnancy in DDAH1 WT and DDAH1$^{-/-}$ mice. (A) HR in DDAH1 WT and DDAH1$^{-/-}$ mice whilst not pregnant (Baseline), throughout gestation, and for 2 days post-partum (1DPP-2DPP) data shown as 24-hour mean average ± SEM (n=2-4) (B) ΔHR from baseline in DDAH1 WT and DDAH1$^{-/-}$ mice. Data shown as 24-hour mean average ± SEM (DDAH1 WT, n=4; DDAH1$^{-/-}$, n=4).

7.2.3 Activity during Pregnancy in CD1 Mice

There were no significant differences between the activity levels of DDAH1 WT and DDAH1$^{-/-}$mice. There was a very similar pattern in %TSI throughout gestation between both DDAH1 WT and DDAH1$^{-/-}$ (and CD1 behaviour as documented previously), where the %TSI gradually increased towards the time of labour (Figure 7.6). In the post-partum period %TSI decreased, likely due to weaning behaviours and reduced size of the mother. %TSI correlated with a decrease in activity and in the intensity of activity (activity>0; Figure 7.7, 7.8). The activity of DDAH1 WT mice was seen to be greater at baseline than DDAH1$^{-/-}$ mice, although not significantly so. This may explain why the ΔActivity in DDAH1 WT was seen to be decreased (Figure 7.7B).

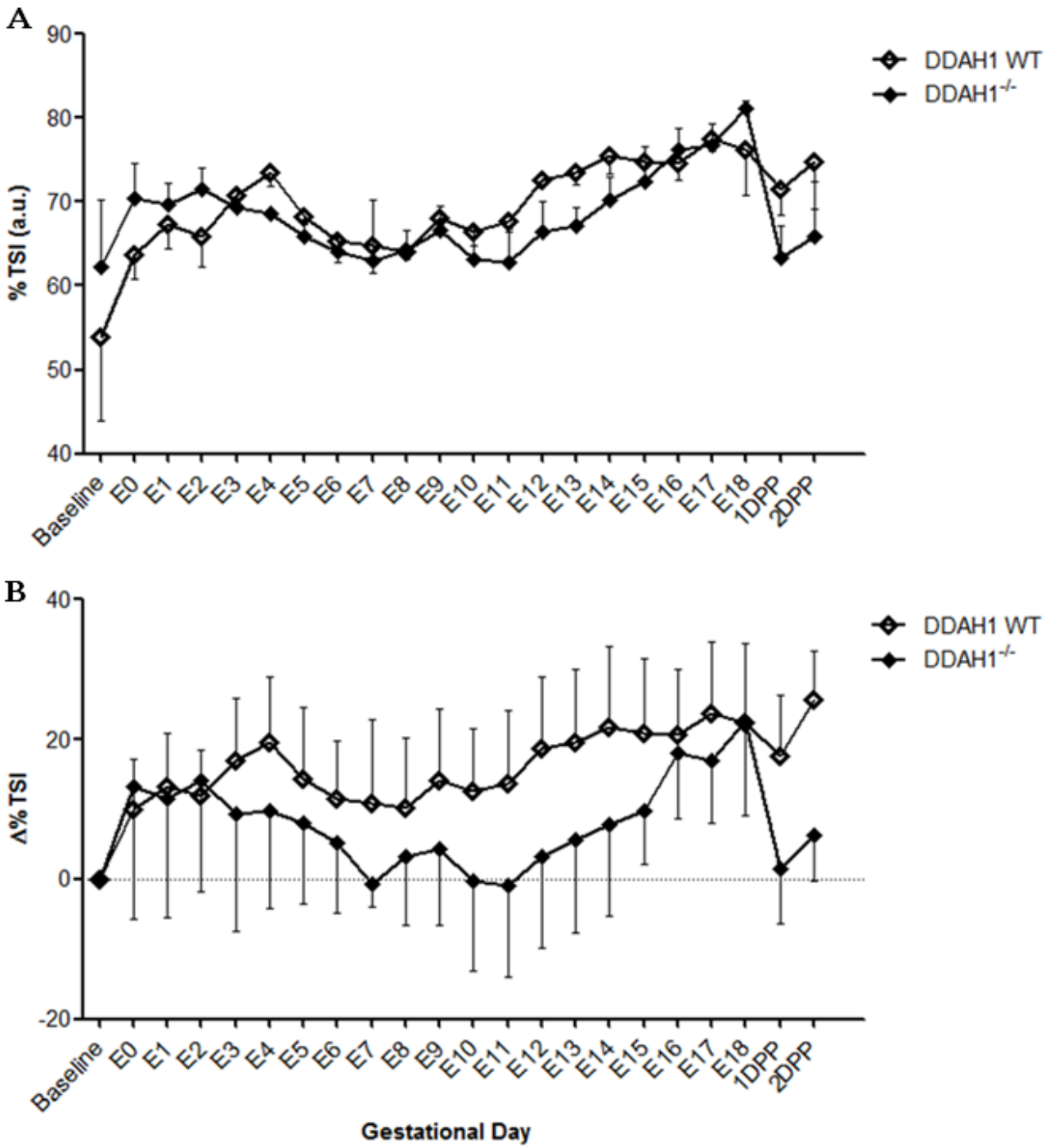


Figure 7.6: Continuous measurement of the percentage of time spent inactive (%TSI) throughout pregnancy in DDAH1 WT and DDAH1$^{-/-}$ mice. (A) %TSI in DDAH1 WT and DDAH1$^{-/-}$ mice whilst not pregnant (Baseline), throughout gestation, and for 2 days post-partum (1DPP-2DPP) data shown as 24-hour mean average ± SEM (n=2-4) (B) Δ%TSI from baseline in DDAH1 WT and DDAH1$^{-/-}$ mice. Data shown as 24-hour mean average ± SEM (DDAH1 WT, n=4; DDAH1$^{-/-}$, n=4).

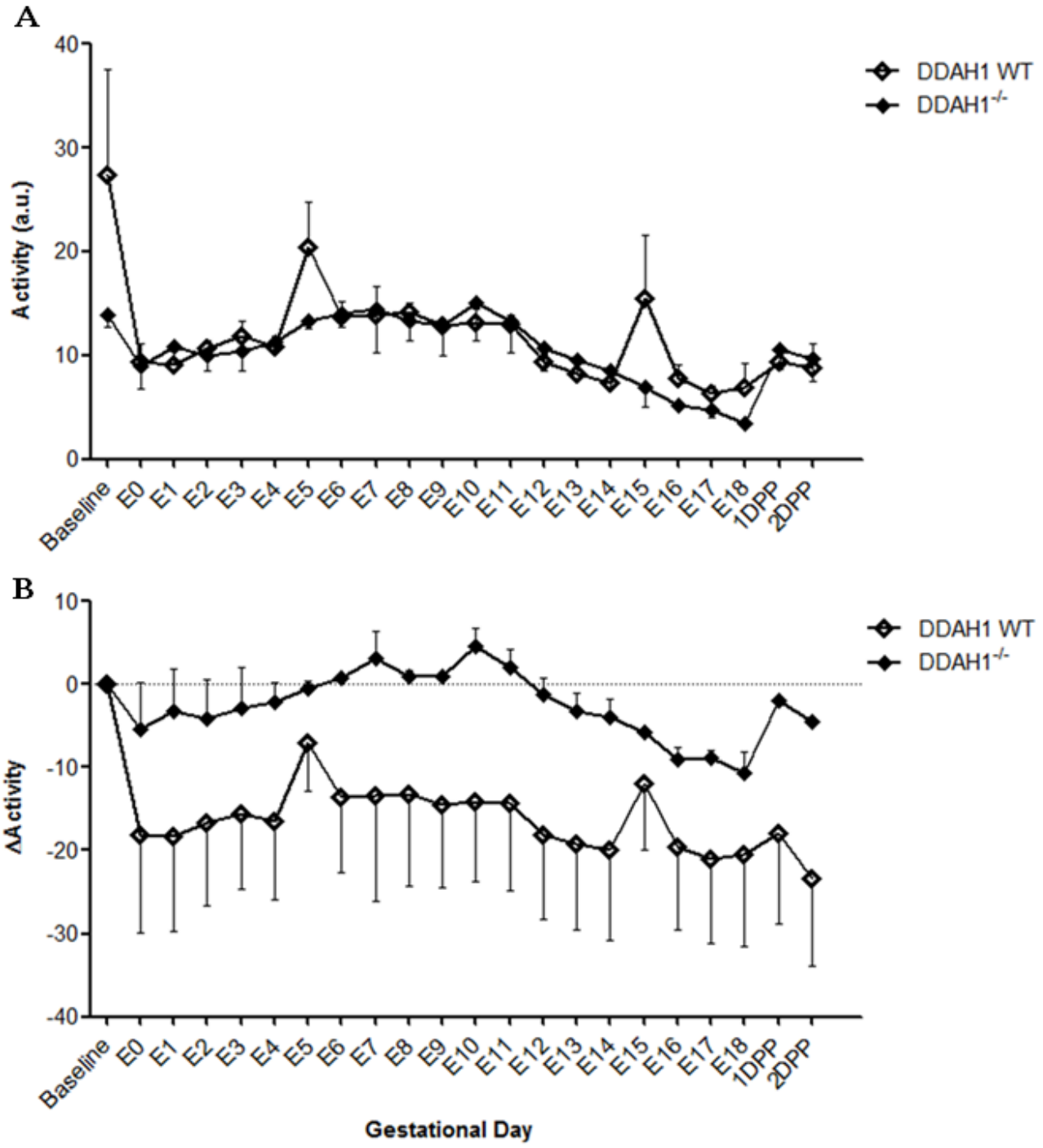


Figure 7.7: Continuous measurement of activity throughout pregnancy in DDAH1 WT and DDAH1$^{-/-}$ mice. (A) Activity in DDAH1 WT and DDAH1$^{-/-}$ mice whilst not pregnant (Baseline), throughout gestation, and for 2 days post-partum (1DPP-2DPP) data shown as 24-hour mean average ± SEM (n=2-4) (B) ΔActivity from baseline in DDAH1 WT and DDAH1$^{-/-}$ mice. Data shown as 24-hour mean average ± SEM (DDAH1 WT, n=4; DDAH1$^{-/-}$, n=4).

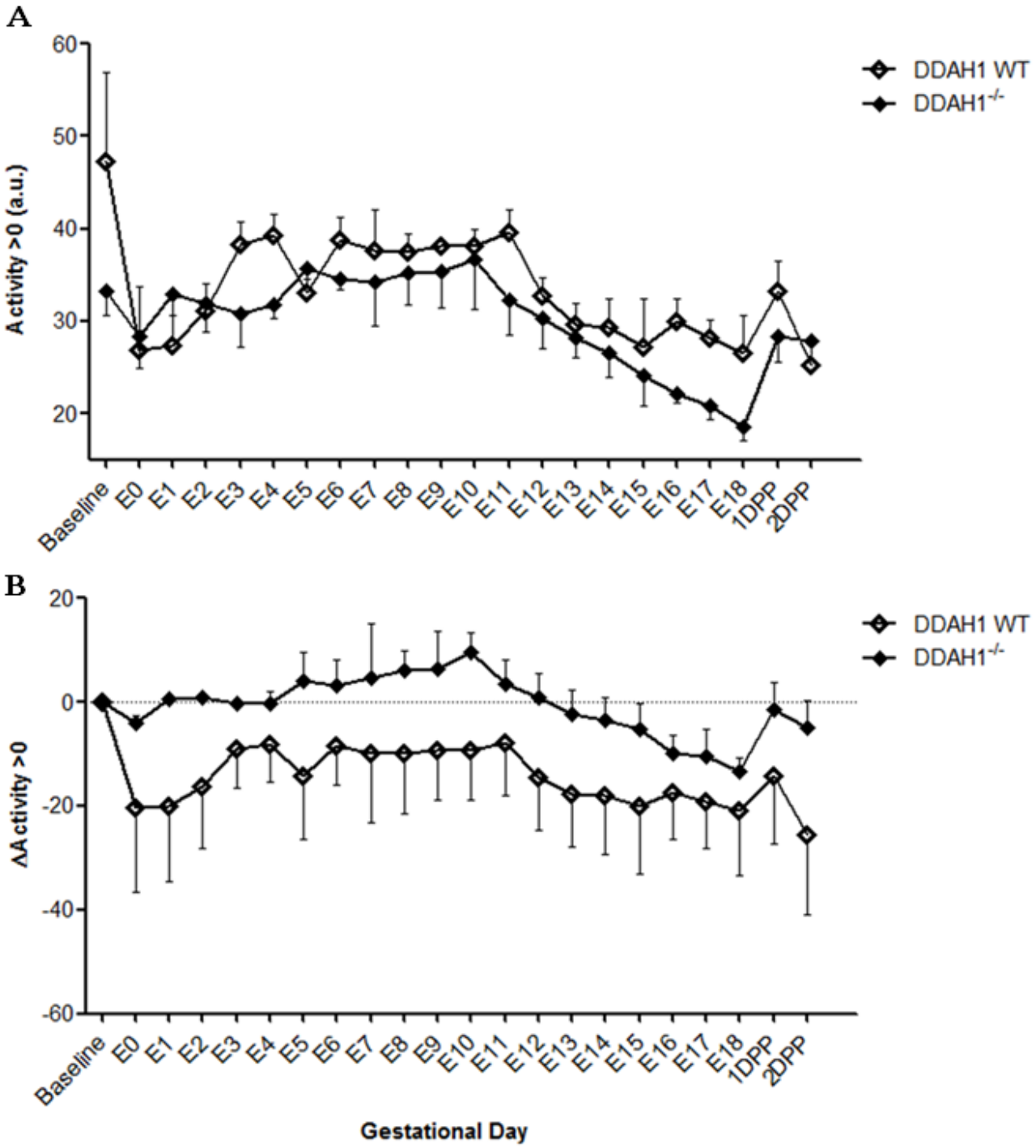


Figure 7.8: Continuous measurement of activity >0 throughout pregnancy in DDAH1 WT and DDAH1$^{-/-}$ mice. (A) Activity >0 in DDAH1 WT and DDAH1$^{-/-}$ mice whilst not pregnant (Baseline), throughout gestation, and for 2 days post-partum (1DPP-2DPP) data shown as 24-hour mean average ± SEM (n=2-4) (B) ΔActivity>0 from baseline in DDAH1 WT and DDAH1$^{-/-}$ mice. Data shown as 24-hour mean average ± SEM (DDAH1 WT, n=4; DDAH1$^{-/-}$, n=4).

7.2.4 Latency to Labour and Pup Survival Outcomes after LPS administration in DDAH1 Knockout Mice

After i.p. PBS on E16, DDAH1 WT and DDAH1$^{-/-}$ mice laboured at term, at 58.6 ± 12.26 hours and 55.4 ± 4.61 hours respectively and birthed live litters (Figure 7.9A, 7.9B). 10μg LPS i.p on E16 significantly reduced latency to labour to 22.56 ± 2.5 hours in DDAH1 WT and 21.8 ± 2.12 hours in DDAH1$^{-/-}$ mice ($p<0.001$; Figure 7.9A). There were no significant differences from the effects of LPS between WT and knockout. In contrast to previous findings in CD1 mice, 10μg LPS did not lead to 100% pup death in DDAH1 WT or DDAH1$^{-/-}$ mice, where by the time of labour 10-25% of pups survived for at least 3 days post-partum. This could be accounted for by strain differences as these mice are on an inbred C57BL/6 background. Furthermore, there were no significant differences between pup survival at 6 and 12 hours and at labour between DDAH1 WT and DDAH1$^{-/-}$, although there was a strong trend towards decreasing pup survival over time in both strains. This could be accounted for by high variability.

During the process of timed-mating, it was observed that many of the animals that were plugged and had pregnancy confirmed by palpation on E8, were no longer pregnant on what would have been E15. Upon analysis, only 50% of DDAH1$^{-/-}$ pregnancies resulted in success. Initial thoughts were that as DDAH1 has been previously shown to be important in mammalian development and that DDAH1 null embryos (deletion of DDAH1 exon 1) could be generated at much lower frequency than DDAH2 null (and could not progress through embryonic development), that these DDAH1$^{-/-}$ mice could be resorbing pregnancies at a higher frequency due to developmental defects. However, it was determined that DDAH1 WT mice had equally as many 'failed' pregnancies (Figure 7.10A). Therefore, this phenomenon was likely to be due to inbred strain differences compared to the outbred CD1 strain used in previous experiments.

Subsequently, because of the number of failed pregnancies and the consequent difficulty in timed-mating these strains, the n numbers for the longitudinal study (where haemodynamics throughout gestation were studied) were much lower than those used to determine non-pregnant baseline.

Therefore because of the finite number of instrumented animals, this meant that no haemodynamic data could be collected in mice after LPS injection on E16 and it was not possible to study the haemodynamic response to LPS in DDAH1$^{-/-}$ animals.

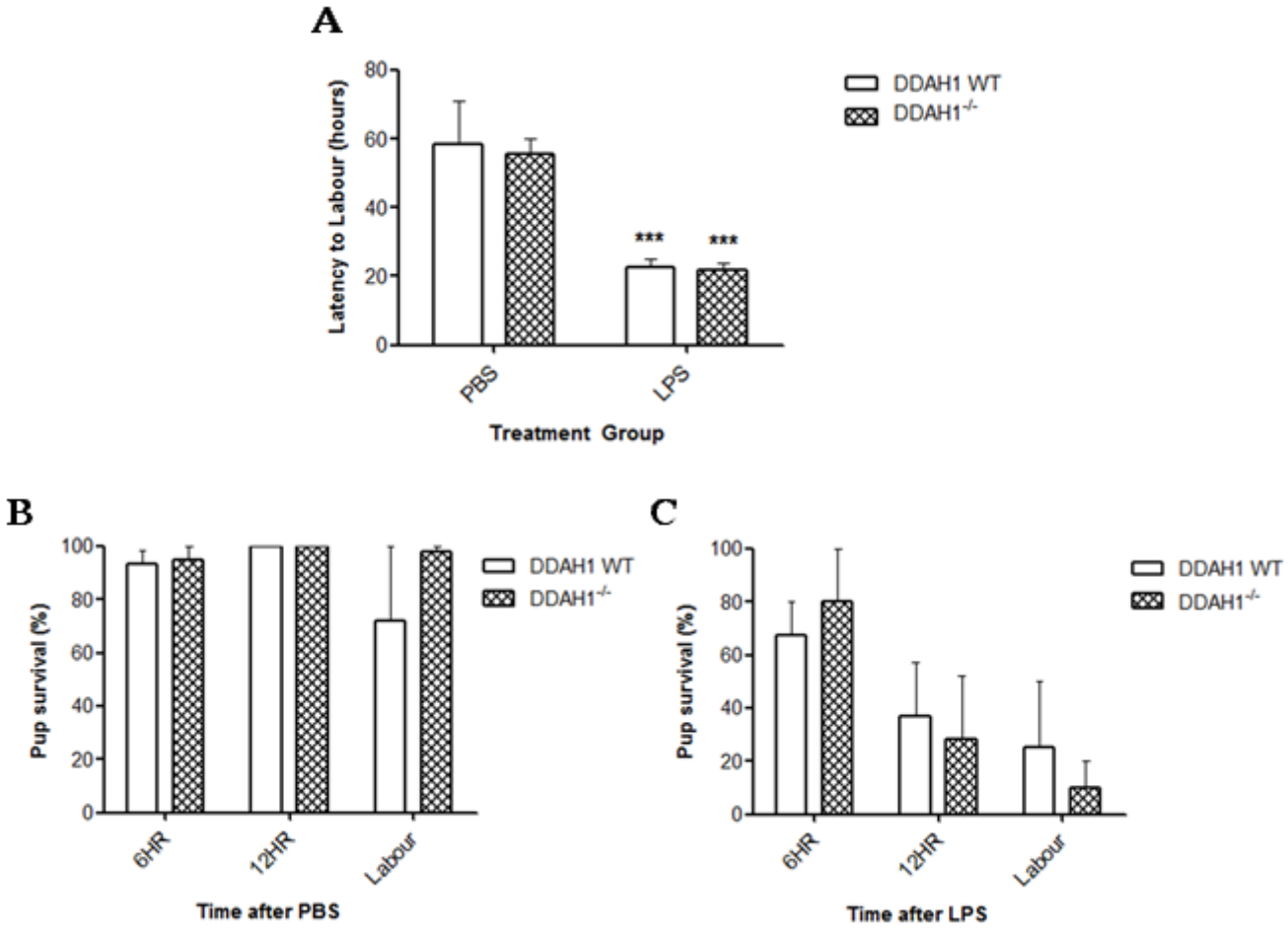


Figure 7.9: Latency to labour and pup survival outcomes after LPS administration in DDAH1 WT and DDAH1$^{-/-}$ mice. Latency to labour (A), pup survival after PBS (vehicle) (B) and pup survival after 10µg LPS administration were observed as outcomes after in DDAH1 WT and DDAH1$^{-/-}$ mice. Latency to labour was assessed in telemetered mice ***P<0.001 compared to PBS control, 2-way ANOVA showing treatment but not genotype was significant. Data expressed as mean ± SEM (PBS groups, n=4; LPS groups, n=5). (B) and (C) Pup survival was noted during tissue collections at 6 and 12 hours post-LPS and at labour in telemetered animals. Data expressed as mean ± SEM (DDAH1 WT 6 HR, 12HR and Labour, n=4; DDAH1$^{-/-}$ 6 HR, 12HR and Labour, n=5).

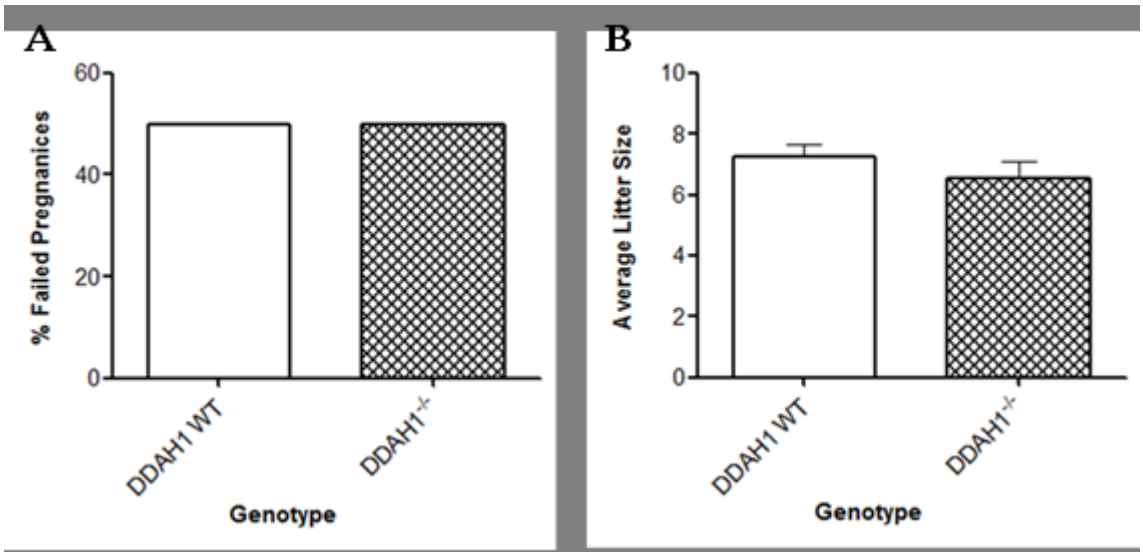


Figure 7.10: The extent of failed pregnancies and average litter sizes in DDAH1 WT and DDAH1$^{-/-}$ mice. (A) Failed pregnancies were counted in DDAH1 WT and DDAH1$^{-/-}$ mice. After plug detection on E0 and confirmation of pregnancy by embryo/placenta palpation on E8, failed pregnancies were then counted if the mouse was no longer gravid on what would be E15. Data are expressed as a percentage of the total pregnancies counted (n=11-13). (B) Litter sizes were recorded from litters born to telemetered animals as well as at the time of tissue collections (6 or 12 hours after PBS/LPS i.p.; DDAH1 WT, n=29; DDAH1$^{-/-}$. n=34).

Further to this, it was noticed that DDAH1$^{-/-}$ litters seemed to be smaller. The numbers of pups in each litter were counted after labour in telemetered animals, and also after opening the abdomen and uterus during 6 and 12 hour time point tissue collections. Whilst there was a slight trend towards smaller litter sizes in the DDAH1$^{-/-}$ mice, this was not found to be significant (Figure 7.10B). The numbers noted (mean litter size of 7.2 ± 0.4 and 6.5 ± 0.5 for DDAH1 WT and DDAH1$^{-/-}$ respectively) were consistent with previous reports in the literature [441, 442] and Jackson Laboratories state that C57BL/6 average litter sizes are typically 6-8.

7.2.5 Circulating Expression of Vasoactive Factors in Response to LPS in Pregnant DDAH1 Knockout Mice

NO and ADMA concentrations in serum from pregnant DDAH1 WT and DDAH1$^{-/-}$ mice 6 and 12 hours after LPS or vehicle control (PBS) were determined using the Seivers nitric oxide analyser and mass spectrometry respectively. Absolute concentrations of vasoactive factors in serum were measured using the Millipore MAGpix multiplex assay system to evaluate the systemic response.

There were no significant differences in circulating NO concentrations on E16 after PBS injections between DDAH1 WT and DDAH1$^{-/-}$ mice (Figure 7.11A). In DDAH1 WT mice, NO concentrations were significantly increased after LPS injection at 6 hours (from 7.39 ± 0.15 μM to 59.6 ±12.22 μM, $p<0.01$) and at 12 hours (from 17.65 ± 3.5 to 107.6 ± 37.72, $p<0.05$). However, whilst LPS increased NO concentration in DDAH1$^{-/-}$ mice this was only significant at 12 hours (from 19.97 ± 2.24 μM to 50.35 ± 8.01 μM after LPS, $p<0.05$).

As there were no differences between circulating NO concentrations in DDAH1 WT and DDAH1$^{-/-}$ on E16 12 hours after LPS, circulating ADMA concentrations were measured (Figure 7.11B). ADMA levels were not changed after LPS administration, but DDAH1$^{-/-}$ mice had significantly higher ADMA concentrations than DDAH1 WT mice at both time points ($p<0.05$). In PBS controls (at 6 hours), ADMA was elevated in DDAH1$^{-/-}$ mice to 119.4 ± 15.06 pmoles compared to 64.75 ± 5.1 pmoles in DDAH1 WT mice. Similar results were seen in LPS-treated mice where in DDAH1$^{-/-}$ ADMA measured 89.65 ± 9.5 pmoles compared to 65.27 ± 4.58 pmoles in DDAH1 WT mice. It therefore appeared that in pregnant DDAH1$^{-/-}$ mice, NO levels were not affected by the increase in ADMA brought about by deletion of DDAH1.

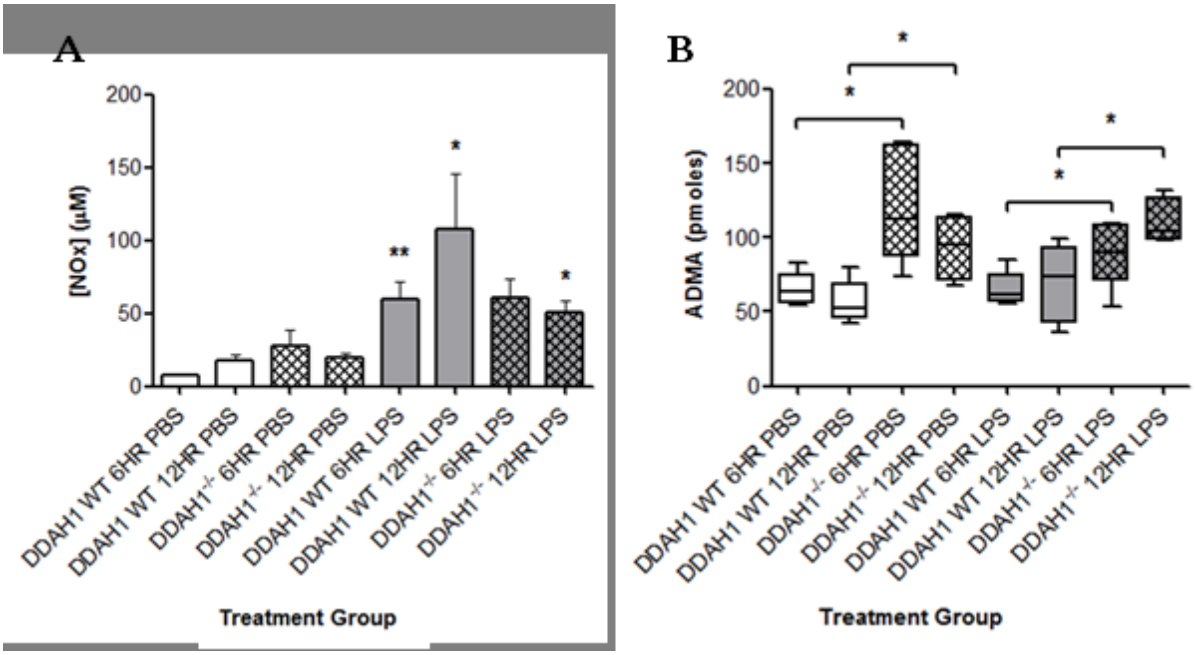


Figure 7.11: Circulating concentrations of nitric oxide and asymmetric dimethylarginine in the serum of pregnant DDAH1 WT and DDAH1$^{-/-}$ mice treated with LPS or vehicle. Measurements were made in serum samples taken 6 or 12 hours after LPS or vehicle in DDAH1 WT and DDAH1$^{-/-}$ mice. (A) Concentration of total nitrates and nitrites (NOx) as measured by nitric oxide analyser (B) ADMA as measured by mass spectrometry. *p<0.05, **p<0.01, compared to PBS control unless otherwise indicated, pairwise t-test comparisons or Mann Whitney U tests were used where appropriate. Data shown as mean ± SEM, or as median ± interquartile range showing minimum and maximum (DDAH1 WT 6HR PBS, n=4; DDAH1 WT 12HR PBS, n=6; DDAH1$^{-/-}$ 6HR PBS, n=6; DDAH1$^{-/-}$ 12HR PBS, n=5; DDAH1 WT 6HR LPS, n=8; DDAH1 WT 12HR LPS, n=6; DDAH1$^{-/-}$ 6HR LPS, n=5; DDAH1$^{-/-}$ 12HR LPS, n=4).

VEGF was not altered by DDAH1 deficiency or the administration of LPS in these animals (Figure 7.12A). The isoform VEGF-D was not altered by DDAH1 deficiency; however compared to PBS control VEGF-D was both reduced at 6 hours post-LPS and increased 12 hours post-LPS in DDAH1 WT mice (p<0.05; Figure 7.12B). There was no change in VEGF-D after LPS administration in DDAH1$^{-/-}$ mice. PLGF2 was significantly increased after LPS (p<0.01), but only at 12 hours post-LPS in DDAH1 WT and DDAH1$^{-/-}$ mice (Figure 7.12C). PLGF2 levels were elevated to 83.05 ± 25.01 pg/mL and 98.39 ± 36.17 pg/mL in DDAH1 WT and DDAH1$^{-/-}$ respectively from 12 hours post-PBS controls which were measured to be 5.94 ± 2.02 and 6.77 ± 2.4 pg/mL. ET-1 was not significantly different between DDAH1 WT and DDAH1$^{-/-}$ mice in PBS controls (Figure 7.12D). There were also no differences in ET-1 levels after LPS administration in DDAH1 WT mice, however in DDAH$^{-/-}$ mice, ET-1 was significantly increased to 38.87 ± 4.8 pg/mL 6 hours post-LPS compared to 21.85 ±

3.17 pg/mL 6 hours post-PBS ($p<0.05$). This elevation was attenuated by 12 hours post-LPS. Although significantly different from PBS controls, this elevation was not significantly different from LPS-treated DDAH1 WT mice at 6 hours.

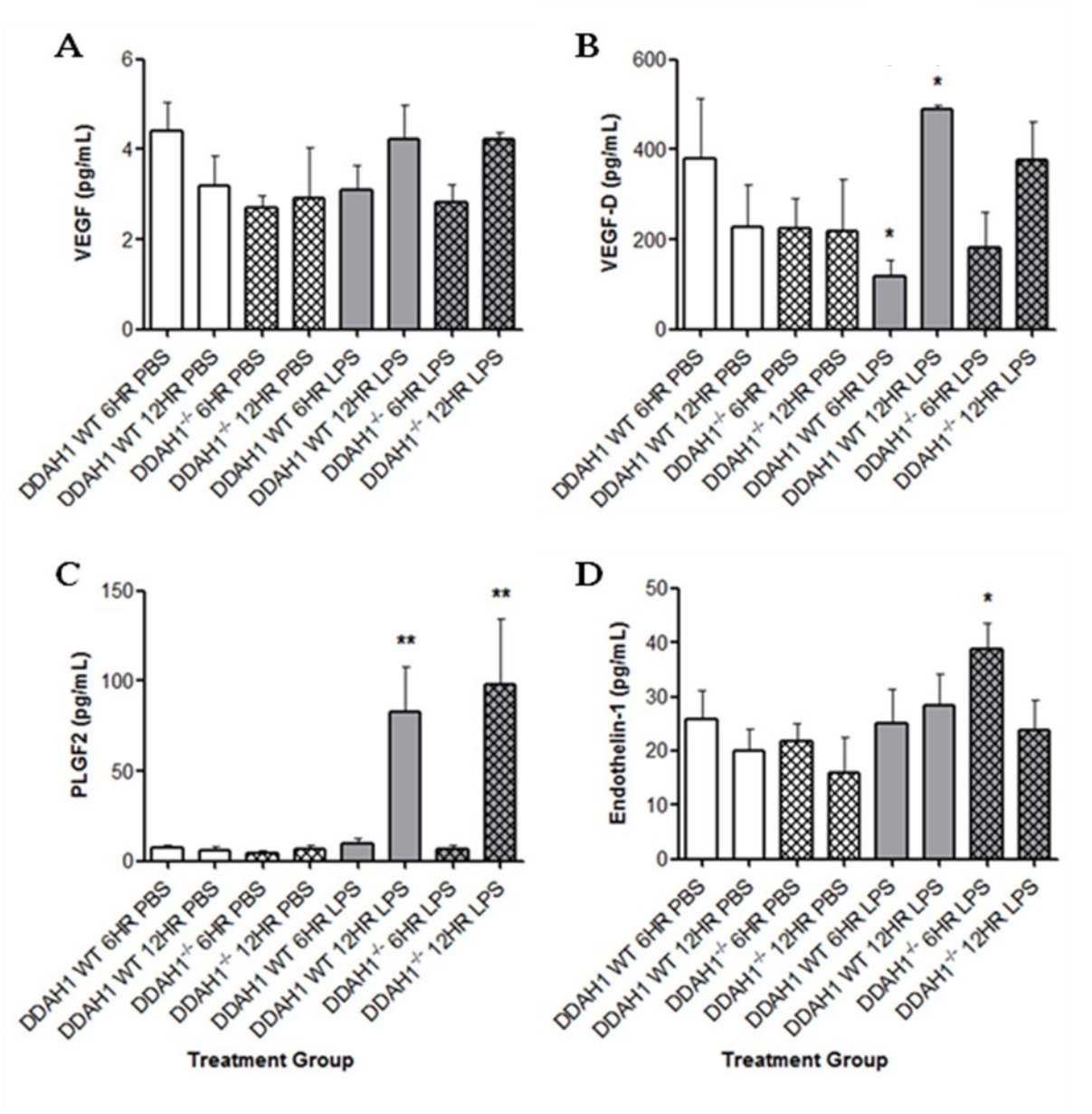


Figure 7.12: **Circulating concentrations of vasoactive factors in serum of pregnant DDAH1 WT and DDAH1$^{-/-}$ mice treated with LPS or vehicle.** (A) VEGF (B) VEGF-D (C) PLGF2 (D) Endothelin-1. *$p<0.05$, **$p<0.01$, compared to vehicle control unless otherwise indicated, pairwise t-test comparisons or Mann Whitney U tests were used where appropriate. Data shown as mean ± SEM (n numbers as for Figure 7.11).

7.2.6 The Production of Inflammatory Markers, Markers of Cardiac Dysfunction and Apoptotic Markers in Left Ventricular Tissue in Response to LPS in Pregnant DDAH1 Knockout Mice

To assess the extent of cardiac sensitivity, the relative expression of various markers of inflammation, cardiac dysfunction and apoptosis were assessed in maternal left ventricular tissue using RT-PCR.

In the left ventricle, IL-1β mRNA expression was not altered by DDAH1 deficiency or by LPS administration in these mice (Figure 7.13A). IL-6 expression was increased at 6 hours post-LPS in DDAH1 WT mice, but not significantly when compared to PBS control (Figure 7.13B). In DDAH1$^{-/-}$ mice, IL-6 expression was significantly increased compared to PBS control ($p<0.01$) which was then significantly ameliorated by 12 hours post-LPS ($p<0.05$). The pro-inflammatory cytokine TNF-α was increased in DDAH1 WT and DDAH1$^{-/-}$ mice ($p<0.01$ 12 hours post-LPS in DDAH1 WT, $p<0.05$ 6 and 12 hours post-LPS in DDAH1$^{-/-}$; Figure 7.13C). High variability in the DDAH1 WT at 6 hours post-LPS and in the PBS control is the likely reason for a lack of significance at 6 hours post-LPS. There were also significant increases in Cox-2 (6 hours post-LPS only, $p<0.01$; Figure 7.13E), and the chemokines CXCL1 (at 6 and 12 hours post-LPS, $p<0.05$ and $p<0.01$; Figure 7.13F) and CXCL2 (at 6 and 12 hours post-LPS; Figure 7.13G). There were no changes in the anti-inflammatory cytokine IL-10 (Figure 7.13D).

Interestingly, 6 hours after LPS administration, iNOS mRNA expression in the left ventricle was significantly reduced in DDAH1 WT ($p<0.001$) and DDAH1$^{-/-}$ mice ($p<0.01$; Figure 7.14A). There was no change in iNOS expression due to DDAH1 deficiency. Similarly, there was no change in eNOS expression due to DDAH1 deficiency in left ventricle (Figure 7.14B). However, 6 hours after LPS eNOS expression was significantly decreased in DDAH1$^{-/-}$ ($p<0.001$) and not in the DDAH1 WT ($p<0.01$ compared to DDAH1$^{-/-}$). There were no changes in ANP (Figure 7.14C), but BNF was significantly increased 6 hours post-LPS in DDAH1 WT ($p<0.01$) and DDAH1$^{-/-}$ mice ($p<0.01$; Figure 7.14D). Interestingly, the increase in BNF was greater in DDAH1$^{-/-}$ ($p<0.05$ compared to DDAH1 WT 6 hours post-LPS; Figure 7.14D). There were no changes in αMHC, βMHC or SERCA expression (Figure 7.14E, 7.14F, 7.14G). ET-1 expression in the left ventricle was increased 6 hours

after LPS, but this was only significant in DDAH1$^{-/-}$ mice ($p<0.05$), likely due to high variability in DDAH1 WT response (Figure 7.14H). Surprisingly, VEGF was found to be significantly decreased after LPS, but only in the DDAH1 WT mice at 12 hours ($p<0.01$ compared to PBS control). It must be considered that VEGF expression, although decreased from PBS control, was not significantly different from DDAH1 WT 6 hours post-LPS or from DDAH1$^{-/-}$ 12 hours post-LPS, and therefore may just be a reflection of an increase in VEGF 12 hours post-PBS in DDAH1 WT mice.

In the left ventricle, Bcl-2 mRNA expression was decreased 6 and 12 hours after LPS, although this effect was only able to reach significance in the DDAH1$^{-/-}$ mice ($p<0.05$; Figure 7.15A). This is likely to be due to high variability in Bcl-2 expression in the PBS controls in DDAH1 WT mice. There were no differences between DDAH1 WT and DDAH1$^{-/-}$ mice, indicating that DDAH1 deficiency did not alter Bcl-2. Bad expression was not altered in PBS controls between DDAH1 WT and DDAH$^{-/-}$ mice (Figure 7.15B).

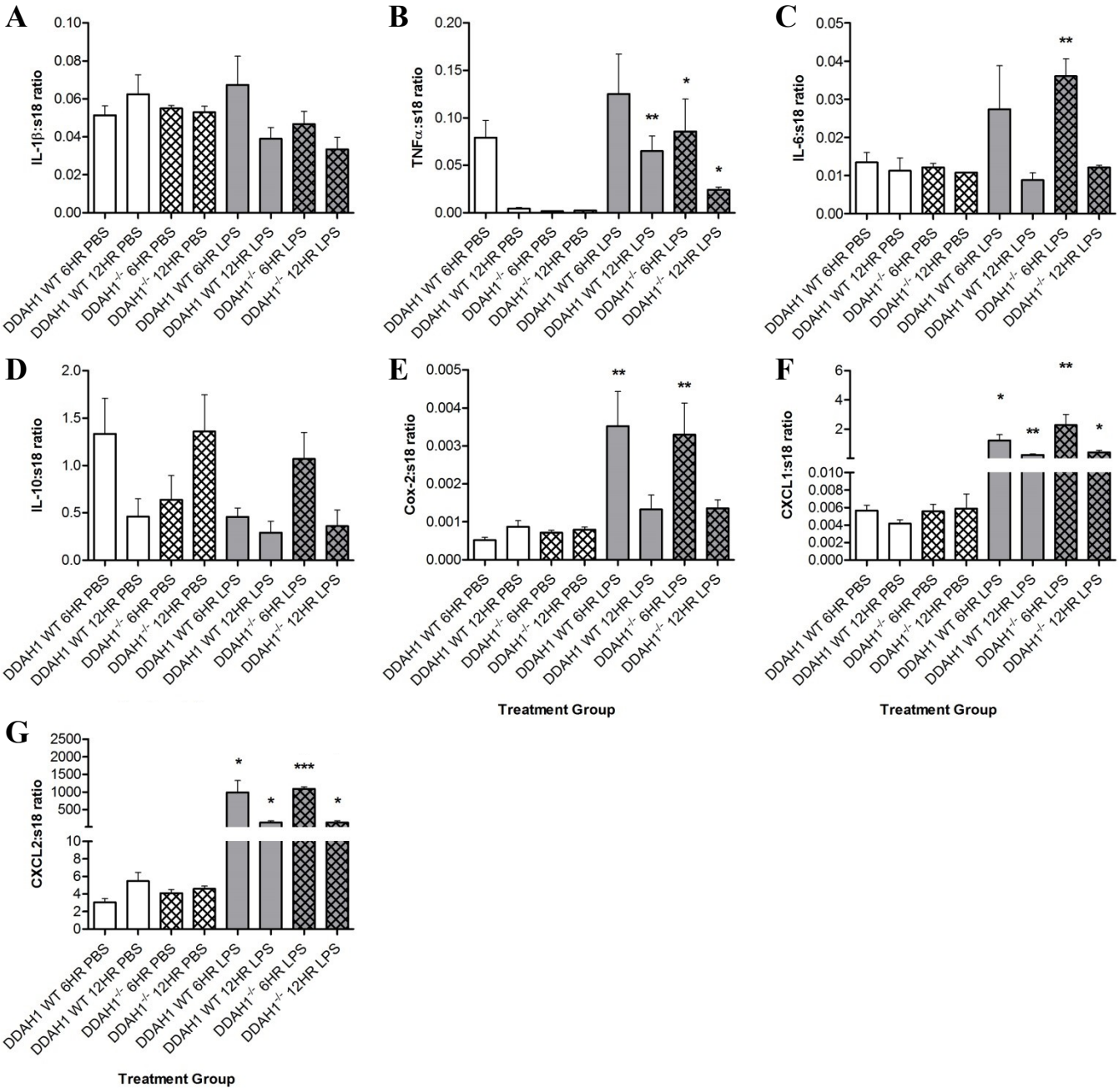


Figure 7.13: **mRNA expression of pro- and anti-inflammatory cytokines, inflammatory regulators and chemokines in left ventricular tissue taken from DDAH1 WT and DDAH1$^{-/-}$ mice treated with LPS or vehicle.** (A) IL-1β (B) IL-6 (C) TNF-α (D) IL-10 (E) Cox-2 (F) CXCL1 (G) CXCL2. *p<0.05, **p<0.01 compared to PBS control unless otherwise indicated, pairwise t-test comparisons or Mann Whitney U tests were used where appropriate. Data are expressed as mean ± SEM (DDAH$^{-/-}$ 12HR PBS, n=5; DDAH1$^{-/-}$ 6HR LPS, n=5; DDAH1$^{-/-}$ 12HR LPS, n=4; all other groups n=6).

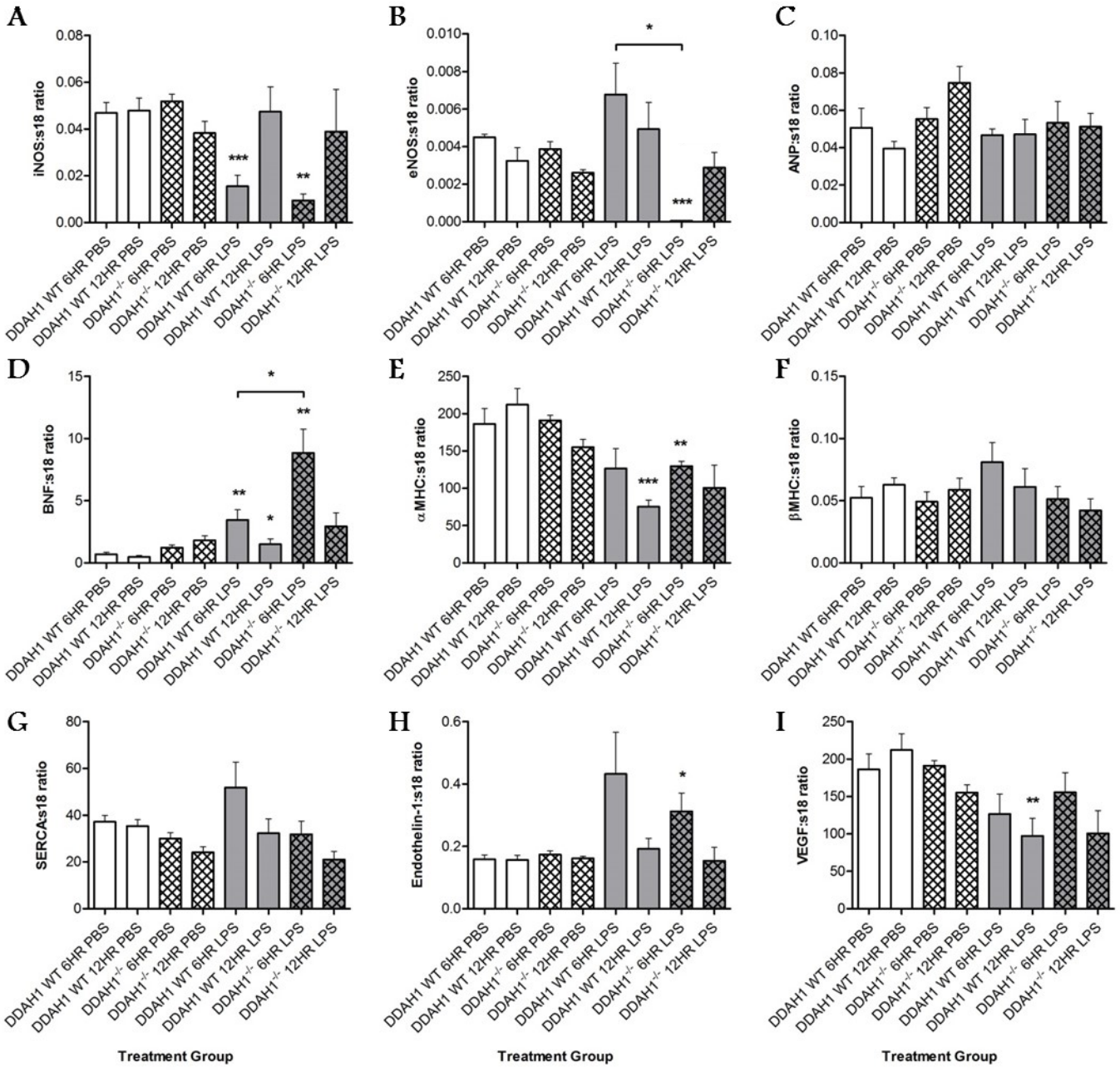


Figure 7.14: **mRNA expression of markers of cardiac dysfunction in left ventricular tissue taken from DDAH1 WT or DDAH1$^{-/-}$ mice treated with LPS or vehicle**. (A) iNOS (B) eNOS (C) ANP (D) BNF (E) αMHC (F) βMHC (G) SERCA (H) Endothelin-1 (I) VEGF. *p<0.05, **p<0.01, ***p<0.001 compared to PBS control unless otherwise indicated, pairwise t-test comparisons or Mann Whitney U tests were used where appropriate. Data are expressed as mean ± SEM (DDAH$^{-/-}$ 12HR PBS, n=5; DDAH1$^{-/-}$ 6HR LPS, n=5; DDAH1$^{-/-}$ 12HR LPS, n=4; all other groups n=6).

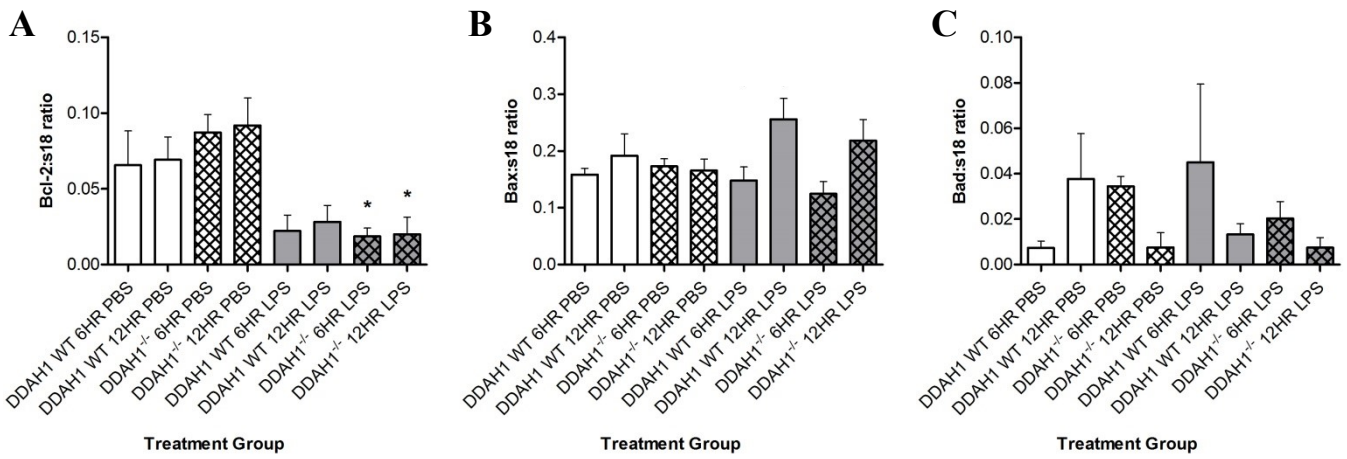


Figure 7.15: **mRNA expression of markers of apoptosis in left ventricular tissue taken from DDAH1 WT or DDAH1$^{-/-}$ mice treated with LPS or vehicle**. (A) Bcl-2 (B) Bax (C) Bad. *p<0.05, compared to PBS control unless otherwise indicated, pairwise t-test comparisons or Mann Whitney U tests were used where appropriate. Data are expressed as mean ± SEM (DDAH$^{-/-}$ 12HR PBS, n=5; DDAH1$^{-/-}$ 6HR LPS, n=5; DDAH1$^{-/-}$ 12HR LPS, n=4; all other groups n=6).

7.2.7 The Production of Vasoactive Factors in DDAH1 Knockout Mouse Placenta

Placental tissue taken 6 or 12 hours after PBS i.p from DDAH1 WT and DDAH1$^{-/-}$ mice were analysed to investigate vasoactive factors that could influence maternal haemodynamics. As there were no significant differences between any of the factors measured between 6 and 12 hours post-PBS these tissues were pooled and referred to as DDAH1 WT or DDAH1$^{-/-}$ only.

Placental tissue from DDAH1$^{-/-}$ mice had significantly higher concentrations of ADMA compared to WT (14.51 ± 1.18 vs. 8.22 ± 0.68 pmol/mg tissue; Figure 7.16A). In accordance with this finding, placentas from DDAH1$^{-/-}$ mice had significantly lower concentrations of L-arginine (1.42 ± 0.09 pmol/mg tissue) compared to WT (1.90 ± 0.12 pmol/mg tissue; Figure 7.16B). Similar to circulating concentrations (Figure 7.11A) placental NO concentrations were not significantly different in DDAH1 deficient mice (Figure 7.16C).

sFlt-1 is the soluble form of the VEGF/PLGF receptor Flt-1 (also known as sVEGFR1) which has been shown to act as a VEGF and PLGF antagonist [443, 444]. sFlt-1 produced by the placenta in response to hypoxia is released into the maternal circulation and can both antagonise the angiogenic effects of VEGF and PLGF as well as sensitise endothelial cells to the effects of pro-inflammatory cytokines [444, 445]. sFlt-1 concentration did not significantly differ between DDAH1 WT and placental tissue from DDAH1$^{-/-}$ mice (Figure 7.16D). Placentas from DDAH1$^{-/-}$ mice overall exhibited higher concentrations of sFlt-1 with a mean concentration of 11.1 ± 0.47 ng/μg tissue vs. 9.86 ± 0.51 ng/μg tissue in DDAH1 WT placenta but this did not reach significance.

Placental tissue from DDAH1$^{-/-}$ mice had significantly lower mRNA expression of iNOS ($p<0.05$; Figure 7.16E) and VEGF-B ($p<0.05$; Figure 7.16H) compared to DDAH1 WT mice. There was no significant difference in expression of eNOS, VEGF, ET-1 or Hsp70 (Figure 7.16F, 7.16G, 7.16I, 7.16J) between DDAH1 WT and placental tissue from DDAH1$^{-/-}$ mice. In addition, expression of PPAR-γ, PGC1-α, VEGF-C and VEGF-D did not significantly differ between DDAH1$^{-/-}$ and DDAH1 WT placenta (data not shown). Interestingly, 4 of the 11 placentas from DDAH1$^{-/-}$ mice exhibited a

mean mRNA expression of Hsp70 that was 40-fold higher than the mean expression of Hsp70 in DDAH1 WT placentae and 2.5-fold higher than the 7 other placenta from DDAH1$^{-/-}$ mice.

Placental tissue from DDAH1$^{-/-}$ mice exhibited lower protein expression of DDAH1 compared to DDAH1 WT mice (Figure 7.17A, 7.17B). DDAH-1 expression is still observed in these placentas, as homozygous female DDAH1$^{-/-}$ mice were mated with CD1 (DDAH1$^{+/+}$) stud males, therefore the resulting placentas, which consist of tissue of both maternal and fetal origin, display heterozygous expression of DDAH1. Densitometry analysis which calculated the ratio of DDAH1 to GAPDH (loading control) confirmed this observation ($p<0.001$; Figure 7.17B). There was no significant difference in the protein expression of DDAH2 between DDAH1 WT and placentas from DDAH1$^{-/-}$ mice (Figure 7.17A, 7.17C).

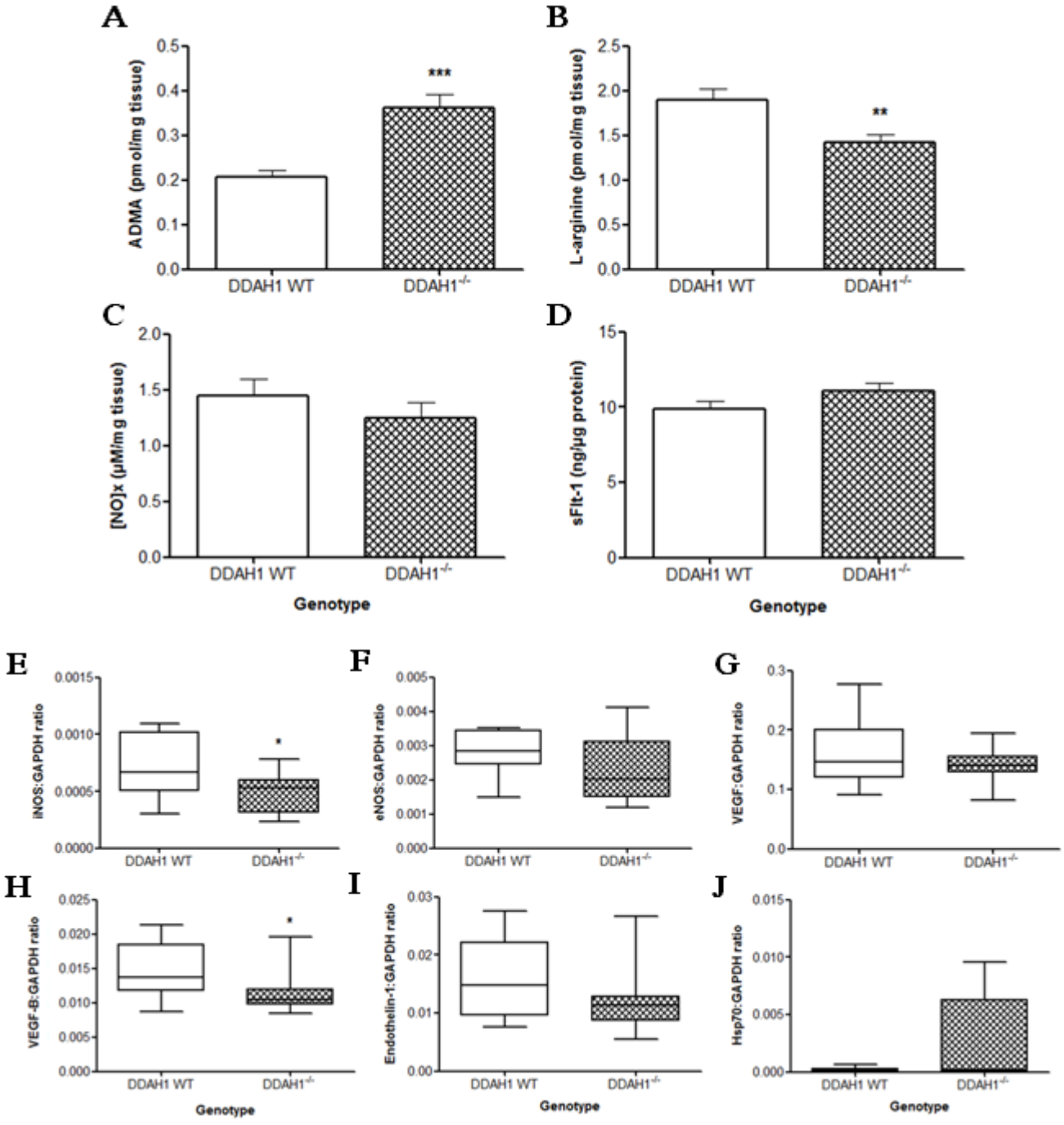


Figure 7.16: Placental concentrations of vasoactive factors in DDAH1 WT and DDAH1$^{-/-}$ mice. (A) ADMA concentations in the placenta as measured by mass spectrometry. ***p<0.001, student's t-test (B) L-Arginine concentrations in the placenta as measured by mass spectrometry. **<0.01, student's t-test (C) Concentration of total nitrates and nitrites (NOx) as measured by nitric oxide analyser (D) Concentration of sFlt-1 as measured by ELISA, normalised to protein content. Data expressed as mean ± SEM (n=11-12). mRNA expression of (E) iNOS (F) eNOS (G) VEGF (H) VEGF-B (I) ET-1 (F) Hsp70, *p<0.01, student's t-test or Mann Whitney U test as appropriate. Data shown as median ± interquartile range showing minimum and maximum (DDAH1 WT, n=11; DDAH1$^{-/-}$, n=12).

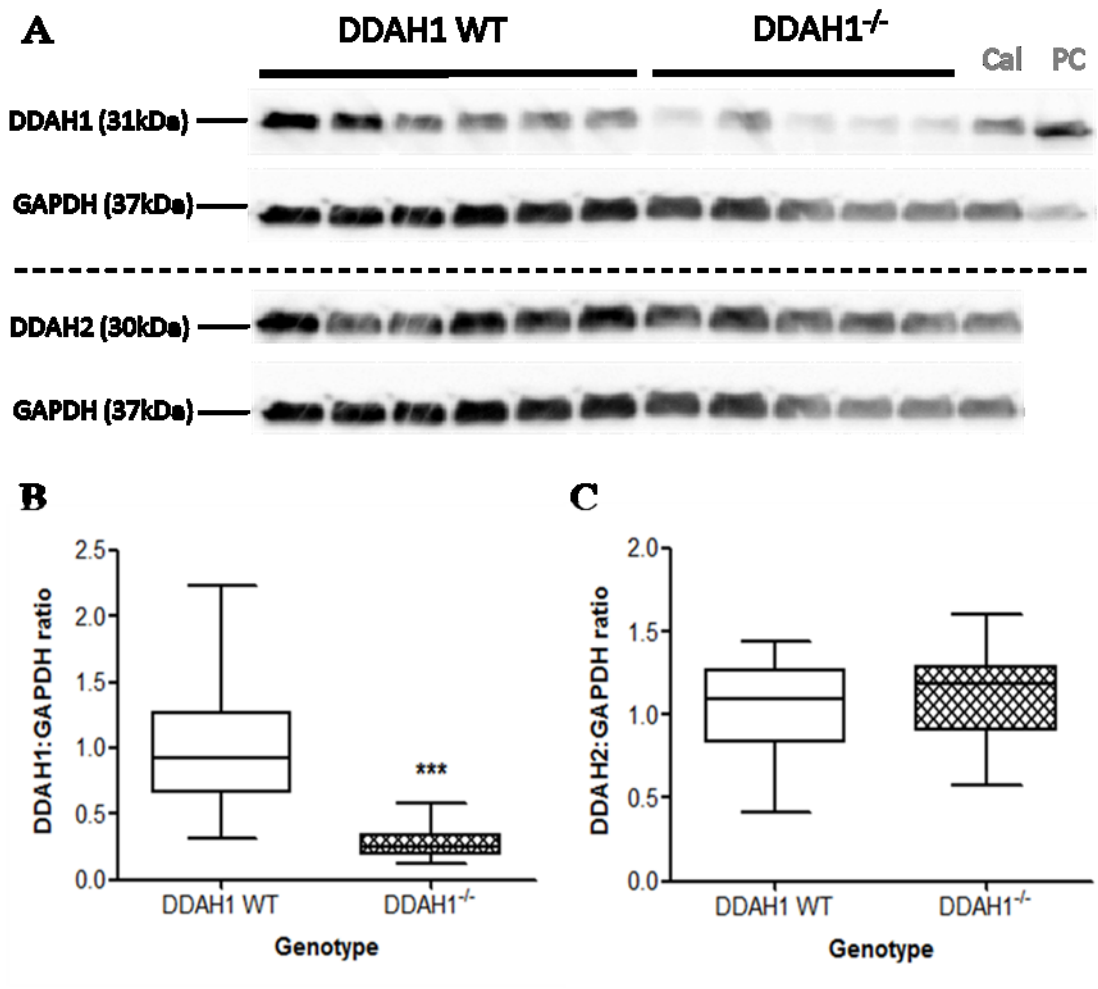


Figure 7.17: Expression of DDAH1 and DDAH2 in placental tissue taken from DDAH1 WT and DDAH1$^{-/-}$ mice. (A) Representative western blots showing DDAH1 and DDAH2 expression in DDAH1 WT and DDAH1$^{-/-}$ mice including GAPDH loading controls. Densitometry analysis was performed with ImageQuant software using GAPDH as loading control for DDAH1 (B) and DDAH2 (C). ***p<0.001 student's t-test (DDAH1 WT, n=11; DDAH1$^{-/-}$, n=12). Cal- calibrator, PC- positive control.

7.3 Summary and Discussion

Non-pregnant female DDAH1$^{-/-}$ mice had significantly elevated MAP, SAP and HR compared to DDAH1 WT. There was an increase in DAP but this was not significant. There were no significant changes in activity level between DDAH1 WT and DDAH1$^{-/-}$. In pregnant mice the haemodynamic profile of DDAH1 WT (C57BL/6) did not follow the same pattern as seen in the CD1 mice. There was a drop in MAP at mid-gestation but this was not significantly different from non-pregnant baseline. Similar patterns were observed in SAP and DAP. HR was increased at the post-implantation stage and peaked at E7 before returning to baseline. Surprisingly, DDAH1$^{-/-}$ mice exhibited a very similar haemodynamic profile throughout pregnancy and there were no significant differences between DDAH1$^{-/-}$ and DDAH1 WT mice for MAP, SAP or DAP. Likewise, although HR was consistently higher in DDAH1$^{-/-}$ mice, a very similar pattern to DDAH1 WT was observed throughout the course of gestation. One interesting observation was that DDAH1$^{-/-}$ mice had elevated MAP and SAP during the first trimester which was not different from their hypertensive baseline measurements. This may have implications in placental development and implantation. Additionally, another finding of note was that after labour and during the post-partum period, MAP, SAP and DAP all increased in DDAH1$^{-/-}$ mice to baseline levels or higher, demonstrating that the hypertensive phenotype of the non-pregnant DDAH1$^{-/-}$ mouse was quickly re-established after expulsion of the fetuses and placentas. There were no significant differences in activity levels between DDAH1 WT and DDAH1$^{-/-}$ mice during pregnancy or the post-partum period.

Latency to labour and pup survival after LPS administration (10μg) and vehicle control in DDAH1$^{-/-}$ mice were not significantly different to WT mice. The number of failed pregnancies and average litter sizes were also not different between DDAH1 WT and DDAH1$^{-/-}$ mice. Circulating NO levels were significantly increased after LPS in both strains compared to vehicle control. In contrast, ADMA levels were significantly increased in DDAH1$^{-/-}$ mice compared to DDAH1 WT in both LPS- and vehicle-treated mice and LPS was not seen to affect ADMA levels. There were no significant differences in VEGF or PLGF2 levels between DDAH1 WT and DDAH1$^{-/-}$, but 6 hours after LPS

administration, ET-1 was significantly increased in DDAH1$^{-/-}$ and not in DDAH1 WT. Cytokine/chemokine expression in response to LPS in left ventricular tissue was not altered in DDAH1$^{-/-}$ mice, however eNOS mRNA expression was significantly downregulated after LPS compared to vehicle, which did not occur in DDAH1 WT mice. BNF was also altered in DDAH1$^{-/-}$ mice, where in response to LPS BNF elevation was significantly greater.

In placental tissue, ADMA concentrations were significantly increased and L-arginine levels were correspondingly decreased in DDAH1$^{-/-}$ compared to DDAH1 WT. There were no changes in NO concentrations or sFlt-1. mRNA expression of iNOS, but not eNOS, was significantly decreased in placenta from DDAH1$^{-/-}$ mice and VEGF-B expression was also downregulated. Not surprisingly, DDAH1 protein expression was significantly reduced in placentas from DDAH1$^{-/-}$ mice compared to DDAH1 WT. The presence of low DDAH1 expression is likely due to the fetal component of the placenta, as fetal genotype was DDAH1 heterozygous. There was no change in DDAH2 levels.

The non-pregnant female DDAH1$^{-/-}$ mice displayed a hypertensive phenotype that was consistent with previous work done using male DDAH1$^{-/-}$ mice both in our group and others [437, 440]. When the haemodynamic profiles of both DDAH1$^{-/-}$ and DDAH1 WT were examined during pregnancy, there was some discrepancy between the data presented here and that previously seen in outbred CD1 mice, where DDAH1 WT mice did not display the same characteristic decline in MAP to mid-gestation which then recovered before labour (Chapter 3). It is possible that in C57BL/6 mice the cardiovascular adaptations that occur during pregnancy are dysregulated, however this would contradict several reports in the literature. Several studies have used C57BL/6 mice to look at haemodynamics in pregnancy and have been able to replicate the general trend of a mid-gestational nadir in MAP [250, 429, 446]. Therefore it is more likely that due to the low n numbers in this study, there is an erroneous finding that may have skewed the results.

The finding that there was no significant difference between DDAH1 WT and DDAH1$^{-/-}$ mice throughout pregnancy, and that the basal hypertension seen in DDAH1$^{-/-}$ females before pregnancy

did not persist, indicates that the cardiovascular adaptations that occur during pregnancy can override the contribution of DDAH/ADMA in the regulation of vascular tone. Whilst in pregnant DDAH1$^{-/-}$ mice (on E16) ADMA was found to be significantly increased compared to DDAH1 WT, this did not impact on the circulating levels of NO. Furthermore, the administration of LPS did not elicit a differential effect in DDAH1$^{-/-}$ compared to DDAH1 WT as there was an LPS-induced increase in NO in both strains. These results did not mirror the effect of DDAH deficiency in male mice, where Hu *et al*., reported that relative urinary NO content and plasma NO concentration were decreased in DDAH1$^{-/-}$ mice [440]. The authors suggested that DDAH1 was therefore responsible for maintaining both tissue and systemic NO bioavailability. In the DDAH1 transgenic mouse where DDAH1 is globally overexpressed, NO production in explanted heart tissue was found to be increased accordingly [447]. In concordance with these results, pharmacological inhibition of DDAH1 using the selective inhibitor L-257 was able to significantly attenuate NO production in male mice in response to experimental model of polymicrobial sepsis [448].

It is still unclear as to the underlying mechanism that would override the initial hypertensive phenotype of the DDAH1$^{-/-}$ mouse in pregnancy and result in similar levels of NO to DDAH1 WT control despite elevated ADMA concentrations. An important investigation to try and elicit the effect of DDAH1 deficiency on haemodynamics in pregnancy would be to measure blood pressure following LPS administration in pregnant DDAH1$^{-/-}$ mice. It may be that as the endogenous vasoconstrictor ET-1 was seen to be increased in DDAH1$^{-/-}$ and not in DDAH1 WT 6 hours after LPS, that in pregnancy DDAH1 deficiency would confer a protective phenotype against LPS-induced hypotension.

One possible explanation may be that LPS has been seen to elevate ADMA concentrations and reduce DDAH activity in human umbilical cord endothelial cells (hUVECs) [449]. Therefore, after LPS challenge, DDAH activity could be diminished to levels similar to those seen in DDAH1$^{-/-}$ mice. However, in this model, ADMA levels were not elevated further after LPS treatment so this is unlikely. Conversely, there have been reports that found arterial plasma concentrations of ADMA to

be lower after LPS infusion in rats [450]. Nijveldt *et al*., suggested that this finding could be due to an increased uptake by cells having the cationic amino acid transporter of system y^+. The expression of this transporter is known to be upregulated by LPS in several organs resulting in increased transport capacity. However, this transporter has also been shown to be abundantly expressed independent of LPS treatment [450]. It is important to consider whilst comparing these systems that changes in plasma ADMA levels may not be accurately reflected in cellular models, as changes in cellular ADMA concentrations may be not be evident in the plasma pool due to the effects of haemodilution.

Furthermore in the study presented in this chapter, a relatively mild dose of LPS was used, which was evident when examining the expression of cytokines and chemokines present in left ventricular tissue. Only CXCL1 and CXCL2 were upregulated in all groups that had been treated with LPS and IL-1β was not upregulated at all. Furthermore, iNOS mRNA expression was not elevated in the left ventricle after LPS and was actually seen to be downregulated 6 hours post-LPS. In a study that used LPS to model acute lung injury (ALI), 28 cytokines were found to be upregulated in BAL fluid, of which 13 of these were attenuated after DDAH2 overexpression [451]. This could suggest that DDAH deficiency could exacerbate the cytokine cascade after LPS and potentiate inflammation. This notion would be supported by *in vitro* evidence that CCL2 and IL-8 secretion was augmented after exogenous ADMA treatment in hUVECs and that DDAH2-transfected fibroblast-like synoviocytes upon stimulation with TNF-α produced significantly less IL-1β and IL-6 [452, 453]. However this may be reflective of only DDAH2 manipulation as we know that DDAH2 is the only isoform found in immune cells [97].

BNF mRNA expression was found to be upregulated after LPS in both DDAH1 WT and DDAH1$^{-/-}$, but interestingly the effect in DDAH1$^{-/-}$ mice was significantly greater. BNF has been seen to be significantly elevated both in animal models of LPS-induced endotoxaemia and in humans with endotoxic shock [153, 454]. Witthaut *et al*., were able to conclude from their clinical study in patients with sepsis that although ANP and BNF were increased in patients with septic shock, BNF reflected left ventricular dysfunction and ANP was related to IL-6 production rather than to cardiovascular

dysfunction [153]. Therefore the greater increase in BNF after LPS in DDAH1$^{-/-}$ mice may reflect increased sensitivity to LPS-induced ventricular dysfunction.

An important factor to consider would be that in this study, only circulating NO and ADMA concentrations were measured in DDAH1 WT and DDAH1$^{-/-}$ mice after LPS. Nijveldt *et al*., showed the capacity for alternative handling of ADMA in different tissues and it could therefore be hypothesised that as NO and ADMA were not measured in the heart that the serum levels cannot be taken as indicative of the levels in the left ventricle [450]. This notion would be supported by other findings that showed despite a 3-4 fold ADMA increase measured in restenotic lesions and the ischemia-reperfused myocardium, this was not associated with increased plasma ADMA and would therefore not be expected to contribute to systemic vascular pathology [90, 91, 455]. It may be then that elevated circulating ADMA would not be an indication of increased endothelial ADMA.

Similar to the finding in the circulation, NO was not decreased in the placenta despite increased ADMA. Additionally in placenta iNOS was found to be significantly downregulated, this would be expected to have an effect on overall NO production. This finding, in part, supports the work of Pope *et al*., where DDAH1 knockdown let to a modest reduction in NO bioavailability but a 48% reduction in L-arginine/ADMA ratio, whereas DDAH2 knockdown led to a 57% reduction in NO bioavailability and had no effect in L-arginine/ADMA ratio [91]. This led the authors to suggest that DDAH1 may exert its effects via an ADMA-dependent pathway and DDAH2 through an ADMA-independent pathway. Heterozygous expression of DDAH1 in the placentas of DDAH1$^{-/-}$ mice resulted in elevated placental ADMA which did not affect NO production, further supported by the finding that DDAH2 levels were not changed in the placentas of these mice.

Therefore, alongside the finding that female DDAH-1$^{-/-}$ mice have significantly higher mean arterial BP basally, and that there may be an effect of persistent hypertension throughout the first trimester of pregnancy; the reduction in placental iNOS expression, increased placental and serum concentrations of ADMA and no change in circulating or placental NO production in this study suggests that

DDAH1 functions to regulate ADMA levels which has a subsequent impact on haemodynamic regulation, possibly independent of NO.

Chapter 8: General Discussion

8.1 Summary of Main Findings

Sepsis is now the leading cause of direct maternal mortality in the UK and work conducted in the USA has shown that the rates of severe maternal sepsis and the risk of sepsis-related death has doubled since 2003 [227, 228, 235, 236]. The susceptibility to and severity of infections during pregnancy has been shown to be increased, where, for example, during the 2009 H1N1 influenza pandemic, over a third of all pregnant women diagnosed were hospitalised, and accounted for 5-7% of all deaths, hospitalisations and ICU admissions despite accounting for less than 1% of the population [110]. However, the mechanisms behind this increased morbidity and mortality during pregnancy are not fully understood.

The work described in this thesis was performed to address the two main hypotheses:

- The haemodynamic response to infection and inflammation is altered in pregnancy.
- Agents targeting the chemokine and NO signaling pathways given in pregnancy could alter the maternal response to infection and inflammation.

To explore these hypotheses, first, a telemetric method of measuring haemodynamic parameters during murine pregnancy in conscious mice was established. Telemetry recordings throughout gestation showed that MAP, DAP and SAP significantly decreased to a mid-gestational nadir at E8-E9 before returning to baseline by E16 accompanied by no change in HR. This fall in MAP is likely a consequence of peripheral vasodilation driven by early maternal hormonal changes. Over the course of gestation it was observed that activity decreased, although the time spent inactive decreased just before labour which continued post-partum. This was likely due to overwhelming nesting and weaning behaviours. These data were comparable with previously published data examining haemodynamic parameters during pregnancy in other mouse strains such as B6 and Balb/c [2].

The telemetric method established then allowed for the investigation of the cardiovascular response to inflammation in pregnancy. A non-invasive route to induce non-fatal endotoxaemia during pregnancy was established. A dose of 10μg LPS resulted in no maternal mortality and reproducible PTL with

delivery at a mean of approximately 20 hours post-injection. Pup survival was approximately 10% in these animals. Endotoxaemia in pregnancy led to significantly reduced MAP in pregnant compared to non-pregnant CD1 mice. Contrary to our hypothesis however, this was accompanied by a very similar systemic cytokine reaction suggesting that the response of the maternal innate immune system is neither impaired nor excessive. Although several cytokines and chemokines were elevated after LPS administration, there were no significant differences observed between pregnant and non-pregnant responses. These data suggest that during pregnancy the cardiovascular system is more sensitive to inflammation and potentially for this reason is less able to maintain blood pressure in the face of an inflammatory stimulus. Therefore the hypotensive response and any bearing this may have on maternal susceptibility to infection are not due to greater increases in cytokine and chemokines in pregnant animals. Levels of both NO and VEGF were significantly increased in non-pregnant mice after LPS, but this response was attenuated in pregnant mice. These results suggest that LPS-induced vasodilation (and consequently hypotension) should be more pronounced in non-pregnant mice, which is opposite to what was actually observed. Potentially, a pregnancy-induced increased sensitivity to the vasodilator action of VEGF and NO could account for these results but the vessels taken from pregnant animals did not respond differently to the NO donor, SNP. The most marked difference between the two groups was in the infiltration of the lungs, where pregnant animals had decreased neutrophils and increased monocytes. If greater monocytic infiltration were to lead to impaired arteriolar function as a result of an increase in inflammation and release of locally active vasoactive factors, this might contribute to the marked hypotension observed in pregnant animals.

The role of progesterone in LPS-induced haemodynamic alterations in pregnancy was investigated using progesterone supplementation. 10mg P4 was given daily between E14 and 16 and 10μg of LPS was administered i.p. on E16. P4 administration led to a reproducible extended latency to labour but there were no differences in pup survival compared to vehicle control (0% survival). After P4 supplementation, the LPS-induced hypotensive response observed in control animals was ameliorated. As circulating pro-inflammatory cytokines and chemokines as well as VEGF, NO and ADMA

concentrations were not altered by P4 supplementation, the underlying mechanism behind this result is unclear. The action of P4 in this circumstance is likely to be through an NO-independent pathway, potentially via membrane PRs or prostacyclin. Together, these data suggest that increased progesterone concentrations in pregnant mice do not drive the hypotensive response to LPS observed in pregnant animals. This finding was surprising as the initial hypothesis was that P4 would cause a further drop in MAP, implicating progesterone responsible for the different response observed in pregnancy.

To try and understand the involvement of chemokines, specifically signalling via CCL2/CCR2, in the inflammation-induced haemodynamic and immune responses in pregnancy, a CCR2-deficient mouse model and a CCR2 antagonist were used. Female non-pregnant $CCR2^{-/-}$ mice did not display significant alterations in blood pressure. Latency to labour and pup survival after LPS administration in $CCR2^{-/-}$ mice was not significantly different to CD1 mice. After LPS administration in $CCR2^{-/-}$ mice, there was no hypotension observed, in fact MAP increased to a peak at 5 hours post-LPS (which corresponded with elevated ET-1 at 6 hours) and then returned to baseline. At intermediate time points between LPS administration and labour, circulating concentrations of TNF-α were significantly reduced and IL-4 and IL-10 were significantly increased in $CCR2^{-/-}$ mice compared to CD1. Circulating NO and ADMA concentrations were significantly reduced in $CCR2^{-/-}$ mice both basally and after LPS challenge which is likely to be due to a lack of CCL2-induced monocyte (and neutrophil) recruitment to off-target sites, thus reducing excessive macrophage infiltration and NO release. This conclusion may also explain the reduced concentration of TNF-α in serum. Taken together, these data suggest a blockade of CCR2 results in the attenuation of an exacerbated innate immune response. Whilst this seems to contradict the conclusions drawn from previous observations in WT mice, where it was suggested that LPS administered in pregnancy does not elicit an excessive cytokine response over and above that in non-pregnant mice, it may be that manipulation of CCL2/CCR2 signalling is able to alter the Th1/Th2 balance. It may be however, that the results observed here at 12 hours post-LPS injection are unlikely to reflect the more long-term changes that

reflect a modulated adaptive immune response. The CCR2 antagonist RS504393 was able to reproduce the majority of the effects observed in the CCR2 knockout mouse. Whilst it was promising to be able to recreate the effects of CCR2 knockout with the CCR2 antagonist on LPS-induced haemodynamic changes, to be able to draw further conclusions from these data increased numbers of animals would be necessary.

Finally, to try and understand the contribution of NO signalling to the altered haemodynamic responses in pregnancy, the upstream endogenous ADMA inhibitor DDAH was targeted. In pregnant mice the haemodynamic profile of DDAH1 WT (C57BL/6) did not follow the same pattern as seen in the CD1 mice. There was a decrease in MAP at the mid-gestational point but this was not significantly different from non-pregnant baseline. HR was increased at the post-implantation stage and peaked at E7 before returning to baseline. Surprisingly, DDAH1$^{-/-}$ mice exhibited a very similar haemodynamic profile throughout pregnancy and there were no significant differences in the overall gestational MAP profile between DDAH1$^{-/-}$ and DDAH1 WT mice. One interesting observation was that DDAH1$^{-/-}$ mice exhibit a persistent hypertension during the first trimester that was not different from their hypertensive baseline measurements, which may have implications in placental development and implantation. This may be due to increased ET-1 which was only observed in DDAH1$^{-/-}$ and not in WT littermates. Or potentially, the lack of DDAH could lead to raised local ADMA preventing local NO production and thus the expected fall in MAP. Additionally, another finding of note was that after labour and during the post-partum period, MAP increased in DDAH1$^{-/-}$ mice to baseline levels or higher, demonstrating that the hypertensive phenotype of the non-pregnant DDAH1$^{-/-}$ mouse was quickly re-established after expulsion of the fetuses and placentas. Upon investigation, the placentae from these animals (genetically heterozygous for DDAH1) had reduced iNOS expression, increased ADMA concentrations and no change in NO levels when compared to WT littermates. These data suggest that the effect of DDAH1 on ADMA has a subsequent impact on haemodynamic regulation, but this may be independent of NO.

In summary, it has been shown here for the first time that a telemetric murine model of infection in pregnancy can be utilised in studying the effects of inflammation on maternal haemodynamics and the effects this may have on several outcomes in pregnancy. This model has been used to demonstrate that low levels of inflammation in pregnancy can lead to hypotension. Additionally, the increased levels of progesterone characteristic of pregnancy were shown not to be responsible for this hypotension. Manipulation of CCL2 signalling was able to reverse inflammation-induced hypotension in pregnancy, both by genetic knockout and pharmacological inhibition. DDAH1 knockout, whilst conferring initial hypertension, did not significantly impact the gestational haemodynamic profile.

8.2 Limitations of Study

Here we show that by using telemetric technique in combination with endotoxin to model maternal sepsis, it is possible to study the potential mechanisms behind the effects of inflammation during pregnancy. Clearly, it would be extremely difficult to conduct such investigations in human pregnancy with regards to ethical concerns and to the lack of tools to explore the underlying mechanisms (e.g. genetically modified mouse models). Despite this, there are several limitations, both experimental and technical, that should be considered when interpreting these results.

8.2.1 Experimental Limitations

There are several experimental limitations that should be taken into account when interpreting the results described in this thesis. The first of these is the consideration of the choice of experimental time points. In this thesis the time points of 6 and 12 hours were chosen to evaluate the cytokine profile after LPS or vehicle in non-pregnant and pregnant mice. The 12 hour time point was chosen to allow for the further investigation of the haemodynamic data where the nadir in blood pressure elicited by LPS in pregnant mice was at 12 hours post LPS injection. The time point of 6 hours was chosen as an intermediate. Several laboratories have noted that the induction of the main pro-inflammatory cytokines reach peak levels at approximately 1-2.5 hours post-LPS (IL-1β, IL-6 and TNF-α), regardless of the route of administration [456, 457]. Although, the temporal profile of IL-1β release is less well-defined, as others have found peak concentrations of plasma IL-1β to be much later, at around 6 hours, similar to the temporal profile of IFN-γ [458]. Consequently, the employment of a 6 hour time point may have led to the peak concentrations of some circulating cytokines being missed; however the emphasis in this study was not on the determination of the cytokine profile evoked by LPS, but to allow for the comparison of haemodynamic responses between non-pregnant and pregnant mice. Equally, the majority of serum cytokines examined were significantly elevated after LPS at the 6 hour time point when compared to vehicle control.

Secondly, only a subset of the cytokines that might be affected by pregnancy-induced immune system adaptations was studied. For example, despite the understanding that G-CSF is increased during pregnancy, and both G-CSF and GM-CSF have been shown to be elevated after LPS administration, neither were examined in the chapters of this thesis [80, 459]. In fact, whilst 'fingerprinting' the murine TLR4-induced inflammatory response, Bosmann *et al*., showed that amongst others IL-1α, IL-2, IL-3, IL-5, IL-9, IL-12(p40), IL-13, CCL11, G-CSF and GM-CSF were observed to have elevated plasma concentrations between 3 and 24 hours post-LPS administration [459], none of which were examined here. This was due to several technical and financial restrictions including, but not limited to, the unavailability of some of these cytokines on the multiplex cytokine panel.

8.2.2 Technical Limitations

When using a mouse model to investigate the changes that are conferred during pregnancy, it is important to consider the differences between mouse and human pregnancies. Aside from the dissimilarities in gestational length, and the number of fetuses carried in mouse pregnancy, there are also some important anatomical and endocrine differences. One critical difference is the withdrawal of progesterone to initiate labour. In most mammalian species, including the mouse, the levels of progesterone fall and oestrogen rises at the end of pregnancy to induce parturition. In humans, parturition occurs without this fall in progesterone and thus the initiation of labour is said to occur after a 'functional' withdrawal of progesterone, likely through diminished target tissue responsiveness facilitated by altered progesterone receptor expression [460].

Anatomically, both the uterus and placenta are very different when comparing the mouse and human. The rodent uterus has a bicornuate shape with two distinct uterine horns and a discrete longitudinal/circular muscle arrangement. Also, the differences in placentation, endocrine function and morphogenesis of the placenta can be considered to be of critical importance. During the first trimester of human pregnancy, extravillous trophoblast cells breach maternal spiral arteries and replace the residual endothelial cells leading to the remodelling of the spiral arteries and arterial vasodilation. In mice, trophoblast invasion into the maternal vasculature is negligible and the

exchange of nutrients occurs in the placental labyrinth region. The vascular remodelling that occurs does so independently of trophoblast cells invasion [461]. Consequently the immunological adaptations that occur particularly at the fetomaternal interface are potentially very different between mice and humans, therefore affecting the maternal immune response to infection. With respect to endocrine function, the principal difference between mice and humans is the mechanism controlling transition of the cyclic corpus luteum into a gestational corpus luteum, allowing the maintenance of progesterone secretion [274]. In mice, the corpus luteum has to produce progesterone throughout gestation. The consequent production of progesterone, and to some extent oestrogen, is much greater in humans than in other mammals.

Many researchers have suggested the guinea pig as a potentially much better model than other species (rodents, pigs and sheep) due to the relative similarity of placental structure and function to humans as well as a similar 'functional' withdrawal of progesterone before labour. Guinea pig placenta shares both the haemochorial placental type and the process of trophoblast invasion [462]. However, there are still obvious differences including the labyrinthine (rather than villous) placentation and further complicated lobular structure. Furthermore, there is not currently the capability to use genetic manipulation in the guinea pig to probe the pathways and mechanisms that lie behind the responses to inflammation and infection in pregnancy.

Along with considerations for the use of animal models in pregnancy research, there must be consideration of the technical limitations of the animal models used to study inflammation and sepsis. For example, the inhibition of inflammatory markers that has proven to be beneficial in endotoxin models, has not translated into an effective therapy in clinical trials [463]. Both TNF-α and IL-1 have been shown to be fundamental mediators of inflammation after LPS administration and have therefore attracted attention as potential targets in sepsis research. Promising results from TNF-α blockade in LPS animal studies led to several clinical trials for TNF-α antibodies or soluble receptors (TNF-SR p55, or p75), all of which showed either no improvement or actually led to increased mortality [464]. The limitations of TNF-α blockade likely includes the difficulty of the identification of the subset of

sepsis patients that would benefit. Similarly, blockade of IL-1 by IL-1 receptor antagonist (IL-1RA) was also shown to be ineffective in large clinical trials [465]; where only those patients identified as being most at risk of sepsis-induced mortality were seen to benefit from IL-1RA administration [466]. In fact, between 1981 and 2014 there has been at least 15 studies that have shown selected sepsis drugs that improved survival in animal models (including LPS and bacterial inoculation) but that had no beneficial effect in humans (or this effect was too small to achieve statistical significance) [467].

Given the lack of efficacy of these human clinical trials based on targets identified in the endotoxin studies, the endotoxin sepsis model has been called into question [213]. Several review articles have discussed and highlighted a number of putative differences between animal models of sepsis and what is presented in the clinic. Firstly, the systemic administration of LPS to model inflammation and sepsis relies on the assumption that the onset of sepsis is caused by the host-response and not the intact pathogen [214]. Undoubtedly, LPS administered via several different routes can bring about sepsis-like pathophysiological responses in these models, inducing increases in many circulating cytokines; however the contemporaneous nature of cytokine release has been shown to be very different between LPS models (in both animals and humans) and human sepsis, where in LPS models TNF-α, IL-6 and CXC chemokines were shown to peak much earlier and in far greater quantities [468, 469]. Secondly, the discrepancy of several orders of magnitude in the sensitivity of mice and humans to LPS *in vivo* has recently been shown to not be present when researchers looked at the response of macrophages from the two species *in vitro* [470]. This is unlike the responses to LPS of other cells taken from both species and grown in culture under identical conditions. Warren *at el*., showed that proteins present in mouse serum were able to markedly supress the induction of pro-inflammatory cytokines compared to in human serum. To the author's knowledge the specific proteins present in mouse, but not human, serum that exerted this immunosuppressant effect have not been identified. Thirdly, there should be consideration of the vast differences in the administration of endotoxin between studies: dose, bolus vs infusion, serotype and route of administration are extremely variable. Not only does that make it more difficult to compare results between studies, but leads to the

production of quite different models. For example, models that use sub-lethal doses of LPS have been shown to produce a hyperdynamic cardiovascular response compared to the hypodynamic response that accompanies larger typically lethal doses [215].

Mouse models to study inflammation and the immune system are improving though, and since the earlier 2000s, immunodeficient mice appropriate for generating "humanized mice" have been successfully developed. These mice were established by introducing the mutant *IL2ra* gene into severe combined immunodeficiency (SCID) or RAG1/2$^{-/-}$ mice to produce NOD/SCID/γc$^{-/-}$ and Rag1/2$^{-/-}$γc$^{-/-}$ mice respectively. These mice exhibit manifold immunodeficiencies including defects on T, B and NK cells as well as reduced macrophages and dendritic cell function. This means that due to the high human engraftment rates it is possible to generate mice that retain human immune cells to facilitate the analysis of the mechanisms behind the human immune responses in sepsis [471, 472]. There has been several studies examining the mechanisms behind sepsis (using LPS and CLP models) and viruses in 'humanized mice', but the use of these mice have not yet been explored in maternal infection research [473, 474].

Fink *et al*., commented that even though most animal models of human sepsis are flawed and the results from preclinical studies cannot be directly extrapolated to the problem of human sepsis, experiments using these models remain central to the development of new agents for the pharmacological treatment severe sepsis [475]. It is important to recognise the limitations of each model for them to be able to provide relevant information for application to humans.

One important technical limitation that affected the design of this study was the concern of pairing two surgical techniques: that of insertion of the telemetry probe, and CLP. This was dictated by the limitations of the PPL that this work was conducted under that did not permit multiple invasive surgeries on the same animal (such as the implantation of the telemetry device coupled with CLP). As discussed previously, the CLP model is considered to more closely resemble the polymicrobial characteristics of human sepsis than a bolus injection of endotoxin, producing a more representative

host response and appropriately timed cytokine release. Going forward, the combination of these techniques would provide further insight into the mechanisms behind maternal sepsis and the differences between the immune response in the non-pregnant state and during pregnancy.

8.3 Further Research

The results described in this thesis contribute towards our understanding of the maternal cardiovascular and immune response to inflammation. However, further work would complement and build upon the work presented here. For example, as there was no evidence to suggest excessive activation of the innate immune system by way of a resulting cytokine/chemokine storm in pregnant animals, the differences in cardiovascular response are likely to be perpetuated by different mechanisms. The greatest difference between pregnant and non-pregnant animals was observed in the immune cell infiltration of the lungs, where pregnant animals had fewer neutrophils and more monocytes. As previously stated, if greater monocytic infiltration can lead to impaired arteriolar function as a result of an increase in inflammation and release of locally active vasoactive factors, this could contribute to the marked hypotension observed. To investigate this further, it would be beneficial to explore the composition of these infiltrating cells into the lung and other tissues in greater detail by differentiating between the monocytic populations (that is, resident and infiltrating, or 'patrolling' monocytes) in the aim of assessing the dynamics of leukocyte trafficking following LPS challenge [476]. Other studies have suggested it is the failure of neutrophil migration that has the most deleterious effect on survival outcomes [477]. Therefore, further study of neutrophil trafficking is warranted as if there is impaired neutrophil migration in pregnant animals, this dysregulation would indicate impaired clearance of the infectious insult, reduced production of reactive oxygen species and decrease recruitment to infected sites.

Further to this, because of the difference observed in vasoactive factors such as VEGF in the maternal response to inflammation, it would be interesting to explore the effects of VEGF on vessel function using wire myography. In this thesis, VEGF was significantly elevated in response to LPS in non-pregnant but not pregnant animals. This was surprising as VEGF has been previously found to be increased in maternal serum and thought to contribute to vasodilation of the uterine and uteroplacental vasculature [478, 479]. A comparison of the vessel responses to VEGF taken from pregnant and non-

pregnant animals pre-treated with LPS or vehicle may lead to a greater understanding of the role of the VEGF in the cardiovascular response to inflammation in pregnancy.

In $CCR2^{-/-}$ mice we supposed that a lack of CCL2/CCR2 signalling was able to infer decreased monocyte and neutrophil recruitment to off-target sites and thus prevent excessive macrophage infiltration and subsequent release of NO and other pro-inflammatory cytokines. This explanation could account for the decrease in circulating TNF-α and NO concentrations also seen in pregnant $CCR2^{-/-}$ mice after LPS challenge. In turn, the reduction in NO could account for the failure of LPS to elicit hypotension in these animals. These data are of particular note as the manipulation of this pathway seems a promising avenue for the potential attenuation of inflammation-induced hypotension and warrants further investigation. The pharmacological blockade of CCR2 also led to promising results where LPS-induced hypotension was reversed, however although inhibition was achieved it may have only been partial antagonism. Experiments designed to define a more appropriate dose and dosing regimen may lead to maximum drug efficacy. Equally, with more time greater numbers of animals in each experimental group would strengthen the conclusions drawn from these data as it would minimise error and increase statistical power. Further to this, it would be interesting to compare these results with the effects of a BSCI, which has previously been shown to be an effective tocolytic agent in models of LPS-induced PTL [411].

Work presented in this thesis showed that $DDAH1^{-/-}$ mice exhibited a very similar haemodynamic profile throughout pregnancy to DDAH1 WT mice. This was a surprising result and it remains unclear as to the underlying mechanism that would override the initial hypertensive phenotype of the $DDAH1^{-/-}$ mouse in pregnancy and result in similar levels of NO to DDAH1 WT control despite elevated ADMA concentrations. Due to time constraints it was not possible to administer LPS to pregnant $DDAH1^{-/-}$ mice as intended to try and establish the role of this pathway during infectious insult and inflammation. Advancing the work presented in this thesis would unquestionably involve the exploration of the cardiovascular response of $DDAH1^{-/-}$ mice to LPS. The measurement of blood pressure in pregnant $DDAH1^{-/-}$ mice would enable the further investigation of the ET-1 response and

determine whether DDAH1 deficiency confers a protective phenotype against LPS-induced hypotension.

Similar to the premise behind introducing a pharmacological antagonist to target the CCL2/CCR2 signalling pathway, namely to determine if the same results can be observed when compensatory pathways are removed, it would be beneficial to test a DDAH inhibitor to confirm the effects of DDAH blockade. To date, the only compounds that show selectivity for DDAH over NOS are the guanidine substituted arginines NG-(2-methoxyethyl)-L-arginine (L-257) and NG-(2-methoxyethyl)-L-arginine methylester (L-291) [480]. Inhibition of NO by L-257, which binds to the active site of DDAH1, would result in increased levels of ADMA which as an endogenous NO inhibitor, may have the potential to improve the inflammation-induced hypotension observed after LPS challenge in pregnant animals. Previous research has shown that haemodynamic performance, including the degree of tachycardia and microvascular perfusion, in rat model of septic shock (induced by LPS or faecal slurry) could be preserved by treating with L-257. Importantly, L-257 was shown to prolong survival in these models [448].

8.3.1 Future Directions

To address some of the limitations of using LPS to induce inflammation, the combination of telemetry and CLP could provide further insight into the mechanisms behind maternal sepsis and the differences between the immune response in the non-pregnant state and during pregnancy. After a surgical procedure for conducting CLP in pregnancy is established and survival studies completed, this model could be used in conjunction with telemetry to monitor maternal cardiovascular responses to polymicrobial sepsis. In a similar fashion to the experiments described in this thesis, the haemodynamic data gathered could be understood in greater detail by taking tissues and maternal blood at several time points between the induction of sepsis by CLP and defined humane endpoints. These tissues could then be used to explore any differences in leukocyte densities, dysregulated leukocyte trafficking, the induction of cytokine/chemokines and the role of NO. The use of a

polymicrobial model would allow for the consideration of the effects of combination therapies (such as a combination of CCR2 antagonist or DDAH antagonist with broad spectrum antibiotics). The advantage of this approach would be to use a more representative model of sepsis, allowing for potentially more relevant conclusions to be drawn.

8.4 Conclusions

These data demonstrate that pregnant mice exhibit a marked hypotensive response to LPS and that this is associated with evidence of cardiac compromise, but normal vascular function. The administration of progesterone did not lead to a worsened hypotensive outcome, thus suggesting it is not progesterone that is responsible for the increased response to LPS in pregnancy. Conversely, although is it unlikely that pregnancy-induced immune adaptations in CCL2/CCR2 signalling are solely responsible for the altered response to inflammation during pregnancy, blockade of this pathway resulted in a reversal of LPS-induced hypotension in pregnancy. The marked fall in blood pressure in response to LPS may help to explain the greater 'susceptibility' of pregnant women to sepsis. Further research is necessary to understand the mechanisms responsible to allow for the development of a specifically targeted therapeutic response and an improvement in the management of severe infection in pregnant women.

9. References

1. Hunter, S. and S.C. Robson, *Adaptation of the maternal heart in pregnancy.* British Heart Journal, 1992. **68**(6): p. 540-543.
2. Burke, S.D., et al., *Spiral Arterial Remodeling Is Not Essential for Normal Blood Pressure Regulation in Pregnant Mice.* Hypertension, 2010. **55**(3): p. 729-737.
3. Capeless, E.L. and J.F. Clapp, *Cardiovascular changes in early phase of pregnancy.* Am J Obstet Gynecol, 1989. **161**(6 Pt 1): p. 1449-53.
4. Clapp, J.F., 3rd, et al., *Maternal physiologic adaptations to early human pregnancy.* Am J Obstet Gynecol, 1988. **159**(6): p. 1456-60.
5. Pecins-Thompson, M. and M. Keller-Wood, *Effects of progesterone on blood pressure, plasma volume, and responses to hypotension.* American Journal of Physiology-Regulatory Integrative and Comparative Physiology, 1997. **272**(1): p. R377-R385.
6. Kristiansson, P. and J.X. Wang, *Reproductive hormones and blood pressure during pregnancy.* Human Reproduction, 2001. **16**(1): p. 13-17.
7. Melchiorre, K., R. Sharma, and B. Thilaganathan, *Cardiac structure and function in normal pregnancy.* Curr Opin Obstet Gynecol, 2012. **24**(6): p. 413-21.
8. Ahokas, R.A., B.M. Sibai, and G.D. Anderson, *Lack of evidence of a vasodepressor role for relaxin in spontaneously hypertensive and normotensive pregnant rats.* American Journal of Obstetrics and Gynecology, 1989. **161**(3): p. 618-22.
9. Weinberger, M.H., et al., *The effect of posture and saline loading on plasma renin activity and aldosterone concentration in pregnant, non-pregnant and estrogen-treated women.* J Clin Endocrinol Metab, 1977. **44**(1): p. 69-77.
10. Longo, L.D., *Maternal blood volume and cardiac output during pregnancy: a hypothesis of endocrinologic control.* Am J Physiol, 1983. **245**(5 Pt 1): p. R720-9.
11. Lumbers, E.R. and K.G. Pringle, *Roles of the circulating renin-angiotensin-aldosterone system in human pregnancy.* Am J Physiol Regul Integr Comp Physiol, 2014. **306**(2): p. R91-101.
12. Brunton, P.J., S. Arunachalam, and J.A. Russel, *Control of neurohypophysial hormone secretion, blood osmolality and volume in pregnancy.* Journal of physiology and pharmacology : an official journal of the Polish Physiological Society, 2008. **59 Suppl 8**: p. 27-45.
13. Costantine, M.M., *Physiologic and pharmacokinetic changes in pregnancy.* Frontiers in Pharmacology, 2014. **5**: p. 65.
14. Jansen, A.J., et al., *Postpartum hemorrhage and transfusion of blood and blood components.* Obstet Gynecol Surv, 2005. **60**(10): p. 663-71.
15. Osol, G. and M. Mandala, *Maternal Uterine Vascular Remodeling During Pregnancy.* Physiology, 2009. **24**(1): p. 58-71.
16. Tan, E.K. and E.L. Tan, *Alterations in physiology and anatomy during pregnancy.* Best Pract Res Clin Obstet Gynaecol, 2013. **27**(6): p. 791-802.
17. De Wolf, F., et al., *The human placental bed: electron microscopic study of trophoblastic invasion of spiral arteries.* American Journal of Obstetrics and Gynecology, 1980. **137**(1): p. 58-70.
18. Valensise, H., et al., *Maternal cardiac systolic and diastolic function: relationship with uteroplacental resistances. A Doppler and echocardiographic longitudinal study.* Ultrasound in obstetrics & gynecology : the official journal of the International Society of Ultrasound in Obstetrics and Gynecology, 2000. **15**(6): p. 487-97.
19. Kelly, B., S. Stone, and L. Poston, *Cardiovascular adaptation to pregnancy: the role of altered vascular structure.* Fetal and Maternal Medicine Review, 1999. **11**(03): p. 105-116.
20. Johansson, E.D.B., *Plasma Levels of Progesterone in Pregnancy Measured by a Rapid Comptetitive Protein Binding Technique.* Acta Endocrinologica, 1969. **61**(4): p. 607-617.

21. Johnson, M.H., *Maternal Recognition and Support of Pregnancy*, in *Reproduction*. 2007, Blackwell Publishing: 350 Main Street, Malden, Massachusets. p. 212-221.
22. Spencer, T.E., et al., *Conceptus signals for establishment and maintenance of pregnancy.* Animal Reproduction Science, 2004. **82-83**: p. 537-50.
23. O'Leary, P., et al., *Longitudinal assessment of changes in reproductive hormones during normal pregnancy.* Clinical chemistry, 1991. **37**(5): p. 667-72.
24. Nachtigall, L., et al., *Plasma estriol levels in normal and abnormal pregnancies: An index of fetal welfare.* American Journal of Obstetrics & Gynecology, 1968. **101**(5): p. 638-648.
25. Wenner, M.M. and N.S. Stachenfeld, *Blood pressure and water regulation: understanding sex hormone effects within and between men and women.* J Physiol, 2012. **590**(Pt 23): p. 5949-61.
26. Omar, H.A., R. Ramirez, and M. Gibson, *Properties of a progesterone-induced relaxation in human placental arteries and veins.* Journal of Clinical Endocrinology & Metabolism, 1995. **80**(2): p. 370-3.
27. Rylance, P.B., et al., *Natural progesterone and antihypertensive action.* Br Med J (Clin Res Ed), 1985. **290**(6461): p. 13-4.
28. Fischer, G.M., *In vivo effects of estradiol on collagen and elastin dynamics in rat aorta.* Endocrinology, 1972. **91**(5): p. 1227-32.
29. Fischer, G.M. and M.L. Swain, *Influence of contraceptive and other sex steroids on aortic collagen and elastin.* Experimental and molecular pathology, 1980. **33**(1): p. 15-24.
30. Chang, K. and Z. Lubo, *Review article: steroid hormones and uterine vascular adaptation to pregnancy.* Reprod Sci, 2008. **15**(4): p. 336-48.
31. Magness, R.R. and C.R. Rosenfeld, *Local and systemic estradiol-17 beta: effects on uterine and systemic vasodilation.* Am J Physiol, 1989. **256**(4 Pt 1): p. E536-42.
32. Mendelsohn, M.E. and R.H. Karas, *The protective effects of estrogen on the cardiovascular system.* The New England journal of medicine, 1999. **340**(23): p. 1801-11.
33. Conrad, K.P., *Maternal vasodilation in pregnancy: the emerging role of relaxin.* Am J Physiol Regul Integr Comp Physiol., 2011. **301**(2): p. R267-R275.
34. Novak, J., et al., *Relaxin is essential for renal vasodilation during pregnancy in conscious rats.* J Clin Invest, 2001. **107**(11): p. 1469-75.
35. Massicotte, G., A. Parent, and J. St-Louis, *Blunted responses to vasoconstrictors in mesenteric vasculature but not in portal vein of spontaneously hypertensive rats treated with relaxin.* Proceedings of the Society for Experimental Biology and Medicine. Society for Experimental Biology and Medicine (New York, N.Y.), 1989. **190**(3): p. 254-9.
36. Gant, N.F., et al., *Control of vascular responsiveness during human pregnancy.* Kidney international, 1980. **18**(2): p. 253-8.
37. Baker, P.N., F. Broughton Pipkin, and E.M. Symonds, *Platelet angiotensin II binding and plasma renin concentration, plasma renin substrate and plasma angiotensin II in human pregnancy.* Clinical science (London, England : 1979), 1990. **79**(4): p. 403-8.
38. Jauniaux, E., et al., *The role of relaxin in the development of the uteroplacental circulation in early pregnancy.* Obstetrics and Gynecology, 1994. **84**(3): p. 338-42.
39. McGuane, J.T., et al., *Angiogenic growth factors are new and essential players in the sustained relaxin vasodilatory pathway in rodents and humans.* Hypertension, 2011. **57**(6): p. 1151-60.
40. Danielson, L.A., L.J. Kercher, and K.P. Conrad, *Impact of gender and endothelin on renal vasodilation and hyperfiltration induced by relaxin in conscious rats.* 2000. **279**(4): p. R1298-R1304.
41. Granger, J.P., *Maternal and fetal adaptations during pregnancy: lessons in regulatory and integrative physiology.* American Journal of Physiology - Regulatory, Integrative and Comparative Physiology, 2002. **283**(6): p. R1289-R1292.
42. Li, Y., Z.L. Brookes, and S. Kaufman, *Acute and chronic effects of relaxin on vasoactivity, myogenic reactivity and compliance of the rat mesenteric arterial and venous vasculature.* Regulatory Peptides, 2005. **132**(1-3): p. 41-6.

43. Pazos, M., et al., *The influence of pregnancy on systemic immunity.* Immunologic Research, 2012. **54**(1-3): p. 254-261.
44. Pierdominici, M., et al., *Estrogen receptor profiles in human peripheral blood lymphocytes.* Immunology letters, 2010. **132**(1-2): p. 79-85.
45. Damber, M.-G., B. von Schoultz, and T. Stigbrand, *The Immunological Paradox of Pregnancy.* Acta Obstetricia et Gynecologica Scandinavica, 1977. **56**(S66): p. 39-47.
46. Medawar, P.B., *Some immunological and endocrinological problems raised by the evolution of viviparity in vertebrates.* . Symposia of the Society for Experimental Biology, 1953. **7**: p. 320-338.
47. Lin, H., et al., *Synthesis of T helper 2-type cytokines at the maternal-fetal interface.* J Immunol, 1993. **151**(9): p. 4562-73.
48. Chaouat, G., *The Th1/Th2 paradigm: still important in pregnancy?* Semin Immunopathol, 2007. **29**(2): p. 95-113.
49. Kourtis, A.P., J.S. Read, and D.J. Jamieson, *Pregnancy and infection.* N Engl J Med, 2014. **371**(11): p. 1077.
50. Klipple, G.L. and F.A. Cecere, *Rheumatoid arthritis and pregnancy.* Rheumatic diseases clinics of North America, 1989. **15**(2): p. 213-39.
51. Confavreux, C., et al., *Rate of pregnancy-related relapse in multiple sclerosis. Pregnancy in Multiple Sclerosis Group.* The New England journal of medicine, 1998. **339**(5): p. 285-91.
52. Lissauer, D., et al., *Fetal-specific CD8+ cytotoxic T cell responses develop during normal human pregnancy and exhibit broad functional capacity.* J Immunol, 2012. **189**(2): p. 1072-80.
53. Constantin, C.M., et al., *Normal establishment of virus-specific memory CD8 T cell pool following primary infection during pregnancy.* J Immunol, 2007. **179**(7): p. 4383-9.
54. Sacks, G.P., C.W.G. Redman, and I.L. Sargent, *Monocytes are primed to produce the Th1 type cytokine IL-12 in normal human pregnancy: an intracellular flow cytometric analysis of peripheral blood mononuclear cells.* Clinical and experimental immunology, 2003. **131**(3): p. 490-497.
55. Sperling, R.S., et al., *Immunogenicity of trivalent inactivated influenza vaccination received during pregnancy or postpartum.* Obstetrics and Gynecology, 2012. **119**(3): p. 631-9.
56. Munoz, F.M., et al., *Safety and immunogenicity of tetanus diphtheria and acellular pertussis (Tdap) immunization during pregnancy in mothers and infants: a randomized clinical trial.* JAMA, 2014. **311**(17): p. 1760-9.
57. Mor, G. and I. Cardenas, *The immune system in pregnancy: a unique complexity.* Am J Reprod Immunol, 2010. **63**(6): p. 425-33.
58. Sacks, G., I. Sargent, and C. Redman, *An innate view of human pregnancy.* Immunology Today, 1999. **20**(3): p. 114-118.
59. Szekeres-Bartho, J., et al., *Progesterone as an immunomodulatory molecule.* Int Immunopharmacol, 2001. **1**(6): p. 1037-48.
60. Huber, S.A., J. Kupperman, and M.K. Newell, *Estradiol prevents and testosterone promotes Fas-dependent apoptosis in CD4+ Th2 cells by altering Bcl 2 expression.* Lupus, 1999. **8**(5): p. 384-387.
61. Straub, R.H., *The Complex Role of Estrogens in Inflammation.* Endocr Rev, 2007. **28**(5): p. 521-574.
62. Racicot, K., et al., *Understanding the Complexity of the Immune System during Pregnancy.* American Journal of Reproductive Immunology, 2014. **72**(2): p. 107-116.
63. Sacks, G.P., et al., *Normal pregnancy and preeclampsia both produce inflammatory changes in peripheral blood leukocytes akin to those of sepsis.* American Journal of Obstetrics and Gynecology, 1998. **179**(1): p. 80-6.
64. Koumandakis, E., et al., *Enhanced phagocytosis of mononuclear phagocytes in pregnancy.* British journal of obstetrics and gynaecology, 1986. **93**(11): p. 1150-4.
65. Takeuchi, O., et al., *Differential Roles of TLR2 and TLR4 in Recognition of Gram-Negative and Gram-Positive Bacterial Cell Wall Components.* Immunity, 1999. **11**(4): p. 443-451.

66. Peck, A. and E.D. Mellins, *Plasticity of T-cell phenotype and function: the T helper type 17 example.* Immunology, 2010. **129**(2): p. 147-153.
67. Crome, S.Q., A.Y. Wang, and M.K. Levings, *Translational Mini-Review Series on Th17 Cells: Function and regulation of human T helper 17 cells in health and disease.* Clinical and experimental immunology, 2010. **159**(2): p. 109-119.
68. Saito, S., et al., *Th1/Th2/Th17 and Regulatory T-Cell Paradigm in Pregnancy.* American Journal of Reproductive Immunology, 2010. **63**(6): p. 601-610.
69. Miossec, P. and J.K. Kolls, *Targeting IL-17 and TH17 cells in chronic inflammation.* Nature reviews. Drug discovery, 2012. **11**(10): p. 763-76.
70. Sykes, L., et al., *The Th1:Th2 Dichotomy of Pregnancy and Preterm Labour.* Mediators Inflamm, 2012.
71. Tafuri, A., et al., *T cell awareness of paternal alloantigens during pregnancy.* Science (New York, N.Y.), 1995. **270**(5236): p. 630-3.
72. Sakaguchi, S., et al., *Regulatory T Cells and Immune Tolerance.* Cell, 2008. **133**(5): p. 775-787.
73. Leber, A., A. Teles, and A.C. Zenclussen, *Regulatory T cells and their role in pregnancy.* Am J Reprod Immunol, 2010. **63**(6): p. 445-59.
74. Terness, P., et al., *Tolerance Signaling Molecules and Pregnancy: IDO, Galectins, and the Renaissance of Regulatory T Cells.* American Journal of Reproductive Immunology, 2007. **58**(3): p. 238-254.
75. Jasper, M.J., K.P. Tremellen, and S.A. Robertson, *Primary unexplained infertility is associated with reduced expression of the T-regulatory cell transcription factor Foxp3 in endometrial tissue.* Molecular Human Reproduction, 2006. **12**(5): p. 301-8.
76. Zenclussen, A.C., *Adaptive immune responses during pregnancy.* Am J Reprod Immunol, 2013. **69**(4): p. 291-303.
77. Muzzio, D., A.C. Zenclussen, and F. Jensen, *The role of B cells in pregnancy: the good and the bad.* Am J Reprod Immunol, 2013. **69**(4): p. 408-12.
78. Zhang, J.-M. and J. An, *Cytokines, Inflammation and Pain.* International anesthesiology clinics, 2007. **45**(2): p. 27-37.
79. Graves, D.T. and Y. Jiang, *Chemokines, a family of chemotactic cytokines.* Critical reviews in oral biology and medicine : an official publication of the American Association of Oral Biologists, 1995. **6**(2): p. 109-18.
80. Kraus, T.A., et al., *Peripheral Blood Cytokine Profiling During Pregnancy and Post-partum Periods.* American Journal of Reproductive Immunology, 2010. **64**(6): p. 411-426.
81. Sabat, R., et al., *Biology of interleukin-10.* Cytokine & growth factor reviews, 2010. **21**(5): p. 331-44.
82. Kishimoto, T., *Interleukin-6: from basic science to medicine--40 years in immunology.* Annual review of immunology, 2005. **23**: p. 1-21.
83. Mosmann, T.R. and R.L. Coffman, *TH1 and TH2 cells: different patterns of lymphokine secretion lead to different functional properties.* Annual review of immunology, 1989. **7**: p. 145-73.
84. Bredt, D.S. and S.H. Snyder, *Nitric oxide: a physiologic messenger molecule.* Annual review of biochemistry, 1994. **63**: p. 175-95.
85. Stuehr, D.J., *Mammalian nitric oxide synthases.* Biochimica et Biophysica Acta (BBA) - Bioenergetics, 1999. **1411**(2–3): p. 217-230.
86. Slaghekke, F., G. Dekker, and B. Jeffries, *Endogenous inhibitors of nitric oxide and preeclampsia: A review.* The Journal of Maternal-Fetal & Neonatal Medicine, 2006. **19**(8): p. 447-452.
87. Bogdan, C., *Nitric oxide synthase in innate and adaptive immunity: an update.* Trends in Immunology, 2015. **36**(3): p. 161-178.
88. Boger, R.H., et al., *The role of nitric oxide synthase inhibition by asymmetric dimethylarginine in the pathophysiology of preeclampsia.* Gynecol Obstet Invest, 2010. **69**(1): p. 1-13.

89. Vallance, P., et al., *Accumulation of an endogenous inhibitor of nitric oxide synthesis in chronic renal failure.* Lancet (London, England), 1992. **339**(8793): p. 572-5.
90. Cardounel, A.J., et al., *Evidence for the pathophysiological role of endogenous methylarginines in regulation of endothelial NO production and vascular function.* J Biol Chem, 2007. **282**(2): p. 879-87.
91. Pope, A.J., K. Karuppiah, and A.J. Cardounel, *Role of the PRMT-DDAH-ADMA axis in the regulation of endothelial nitric oxide production.* Pharmacol Res, 2009. **60**(6): p. 461-5.
92. Achan, V., et al., *Asymmetric dimethylarginine causes hypertension and cardiac dysfunction in humans and is actively metabolized by dimethylarginine dimethylaminohydrolase.* Arterioscler Thromb Vasc Biol, 2003. **23**(8): p. 1455-9.
93. Palm, F., et al., *Dimethylarginine dimethylaminohydrolase (DDAH): expression, regulation, and function in the cardiovascular and renal systems.* Am J Physiol Heart Circ Physiol, 2007. **293**(6): p. H3227-45.
94. Leiper, J.M., et al., *Identification of two human dimethylarginine dimethylaminohydrolases with distinct tissue distributions and homology with microbial arginine deiminases.* Biochem J, 1999. **343 Pt 1**: p. 209-14.
95. Nijveldt, R.J., et al., *Handling of asymmetrical dimethylarginine and symmetrical dimethylarginine by the rat kidney under basal conditions and during endotoxaemia.* Nephrology Dialysis Transplantation, 2003. **18**(12): p. 2542-2550.
96. Nijveldt, R.J., et al., *Elimination of Asymmetric Dimethylarginine by the Kidney and the Liver: A Link to the Development of Multiple Organ Failure?* The Journal of Nutrition, 2004. **134**(10): p. 2848S-2852S.
97. Tran, C.T., et al., *Chromosomal localization, gene structure, and expression pattern of DDAH1: comparison with DDAH2 and implications for evolutionary origins.* Genomics, 2000. **68**(1): p. 101-5.
98. Wang, D., et al., *Isoform-Specific Regulation by NG,NG-Dimethylarginine Dimethylaminohydrolase of Rat Serum Asymmetric Dimethylarginine and Vascular Endothelium-Derived Relaxing Factor/NO.* Circulation Research, 2007. **101**(6): p. 627-635.
99. Konishi, H., K. Sydow, and J.P. Cooke, *Dimethylarginine dimethylaminohydrolase promotes endothelial repair after vascular injury.* J Am Coll Cardiol, 2007. **49**(10): p. 1099-1105.
100. Xu, D.L., et al., *Upregulation of endothelial and neuronal constitutive nitric oxide synthase in pregnant rats.* Am J Physiol, 1996. **271**(6 Pt 2): p. R1739-45.
101. Weiner, C.P., R.G. Knowles, and S. Moncada, *Induction of nitric oxide synthases early in pregnancy.* American Journal of Obstetrics and Gynecology, 1994. **171**(3): p. 838-43.
102. Weiner, C., et al., *In vitro release of endothelium-derived relaxing factor by acetylcholine is increased during the guinea pig pregnancy.* American Journal of Obstetrics and Gynecology, 1989. **161**(6 Pt 1): p. 1599-605.
103. Valdes, G., et al., *Vasodilator factors in the systemic and local adaptations to pregnancy.* Reproductive biology and endocrinology : RB&E, 2009. **7**: p. 79.
104. Sladek, S.M., R.R. Magness, and K.P. Conrad, *Nitric oxide and pregnancy.* American Journal of Physiology - Regulatory, Integrative and Comparative Physiology, 1997. **272**(2): p. R441-R463.
105. Ito, E., et al., *Regulation of myometrial contractivity during pregnancy in the rat: potential role for DDAH.* Molecular Human Reproduction, 2009. **15**(8): p. 507-12.
106. Hale, S.A., et al., *Reduced NO signaling during pregnancy attenuates outward uterine artery remodeling by altering MMP expression and collagen and elastin deposition.* American Journal of Physiology - Heart and Circulatory Physiology, 2011. **301**(4): p. H1266-H1275.
107. Matuszkiewicz-Rowinska, J., J. Malyszko, and M. Wieliczko, *Urinary tract infections in pregnancy: old and new unresolved diagnostic and therapeutic problems.* Archives of medical science : AMS, 2015. **11**(1): p. 67-77.
108. Morgan, J. and S. Roberts, *Maternal Sepsis.* Obstetrics and Gynecology Clinics of North America, 2013. **40**(1): p. 69-87.
109. Batts, J.A., Jr., *Chorioamnionitis.* J Reprod Med, 1976. **17**(5): p. 296-8.

110. Sappenfield, E., D.J. Jamieson, and A.P. Kourtis, *Pregnancy and susceptibility to infectious diseases.* Infect Dis Obstet Gynecol, 2013. **2013**: p. 752852.
111. Kraus, T., et al., *Characterizing the Pregnancy Immune Phenotype: Results of the Viral Immunity and Pregnancy (VIP) Study.* Journal of Clinical Immunology, 2012. **32**(2): p. 300-311.
112. Priddy, K.D., *Immunologic Adaptations During Pregnancy.* Journal of Obstetric, Gynecologic, & Neonatal Nursing, 1997. **26**(4): p. 388-394.
113. Harris, J.W., *Influenza occurring in pregnant women: A statistical study of thirteen hundred and fifty cases.* Journal of the American Medical Association, 1919. **72**(14): p. 978-980.
114. Freeman, D.W. and A. Barno, *Deaths from Asian influenza associated with pregnancy.* Am J Obstet Gynecol, 1959. **78**: p. 1172-5.
115. Pramanick, A., et al., *Pandemic (H1N1) 2009 virus infection during pregnancy in South India.* International Journal of Gynecology & Obstetrics, 2011. **113**(1): p. 32-35.
116. Rolland-Harris, E., et al., *Hospitalization of pregnant women with pandemic A(H1N1) 2009 influenza in Canada.* Epidemiology & Infection, 2012. **140**(07): p. 1316-1327.
117. Mickiene, A., et al., *Hospitalized adult patients with 2009 pandemic influenza A (H1N1) in Kaunas, Lithuania.* Medicina (Kaunas), 2011. **47**(1): p. 11-8.
118. Kay, A.W., et al., *Enhanced natural killer-cell and T-cell responses to influenza A virus during pregnancy.* Proceedings of the National Academy of Sciences, 2014. **111**(40): p. 14506-14511.
119. Brandes, M., et al., *A Systems Analysis Identifies a Feed-forward Inflammatory Circuit Leading to Lethal Influenza Infection.* Cell, 2013. **154**(1): p. 197-212.
120. Marcelin, G., et al., *Fatal Outcome of Pandemic H1N1 2009 Influenza Virus Infection Is Associated with Immunopathology and Impaired Lung Repair, Not Enhanced Viral Burden, in Pregnant Mice.* Journal of Virology, 2011. **85**(21): p. 11208-11219.
121. McLean, A.R., et al., *Malaria and immunity during pregnancy and postpartum: a tale of two species.* Parasitology, 2015. **142**(8): p. 999-1015.
122. Desai, M., et al., *Epidemiology and burden of malaria in pregnancy.* The Lancet. Infectious diseases, 2007. **7**(2): p. 93-104.
123. Rijken, M.J., et al., *Malaria in pregnancy in the Asia-Pacific region.* The Lancet Infectious Diseases, 2012. **12**(1): p. 75-88.
124. WHO, *Severe Malaria.* Tropical Medicine & International Health, 2014. **19**: p. 7-131.
125. McClure, E.M., et al., *A systematic review of the impact of malaria prevention in pregnancy on low birth weight and maternal anemia.* International Journal of Gynecology & Obstetrics, 2013. **121**(2): p. 103-109.
126. Eisele, T.P., et al., *Malaria prevention in pregnancy, birthweight, and neonatal mortality: a meta-analysis of 32 national cross-sectional datasets in Africa.* The Lancet. Infectious diseases, 2012. **12**(12): p. 942-9.
127. Rogerson, S.J., et al., *Malaria in pregnancy: pathogenesis and immunity.* The Lancet Infectious Diseases, 2007. **7**(2): p. 105-117.
128. Riley, E.M., et al., *Suppression of cell-mediated immune responses to malaria antigens in pregnant Gambian women.* The American journal of tropical medicine and hygiene, 1989. **40**(2): p. 141-4.
129. Fievet, N., et al., *Immune response to Plasmodium falciparum antigens in Cameroonian primigravidae: evolution after delivery and during second pregnancy.* Clinical and experimental immunology, 1997. **107**(3): p. 462-7.
130. Fievet, N., et al., *Cellular immune response to Plasmodium falciparum after pregnancy is related to previous placental infection and parity.* Malaria journal, 2002. **1**: p. 16.
131. Urban, B.C. and S. Todryk, *Malaria pigment paralyzes dendritic cells.* Journal of biology, 2006. **5**(2): p. 4.
132. Urban, B.C., et al., *Plasmodium falciparum-infected erythrocytes modulate the maturation of dendritic cells.* Nature, 1999. **400**(6739): p. 73-7.

133. Artavanis-Tsakonas, K., et al., *Activation of a subset of human NK cells upon contact with Plasmodium falciparum-infected erythrocytes.* J Immunol, 2003. **171**(10): p. 5396-405.
134. Duarte, G., et al., *[Urinary tract infection in pregnancy]*. Revista brasileira de ginecologia e obstetricia : revista da Federacao Brasileira das Sociedades de Ginecologia e Obstetricia, 2008. **30**(2): p. 93-100.
135. Sujatha, R. and M. Nawani, *Prevalence of asymptomatic bacteriuria and its antibacterial susceptibility pattern among pregnant women attending the antenatal clinic at kanpur, India.* Journal of clinical and diagnostic research : JCDR, 2014. **8**(4): p. DC01-3.
136. Celen, S., et al., *Asymptomatic bacteriuria and antibacterial susceptibility patterns in an obstetric population.* ISRN obstetrics and gynecology, 2011. **2011**: p. 721872.
137. Farkash, E., et al., *Acute antepartum pyelonephritis in pregnancy: a critical analysis of risk factors and outcomes.* European journal of obstetrics, gynecology, and reproductive biology, 2012. **162**(1): p. 24-7.
138. Wing, D.A., M.J. Fassett, and D. Getahun, *Acute pyelonephritis in pregnancy: an 18-year retrospective analysis.* American Journal of Obstetrics and Gynecology, 2014. **210**(3): p. 219 e1-6.
139. Chaemsaithong, P., et al., *Soluble TRAIL in normal pregnancy and acute pyelonephritis: a potential explanation for the susceptibility of pregnant women to microbial products and infection.* The Journal of Maternal-Fetal & Neonatal Medicine, 2013. **26**(16): p. 1568-1575.
140. McGrath, E.E., et al., *TNF-related apoptosis-inducing ligand (TRAIL) regulates inflammatory neutrophil apoptosis and enhances resolution of inflammation.* J Leukoc Biol, 2011. **90**(5): p. 855-65.
141. Cziupka, K., et al., *Tumor necrosis factor-related apoptosis-inducing ligand (TRAIL) improves the innate immune response and enhances survival in murine polymicrobial sepsis.* Critical care medicine, 2010. **38**(11): p. 2169-74.
142. Dejager, L., et al., *Cecal ligation and puncture: the gold standard model for polymicrobial sepsis?* Trends in Microbiology, 2011. **19**(4): p. 198-208.
143. Lucas, D.N., P.N. Robinson, and M.R. Nel, *Sepsis in obstetrics and the role of the anaesthetist.* International Journal of Obstetric Anesthesia, 2012. **21**(1): p. 56-67.
144. Bosmann, M. and P.A. Ward, *The inflammatory response in sepsis.* Trends in Immunology, 2013. **34**(3): p. 129-36.
145. Charpentier, J., et al., *Brain natriuretic peptide: A marker of myocardial dysfunction and prognosis during severe sepsis.* Critical Care Medicine, 2004. **32**(3): p. 660-5.
146. Zaky, A., et al., *Characterization of cardiac dysfunction in sepsis: an ongoing challenge.* Shock (Augusta, Ga.), 2014. **41**(1): p. 12-24.
147. Blanco, J., et al., *Incidence, organ dysfunction and mortality in severe sepsis: a Spanish multicentre study.* Critical Care, 2008. **12**(6): p. R158-R158.
148. Zhang, T. and Q. Feng, *Nitric oxide and calcium signaling regulate myocardial tumor necrosis factor-alpha expression and cardiac function in sepsis.* Canadian Journal of Physiology and Pharmacology, 2010. **88**(2): p. 92-104.
149. Brown, M.A. and W.K. Jones *NF-kappaB action in sepsis: the innate immune system and the heart*. Frontiers in bioscience : a journal and virtual library, 2004. **9**, 1201-1217.
150. Li, X., et al., *Cleavage of IkappaBalpha by calpain induces myocardial NF-kappaB activation, TNF-alpha expression, and cardiac dysfunction in septic mice.* Am J Physiol Heart Circ Physiol, 2014. **306**(6): p. H833-43.
151. ver Elst, K.M., et al., *Cardiac troponins I and T are biological markers of left ventricular dysfunction in septic shock.* Clinical chemistry, 2000. **46**(5): p. 650-7.
152. Balija, T.M. and S.F. Lowry, *Lipopolysaccharide and sepsis-associated myocardial dysfunction.* Curr Opin Infect Dis, 2011. **24**(3): p. 248-53.
153. Witthaut, R., et al., *Plasma atrial natriuretic peptide and brain natriuretic peptide are increased in septic shock: impact of interleukin-6 and sepsis-associated left ventricular dysfunction.* Intensive Care Med, 2003. **29**(10): p. 1696-702.

154. Stein, B.C. and R.I. Levin, *Natriuretic peptides: physiology, therapeutic potential, and risk stratification in ischemic heart disease.* American heart journal, 1998. **135**(5 Pt 1): p. 914-23.
155. Chua, G. and L. Kang-Hoe, *Marked elevations in N-terminal brain natriuretic peptide levels in septic shock.* Critical Care, 2004. **8**(4): p. R248-R250.
156. Ouzounian, J.G. and U. Elkayam, *Physiologic changes during normal pregnancy and delivery.* Cardiology clinics, 2012. **30**(3): p. 317-29.
157. Adam, B., et al., *Plasma Atrial Natriuretic Peptide Levels in Preeclampsia and Eclampsia.* Journal of maternal-fetal investigation : the official journal of French Society of Ultrasound in Medicine and Biology, 1998. **8**(2): p. 85-8.
158. Uchiba, M., et al., *Endotoxin-induced pulmonary vascular injury is mainly mediated by activated neutrophils in rats.* Thrombosis Research, 1995. **78**(2): p. 117-125.
159. Gill, S.E., et al., *Pulmonary microvascular albumin leak is associated with endothelial cell death in murine sepsis-induced lung injury in vivo.* PLoS ONE, 2014. **9**(2): p. e88501.
160. Wu, P.Y., et al., *Colloid osmotic pressure: variations in normal pregnancy.* Journal of perinatal medicine, 1983. **11**(4): p. 193-9.
161. Snyder, C.C., et al., *Severe sepsis and septic shock in pregnancy: indications for delivery and maternal and perinatal outcomes.* The journal of maternal-fetal & neonatal medicine : the official journal of the European Association of Perinatal Medicine, the Federation of Asia and Oceania Perinatal Societies, the International Society of Perinatal Obstetricians, 2013. **26**(5): p. 503-6.
162. Barton, J.R.M.D. and B.M.M.D. Sibai, *Severe Sepsis and Septic Shock in Pregnancy.* Obstetrics & Gynecology, 2012. **120**(3): p. 689-706.
163. Cunningham, F.G., *Appendix B: Laboratory Values in Normal Pregnancy*, in *Protocols for High-Risk Pregnancies*. 2010, Wiley-Blackwell. p. 587-595.
164. Rollins, B.J., *Chemokines.* Blood, 1997. **90**(3): p. 909-28.
165. Benjamim, C.F., C.M. Hogaboam, and S.L. Kunkel, *The chronic consequences of severe sepsis.* J Leukoc Biol, 2004. **75**(3): p. 408-412.
166. Sallusto, F., A. Lanzavecchia, and C.R. Mackay, *Chemokines and chemokine receptors in T-cell priming and Th1/Th2-mediated responses.* Immunology Today, 1998. **19**(12): p. 568-74.
167. He, Y.Y., et al., *The decidual stromal cells-secreted CCL2 induces and maintains decidual leukocytes into Th2 bias in human early pregnancy.* Clin Immunol, 2012. **145**(2): p. 161-73.
168. Menzies, F.M., et al., *The chemokine receptor CCR2 is not required for successful initiation of labor in mice.* Biol Reprod, 2012. **86**(4): p. 118.
169. Nakano, Y., et al., *Protection against lethal bacterial infection in mice by monocyte-chemotactic and -activating factor.* Infection and Immunity, 1994. **62**(2): p. 377-383.
170. Gomes, R.N., et al., *Bacterial Clearance in Septic Mice is Modulated by MCP-1/CCL2 and Nitric Oxide.* Shock (Augusta, Ga.), 2013. **39**(1): p. 63-69.
171. Gomes, R.N., et al., *Increased susceptibility to septic and endotoxic shock in monocyte chemoattractant protein 1/cc chemokine ligand 2-deficient mice correlates with reduced interleukin 10 and enhanced macrophage migration inhibitory factor production.* Shock (Augusta, Ga.), 2006. **26**(5): p. 457-63.
172. Souto, F.O., et al., *Essential role of CCR2 in neutrophil tissue infiltration and multiple organ dysfunction in sepsis.* Am J Respir Crit Care Med, 2011. **183**(2): p. 234-42.
173. Speyer, C.L., et al., *Novel Chemokine Responsiveness and Mobilization of Neutrophils during Sepsis.* The American Journal of Pathology, 2004. **165**(6): p. 2187-2196.
174. Thiemermann, C., et al., *The multiple organ dysfunction syndrome caused by endotoxin in the rat: attenuation of liver dysfunction by inhibitors of nitric oxide synthase.* British Journal of Pharmacology, 1995. **116**(7): p. 2845-51.
175. Thiemermann, C. and J. Vane, *Inhibition of nitric oxide synthesis reduces the hypotension induced by bacterial lipopolysaccharides in the rat in vivo.* European Journal of Pharmacology, 1990. **182**(3): p. 591-595.
176. Feihl, F., B. Waeber, and L. Liaudet, *Is nitric oxide overproduction the target of choice for the management of septic shock?* Pharmacology & therapeutics, 2001. **91**(3): p. 179-213.

177. Holden, D.P., et al., *Plasma concentrations of asymmetric dimethylarginine, a natural inhibitor of nitric oxide synthase, in normal pregnancy and preeclampsia.* American Journal of Obstetrics and Gynecology, 1998. **178**(3): p. 551-6.
178. Avontuur, J.A., et al., *Pulmonary hypertension and reduced cardiac output during inhibition of nitric oxide synthesis in human septic shock.* Shock (Augusta, Ga.), 1998. **9**(6): p. 451-4.
179. Ninkovic, M.B., et al., *Nitric oxide synthase inhibitors partially inhibit oxidative stress development in the rat brain during sepsis provoked by cecal ligation and puncture.* Gen Physiol Biophys, 2009. **28**: p. 243-50.
180. Bakker, J., et al., *Administration of the nitric oxide synthase inhibitor NG-methyl-L-arginine hydrochloride (546C88) by intravenous infusion for up to 72 hours can promote the resolution of shock in patients with severe sepsis: results of a randomized, double-blind, placebo-controlled multicenter study (study no. 144-002).* Critical Care Medicine, 2004. **32**(1): p. 1-12.
181. Lopez, A., et al., *Multiple-center, randomized, placebo-controlled, double-blind study of the nitric oxide synthase inhibitor 546C88: effect on survival in patients with septic shock.* Crit Care Med, 2004. **32**(1): p. 21-30.
182. Lamont, R.F., *Infection in the prediction and antibiotics in the prevention of spontaneous preterm labour and preterm birth.* BJOG: An International Journal of Obstetrics & Gynaecology, 2003. **110**: p. 71-75.
183. Agrawal, V. and E. Hirsch, *Intrauterine infection and preterm labor.* Seminars in Fetal and Neonatal Medicine, 2012. **17**(1): p. 12-19.
184. Romero, R., et al., *The Preterm Labor Syndrome.* Annals of the New York Academy of Sciences, 1994. **734**(1): p. 414-429.
185. Romero, R., T. Chaiworapongsa, and J. Espinoza, *Micronutrients and Intrauterine Infection, Preterm Birth and the Fetal Inflammatory Response Syndrome.* The Journal of Nutrition, 2003. **133**(5): p. 1668S-1673S.
186. Norman, J., et al., *Inflammatory pathways in the mechanism of parturition.* BMC Pregnancy and Childbirth, 2007. **7**(Suppl 1): p. S7.
187. Keelan, J.A., *Pharmacological inhibition of inflammatory pathways for the prevention of preterm birth.* Journal of Reproductive Immunology, 2011. **88**(2): p. 176-184.
188. Saji, F., et al., *Cytokine production in chorioamnionitis.* Journal of Reproductive Immunology, 2000. **47**(2): p. 185-196.
189. Menon, R.P., et al., *Amniotic Fluid Eicosanoids in Preterm and Term Births: Effects of Risk Factors for Spontaneous Preterm Labor.* Obstetrics & Gynecology, 2011. **118**(1): p. 121-134.
190. Challis, et al., *Prostaglandins and mechanisms of preterm birth.* Reproduction, 2002. **124**(1): p. 1-17.
191. Young, A., et al., *Immunolocalization of Proinflammatory Cytokines in Myometrium, Cervix, and Fetal Membranes During Human Parturition at Term.* Biology of Reproduction, 2002. **66**(2): p. 445-449.
192. Gravett, M.G., et al., *An experimental model for intraamniotic infection and preterm labor in rhesus monkeys.* Am J Obstet Gynecol, 1994. **171**(6): p. 1660-7.
193. Kelly, R.W., *Inflammatory mediators and cervical ripening.* J Reprod Immunol, 2002. **57**(1-2): p. 217-24.
194. Baggia, S., et al., *Interleukin-Iβ Intra-Amniotic Infusion Induces TUmor Necrosis Factor-α, Prostaglandin Production, and Preterm Contractions in Pregnant Rhesus Monkeys.* Journal of the Society for Gynecologic Investigation, 1996. **3**(3): p. 121-126.
195. Pirianov, G., et al., *The Cyclopentenone 15-Deoxy-Î"12,14-Prostaglandin J2 Delays Lipopolysaccharide-Induced Preterm Delivery and Reduces Mortality in the Newborn Mouse.* Endocrinology, 2009. **150**(2): p. 699-706.
196. Hillier, S.L., et al., *The relationship of amniotic fluid cytokines and preterm delivery, amniotic fluid infection, histologic chorioamnionitis, and chorioamnion infection.* Obstet Gynecol, 1993. **81**(6): p. 941-8.

197. Jefferson, K.K., *The bacterial etiology of preterm birth.* Adv Appl Microbiol, 2012. **80**: p. 1-22.
198. Whitworth, M. and S. Quenby, *Prophylactic oral betamimetics for preventing preterm labour in singleton pregnancies.* Cochrane Database Syst Rev, 2008(1).
199. Adams Waldorf, K.M., et al., *Pretreatment With Toll-like Receptor 4 Antagonist Inhibits Lipopolysaccharide-Induced Preterm Uterine Contractility, Cytokines, and Prostaglandins in Rhesus Monkeys.* Reproductive Sciences, 2008. **15**(2): p. 121-127.
200. Carroll, S.G., et al., *Preterm prelabour amniorrhexis: intrauterine infection and interval between membrane rupture and delivery.* Archives of Disease in Childhood - Fetal and Neonatal Edition, 1995. **72**(1): p. F43-F46.
201. Gomez, R., et al., *The fetal inflammatory response syndrome.* American Journal of Obstetrics and Gynecology, 1998. **179**(1): p. 194-202.
202. Dessardo, N.S., et al., *Chronic lung disease of prematurity and early childhood wheezing: Is foetal inflammatory response syndrome to blame?* Early Human Development, 2014. **90**(9): p. 493-499.
203. Bashiri, A., E. Burstein, and M. Mazor, *Cerebral palsy and fetal inflammatory response syndrome: a review.* J Perinat Med, 2006. **34**(1): p. 5-12.
204. Hofer, N., et al., *The fetal inflammatory response syndrome is a risk factor for morbidity in preterm neonates.* American Journal of Obstetrics and Gynecology, 2013. **209**(6): p. 542.e1-542.e11.
205. Lu, Y.-C., W.-C. Yeh, and P.S. Ohashi, *LPS/TLR4 signal transduction pathway.* Cytokine, 2008. **42**(2): p. 145-151.
206. Wright, S.D., et al., *Lipopolysaccharide (LPS) binding protein opsonizes LPS-bearing particles for recognition by a novel receptor on macrophages.* J Exp Med, 1989. **170**(4): p. 1231-1241.
207. Cohen, J., *The immunopathogenesis of sepsis.* Nature, 2002. **420**(6917): p. 885-891.
208. Sharp, G.C., et al., *A Computational Model of Lipopolysaccharide-Induced Nuclear Factor Kappa B Activation: A Key Signalling Pathway in Infection-Induced Preterm Labour.* PLoS ONE, 2013. **8**(7): p. e70180.
209. Newton, R., et al., *Evidence for involvement of NF-kappaB in the transcriptional control of COX-2 gene expression by IL-1beta.* Biochemical and Biophysical Research Communications, 1997. **237**(1): p. 28-32.
210. Popov, D. and G. Pavlov, *Sepsis Models in Experimental Animals.* Trakia Journal of Sciences, 2013. **1**: p. 13-23.
211. Wintersteller, S., et al., *Molecular mediators of polymicrobial sepsis.* Frontiers in bioscience (Elite edition), 2012. **4**: p. 2584-604.
212. van de Sandt, A.M., et al., *Endothelial NOS (NOS3) impairs myocardial function in developing sepsis.* Basic Research in Cardiology, 2013. **108**(2): p. 330.
213. Remick, D.G. and P.A. Ward, *Evaluation of Endotoxin Models for the Study of Sepsis.* Shock, 2005. **24** (1): p. 7-11.
214. Rittirsch, D., L.M. Hoesel, and P.A. Ward, *The disconnect between animal models of sepsis and human sepsis.* J Leukoc Biol, 2007. **81**(1): p. 137-143.
215. Deitch, E.A., *Animal Models of Sepsis and Shock: A Review and Lessons Learned.* Shock, 1998. **9**(1): p. 1-11.
216. Warren, H.S., *Editorial: Mouse models to study sepsis syndrome in humans.* J Leukoc Biol, 2009. **86**(2): p. 199-201.
217. Lowry, S.F., *Human endotoxemia: a model for mechanistic insight and therapeutic targeting.* Shock (Augusta, Ga.), 2005. **24**: p. 94-100.
218. Taveira da Silva, A.M., et al., *Brief report: shock and multiple-organ dysfunction after self-administration of Salmonella endotoxin.* The New England journal of medicine, 1993. **328**(20): p. 1457-60.

219. Hirsch, E., et al., *Bacterially induced preterm labor in the mouse does not require maternal interleukin-1 signaling.* American Journal of Obstetrics and Gynecology, 2002. **186**(3): p. 523-530.
220. Mussalli, G.M., et al., *Inflammatory Cytokines in a Murine Model of Infection-Induced Preterm Labor: Cause or Effect?* Journal of the Society for Gynecologic Investigation, 1999. **6**(4): p. 188-195.
221. Normann, E., et al., *A Novel Mouse Model of Ureaplasma-Induced Perinatal Inflammation: Effects on Lung and Brain Injury.* Pediatr Res, 2009. **65**(4): p. 430-436.
222. Han, Y.W., et al., *Fusobacterium nucleatum Induces Premature and Term Stillbirths in Pregnant Mice: Implication of Oral Bacteria in Preterm Birth.* Infection and Immunity, 2004. **72**(4): p. 2272-2279.
223. Mai, S., et al., *Experimental Sepsis Models: Sepsis - An Ongoing and Significant Challenge*. Luciano Azevedo ed. 2012.
224. Zantl, N., et al., *Essential role of gamma interferon in survival of colon ascendens stent peritonitis, a novel murine model of abdominal sepsis.* Infection and Immunity, 1998. **66**(5): p. 2300-9.
225. Traeger, T., et al., *Colon Ascendens Stent Peritonitis (CASP) - a Standardized Model for Polymicrobial Abdominal Sepsis.* Journal of Visualized Experiments : JoVE, 2010. **46**: p. 2299.
226. Schabbauer, G., *Polymicrobial sepsis models: CLP versus CASP.* Drug Discovery Today: Disease Models, 2012. **9**(1): p. e17-e21.
227. Mander, R. and G.D. Smith, *Saving Mothers' Lives (formerly Why Mothers die): Reviewing maternal deaths to make motherhood safer 2003–2005.* Midwifery, 2008. **24**(1): p. 8-12.
228. *Centre for Maternal and Child Enquiries (CMACE). Saving Mothers' Lives: reviewing maternal deaths to make motherhood safer: 2006–08. The Eighth Report on Confidential Enquiries into Maternal Deaths in the United Kingdom.* BJOG, 2011. **118**(Suppl. 1): p. 1-203.
229. Olamijulo, J.A., et al., *Trends in maternal mortality at the Lagos University Teaching Hospital, Lagos, Nigeria.* Nig Q J Hosp Med, 2012. **22**(2): p. 72-9.
230. Cantwell, R., et al., *Saving Mothers' Lives: Reviewing maternal deaths to make motherhood safer: 2006-2008. The Eighth Report of the Confidential Enquiries into Maternal Deaths in the United Kingdom.* BJOG, 2011. **118**: p. 1-203.
231. Acosta, C.D., et al., *Maternal sepsis: a Scottish population-based case–control study.* BJOG: An International Journal of Obstetrics & Gynaecology, 2012. **119**(4): p. 474-483.
232. Kramer, H.M., et al., *Maternal mortality and severe morbidity from sepsis in the Netherlands.* Acta Obstet Gynecol Scand, 2009. **88**(6): p. 647-53.
233. van Dillen, J., et al., *Maternal sepsis: epidemiology, etiology and outcome.* Curr Opin Infect Dis, 2010. **23**(3): p. 249-54.
234. Acosta, C.D., et al., *Severe maternal sepsis in the UK, 2011-2012: a national case-control study.* PLoS Med, 2014. **11**(7): p. e1001672.
235. Acosta, C.D., et al., *The Continuum of Maternal Sepsis Severity: Incidence and Risk Factors in a Population-Based Cohort Study.* PLoS ONE, 2013. **8**(7): p. e67175.
236. Bauer, M.E., et al., *Maternal sepsis mortality and morbidity during hospitalization for delivery: temporal trends and independent associations for severe sepsis.* Anesth Analg, 2013. **117**(4): p. 944-50.
237. Oud, L., P. Watkins, and M. Hampton, *Trending the association of pregnancy-associated severe sepsis and maternal death: a population study.* Obstet Gynecol, 2014. **123 Suppl 1**: p. 132S.
238. Hoffman, M.K. and A.C. Sciscione, *Sepsis and multisystem organ failure in a woman attempting interval delivery in a triplet pregnancy: a case report.* J Reprod Med, 2004. **49**(5): p. 387-8.
239. Plachouras, N., et al., *Fulminant sepsis after invasive prenatal diagnosis.* Obstet Gynecol, 2004. **104**(6): p. 1244-7.

240. Lawn, J., et al., *Global report on preterm birth and stillbirth (1 of 7): definitions, description of the burden and opportunities to improve data.* BMC Pregnancy and Childbirth, 2010. **10**(Suppl 1): p. S1.
241. Romero, R., S.K. Dey, and S.J. Fisher, *Preterm labor: One syndrome, many causes.* Science, 2014. **345**(6198): p. 760-765.
242. Goldenberg, R.L. and J.F. Culhane, *Low birth weight in the United States.* The American Journal of Clinical Nutrition, 2007. **85**(2): p. 584S-590S.
243. Murphy, D.J. and S. Sellers, *Case-control study of antenatal and intrapartum risk.* Lancet, 1995. **346**(8988): p. 1449.
244. Gibbs, R.S., et al., *A review of premature birth and subclinical infection.* Am J Obstet Gynecol, 1992. **166**(5): p. 1515-28.
245. Kenyon S, Hagberg H, and N. JE, *Preterm Labour, Antibiotics, and Cerebral Palsy. Scientific Impact Paper no 33.* Royal College of Obstetricians and Gynaecologists, 2013.
246. Romero, R., et al., *The role of infection in preterm labour and delivery.* Paediatric and Perinatal Epidemiology, 2001. **15**: p. 41-56.
247. Villarini, M., et al., *Brain hsp70 expression and DNA damage in mice exposed to extremely low frequency magnetic fields: a dose-response study.* Int J Radiat Biol, 2013. **89**(7): p. 562-70.
248. Boring, L., et al., *Impaired monocyte migration and reduced type 1 (Th1) cytokine responses in C-C chemokine receptor 2 knockout mice.* J Clin Invest, 1997. **100**(10): p. 2552-61.
249. Breckenridge, R.A., et al., *A role for Dimethylarginine Dimethylaminohydrolase 1 (DDAH1) in mammalian development.* Int J Dev Biol, 2010. **54**(1): p. 215-20.
250. Butz, G.M. and R.L. Davisson, *Long-term telemetric measurement of cardiovascular parameters in awake mice: a physiological genomics tool.* Physiological Genomics, 2001. **5**(2): p. 89-97.
251. Boksa, P., *Effects of prenatal infection on brain development and behavior: A review of findings from animal models.* Brain, Behavior, and Immunity, 2010. **24**(6): p. 881-897.
252. Elovitz, M.A., et al., *A New Model for Inflammation-Induced Preterm Birth: The Role of Platelet-Activating Factor and Toll-Like Receptor-4.* The American Journal of Pathology, 2003. **163**(5): p. 2103-2111.
253. Spiers, A. and N. Padmanabhan, *A Guide to Wire Myography*, in *Hypertension*, J. Fennell and A. Baker, Editors. 2005, Humana Press. p. 91-104.
254. Sena, S., et al., *Cardiac hypertrophy caused by peroxisome proliferator- activated receptor-gamma agonist treatment occurs independently of changes in myocardial insulin signaling.* Endocrinology, 2007. **148**(12): p. 6047-53.
255. Deepak, S., et al., *Real-Time PCR: Revolutionizing Detection and Expression Analysis of Genes.* Curr Genomics, 2007. **8**(4): p. 234-51.
256. Lowry, O.H., et al., *Protein Measurement With the Folin Phenol Reagent.* Journal of Biological Chemistry, 1951. **193**(1): p. 265-275.
257. DiPalma, T., et al., *The placenta growth factor gene of the mouse.* Mamm Genome, 1996. **7**(1): p. 6-12.
258. Tarallo, V., L. Tudisco, and S. De Falco, *A placenta growth factor 2 variant acts as dominant negative of vascular endothelial growth factor A by heterodimerization mechanism.* Am J Cancer Res, 2011. **1**(2): p. 265-274.
259. Yu, M., et al., *Mechanism of cGMP contribution to the vasodilator response to NO in rat middle cerebral arteries.* 2002. **282**(5): p. H1724-H1731.
260. Lincoln, T.M., N. Dey, and H. Sellak, *Invited review: cGMP-dependent protein kinase signaling mechanisms in smooth muscle: from the regulation of tone to gene expression.* J Appl Physiol (1985), 2001. **91**(3): p. 1421-30.
261. Bryan, N.S. and M.B. Grisham, *Methods to detect nitric oxide and its metabolites in biological samples.* Free Radic Biol Med, 2007. **43**(5): p. 645-57.
262. Hytten, F., *Blood volume changes in normal pregnancy.* Clin Haematol, 1985. **14**(3): p. 601-12.

263. Duvekot, J.J., et al., *Early pregnancy changes in hemodynamics and volume homeostasis are consecutive adjustments triggered by a primary fall in systemic vascular tone.* Am J Obstet Gynecol, 1993. **169**(6): p. 1382-92.
264. Schrier, R.W. and V.A. Briner, *Peripheral arterial vasodilation hypothesis of sodium and water retention in pregnancy: implications for pathogenesis of preeclampsia-eclampsia.* Obstet Gynecol, 1991. **77**(4): p. 632-9.
265. Chapman, A.B., et al., *Temporal relationships between hormonal and hemodynamic changes in early human pregnancy.* Kidney Int, 1998. **54**(6): p. 2056-2063.
266. Zhao, X., et al., *Arterial Pressure Monitoring in Mice*, in *Current Protocols in Mouse Biology*. 2011, John Wiley & Sons, Inc.
267. Mills, P.A., et al., *A new method for measurement of blood pressure, heart rate, and activity in the mouse by radiotelemetry.* J Appl Physiol, 2000. **88**(5): p. 1537-44.
268. Carlson, S.H. and J.M. Wyss, *Long-term telemetric recording of arterial pressure and heart rate in mice fed basal and high NaCl diets.* Hypertension, 2000. **35**(2): p. E1-5.
269. Van Vliet, B.N., et al., *Phenotyping the Level of Blood Pressure by Telemetry in Mice.* Clinical and Experimental Pharmacology and Physiology, 2006. **33**(11): p. 1007-1015.
270. Tanaka, T., *Effects of litter size on behavioral development in mice.* Reproductive Toxicology, 1998. **12**(6): p. 613-617.
271. James, P.R. and C. Nelson-Piercy, *Management of hypertension before, during, and after pregnancy.* Heart, 2004. **90**(12): p. 1499-1504.
272. Hermida, R.C., D.E. Ayala, and M. Iglesias, *Predictable blood pressure variability in healthy and complicated pregnancies.* Hypertension, 2001. **38**(3 Pt 2): p. 736-41.
273. Robson, S.C., et al., *Serial study of factors influencing changes in cardiac output during human pregnancy.* Am J Physiol, 1989. **256**(4 Pt 2): p. H1060-5.
274. Malassine, A., J.L. Frendo, and D. Evain-Brion, *A comparison of placental development and endocrine functions between the human and mouse model.* Hum Reprod Update, 2003. **9**(6): p. 531-9.
275. Deng, A., K. Engels, and C. Baylis, *Impact of nitric oxide deficiency on blood pressure and glomerular hemodynamic adaptations to pregnancy in the rat.* Kidney Int, 1996. **50**(4): p. 1132-8.
276. Conrad, K.P., et al., *Identification of increased nitric oxide biosynthesis during pregnancy in rats.* FASEB J, 1993. **7**(6): p. 566-71.
277. Kopp, L., G. Paradiz, and J.R. Tucci, *Urinary excretion of cyclic 3',5'-adenosine monophosphate and cyclic 3',5'-guanosine monophosphate during and after pregnancy.* J Clin Endocrinol Metab, 1977. **44**(3): p. 590-4.
278. Majed, B.H. and R.A. Khalil, *Molecular Mechanisms Regulating the Vascular Prostacyclin Pathways and Their Adaptation during Pregnancy and in the Newborn.* Pharmacological Reviews, 2012. **64**(3): p. 540-582.
279. Scott, P.-A., et al., *Vasorelaxant action of 17β-estradiol in rat uterine arteries: role of nitric oxide synthases and estrogen receptors.* 2007. **293**(6): p. H3713-H3719.
280. Gangula, P.R., et al., *Pregnancy and steroid hormones enhance the vasodilation responses to CGRP in rats.* Am J Physiol, 1999. **276**(1 Pt 2): p. H284-8.
281. Chakrabarti, S., J.S. Morton, and S.T. Davidge, *Mechanisms of estrogen effects on the endothelium: an overview.* Can J Cardiol, 2014. **30**(7): p. 705-12.
282. Zhou, K., et al., *17beta-estradiol induces vasorelaxation by stimulating endothelial hydrogen sulfide release.* Mol Hum Reprod, 2013. **19**(3): p. 169-76.
283. Rosenfeld, C.R., et al., *Effect of estradiol-17beta on blood flow to reproductive and nonreproductive tissues in pregnant ewes.* Am J Obstet Gynecol, 1976. **124**(6): p. 618-29.
284. Rosenfeld, C.R. and T. Roy, *Large Conductance Ca(2+)-Activated and Voltage-Activated K(+) Channels Contribute to the Rise and Maintenance of Estrogen-Induced Uterine Vasodilation and Maintenance of Blood Pressure.* Endocrinology, 2012. **153**(12): p. 6012-6020.

285. Paller, M.S., G. Gregorini, and T.F. Ferris, *Pressor responsiveness in pseudopregnant and pregnant rats: role of maternal factors.* Am J Physiol, 1989. **257**(4 Pt 2): p. R866-71.
286. Lotgering, F.K., et al., *Maximal aerobic exercise in pregnant women: heart rate, O2 consumption, CO2 production, and ventilation.* 1991. **70**(3): p. 1016-1023.
287. Yamashita, T., et al., *Resistance to Endotoxin Shock in Transgenic Mice Overexpressing Endothelial Nitric Oxide Synthase.* Circulation, 2000. **101**(8): p. 931-937.
288. Lv, K.-Y., et al., *Deficiency of Smad3 results in enhanced inducible nitric oxide synthase–mediated hypotension in lipopolysaccharide-induced endotoxemia.* Journal of Surgical Research, 2014. **187**(2): p. 640-645.
289. Schmidt, C., et al., *Regulation of Renal Sodium Transporters during Severe Inflammation.* Journal of the American Society of Nephrology, 2007. **18**(4): p. 1072-1083.
290. Mederle, K., et al., *The angiotensin II AT1 receptor-associated protein Arap1 is involved in sepsis-induced hypotension.* Critical Care, 2013. **17**(4): p. R130.
291. Isobe, H., et al., *Activated Protein C Prevents Endotoxin-Induced Hypotension in Rats by Inhibiting Excessive Production of Nitric Oxide.* Circulation, 2001. **104**(10): p. 1171-1175.
292. Molor-Erdene, P., et al., *Urinary trypsin inhibitor reduces LPS-induced hypotension by suppressing tumor necrosis factor-α production through inhibition of Egr-1 expression.* 2005. **288**(3): p. H1265-H1271.
293. Redl, H., et al., *Clinical detection of LPS and animal models of endotoxemia.* Immunobiology, 1993. **187**(3-5): p. 330-45.
294. Munford, R.S., *Murine Responses to Endotoxin: Another Dirty Little Secret?* Journal of Infectious Diseases, 2010. **201**(2): p. 175-177.
295. Coyle, S.M., S.E. Calvano, and S.F. Lowry, *Gender influences in vivo human responses to endotoxin.* Shock, 2006. **26**(6): p. 538-43.
296. Wirtz, P.H., et al., *Monocyte proinflammatory cytokine release is higher and glucocorticoid sensitivity is lower in middle aged men than in women independent of cardiovascular risk factors.* Heart, 2004. **90**(8): p. 853-8.
297. Aulock, S.V., et al., *Gender difference in cytokine secretion on immune stimulation with LPS and LTA.* J Interferon Cytokine Res, 2006. **26**(12): p. 887-92.
298. van Eijk, L.T., et al., *Gender differences in the innate immune response and vascular reactivity following the administration of endotoxin to human volunteers.* Crit Care Med, 2007. **35**(6): p. 1464-9.
299. Speyer, C.L., et al., *Regulatory effects of estrogen on acute lung inflammation in mice.* Am J Physiol Cell Physiol, 2005. **288**(4): p. C881-90.
300. Card, J.W., et al., *Gender differences in murine airway responsiveness and lipopolysaccharide-induced inflammation.* J Immunol, 2006. **177**(1): p. 621-30.
301. Angele, M.K., et al., *Effect of gender and sex hormones on immune responses following shock.* Shock, 2000. **14**(2): p. 81-90.
302. Raju, R., K.I. Bland, and I.H. Chaudry, *Estrogen: a novel therapeutic adjunct for the treatment of trauma-hemorrhage-induced immunological alterations.* Mol Med, 2008. **14**(3-4): p. 213-21.
303. Elovitz, M.A. and C. Mrinalini, *Animal models of preterm birth.* Trends in Endocrinology & Metabolism, 2004. **15**(10): p. 479-487.
304. Wang, X., et al., *Lipopolysaccharide-induced inflammation and perinatal brain injury.* Semin Fetal Neonatal Med, 2006. **11**(5): p. 343-53.
305. Silver, R.M., et al., *Bacterial lipopolysaccharide-mediated fetal death. Production of a newly recognized form of inducible cyclooxygenase (COX-2) in murine decidua in response to lipopolysaccharide.* J Clin Invest, 1995. **95**(2): p. 725-31.
306. Cai, Z., et al., *Cytokine induction in fetal rat brains and brain injury in neonatal rats after maternal lipopolysaccharide administration.* Pediatr Res, 2000. **47**(1): p. 64-72.
307. Buhimschi, I.A., C.S. Buhimschi, and C.P. Weiner, *Protective effect of N-acetylcysteine against fetal death and preterm labor induced by maternal inflammation.* Am J Obstet Gynecol, 2003. **188**(1): p. 203-8.

308. Dalitz, P., et al., *Prolonged reductions in placental blood flow and cerebral oxygen delivery in preterm fetal sheep exposed to endotoxin: possible factors in white matter injury after acute infection.* J Soc Gynecol Investig, 2003. **10**(5): p. 283-90.
309. Garnier, Y., et al., *Endotoxemia severely affects circulation during normoxia and asphyxia in immature fetal sheep.* J Soc Gynecol Investig, 2001. **8**(3): p. 134-42.
310. Wei, Y.L., X.H. Li, and J.Z. Zhou, *Prenatal exposure to lipopolysaccharide results in increases in blood pressure and body weight in rats.* Acta Pharmacol Sin, 2007. **28**(5): p. 651-6.
311. Polglase, G.R., et al., *Intrauterine inflammation causes pulmonary hypertension and cardiovascular sequelae in preterm lambs.* J Appl Physiol (1985), 2010. **108**(6): p. 1757-65.
312. Vuorela, P., et al., *Expression of vascular endothelial growth factor and placenta growth factor in human placenta.* Biology of Reproduction, 1997. **56**(2): p. 489-94.
313. Yano, K., et al., *Vascular endothelial growth factor is an important determinant of sepsis morbidity and mortality.* J Exp Med, 2006. **203**(6): p. 1447-58.
314. Yano, K., et al., *Elevated levels of placental growth factor represent an adaptive host response in sepsis.* J Exp Med, 2008. **205**(11): p. 2623-31.
315. Haddad, R., et al., *Angiogenesis gene expression in mouse uterus during the common pathway of parturition.* American Journal of Obstetrics and Gynecology, 2008. **198**(5): p. 539.e1-539.e8.
316. Hassan, S.S., et al., *Signature pathways identified from gene expression profiles in the human uterine cervix before and after spontaneous term parturition.* American Journal of Obstetrics and Gynecology, 2007. **197**(3): p. 250.e1-250.e7.
317. Lappas, M., *Nuclear factor-κB mediates placental growth factor induced pro-labour mediators in human placenta.* Molecular Human Reproduction, 2012. **18**(7): p. 354-361.
318. Nguyen, N.Q., et al., *Prolactin/growth hormone-derived antiangiogenic peptides highlight a potential role of tilted peptides in angiogenesis.* Proc Natl Acad Sci U S A, 2006. **103**(39): p. 14319-24.
319. Leaños-Miranda, A., et al., *Circulating Angiogenic Factors and Urinary Prolactin as Predictors of Adverse Outcomes in Women With Preeclampsia.* Hypertension, 2013. **61**(5): p. 1118-1125.
320. Bajou, K., et al., *PAI-1 mediates the antiangiogenic and profibrinolytic effects of 16K prolactin.* Nat Med, 2014. **20**(7: 10): p. 741-7.
321. Qian, J., et al., *Octylphenol induces apoptosis in cultured rat Sertoli cells.* Toxicology Letters, 2006. **166**(2): p. 178-186.
322. McGinnis, K.M., et al., *Procaspase-3 and Poly(ADP)ribose Polymerase (PARP) Are Calpain Substrates.* Biochemical and Biophysical Research Communications, 1999. **263**(1): p. 94-99.
323. Girsh, E., et al., *Cloprostenol, a prostaglandin F(2alpha) analog, induces hypoxia in rat placenta: BOLD contrast MRI.* NMR Biomed, 2007. **20**(1): p. 28-39.
324. Dowle, S., *Elucidation of the Role of Placental Hypoxia and the Nitric Oxide Signalling Pathway in Pre-eclampsia* in *Department of Surgery and Cancer,* 2014, Imperial College London.
325. Silver, R.M., et al., *Lipopolysaccharide-induced fetal death: the role of tumor-necrosis factor alpha.* Biol Reprod, 1994. **50**(5): p. 1108-12.
326. Casey, M.L., et al., *Cachectin/tumor necrosis factor-alpha formation in human decidua. Potential role of cytokines in infection-induced preterm labor.* J Clin Invest, 1989. **83**(2): p. 430-6.
327. Cotechini, T., et al., *Inflammation in rat pregnancy inhibits spiral artery remodeling leading to fetal growth restriction and features of preeclampsia.* J Exp Med, 2014. **211**(1): p. 165-79.
328. Vizi, E., et al., *Enhanced tumor necrosis factor-alpha-specific and decreased interleukin-10-specific immune responses to LPS during the third trimester of pregnancy in mice.* Journal of Endocrinology, 2001. **171**(2): p. 355-361.

329. Iskit, A.B., et al., *Endothelin receptor antagonist bosentan improves survival in a murine caecal ligation and puncture model of septic shock.* European journal of pharmacology, 2004. **506**(1): p. 83-8.
330. Vo, P.A., et al., *Autoregulatory Role of Endothelium-derived Nitric Oxide (NO) on Lipopolysaccharide-induced Vascular Inducible NO Synthase Expression and Function.* Journal of Biological Chemistry, 2005. **280**(8): p. 7236-7243.
331. Kilbourn, R., C. Szabó, and D. Traber, *Beneficial versus detrimental effects of nitric oxide synthase inhibitors in circulatory shock: lessons learned from experimental and clinical studies.* Shock, 1997. **7**(4): p. 235-46.
332. Conrad, K.P., et al., *Identification of increased nitric oxide biosynthesis during pregnancy in rats.* The FASEB Journal, 1993. **7**(6): p. 566-71.
333. Cooke, C.-L.M. and S.T. Davidge, *Pregnancy-Induced Alterations of Vascular Function in Mouse Mesenteric and Uterine Arteries.* Biology of Reproduction, 2003. **68**(3): p. 1072-1077.
334. Goulopoulou, S., et al., *Augmented dilation to nitric oxide in uterine arteries from rats with type 2 diabetes: implications for vascular adaptations to pregnancy.* Am J Physiol Heart Circ Physiol, 2014. **306**(4): p. H610-8.
335. Klarr, S.A., et al., *Decreased sensitivity of vascular smooth muscle from pregnant rats to phenylephrine may be due to increased Nitric Oxide Synthase activity.* FASEB Journal, 1996. **10**(3).
336. Ungvari, Z., et al., *Increased NO-mediated and reduced TxA2-dependent responses in skeletal muscle arterioles in pregnancy.* Hypertens Pregnancy, 2002. **21**(2): p. 135-46.
337. Di, T., et al., *Pregnancy-Specific Enhancement of Agonist-Stimulated ERK-1/2 Signaling in Uterine Artery Endothelial Cells Increases Ca2+ Sensitivity of Endothelial Nitric Oxide Synthase as well as Cytosolic Phospholipase A2.* Endocrinology, 2001. **142**(7): p. 3014-3026.
338. Wedel Jones, C., et al., *Mechanisms underlying maternal venous adaptation in pregnancy.* Reprod Sci, 2009. **16**(6): p. 596-604.
339. Varpula, M., et al., *Predictive value of N-terminal pro-brain natriuretic peptide in severe sepsis and septic shock.* Critical care medicine, 2007. **35**(5): p. 1277-83.
340. Landesberg, G., et al., *Troponin Elevation in Severe Sepsis and Septic Shock: The Role of Left Ventricular Diastolic Dysfunction and Right Ventricular Dilatation.* Critical Care Medicine, 2014. **42**(4): p. 790-800.
341. Landesberg, G., et al., *Myocardial dysfunction in severe sepsis and septic shock: No correlation with inflammatory cytokines in real-life clinical setting.* Chest, 2015. **148**(1): p. 93-102.
342. McLean, A. and S. Huang, *Brain not processing: is finding a role for BNP in sepsis like fitting a square peg into a round hole?* Critical Care, 2014. **18**(4): p. 161.
343. Rameshrad, M., et al., *Lipopolysaccharide Induced Activation of Toll Like Receptor 4 in Isolated Rat Heart Suggests a Local Immune Response in Myocardium.* Iran J Immunol, 2015. **12**(2).
344. Li, H.L., et al., *Lipopolysaccharide induces apoptosis in adult rat ventricular myocytes via cardiac AT1 receptors.* Am J Physiol Heart Circ Physiol., 2002. **283**(2): p. H461-H467.
345. Chagnon, F., et al., *Endotoxin-Induced Myocardial Dysfunction: Effects of Macrophage Migration Inhibitory Factor Neutralization.* Circulation Research, 2005. **96**(10): p. 1095-1102.
346. Yamamura, Y., et al., *Time-dependent Inhibitory Effect of Lipopolysaccharide Injection on PER1 and PER2 Gene Expression in the Mouse Heart and Liver.* Chronobiology International, 2010. **27**(2): p. 213-232.
347. Park, D.W., et al., *Epidemiological and Clinical Characteristics of Community-Acquired Severe Sepsis and Septic Shock: A Prospective Observational Study in 12 University Hospitals in Korea.* Journal of Korean Medical Science, 2012. **27**(11): p. 1308-1314.
348. Rasmussen, S.A. and D.J. Jamieson, *2009 H1N1 Influenza and Pregnancy — 5 Years Later.* New England Journal of Medicine, 2014. **371**(15): p. 1373-1375.

349. Centre for Maternal and Child Enquiries (CMACE), *Saving Mothers' Lives: reviewing maternal deaths to make motherhood safer: 2006-08 The Eighth Report of the Confidential Enquiries into Maternal Deaths in the United Kingdom.* An International Journal of Obstetrics and Gynaecology, 2011. **118**(1): p. 1-203.
350. Karalis, K., G. Goodwin, and J.A. Majzoub, *Cortisol blockade of progesterone: a possible molecular mechanism involved in the initiation of human labor.* Nat Med, 1996. **2**(5): p. 556-60.
351. Henderson, D. and T. Wilson, *Reduced binding of progesterone receptor to its nuclear response element after human labor onset.* Am J Obstet Gynecol, 2001. **185**(3): p. 579-85.
352. Su, L.L., M. Samuel, and Y.S. Chong, *Progestational agents for treating threatened or established preterm labour.* Cochrane Database Syst Rev, 2014. **1**: p. CD006770.
353. Challis, J.R., et al., *Production of prostaglandin Falpha in ewes following luteal regression induced with a prostaglandin analogue, Estrumate (cloprostenol; I.C.I. 80996).* Prostaglandins, 1976. **11**(3): p. 537-43.
354. Lye, S.J. and D.G. Porter, *Demonstration that progesterone 'blocks' uterine activity in the ewe in vivo by a direct action on the myometrium.* J Reprod Fertil, 1978. **52**(1): p. 87-94.
355. Thorburn, G.D. and J.R. Challis, *Endocrine control of parturition.* Physiol Rev, 1979. **59**(4): p. 863-918.
356. Bogacki, M., et al., *Direct Inhibitory Effect of Progesterone on Oxytocin-Induced Secretion of Prostaglandin F2α from Bovine Endometrial Tissue.* Biology of Reproduction, 2002. **67**(1): p. 184-188.
357. Darblade, B., et al., *Estradiol alters nitric oxide production in the mouse aorta through the alpha-, but not beta-, estrogen receptor.* Circ Res, 2002. **90**(4): p. 413-9.
358. Cannoletta, M. and A. Cagnacci, *Modification of blood pressure in postmenopausal women: role of hormone replacement therapy.* Int J Womens Health, 2014. **6**: p. 745-57.
359. Miyaura, H. and M. Iwata, *Direct and Indirect Inhibition of Th1 Development by Progesterone and Glucocorticoids.* The Journal of Immunology, 2002. **168**(3): p. 1087-1094.
360. Flores-Espinosa, P., et al., *Progesterone Elicits an Inhibitory Effect upon LPS-Induced Innate Immune Response in Pre-Labor Human Amniotic Epithelium.* American Journal of Reproductive Immunology, 2014. **71**(1): p. 61-72.
361. Anbe, H., et al., *Influence of progesterone on myometrial contractility in pregnant mice treated with lipopolysaccharide.* J Obstet Gynaecol Res, 2007. **33**(6): p. 765-71.
362. Jiang, C.W., et al., *Progesterone induces endothelium-independent relaxation of rabbit coronary artery in vitro.* Eur J Pharmacol, 1992. **211**(2): p. 163-7.
363. Barbagallo, M., et al., *Vascular Effects of Progesterone: Role of Cellular Calcium Regulation.* Hypertension, 2001. **37**(1): p. 142-147.
364. Wang, Z.Q., et al., *The novel lipopolysaccharide-binding protein CRISPLD2 is a critical serum protein to regulate endotoxin function.* J Immunol, 2009. **183**(10): p. 6646-56.
365. Wang, T., et al., *CRISPLD2 is expressed at low levels during septic shock and is associated with procalcitonin.* PLoS ONE, 2013. **8**(6): p. e65743.
366. Yoo, J.Y., et al., *CRISPLD2 is a target of progesterone receptor and its expression is decreased in women with endometriosis.* PLoS ONE, 2014. **9**(6): p. e100481.
367. Piccinni, M.P., et al., *Progesterone favors the development of human T helper cells producing Th2-type cytokines and promotes both IL-4 production and membrane CD30 expression in established Th1 cell clones.* The Journal of Immunology, 1995. **155**(1): p. 128-33.
368. Romagnani, S., *The Th1/Th2 paradigm.* Immunology Today, 1997. **18**(6): p. 263-266.
369. Piccinni, M.-P., et al., *Role of hormone-controlled Th1- and Th2-type cytokines in successful pregnancy.* Journal of Neuroimmunology, 2000. **109**(1): p. 30-33.
370. Raghupathy, R., *Pregnancy: success and failure within the Th1/Th2/Th3 paradigm.* Seminars in Immunology, 2001. **13**(4): p. 219-227.
371. Druckmann, R. and M.A. Druckmann, *Progesterone and the immunology of pregnancy.* J Steroid Biochem Mol Biol, 2005. **97**(5): p. 389-96.

372. Miller, L., et al., *Progesterone inhibits inducible nitric oxide synthase gene expression and nitric oxide production in murine macrophages.* J Leukoc Biol, 1996. **59**(3): p. 442-50.
373. Gellersen, B., M.S. Fernandes, and J.J. Brosens, *Non-genomic progesterone actions in female reproduction.* Hum Reprod Update, 2009. **15**(1): p. 119-38.
374. Zhu, Y., J. Bond, and P. Thomas, *Identification, classification, and partial characterization of genes in humans and other vertebrates homologous to a fish membrane progestin receptor.* Proc Natl Acad Sci U S A, 2003. **100**(5): p. 2237-42.
375. Ashley, R.L., et al., *Cloning and characterization of an ovine intracellular seven transmembrane receptor for progesterone that mediates calcium mobilization.* Endocrinology, 2006. **147**(9): p. 4151-9.
376. Hanna, R., et al., *Cell-surface expression, progestin binding, and rapid nongenomic signaling of zebrafish membrane progestin receptors alpha and beta in transfected cells.* J Endocrinol, 2006. **190**(2): p. 247-60.
377. Karteris, E., et al., *Progesterone signaling in human myometrium through two novel membrane G protein-coupled receptors: potential role in functional progesterone withdrawal at term.* Mol Endocrinol, 2006. **20**(7): p. 1519-34.
378. Thomas, P., et al., *Steroid and G protein binding characteristics of the seatrout and human progestin membrane receptor alpha subtypes and their evolutionary origins.* Endocrinology, 2007. **148**(2): p. 705-18.
379. Hagedorn, K.A., et al., *Regulation of Vascular Tone During Pregnancy: A Novel Role for the Pregnane X Receptor.* Hypertension, 2007. **49**(2): p. 328-333.
380. Kliewer, S.A., et al., *An Orphan Nuclear Receptor Activated by Pregnanes Defines a Novel Steroid Signaling Pathway.* Cell, 1998. **92**(1): p. 73-82.
381. Bauer, B., et al., *Pregnane X Receptor Up-Regulation of P-Glycoprotein Expression and Transport Function at the Blood-Brain Barrier.* Molecular Pharmacology, 2004. **66**(3): p. 413-419.
382. Kliewer, S.A., B. Goodwin, and T.M. Willson, *The nuclear pregnane X receptor: a key regulator of xenobiotic metabolism.* Endocr Rev, 2002. **23**(5): p. 687-702.
383. Miller, L. and J.S. Hunt, *Regulation of TNF-alpha production in activated mouse macrophages by progesterone.* J Immunol, 1998. **160**(10): p. 5098-104.
384. Lei, B., et al., *Anti-Inflammatory Effects of Progesterone in Lipopolysaccharide-Stimulated BV-2 Microglia.* PLoS ONE, 2014. **9**(7): p. e103969.
385. Jain, S.K., et al., *Progesterone, but not 17β-estradiol, increases TNF-α secretion in U937 monocytes.* Cytokine, 2004. **26**(3): p. 102-105.
386. Echeverria, P.C. and D. Picard, *Molecular chaperones, essential partners of steroid hormone receptors for activity and mobility.* Biochimica et Biophysica Acta (BBA) - Molecular Cell Research, 2010. **1803**(6): p. 641-649.
387. Foster, H., et al., *Internalisation of membrane progesterone receptor-alpha after treatment with progesterone: Potential involvement of a clathrin-dependent pathway.* Mol Med Rep, 2010. **3**(1): p. 27-35.
388. Kurihara, T. and R. Bravo, *Cloning and functional expression of mCCR2, a murine receptor for the C-C chemokines JE and FIC.* J Biol Chem, 1996. **271**(20): p. 11603-7.
389. Kurihara, T., et al., *Defects in macrophage recruitment and host defense in mice lacking the CCR2 chemokine receptor.* J Exp Med, 1997. **186**(10): p. 1757-62.
390. Mack, M., et al., *Expression and characterization of the chemokine receptors CCR2 and CCR5 in mice.* J Immunol, 2001. **166**(7): p. 4697-704.
391. Mack, M., et al., *Identification of Antigen-Capturing Cells as Basophils.* The Journal of Immunology, 2005. **174**(2): p. 735-741.
392. Vecchi, A., et al., *Differential responsiveness to constitutive vs. inducible chemokines of immature and mature mouse dendritic cells.* J Leukoc Biol, 1999. **66**(3): p. 489-94.
393. Johnston, B., et al., *Chronic inflammation upregulates chemokine receptors and induces neutrophil migration to monocyte chemoattractant protein-1.* J Clin Invest, 1999. **103**(9): p. 1269-76.

394. Tsuda, Y., et al., *CCL2, a product of mice early after systemic inflammatory response syndrome (SIRS), induces alternatively activated macrophages capable of impairing antibacterial resistance of SIRS mice.* J Leukoc Biol, 2004. **76**(2): p. 368-73.
395. Hua, R., et al., *Human Labour is Associated with a Decline in Myometrial Chemokine Receptor Expression: The Role of Prostaglandins, Oxytocin and Cytokines.* American Journal of Reproductive Immunology, 2013. **69**(1): p. 21-32.
396. He, Y.-Y., et al., *Regulation of C-C motif chemokine ligand 2 and its receptor in human decidual stromal cells by pregnancy-associated hormones in early gestation.* Human Reproduction, 2007. **22**(10): p. 2733-2742.
397. Gomez-Lopez, N., et al., *Fetal membranes exhibit selective leukocyte chemotaxic activity during human labor.* Journal of Reproductive Immunology, 2009. **80**(1–2): p. 122-131.
398. Gomez-Lopez, N., L.J. Guilbert, and D.M. Olson, *Invasion of the leukocytes into the fetal-maternal interface during pregnancy.* J Leukoc Biol, 2010. **88**(4): p. 625-633.
399. Esplin, M.S., et al., *Monocyte chemotactic protein-1 is increased in the amniotic fluid of women who deliver preterm in the presence or absence of intra-amniotic infection.* Journal of Maternal-Fetal and Neonatal Medicine, 2005. **17**(6): p. 365-373.
400. Martynowicz, H., et al., *The role of chemokines in hypertension.* Adv Clin Exp Med, 2014. **23**(3): p. 319-25.
401. Antonelli, A., et al., *High serum levels of CXC (CXCL10) and CC (CCL2) chemokines in untreated essential hypertension.* Int J Immunopathol Pharmacol, 2012. **25**(2): p. 387-95.
402. Shen, J.Z., et al., *CCL2-dependent macrophage recruitment is critical for mineralocorticoid receptor-mediated cardiac fibrosis, inflammation, and blood pressure responses in male mice.* Endocrinology, 2014. **155**(3): p. 1057-66.
403. Fu, J., et al., *Targeted delivery of pulmonary arterial endothelial cells overexpressing interleukin-8 receptors attenuates monocrotaline-induced pulmonary vascular remodeling.* Arterioscler Thromb Vasc Biol, 2014. **34**(7): p. 1539-47.
404. Rodríguez-Iturbe, B., et al., *Oxidative stress, renal infiltration of immune cells, and salt-sensitive hypertension: all for one and one for all.* 2004. **286**(4): p. F606-F616.
405. Haller, H., et al., *Monocyte infiltration and c-fms expression in hearts of spontaneously hypertensive rats.* Hypertension, 1995. **25**(1): p. 132-8.
406. Mirzadegan, T., et al., *Identification of the binding site for a novel class of CCR2b chemokine receptor antagonists: binding to a common chemokine receptor motif within the helical bundle.* J Biol Chem, 2000. **275**(33): p. 25562-71.
407. Wakida, N., et al., *CC-chemokine ligand 2 facilitates conditioned place preference to methamphetamine through the activation of dopamine systems.* J Pharmacol Sci, 2014. **125**(1): p. 68-73.
408. Yang, D., et al., *Roles of CC chemokine receptors (CCRs) on lipopolysaccharide-induced acute lung injury.* Respir Physiol Neurobiol, 2010. **170**(3): p. 253-9.
409. Yang, S.J., et al., *Inhibition of the chemokine (C-C motif) ligand 2/chemokine (C-C motif) receptor 2 pathway attenuates hyperglycaemia and inflammation in a mouse model of hepatic steatosis and lipoatrophy.* Diabetologia, 2009. **52**(5): p. 972-81.
410. Awad, A.S., et al., *Monocyte/macrophage chemokine receptor CCR2 mediates diabetic renal injury.* Am J Physiol Renal Physiol, 2011. **301**(6): p. F1358-66.
411. Shynlova, O., et al., *Inhibition of infection-mediated preterm birth by administration of broad spectrum chemokine inhibitor in mice.* J Cell Mol Med, 2014. **18**(9): p. 1816-29.
412. Ishibashi, M., et al., *Critical Role of Monocyte Chemoattractant Protein-1 Receptor CCR2 on Monocytes in Hypertension-Induced Vascular Inflammation and Remodeling.* Circulation Research, 2004. **94**(9): p. 1203-1210.
413. Kvist, S. and M.J. Mulvany, *Contrasting Regression of Blood Pressure and Cardiovascular Structure in Declipped Renovascular Hypertensive Rats.* Hypertension, 2003. **41**(3): p. 540-545.
414. Arango Duque, G. and A. Descoteaux, *Macrophage cytokines: involvement in immunity and infectious diseases.* Front Immunol, 2014. **5**: p. 491.

415. Mettimano, M., et al., *Blood pressure regulation by CCR genes.* Clin Exp Hypertens, 2006. **28**(7): p. 611-8.
416. Mettimano, M., et al., *CCR5 and CCR2 gene polymorphisms in hypertensive patients.* Br J Biomed Sci, 2003. **60**(1): p. 19-21.
417. Koyanagi, M., et al., *Role of monocyte chemoattractant protein-1 in cardiovascular remodeling induced by chronic blockade of nitric oxide synthesis.* Circulation, 2000. **102**(18): p. 2243-8.
418. Peters, W., M. Dupuis, and I.F. Charo, *A mechanism for the impaired IFN-gamma production in C-C chemokine receptor 2 (CCR2) knockout mice: role of CCR2 in linking the innate and adaptive immune responses.* J Immunol, 2000. **165**(12): p. 7072-7.
419. Serbina, N.V. and E.G. Pamer, *Monocyte emigration from bone marrow during bacterial infection requires signals mediated by chemokine receptor CCR2.* Nat Immunol, 2006. **7**(3): p. 311-317.
420. Aldridge, J.R., Jr., et al., *TNF/iNOS-producing dendritic cells are the necessary evil of lethal influenza virus infection.* Proc Natl Acad Sci U S A, 2009. **106**(13): p. 5306-11.
421. Gu, L., et al., *Control of TH2 polarization by the chemokine monocyte chemoattractant protein-1.* Nature, 2000. **404**(6776): p. 407-11.
422. Karpus, W.J., et al., *Differential CC chemokine-induced enhancement of T helper cell cytokine production.* J Immunol, 1997. **158**(9): p. 4129-36.
423. Sato, N., et al., *CC chemokine receptor (CCR)2 is required for langerhans cell migration and localization of T helper cell type 1 (Th1)-inducing dendritic cells. Absence of CCR2 shifts the Leishmania major-resistant phenotype to a susceptible state dominated by Th2 cytokines, b cell outgrowth, and sustained neutrophilic inflammation.* J Exp Med, 2000. **192**(2): p. 205-18.
424. Szymczak, W.A. and G.S. Deepe, Jr., *The CCL7-CCL2-CCR2 axis regulates IL-4 production in lungs and fungal immunity.* J Immunol, 2009. **183**(3): p. 1964-74.
425. Aliberti, J., *Control of Innate and Adaptive Immune Responses during Infectious Diseases*, J. Aliberti, Editor, 2011, Springer.
426. Van Vliet, B.N., L.L. Chafe, and J.-P. Montani, *Characteristics of 24 h Telemetered Blood Pressure in eNOS-Knockout and C57Bl/6J Control Mice.* The Journal of Physiology, 2003. **549**(1): p. 313-325.
427. Connelly, L., M. Madhani, and A.J. Hobbs, *Resistance to Endotoxic Shock in Endothelial Nitric-oxide Synthase (eNOS) Knock-out Mice.* Journal of Biological Chemistry, 2005. **280**(11): p. 10040-10046.
428. Kusinski, L.C., et al., *eNOS knockout mouse as a model of fetal growth restriction with an impaired uterine artery function and placental transport phenotype.* American Journal of Physiology - Regulatory, Integrative and Comparative Physiology, 2012. **303**(1): p. R86-R93.
429. Hefler, L.A., et al., *Endothelial-derived nitric oxide and angiotensinogen: blood pressure and metabolism during mouse pregnancy.* 2001. **280**(1): p. R174-R182.
430. Shesely, E.G., et al., *Nitric oxide synthase gene knockout mice do not become hypertensive during pregnancy.* American Journal of Obstetrics and Gynecology, 2001. **185**(5): p. 1198-1203.
431. Ferrari, A.U., et al., *Nitric oxide-dependent vasodilation and the regulation of arterial blood pressure.* J Cardiovasc Pharmacol, 2001. **38**(2): p. S19-22.
432. Lieberthal, W., et al., *Nitric oxide inhibition in rats improves blood pressure and renal function during hypovolemic shock.* Am J Physiol, 1991. **261**(5 Pt 2): p. F868-72.
433. Pullamsetti, S.S., et al., *Effect of nitric oxide synthase (NOS) inhibition on macro- and microcirculation in a model of rat endotoxic shock.* Thromb Haemost, 2006. **95**(4): p. 720-7.
434. Küng, C.F., et al., *L-NAME Hypertension Alters Endothelial and Smooth Muscle Function in Rat Aorta: Prevention by Trandolapril and Verapamil.* Hypertension, 1995. **26**(5): p. 744-751.
435. Kinasewitz, G.T., et al., *Multicenter, randomized, placebo-controlled study of the nitric oxide scavenger pyridoxalated hemoglobin polyoxyethylene in distributive shock.* Crit Care Med, 2008. **36**(7): p. 1999-2007.

436. Vitecek, J., et al., *Arginine-Based Inhibitors of Nitric Oxide Synthase: Therapeutic Potential and Challenges.* Mediators Inflamm, 2012. **2012**: p. 22.
437. Nandi, M., et al., *Genetic and pharmacological inhibition of dimethylarginine dimethylaminohydrolase 1 is protective in endotoxic shock.* Arterioscler Thromb Vasc Biol, 2012. **32**(11): p. 2589-97.
438. Lind, L., et al., *Genetic variation in the dimethylarginine dimethylaminohydrolase 1 gene (DDAH1) is related to asymmetric dimethylarginine (ADMA) levels, but not to endothelium-dependent vasodilation.* Vasc Med, 2013. **18**(4): p. 192-9.
439. Leiper, J., et al., *Disruption of methylarginine metabolism impairs vascular homeostasis.* Nat Med, 2007. **13**(2): p. 198-203.
440. Hu, X., et al., *Dimethylarginine dimethylaminohydrolase-1 is the critical enzyme for degrading the cardiovascular risk factor asymmetrical dimethylarginine.* Arterioscler Thromb Vasc Biol, 2011. **31**(7): p. 1540-6.
441. Casellas, J. and J.F. Medrano, *Within-Generation Mutation Variance for Litter Size in Inbred Mice.* Genetics, 2008. **179**(4): p. 2147-2155.
442. Walker, M.P., L. Tian, and A.G. Matera, *Reduced Viability, Fertility and Fecundity in Mice Lacking the Cajal Body Marker Protein, Coilin.* PLoS ONE, 2009. **4**(7): p. e6171.
443. Kendall, R.L. and K.A. Thomas, *Inhibition of vascular endothelial cell growth factor activity by an endogenously encoded soluble receptor.* Proc Natl Acad Sci U S A, 1993. **90**(22): p. 10705-9.
444. Clark, D.E., et al., *A vascular endothelial growth factor antagonist is produced by the human placenta and released into the maternal circulation.* Biol Reprod, 1998. **59**(6): p. 1540-8.
445. Ahmad, S. and A. Ahmed, *Elevated placental soluble vascular endothelial growth factor receptor-1 inhibits angiogenesis in preeclampsia.* Circ Res, 2004. **95**(9): p. 884-91.
446. Davisson, R.L., et al., *Discovery of a Spontaneous Genetic Mouse Model of Preeclampsia.* Hypertension, 2002. **39**(2): p. 337-342.
447. Tanaka, M., et al., *Dimethylarginine dimethylaminohydrolase overexpression suppresses graft coronary artery disease.* Circulation, 2005. **112**(11): p. 1549-56.
448. Wang, Z., et al., *Pharmacological inhibition of DDAH1 improves survival, haemodynamics and organ function in experimental septic shock.* Biochem J, 2014. **460**(2): p. 309-16.
449. Xin, H.Y., et al., *Regulation by DDAH/ADMA pathway of lipopolysaccharide-induced tissue factor expression in endothelial cells.* Thromb Haemost, 2007. **97**(5): p. 830-8.
450. Nijveldt, R.J., et al., *Gut and liver handling of asymmetric and symmetric dimethylarginine in the rat under basal conditions and during endotoxemia.* Liver Int, 2004. **24**(5): p. 510-8.
451. Aggarwal, S., et al., *Dimethylarginine dimethylaminohydrolase II overexpression attenuates LPS-mediated lung leak in acute lung injury.* Am J Respir Cell Mol Biol, 2014. **50**(3): p. 614-25.
452. Scalera, F., et al., *Endogenous nitric oxide synthesis inhibitor asymmetric dimethyl L-arginine accelerates endothelial cell senescence.* Arterioscler Thromb Vasc Biol, 2004. **24**(10): p. 1816-22.
453. Chen, X.M., et al., *Involvement of DDAH/ADMA pathway in the pathogenesis of rheumatoid arthritis in rats.* Int Immunopharmacol, 2013. **16**(2): p. 322-31.
454. Aiura, K., et al., *Circulating concentrations and physiologic role of atrial natriuretic peptide during endotoxic shock in the rat.* Crit Care Med, 1995. **23**(11): p. 1898-906.
455. Stuhlinger, M.C., et al., *Asymmetric dimethyl L-arginine (ADMA) is a critical regulator of myocardial reperfusion injury.* Cardiovasc Res, 2007. **75**(2): p. 417-25.
456. Hanamura, T., E. Asakura, and T. Tanabe, *Macrophage colony-stimulating factor (M-CSF) augments cytokine induction by lipopolysaccharide (LPS)-stimulation and by bacterial infections in mice.* Immunopharmacology, 1997. **37**(1): p. 15-23.
457. Kakizaki, Y., et al., *Temporal Profiles of Interleukin-1β, Interleukin-6, and Tumor Necrosis Factor-α in the Plasma and Hypothalamic Paraven-tricular Nucleus after Intravenous or Intraperitoneal Administration of Lipopolysaccharide in the Rat.* Endocrine Journal, 1999. **46**(4): p. 487-496.

458. Fretland, D.J., et al., *Temporal relationships of cytokine production in mouse non-lethal sepsis: effect of nitric oxide synthase inhibitors.* Inflammation research : official journal of the European Histamine Research Society 1997. **46 Suppl 2**: p. S155-6.
459. Bosmann, M., N.F. Russkamp, and P.A. Ward, *Fingerprinting of the TLR4-induced acute inflammatory response.* Experimental and molecular pathology, 2012. **93**(3): p. 319-323.
460. Welsh, T.N., et al., *Progesterone Receptor Expression Declines in the Guinea Pig Uterus during Functional Progesterone Withdrawal and in Response to Prostaglandins.* PLoS ONE, 2014. **9**(8): p. e105253.
461. Arck, P.C. and K. Hecher, *Fetomaternal immune cross-talk and its consequences for maternal and offspring's health.* Nat Med, 2013. **19**(5): p. 548-56.
462. Mess, A., *The Guinea Pig Placenta: Model of Placental Growth Dynamics.* Placenta, 2007. **28**(8–9): p. 812-815.
463. Buras, J.A., B. Holzmann, and M. Sitkovsky, *Animal models of sepsis: setting the stage.* Nature reviews. Drug discovery, 2005. **4**(10): p. 854-65.
464. Fisher, C.J., Jr., et al., *Treatment of septic shock with the tumor necrosis factor receptor:Fc fusion protein. The Soluble TNF Receptor Sepsis Study Group.* The New England journal of medicine, 1996. **334**(26): p. 1697-702.
465. Fisher, C.J., Jr., et al., *Recombinant human interleukin 1 receptor antagonist in the treatment of patients with sepsis syndrome. Results from a randomized, double-blind, placebo-controlled trial. Phase III rhIL-1ra Sepsis Syndrome Study Group.* JAMA, 1994. **271**(23): p. 1836-43.
466. Opal, S.M.M.D., et al., *Confirmatory interleukin-1 receptor antagonist trial in severe sepsis: A phase III, randomized, doubleblind, placebo-controlled, multicenter trial.* Critical Care Medicine, 1997. **25**(7): p. 1115-1124.
467. Fink, M.P. and H.S. Warren, *Strategies to improve drug development for sepsis.* Nature reviews. Drug discovery, 2014. **13**(10): p. 741-758.
468. Remick, D.G., et al., *Comparison of the mortality and inflammatory response of two models of sepsis: lipopolysaccharide vs. cecal ligation and puncture.* Shock (Augusta, Ga.), 2000. **13**(2): p. 110-6.
469. Cavaillon, J.M., et al., *Cytokine cascade in sepsis.* Scandinavian journal of infectious diseases, 2003. **35**(9): p. 535-44.
470. Warren, H.S., et al., *Resilience to bacterial infection: difference between species could be due to proteins in serum.* The Journal of infectious diseases, 2010. **201**(2): p. 223-232.
471. Ito, R., et al., *Current advances in humanized mouse models.* Cell Mol Immunol, 2012. **9**(3): p. 208-214.
472. Ito, M., et al., *NOD/SCID/gamma(c)(null) mouse: an excellent recipient mouse model for engraftment of human cells.* Blood, 2002. **100**(9): p. 3175-82.
473. Li, G., et al., *Plasmacytoid dendritic cells suppress HIV-1 replication but contribute to HIV-1 induced immunopathogenesis in humanized mice.* PLoS pathogens, 2014. **10**(7): p. e1004291.
474. Skirecki, T., et al., *Early severe impairment of hematopoietic stem and progenitor cells from the bone marrow caused by CLP sepsis and endotoxemia in a humanized mice model.* Stem cell research & therapy, 2015. **6**(1): p. 142.
475. Fink, M.P., *Animal models of sepsis.* Virulence, 2014. **5**(1): p. 143-53.
476. Italiani, P. and D. Boraschi, *From Monocytes to M1/M2 Macrophages: Phenotypical vs. Functional Differentiation.* Front Immunol, 2014. **5**: p. 514.
477. Benjamim, C.F., S.H. Ferreira, and F.d.Q. Cunha, *Role of Nitric Oxide in the Failure of Neutrophil Migration in Sepsis.* Journal of Infectious Diseases, 2000. **182**(1): p. 214-223.
478. He, H., et al., *Vascular endothelial growth factor signals endothelial cell production of nitric oxide and prostacyclin through flk-1/KDR activation of c-Src.* J Biol Chem, 1999. **274**(35): p. 25130-5.
479. Itoh, S., et al., *Vasodilation to vascular endothelial growth factor in the uterine artery of the pregnant rat is blunted by low dietary protein intake.* Pediatr Res, 2002. **51**(4): p. 485-91.

480. Rossiter, S., et al., *Selective substrate-based inhibitors of mammalian dimethylarginine dimethylaminohydrolase.* Journal of medicinal chemistry, 2005. **48**(14): p. 4670-8.

10. Appendix 1: Supplementary Data

Statistical Analysis Using Mixed Effects Modelling

This work was done by Dr Fabiana Gordon at Imperial College Statistical Advice Service.

The methodology used to compare pregnant and non-pregnant haemodynamic responses to LPS was Mixed Models for longitudinal data. To capture change over time a quadratic trend was fitted, which meant that missing data points were accounted for. These fitted trends were then compared back to the original data to ensure a good fit.

In some of the outcome measures it was necessary to adjust for before-after treatment (baseline values) to get a better fit. In all outcome measures it was found there was an interaction effect between time (hours) and treatment group. This meant that the trajectory of the outcome measure varies across groups. It also meant that the comparisons between groups were dependent on time. Therefore overall comparisons were done in conjunction with individual time-point analysis.

Activity was assessed using the outcome of logarithm of activity, to correct for skewness and heterogeneity of variances across groups. Furthermore, the 'TSI' parameter (time spent inactive) outcome measure had to be adjusted for whether there was activity or not (activity binary) to account for the 100 % values. In other words, there was a discontinuity in the data which may mean that p-values are less robust.

Lastly, as comparisons of interest were made on multiple outcomes which were measured from the same animal simultaneously, an adjustment for p-value significance should be considered. The level of significance becomes 0.0125 after adjusting for multiple comparisons.

SPSS 22 and Stata 13 were used to obtain the estimated effects.

The overall trends for each parameter measured are shown in the figures below (Figure A1.1 to A1.7).

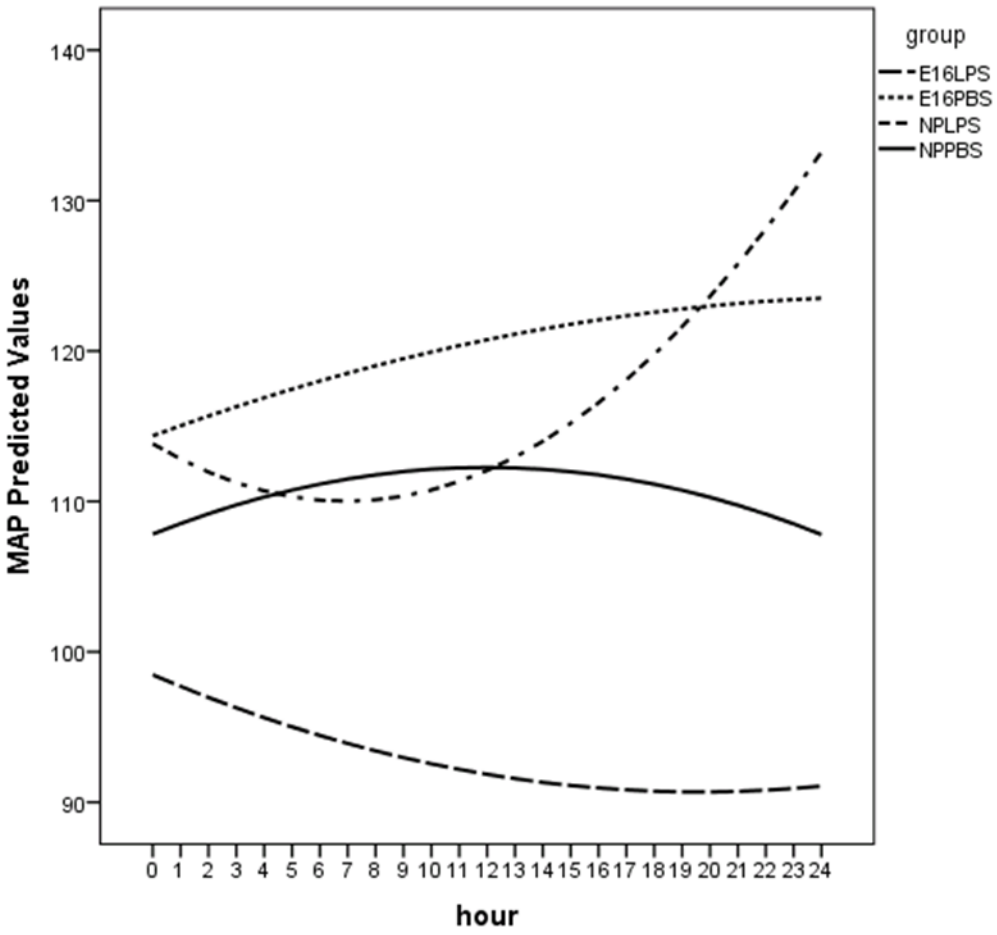


Figure A1.1: Mean arterial pressure (MAP) values from mice in each treatment group were plotted as mmHg over time (24 hours post-i.p. injection). 0 hours represents the baseline (pre-i.p.) time-point. A quadratic trend was fitted and used to calculate statistical significance using mixed effects modelling. n=4-5. E16LPS- pregnant LPS-treated, E16PBS- pregnant PBS-treated, NPLPS- non-pregnant LPS-treated, NPPBS- non-pregnant PBS-treated.

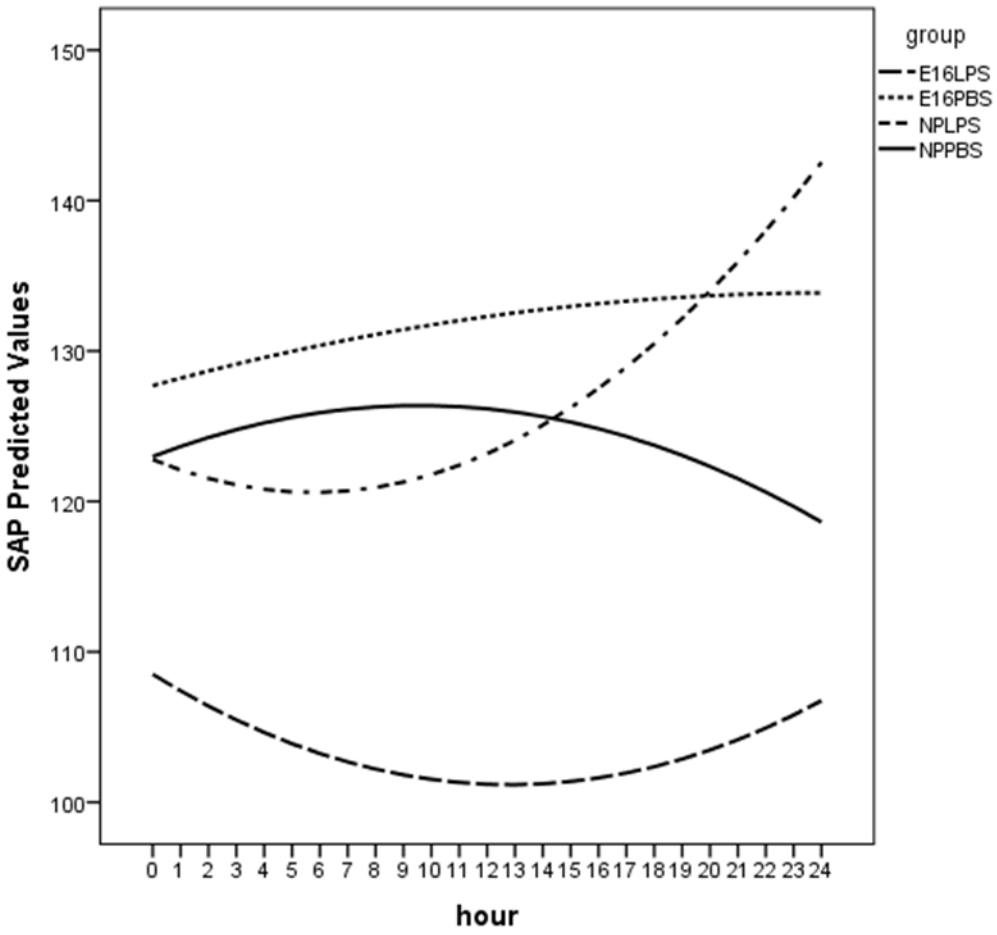


Figure A1.2: Systolic arterial pressure (SAP) values from mice in each treatment group were plotted as mmHg over time (24 hours post-i.p. injection). 0 hours represents the baseline (pre-i.p.) time-point. A quadratic trend was fitted and used to calculate statistical significance using mixed effects modelling. n=4-5. E16LPS- pregnant LPS-treated, E16PBS- pregnant PBS-treated, NPLPS- non-pregnant LPS-treated, NPPBS- non-pregnant PBS-treated.

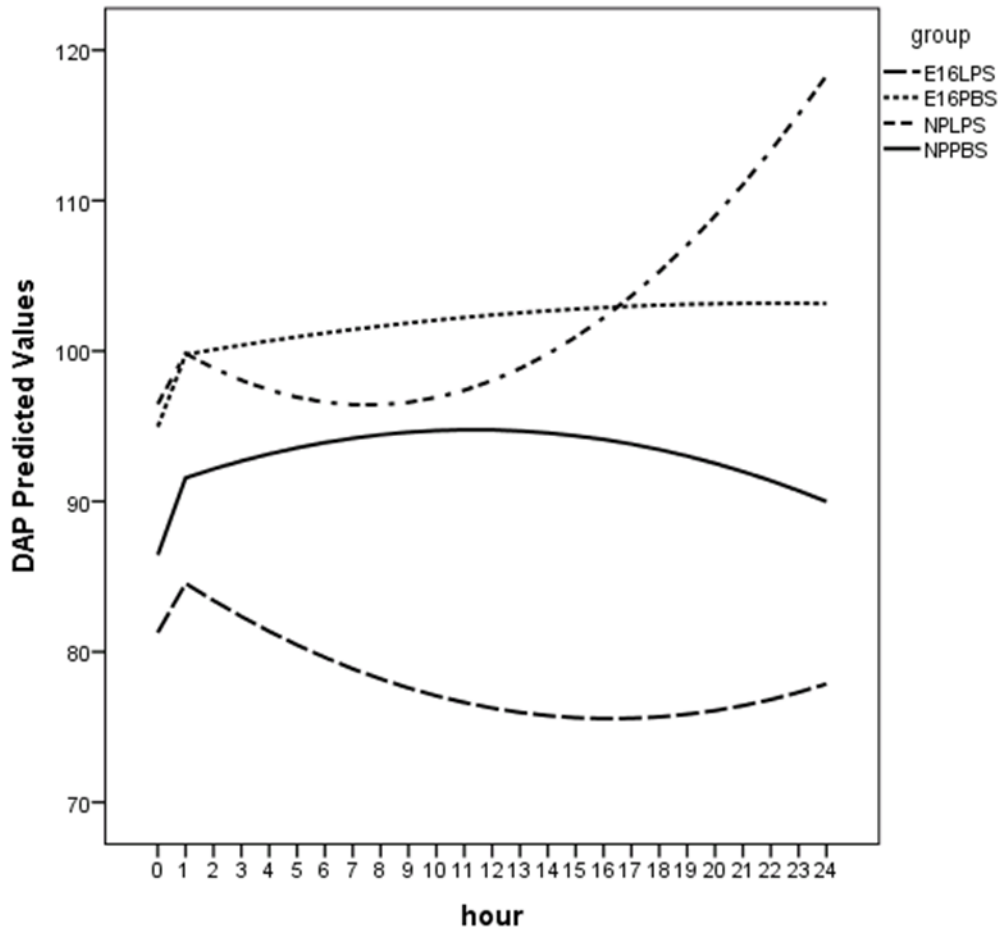


Figure A1.3: Diastolic arterial pressure (DAP) values from mice in each treatment group were plotted as mmHg over time (24 hours post-i.p. injection). 0 hours represents the baseline (pre-i.p.) time-point. A quadratic trend was fitted and used to calculate statistical significance using mixed effects modelling. n=4-5. E16LPS- pregnant LPS-treated, E16PBS- pregnant PBS-treated, NPLPS- non-pregnant LPS-treated, NPPBS- non-pregnant PBS-treated.

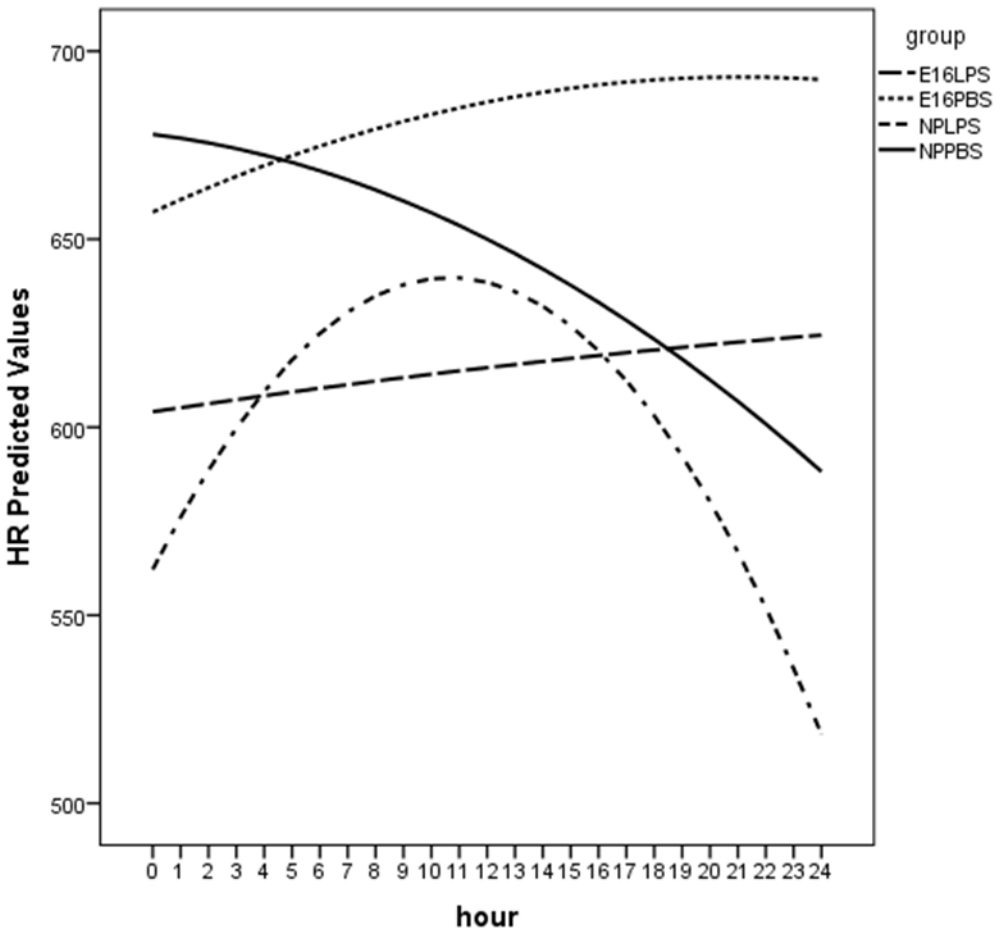


Figure A1.4: Heart rate (HR) values from mice in each treatment group were plotted as beats per minute (bpm) over time (24 hours post-i.p. injection). 0 hours represents the baseline (pre-i.p.) time-point. A quadratic trend was fitted and used to calculate statistical significance using mixed effects modelling. n=4-5. E16LPS- pregnant LPS-treated, E16PBS- pregnant PBS-treated, NPLPS- non-pregnant LPS-treated, NPPBS- non-pregnant PBS-treated.

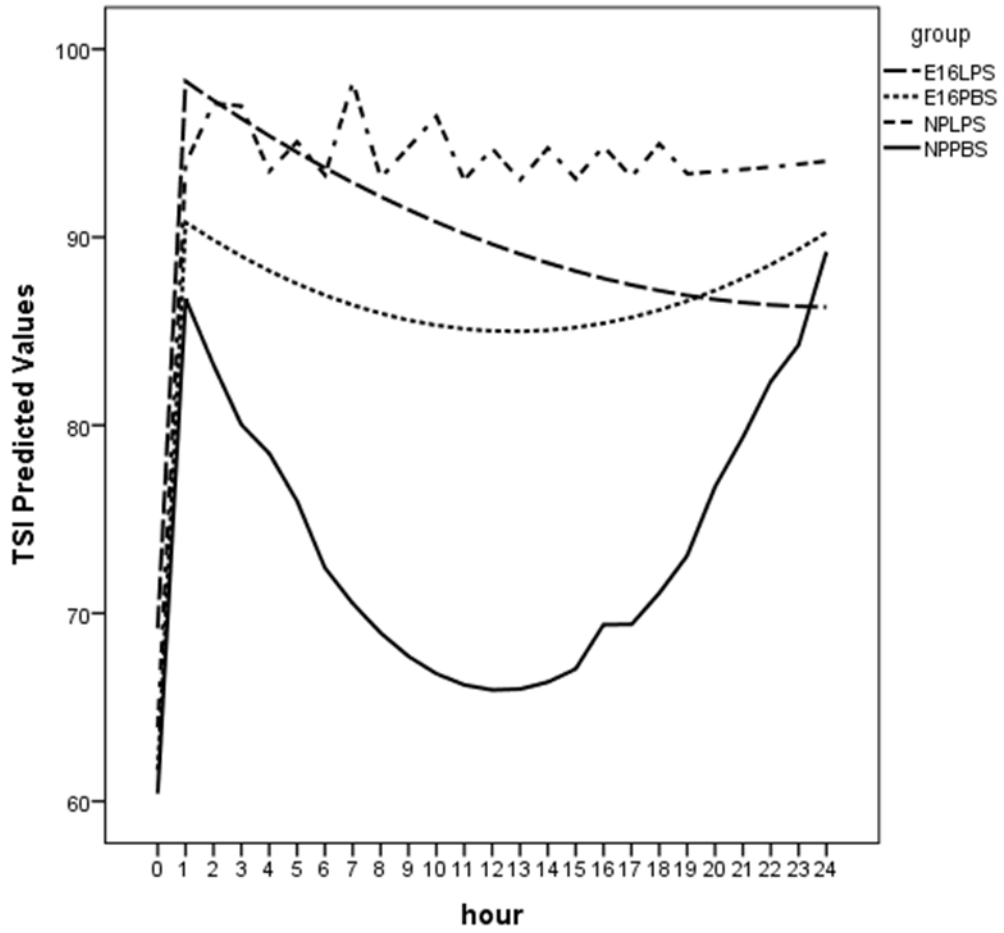


Figure A1.5: Time spent inactive (TSI) values from mice in each treatment group were plotted as percentage (%) over time (24 hours post-i.p. injection). 0 hours represents the baseline (pre-i.p.) time-point. A quadratic trend was fitted and used to calculate statistical significance using mixed effects modelling. n=4-5. E16LPS- pregnant LPS-treated, E16PBS- pregnant PBS-treated, NPLPS- non-pregnant LPS-treated, NPPBS- non-pregnant PBS-treated.

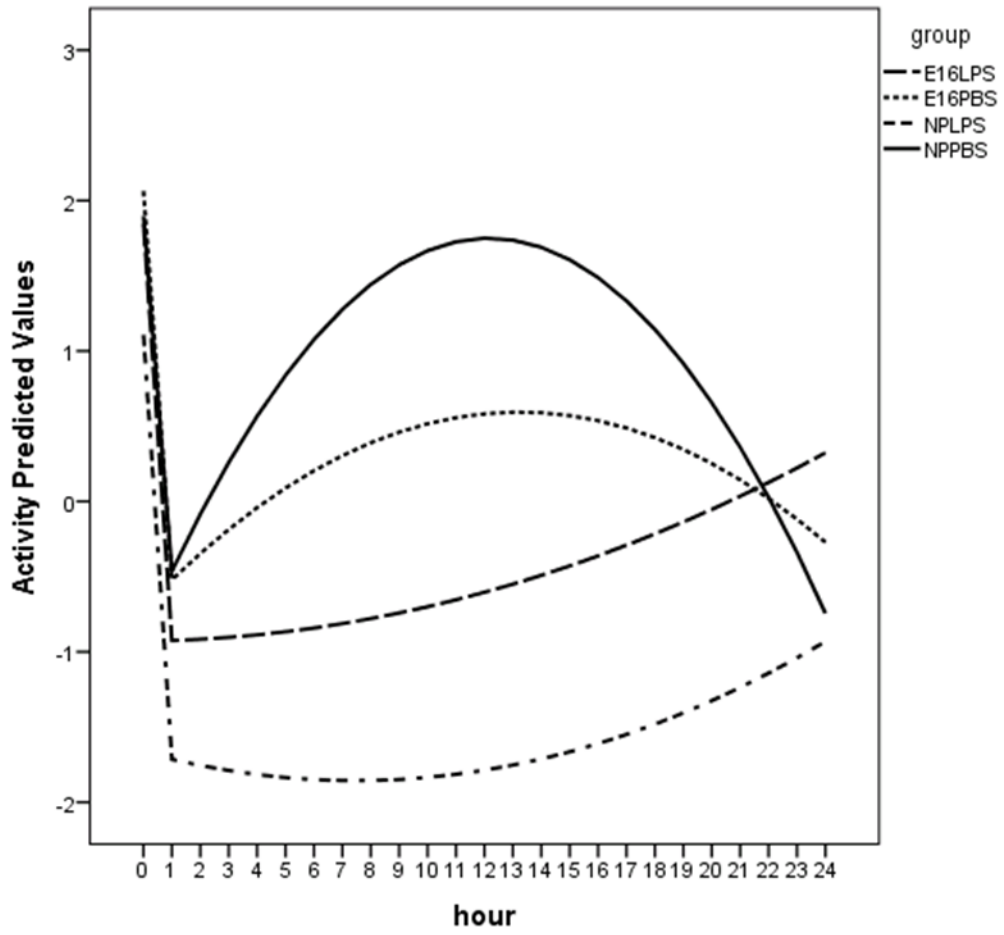


Figure A1.6: Activity (arbitrary units) values from mice in each treatment group were plotted over time (24 hours post-i.p. injection). 0 hours represents the baseline (pre-i.p.) time-point. A quadratic trend was fitted and used to calculate statistical significance using mixed effects modelling. n=4-5. E16LPS- pregnant LPS-treated, E16PBS- pregnant PBS-treated, NPLPS- non-pregnant LPS-treated, NPPBS- non-pregnant PBS-treated.

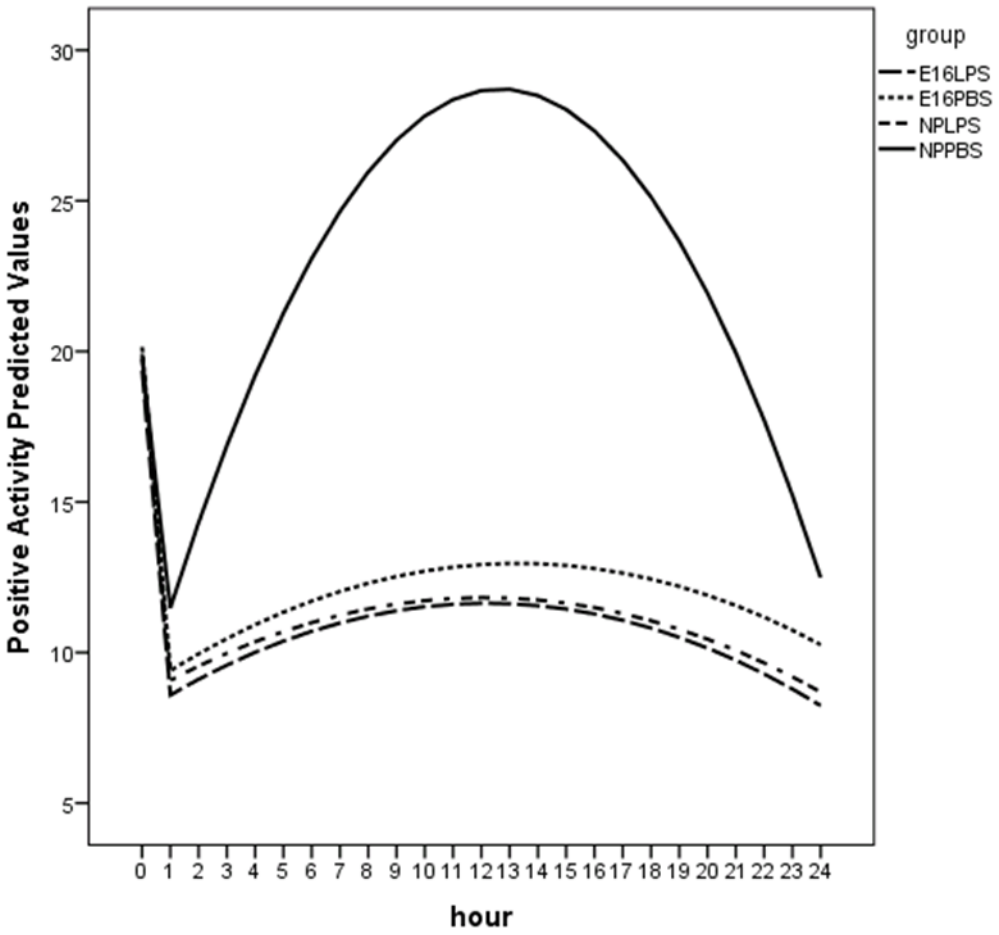


Figure A1.7: Activity >0, or positive activity (arbitrary units) values from mice in each treatment group were plotted over time (24 hours post-i.p. injection). 0 hours represents the baseline (pre-i.p.) time-point. A quadratic trend was fitted and used to calculate statistical significance using mixed effects modelling. n=4-5. E16LPS- pregnant LPS-treated, E16PBS- pregnant PBS-treated, NPLPS- non-pregnant LPS-treated, NPPBS- non-pregnant PBS-treated.